Excerpts from

PROCESSES IN BIOLOGICAL VISION:

including,

ELECTROCHEMISTRY OF THE NEURON

This material is excerpted from the full β-version of the text. The final printed version will be more concise due to further editing and economical constraints. A Table of Contents and an index are located at the end of this paper.

James T. Fulton
Vision Concepts

jtfulton@neuronresearch.net

April 30, 2017

17 Performance descriptors of Vision[1]

PART II: TEMPORAL & SPATIAL PERFORMANCE

The press of work on other parts of the manuscript may delay the final cleanup of this PART but it is too valuable to delay its release for comment. [Author] Any comments are welcome.

It will eventually include an evaluation of the bandwidth of the luminance and chrominance channels in support of the chapter on the tertiary circuits, Chapter 14, including the work of de Lange Dzn and Stockman, MacLeod & Lebrun in Section 17.6.6.5.

17.5 The Temporal Characteristic of the human eye

The overall temporal characteristics of animal vision are difficult to quantify. It is frequently easier to perform experiments in **either** the transient or the steady state domain. To arrive at a unified mathematical model, it is necessary to analyze both classes of data and make the necessary mathematical manipulations to bring all of the data into a single domain. After a general discussion of background material, the main discussion will be separated into a transient section and a frequency response section in order to show how the model correlates with the data from various earlier investigators. A separate discussion of signal delay will be found in **Section 17.6.5.**

The temporal asymmetries of the visual system result in a variety of Effects. These effects can frequently be associated with a specific temporal time constant of the visual system. Many of these effects are infrequently observed. As a result, their description in the technical literature has been spotty and frequently imprecise.

An unusual facet of the literature concerning temporal characteristic of the human eye is that there is virtually no data on light adaptation of the eye, only on dark adaptation. A complete understanding of the temporal performance necessarily involves both sections of the overall temporal performance. Admittedly, the experiments of light adaptation are more difficult, especially for the subject. Poot, Snippe & van Hateren have recently provided new data recognizing the duality of this problem[2].

17.5.1 Background

No discussion was found in the recent literature of the immense range of time intervals that play a significant role in the visual process. The initial photoexcitation process has recently been shown to require less than 200 femto-seconds. On the other hand, subjects with diseases related to night blindness exhibit dark adaptation time constants of over 20 minutes. In between, there are significant processes related to the overall photoexcitation/de-excitation process with *variable* time constants of between 100 and 400 milliseconds, processes related to light adaptation with *variable* time constants of about XXX, and processes related to the iris and with dark adaptation with time constants of a few seconds. A full theoretical discussion of vision should address all of these parameters.

17.5.1.1 Other Investigations

There has been considerable experimental activity with regard to the temporal performance of the human eye. However, it has been primarily exploratory and not always accompanied by careful analytical analysis consistent with an adequate model of the processes involved. This lack of a model has been due primarily to the state of the art in electronics and cytology at the time. Most of the activity falls into two independent categories. First, the exposition of the dark adaptation portion of the overall adaptation characteristic of the eye without accompanying

---

[1]Released April 30, 2017

[2]Poot, L. Snippe, H. & van Hateren, J. (1997) Dynamics of adaptation at high luminances J. Opt. Soc. Am. A vol. 14, no. 9, pp. 2499-2508

analysis. Second, a variety of experiments to determine the temporal bandwidth of the eye. This latter activity has in turn, suffered from two related problems. The various methods available to determine the temporal frequency characteristics have provided conflicting results, even when only one investigator was involved with several methods[3]. And, as expected, their conflicting results are due primarily to differences in assumptions concerning what they are measuring. None of these experimental methods have been implemented based on an adequate model of the system being evaluated.

Most investigators have employed psychophysical experiments in which a linear model of the visual system is assumed in order to evaluate the results of their experiments. This linear model has been a single thread model. Many of the investigators have relied on "white light" illumination. The definition of the light used is normally shown by a single English word within quotation marks. This practice provides an indication of the precision employed in the work. In those experiments involving color, the investigators have generally not chosen illumination sources that only excited one of the chromatic channels of the vision process at a time. This use of illuminants that straddle the chromophoric absorption channels of vision has led to cross-talk in the signal processing that was not adequately anticipated nor recognized by the investigators. In fact, they have frequently relied upon the Principle of Superposition during the interpretation of their data without recognizing there is a chromatically selective subtraction process incorporated in the signal processing system of the retina.

Most of these methods involve quite complex interactions with the visual system of the subject as seen from the overall block diagram. This is especially true where a transform is employed to convert a spatial stimulus into a temporal stimulus. These spatial techniques may employ edges, moving edges and patterns. All of the spatial techniques require a detailed knowledge of the optical system, mosaic characteristic of the retina and electrical circuits of the subjects visual system if accurate results are to be obtained.

17.5.1.1.1 Review of papers of Hecht and associates, pre-1940

The majority of the comprehensive experiments performed with respect to the transient performance of the eye are quite old. Most were performed and reported in the late 1930's by Hecht and his associates and graduate students at Columbia University. Their approach can be described as primarily exploratory as opposed to confirmatory since they relied upon no theoretical model other than the anecdotal functional relationship correlating with the putative physiological difference between rods and cones. Their instrumentation was typical of the time, pre-electronic revolution, and their interpretation was heavily dependent on the assumption of two separate photodetection mechanisms. Hecht was a leading proponent of the Duplex Theory based on functionally distinct rods and cones. Their experimental design was also typical of the time. No tight definition of the "white light" used or the spectral distribution of other lights employed. A few of their graphs, particularly figure 5 of 1937, have been redrawn in this work, based on their tabulations, to more clearly display the data points they relied upon in their discussion. While one might argue whether their instrumentation supports the three digit precision of their data, it appears there are *systematic trends* in the data not supported by either one or two monotonic functions. As stated in their original papers, the repeatability of their data was influenced by the 0.3 log unit day to day variation in the performance of a given subject, and they frequently made piecewise adjustments in their graphics to provide a more comprehensible presentation. Reference to this characteristic has never been found in a subsequent discussion of their work or republication of their graphs.

A major problem with many of their findings was the dependence on data from only one subject. In the paper with Handelbaum[4], sufficient subjects were tested to provide statistical relevance. However, statistical analysis frequently obscures systemic features. Artificial loci were drawn on the published data to encompass the data points (based on the rod/cone premise) instead of showing the actual error bars. They frequently selected the data of one subject for presentation and to press their point. The paper contains a good bibliography and analysis of the work of others during this time period.

There is a significant mathematical problem in finding an equation to represent the conventional description of the dark adaptation characteristic as consisting of two first order mathematical, nominally exponential functions representing a rod and a cone component. Both the product of two exponentials and the sum of two exponentials still look like a single exponential. No "break" is seen in the resulting function. Alternately, a

---

[3]Wyszecki Stiles, Op. cit. Pg 567

[4]Hecht, S. & Mandelbaum, J. (1939) The relation between vitamin A and dark adaptation. Jour. A. M. A., vol. 112, no. 19, pp. 1910-1916

second order system is described by a "damped sinusoid" that, while continuous, does exhibit periodic slope reversals as can be seen in the typical dark adaptation characteristic.

Hecht stressed precision and repeatability in his test instrumentation and listed six important parameters requiring control; (1) the illumination intensity and (2) the duration of the light present before dark adaptation begins, and (3) the area illuminated, (4) the retinal location, (5) the color and (6) the duration of the probe illumination. This work would suggest that their specification of (1) and (5) were inadequate in specifying spectral content adequately.

Overlooking Hecht's role as a primary proponent of the Duplex Theory during his day, the data in Hecht & Mandelbaum can be interpreted quite differently based on the more detailed foundation provided by this work.

Because it becomes important below, it is appropriate to discuss the statistical properties of their data relevant to the relationship between the chromatic and monochromatic thresholds of a given subject. Although they discuss this correlation with tongue and cheek semantics by saying: "The two thresholds are obviously connected, but the correlation is less than half perfect.", **Figure 17.5.1-1** demonstrates their correlation coefficient of 0.44. They suggested further mining of their data to remove the factor of age but did not pursue it. The paper continued to explore the subject of vitamin A depravation on the dark adaptation performance of the eye. A number of important facts were determined:

+ Vitamin A depravation is measurable within a few days and the log of the threshold intensity varies nearly linearly during the first 30 days, linearly for subject L. W. but less so for J. M. The impact is significant for L. W. after 30 days, about 1.6 log units for the monochromatic threshold and 0.9 log units for the chromatic threshold (about 0.9 and 0.5 for J. M.). These results suggest that after removing the expansion factor due to the adaptation amplifier, these two thresholds changed equally.

+ The location of the nominal break point in the dark adaptation characteristic did not change with depravation.

+ A figure from a related study was reproduced in the above paper showing results for one man with serious cirrhosis of the liver[5]. The findings were dramatically different. When placed on intensive vitamin A therapy, the mans visual threshold improved significantly. The changes were both in threshold levels and in location of the breakpoint. The breakpoint was reduced from 15 to seven minutes.

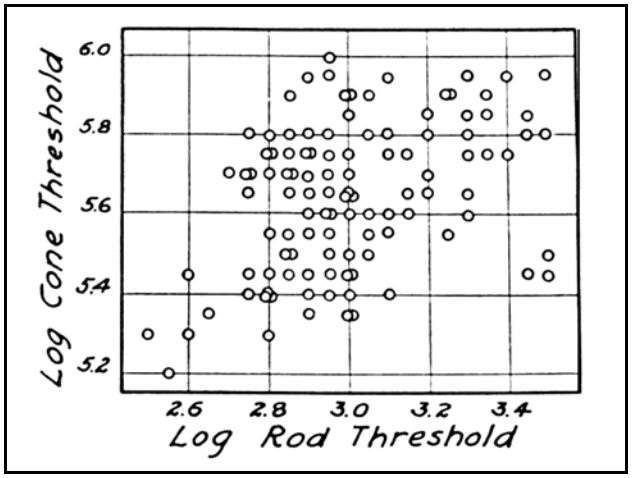

Figure 17.5.1-1 Correlation matrix between chromatic and achromatic thresholds shown by 110 persons. From Hecht & Mandelbaum (1939).

They concluded that: "Thus simple dietary avitaminosis does not change the time of the cone-rod transition point, whereas sever cirrhosis of the liver delays its appearance to almost twice the time, even though the final thresholds may be affected to the same extent in the two instances."

This work assigns distinctly different underlying processes to the determination of the ultimate dark adaptation (separately for the achromatic and monochromatic) thresholds and to the transient response associated with reaching those thresholds. The ultimate thresholds are a reflection of the ultimate threshold of cortical perception circuits, the signal processing in the signal manipulation stage and the amplifier gain associated with the photodetection circuits of stage 1. This gain is normally dominated by that of the adaptation amplifiers (while active) in the appropriate photodetection channels. However, it is also determined by the amount of active chromophore available in the disk stack of the Outer Segments. This chromophore is present as a surface coating of the protein substrates forming the disks of the Outer Segments. On the other hand, the form of the transient response is determined exclusively by the parameters of the vascular-electrostenolytic processes supporting the electrolytic operation of the adaptation amplifiers while they are in the cutoff condition.

---

[5]Haig, C. Hecht, S. & Patek, A. (1938) Vitamin A and rod-cone dark adaptation in cirrhosis of the liver. Science, vol. 87, June 10, pp.534-536

Vitamin A plays a distinctly different role in these two processes. In the first case, it plays a principle role as a chromogen used to form the actual chromophores, the Rhodonines. In the second case, it plays a critical but less direct role as an enzyme facilitating the operation of the vascular-electrostenolytic process of providing electrical power to the adaptation amplifiers specifically but also other neurons of the visual system.

First, depravation of vitamin A resulted in failure of the new disks, produced at a rate of one per hour, and with a life expectancy based on disk transport velocity within the IPM of 7 days, to become fully active on schedule. The depravation of vitamin A clearly reduced the level of the visual chromophores, essentially as a group, available within the IPM to activate the disks. The stored supplies of vitamin A and/or associated retinoids and the diffusion time constants involved insured that the subjects did not go totally blind within the test period. However, their visual thresholds were rising steadily, by as much as a factor of 100 in 35 days, in accordance with their data and similar data from Wald discussed in **Section XXX**.

Second, the intensive vitamin therapy provided to the pathological subject demonstrated that both the visual thresholds, related to vitamin A consumption, and the damping coefficient of the vascular-electrostenolytic process, related to the enzymatic function of vitamin A, were improved. This latter effect was reflected in the change in temporal frequency of the sinusoidal component of the damped sinusoid of dark adaptation. This change reflected the impact of vitamin A acting as an enzyme in cellular growth and maintenance.

Hecht and Mandelbaum attempted short experiments to determine whether intensive vitamin A therapy would improve the thresholds of healthy individuals, without success. The regulatory functions of the body clearly controlled the negative outcome of these experiments.

17.5.1.1.2 Review of more recent work

Whereas it has become *de rigueur* to explain the dark adaptation portion of the adaptation function in terms of rods and cones, the information provided by Rubin & Walls with regard to achromats is very interesting[6]. They showed that a group of total achromats (they did not recognize or define subgroups for typical and atypical achromats) exhibited a typical dark adaptation function including the two distinct regions normally assigned to rods and cones. They finally arrived at an explanation for this in terms of a retina of all blue sensitive cones “able to show” in a dark adaptation curve but “unable to show” in any other aspect of vision. This type of cone could not be found described anywhere else in the literature! The pattern ERG experiment (see discussion above of Dacey) is particularly awkward from the experiment design perspective, especially if broad band luminants are used.

In 1965, Glezer asserted the following, “Of late, the classical views on the mechanism of visual adaptation have undergone considerable modification. Thus it has been shown that during adaptation, nervous influences, both spatial and temporal should be taken into account, as well as changes invisual pigment concentration.” His figure 6 provides good, but not sufficiently fine, data on the dark adaptation process for one subject free of the conventional two-exponentials interpretation. With measurements out to 30 minutes, the “exposine” form of the function defined in this work is clearly evident.

In the 1970's, Spillmann and associates provided threshold luminance information, under both steady state and transient conditions that separated the chromatic and achromatic regimes. Correlating this information with the work of Hecht and associates leads to interesting observations about the performance of the eye and possible new avenues of experimentation. This correlation will be the subject of **Section XXX**. Kelly and associates contributed considerable data concerning temporal frequency response using flicker techniques during the 1970's (See above reference). Hess and associates provided data during the 1990's.[7] This recent work has surfaced the multiple modalities at work in the visual system. Although staying with the Duplex Theory, their work found “at least two different types of temporal signals mediated by rod photoreceptors in the mammalian retina.” They also found that there were significant difference in temporal response as a function of the illumination regime. One of their conclusions was that: “Our results suggest that rod temporal vision is subserved by three temporal channels at all light levels, . . .” The tests were all psychophysical and employed a P4 phosphor screen passed through a green (Wratten #58) filter. This source-filter combination has only a limited similarity to the scotopic visibility function and excites the M-channel chromophore preferentially. The Wratten #58 filter has a spectral transmission almost

---

[6]Rubin, M. & Walls, G. (1969) Fundamentals of visual science. Springfield, Ill: Charles C. Thomas pp. 314-318

[7]Hess, R. Waugh, S. & Nordby, K. (1996) Rod temporal channels Vision Res. vol. 36, no. 4, pp. 613-619

identical to the M-channel chromophore, peak ~523 nm., λ_s = 505, λ_l = 565 nm. and is narrower than the standard scotopic visibility function. They were more careful than earlier investigaters in regard to radiometry. They measured the P4 phosphor with a photometer and then measured the source-filter combination with a tele-spectro-radiometer. Their results were quoted in terms of scotopic trolands. They employed natural pupils and measured them. They employed a "total and complete achromat" in their experiments. His characteristics will be discussed in **Section 18.6.2.**

17.5.1.1.3 Recent chromatic flicker tests

By rearranging and reinterpreting the results of experiments such as those designed by Dacey[8] and Kelly & associates[9], it is possible to uniquely determine whether a given psychophysical experiment is interrogating a single chromophoric channel (a nearly impossible feat in the absence of specific chromatic adaptation techniques) or is interrogating two channels equally. He used a two color checkerboard in which the colors could be alternated as a method of determining the spatial frequency response of an eye. The choice of colors was not based on the chromophoric sensitivity of the photoreceptors. Because of the difference in signal manipulation between the luminance and chrominance channels, it is necessary to understand what chromophoric channels were interrogated and to what extent. Otherwise, the change in brightness becomes a hidden variable in experiments designed to detect chromatic differences, and vice versa. Experiments of this type frequently report a notch in the spatial frequency response of the visual channel. This notch is an artifact in the perception process due to the design of the experiment. For certain spectral distributions of the "colors" used, there is no or limited perceived response at specific spatial frequencies when they are alternated. The exact location of this notch in spatial frequency space has been elusive among different experimenters because of the asymmetric processing by the signal projection stage of vision. The perceived notch is due to a constant net signal in the luminance channel and a constant net signal in the chrominance channel. The older work of Kelly & van Norren explores this situation in more detail without explicitly recognizing the low frequency rolloff in the photosensitive stage of the visual system near 0.1 Hz due to the adaptation amplifiers. They select a frequency of 5 Hz as the boundary between a "chromatic flicker" component and a "brightness flicker" component. By recognizing the existence of a 0.1 Hz pole in the adaptation amplifiers, the rolloff in performance (20 dB, a factor of ten in amplitude, per decade) below 0.1 Hz is recognized immediately as due to that pole (in contrast to some of their more truncated figures that imply a fixed modulation threshold at frequencies below 1 Hz). This rolloff is present in all photosensing channels. It is not related to rods or cones. It is a feature of each adaptation amplifier. Many tests aimed at determining the spatial frequency performance of the eye, generally on axis, do not fully recognize the importance of the properties of the temporal frequency response of the visual system. This subject area will be addressed briefly in **Section 17.8**.

Stockman, MacLeod & Lebrun have provided flicker data focused on the blue photoreceptors that separated the high bandwidth luminance channel signals from the lower bandwidth chrominance channel signals[10].

17.5.1.1.4 Preliminary conclusions from combining theory and experiment

With an adequate model available, many of the conflicting results in the literature can be placed into a consistent context. The basic frequency response of the animal eye are determined by the photoexcitation/de-excitation process within the outer segment of each photoreceptor cell. The temporal characteristics of these processes can be interpreted in terms of transient or frequency terms as the case demands. Following photodetection, all of the signal processing circuits of the visual system prior to the circuits within the brain are all of wider bandwidth than the signal applied to them. The complication, however, is with the signal differencing circuits. These circuits are associated with both the chrominance and the appearance signaling channels. They are both chromatically selective and spatially selective. The result is that the transfer function of the animal as envisioned and widely used by most experimenters in this area, and presented on page 559 of Wyszecki & Stiles is inappropriate!! *The Principle of Superposition (additivity) clearly does not apply to a circuit containing a hidden, or unrecognized, selective subtraction circuit*. This principle is normally used with simple three terminal networks that are known to be linear. It can seldom be applied to a multi-terminal, multi-path, nonlinear network with the complexity of the visual system. An exception is the luminance channel only under small signal conditions.

---

[8]Dacey, XXX

[9]Kelly, D. van Norren, D. (1977) Two-band model of heterochromatic flicker J. Opt. Soc. Am. vol. 67, pp. 1081-1091, *some material also in Wyszecki & Stiles, pg. 565-568*

[10]Stockman, A. MacLeod, D. & Lebrun, S. (1993) Faster than the eye can see: blue cones respond to rapid flicker *J Opt Soc Am A* vol 10(6), pp 1396-1402

This work is consistent with the data of Hess and associates. However, it is not consistent with the Duplicity Theory or their use of the term “three temporal channels” in rod temporal vision. The multiple features they observed are all features appearing in the visual response due to the vascular-electrostenolytic processes supporting the adaptation amplifier of the photoreceptor cells, regardless of their chromatic sensitivity.

17.5.1.2 Foundation from this work

Both the luminance and chrominance channels exhibit a temporal response that is illumination level dependent. By expanding the block diagram of the visual process considerably in this work, it has become possible to delineate the important temporal characteristics of the visual system of animals, with particular emphasis on human. The result can be stated briefly. The visual system of human:

+ is highly non-linear,

+ involves asymmetrical time constants,

+ involves a variable time delay that is frequently confused with a simple RC time constant,

+ is highly dependent on the diffusion characteristics of the vascular bed supporting the Outer Segments of the photoreceptor cells (separate from the supply for the remainder of the cell),

+ and uses asymmetrical encoding techniques in the chrominance channels that results in a variable delay with regard to color perception.

If the instrumentation is not carefully designed, the spectrum of the adapting and test luminants can play a major role in corrupting the data. This problem is aggravated by the variable gain of the various chromophoric photodetection channels in the retina.

In the following discussion, all of the circuit elements in the retina are assumed to be temporally very broadband except for those detailed below. This makes it possible to concentrate on the elements that actually determine the performance characteristics of the eye in **Section 17.6.** The initial discussion will treat the subject from the perspective of transient performance. Later, the frequency performance and the flicker performance will be addressed. These characteristics can be most easily discussed if a broad spectral band square pulse of light is applied to the chromophore of the channel shown.

Figure 17.5.1-2 summarizes the features of the eye that determine its overall temporal performance, assuming the eye lid is open. The figure is a simplified circuit diagram only concerned with temporal performance. This figure is divided into three principle portions:

the significant circuit elements found in the Outer Segment,

the significant circuit elements (shown in lumped form) found in the dendrites of the photoreceptor cell,

the significant circuit elements of the coding and decoding function of the projection neurons.

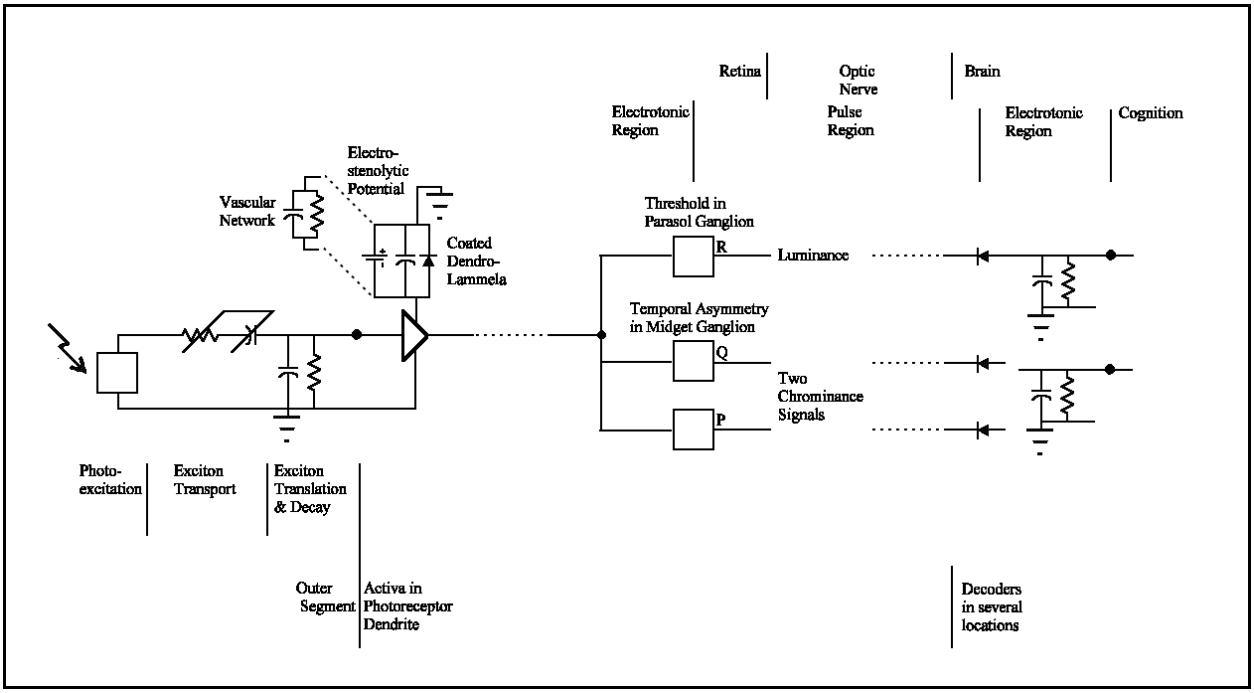

Figure 17.5.1-2 The principle time constants of the eye presented in a idealized composite single channel circuit diagram. See text.

17.5.1.2.1 Critical circuits in the photodetection stage

There are three major and a few minor temporal factors common to both the perceived brightness and the perceived color of an image. These factors affect all of the photoexcitation channels of the animal.

The actual photoexcitation process (the creation of excitons) occurs so quickly that it does not affect the performance of the eye. However, the transport delay associated with those excitons moving to their site of de-excitation (shown diagrammatically by a ganged RC circuit) is frequently a major factor in performance. This time delay is illumination level dependent.

The two other primary temporal factors are related to the performance of the adaptation amplifiers. These amplifiers are highly non-linear and their time constants are asymmetric. The most recognizable time constant of the adaptation amplifier is that related to the restoration of the electrostenolytic voltage across the dendrolemma of the photoreceptor cell. This appears to involve linear vascular activity that can be modeled by a multistage linear RC circuit. In the simplified figure, it is shown as a single RC circuit for convenience.

The R in the vascular equivalent circuit is much larger than the effective output resistance of the dendritic Activa. When the Activa is passing current, the current discharges the capacitor in the lamella very quickly. This lowers the voltage on the Activa collector terminal very quickly and changes the gain of the amplifier dramatically. Because of these two different activities, the adaptation amplifier exhibits significantly different on-transient and off-transient time constants.

17.5.1.2.2 Critical circuits in the signal projection stage

There can be several stages of signal processing between the adaptation amplifier and the ganglion cells. These stages do not affect the transient characteristics of the eye. However, they do determine the polarity of the chrominance signal applied to the midget ganglion cells.

The midget ganglion cells perform the signal encoding function in the chrominance channels by varying the pulse to pulse interval of an otherwise quiescent oscillator in response to a scalar signal. Since the quiescent frequency is low, this can have an impact on the apparent time constant of the signal decoded in the brain. These cells accept a bipolar signal from the signal processing neurons. With a nominal frequency of 30 Hz, electrotonic signals that

shorten the pulse to pulse interval can be recognized by the decoding function more quickly than can signals that lengthen the interval. This involves a portion of Shannon's work that is not normally discussed in elementary texts. The result is that those signals that lengthen the interval exhibit a delay in their cognition. It is interesting that the more saturated the color in the scene, the slower the decoding circuit is to respond. This is a key consideration in the many reported flicker phenomena. It appears that the S- and L-channels cause a lengthening in the interval compared to the M-channel. Because of this characteristic, the NTSC assigned a narrower transmission channel to the signal related to these channels in the standards for color television.

[edit with above paragraph]
The chrominance channels exhibit another temporal effect that has not been discussed or properly modeled in the past. The midget ganglion cells are biased so that they generate a continuous pulse stream at a nominal 30 pulses per second. With higher levels of excitation, these cells can increase this nominal rate to at least 70 pulses per second. Upon reduced levels of excitation, the pulse rate is reduced significantly. However, as the rate approaches zero pulses per second, the information transfer rate becomes very low or non-existent. This situation would suggest that the rate of color perception, in the human at least, may be related to the polarity of the chrominance signals applied to the midget ganglion cells. The data is sparse in this area. However, it appears this feature accounts for the relatively slow perception of changes in the saturated blue and saturated red regions of the chromaticity diagram. Zworykin & Morton[11], working with tristimulus values to define the NTSC color television system, showed that the relative passband of the blue channel is only about 17% of that of the green channel. The red channel passband is only about 40% of that of the green channel. These numbers apply to highly saturated colors. These finding would tend to say that signals in the chrominance channels of the visual system affect the midget ganglion cells differently as suggested above. It appears that an increase in the S-channel signal amplitude causes the midget ganglion cell of the P-channel to lower its pulse frequency. Similarly, an increase in the L-channel signal appears to cause the midget ganglion cell of the Q-channel to lower its pulse frequency. In both cases, the pulse frequencies are increased in the presence of higher levels of M-channel illumination.

The specific characteristics of the actual decoding circuits in the brain are beyond the scope of this work. They are known to occur in at least two locations, the Pretectum and the LGN. The circuits may be different in these two locations. In the figure, simple decoding circuits are shown that can be easily implemented by either passive components or a simple neuron containing one Activa. There is probably an interaction between the decoding circuits of the two chrominance channels. There is clearly an important temporal relationship between the recognition of an initial pulse in the decoder of the luminance channel and the availability of chroma information in the chrominance decoders. It appears that the luminance channel decoder(s) is required to provide an alarm signal as well as an amplitude signal related to the scene. The important fact illustrated by these simple circuits is that the output signal is only a coarse simile of the original analog signal. The summation requires a finite number of pulses to arrive in order to provide a faithful (high accuracy) output signal.

The luminance channel employs a monopolar encoding scheme. The parasol ganglion cells do not create action potentials except when they are excited by a signal above a certain threshold. This threshold is quite low and is only significant in the scotopic region of illumination. At higher illumination levels, the pulse to pulse interval is reduced until the illumination level reaches the bottom of the photopic level. Above that level, the pulse to pulse interval only changes due to changes in signal amplitude within the overall instantaneous dynamic range of the eye, about 100:1. This result is recognized in the literature although its cause is presented differently. Gegenfurtner, et. al. have recently discussed the variation in the response of the luminance channel in the popular press[12]. They noted that as "the light goes down, the world *may appear* to slow" to the human observer. This phenomena is actually due to two processes. The delay assoiciated with transduction and the limited ability of the decoder in the brain to provide a timely signal for cognition. It can provide an initial pulse very quickly for alarm purposes. However, it requires a longer interval, measured in multiples of about 14 milliseconds (reciprocal of a nominal 70 Hertz peak frequency) to provide a meaningful electrotonic signal.

----[**remnants below here take out or relocate]**

This time delay is often modeled differently in the literature. It is either modeled as a simple time constant or as a series of time constants related to a series of individual filter elements. The illumination level dependent feature of

---

[11]Zworykin, V. & Morton, G. (1954) Television, 2nd ed. NY: John Wiley & Sons. pp. 817-825
[12]Gegenfurtner, K. & XXX (1999) Nature, April 8, 1999, pp. XXX

this time delay makes the typical experiment based on a simple constant parameter filter difficult to confirm by repetition.

Because the amplitude transfer function of the adaptation amplifier involves an exponential term of the fifth or sixth power that is time dependent, many investigators have attempted to model the overall passband of the HVS using as many as 12 cascaded stages of simple RC filters, occasionally with one or more variable resistance values. More careful experiment design will illustrate that this multi-stage filter approach is inappropriate.

17.5.1.2.2 Critical circuits in the signal manipulation stage

It is also difficult to quantify the overall transient response of the human eye because of the wide range of parametric values involved. These parameters even involve the Stiles-Crawford effect when large field measurements are made at off-axis locations or with variable pupil sizes (**Section 17.3.7**). Similarly, when off-axis measurements are involved, it is not appropriate to assume first order, Gaussian, optics in experiment design.

17.5.1.3 Principle sources of data

As indicated above, Hecht and his associates have provided a majority of the data in the literature, including the only data based on a large enough group of subjects to derive statistically relevant material. Other investigators have usually used less than five subjects. The work of Hecht is also the most comprehensive in terms of experimental design and parameters explored. Concentrating on the material from Hecht for a moment, it is clear that the temporal characteristics of the eye vary considerably with location in object space, the size of the test object, and frequently the size of the adaptation object. This is primarily due to the imaging qualities of the physiological optics, the variation in population density of a given chromophoric photoreceptor over the mosaic, the variation in capture cross section for light of a given wavelength over the mosaic, and the hydraulic performance of the vascular matrix, supporting the Outer Segments of the photoreceptor cells, as a function of mosaic location. The characteristics of the vascular matrix will be seen to be extremely important in the performance of the human eye where different size adaptation and test fields are employed. This is true for both edge stimuli and area stimuli.

17.5.1.3.1 Composite adaptation performance

Crawford has provided an overall graph of the temporal response of vision to a repetitive square pulse[13]. The published version appears to have discounted the delay internal to the system. This was due to plotting the waveforms so as to coincide near the peak of their rise. Because of the approach taken, the rectangle representing the stimulus should be different for each pulse train. As a result, the graph shows either a precognition of the events or some other form of anticipation. Based on this theory, the peaks in the responses should exhibit a variation due to the delay term in the P/D equation. The responses to higher intensity stimuli should begin earlier and rise more steeply than responses to lower intensity stimuli. Using this approach, the start of a single pulse would have been taken as the reference. The delays relative to this starting time would have indicated the delay in the system. This delay would have consisted of a fixed delay and a variable delay as a function of the intensity of stimulation. Brown & Mueller (1965) and Uttal (1981) have reproduced a version of Crawford's figure but have not reproduced the putative repetitive square pulse.

Using the proposed reinterpretation, Crawfords data would agree with that of Poot, Snippe & van Hateren discussed below.

17.5.1.3.2 Dark adaptation parameters

[This is probably junk replace with discussion including 400,000 Tr frame from Fulton Hecht 1937 fg 5.ai. Stress systematic trends in data points] [xxx see figure 16.4.2-8]
A valuable starting point appears to be **Figure 17.5.1-3. [Drop right hand frame from figure]** This widely distributed figure from Hecht, Haig and Wald has led to some highly misleading statements in the literature. Only one subject was involved and he was quite likely a pathological case. According to this data, the subject had a

---

[13]Crawford, B. (1947) Visual adaptation in relation to brief conditioning stimuli. P. Roy. Soc. vol 134B, pp 283-302 *reproduced* in Boynton, R. (1979) Human Color Vision, NY: Holt Rinehart & Winston, pg 184

object field threshold sensitivity 50:1 lower at the point of fixation than he did at 2 ½ degrees from the fixation point. This author has found his similar performance was less than a factor of two or one stellar magnitude. This loss in sensitivity could was clearly related to the off-axis performance of my lens system. I achieved higher resolution using one eye when imaging the stars along the optical axis of the eye, about 2 ½ degrees from the normal fixation point.

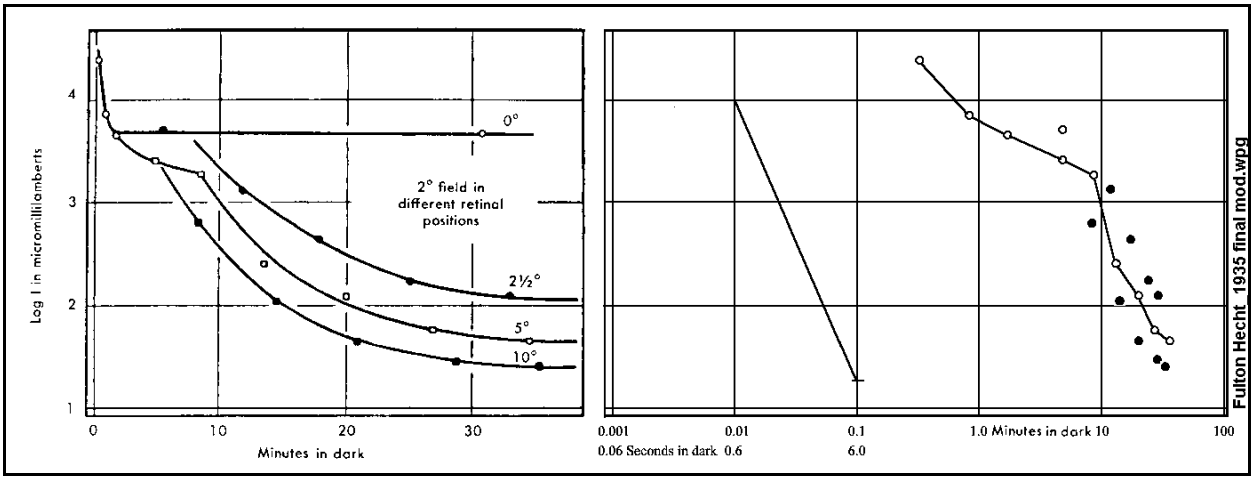

Figure 17.5.1-3 An extension of the classic dark adaptation curve of Hecht, Haig & Wald to demonstrate the presence of only two time constants related to this figure. An exception is the foveal position that only exhibits one time constant. See text.

A particularly good data set is provided by van den Brink for several subjects[14]. Although adhering to the conventional wisdom, he does show the shift of the break point in the dark adaptation characteristic to longer times with higher exposures, generally going beyond his time scale at high illumination levels. The model presented in this work provides a detailed description of the cause of this phenomena.

Stevens & Stevens also provide useful data and an interesting test configuration[15]. They deviated from the conventional wisdom by suggesting that adaptation involved a power law relationship instead of an exponential relationship. They draw this conclusion based on attempts at curve fitting rather than based on a physical model. This work will show that the actual relationship is due to a cascade of mechanisms that can be described via a third order differential equation. The solution to that equation is the product of a sinusoidal function and an exponential function.

17.5.1.3.3 Light adaptation parameters

Figure 17.5.1-4 from Poot, Snippe & van Hateren provides the most recent data on light adaptation.

17.5.1.3.4 Noise data

Copenhagen, Ashmore & Schnapf have provided data on the noise performance of the turtle visual system as a function of adaptation[16]. Although using a model not supported here, Leibrock, Reuter & Lamb have also provided good noise data during dark adaptation[17].

---

[14]Van den Brink, G. (1962) Subjective brightness during dark adaptation. Vision Res. vol. 2, pp 495-502
[15]Stevens, J. & Stevens, S. (1963) Brightness function: Effects of adaptation. J. Opt. Soc. Am. vol. 53, no. 3, pp 375-385
[16]Copenhagen, D. Ashmore, J. & Schnapf, J. (1983) Kinetics of synaptic transmission from photoreceptors to horizontal and bipolar cells in turtle retina, *Vision Res*. vol. 23, pp 363-369
[17]Leibrock, C. Reuter, T. & Lamb, T. (1998) Molecular basis of dark adaptation in rod photoreceptors. *Eye*, vol. 12, pp 511-520

Hay & Chesters has provided an analysis of the noise environment of vision which is sound but needs to be extended[18]. It does not consider the possibility of a limit on the dynamic range of the system. They define the threshold level appropriately based on the effective photon noise (photon noise times an absorption efficiency). This definition is appropriate for the UV–, S– & M–channels without further detailing. For the L–channel, the square law process involved introduces a mathematical complication. They define a suprathreshold state where the luminance is higher and there is excess noise relative to the photon noise and absorption efficiency. Their study concentrates on the change in noise level with the diameter of the illuminated spot (ostensibly being correlated within the visual system). Changes in illumination level are only treated parametrically. They do provide an interesting plot of visual acuity versus luminance. with a shoulder near 1– 2 minutes of arc (depending on eccentricity) at minus one log luminance in millilamberts.

17.5.1.3.5 XXX parameters

It is important to explicitly specify the state of the iris in any experimental undertaking. In general, it is best to use an artificial iris of nominally two mm. diameter if suitable stabilization equipment is available to insure this artificial iris remains centered on the line of fixation. If it does not, vignetting of the optical bundle entering the eye will result. This vignetting will introduce additional uncontrolled variables. If the real iris is used, its state of opening must be described. If sufficient time has not passed, the changing diameter of the iris may be a factor in any measurements.

17.5.2 Transient characteristics of the photodetection system

There are two important and distinct temporal impacts on the photoreceptors of the human eye in response to illumination. One, the in-line characteristic, is directly associated with the individual cell and its support by the metabolic system. The second is the cross-talk characteristic. This is the impact on one photoreceptor cell due to the demands of these other cells immersed in the same diffusion bed of the metabolic system. These transient characteristics are not normally measured directly. Instead, the overall visual system transient performance is measured. By assuming the perceived threshold is essentially a constant of the cortical system, it is possible to determine the perceived amplification as a function of time in the system and compare this perceived amplification to the theoretical amplification proposed here. The functional relationship between the voltage transient associated with the collector of the amplifier and the perceived amplification is precisely the exponential amplification of the adaptation amplifier. Because of this relationship, the general mathematical form of the dark adaptation characteristic of human vision will be shown to be an “expanded exponential sinusoid.” Under special cases, this general form reduces to a simple “expanded exponential” or to an “expanded and extended exponential.” These special cases will be developed below.

17.5.2.1 In-line characteristics

If the total adaptation characteristic of the eye is examined with respect to the location where the stimulus was applied to the retina, considerable information can be gleaned from the available literature. By reviewing the data collected and summarized in this work, the complete adaptation characteristic can be defined conceptually as in **Figure 17.5.2-1** for long pulse illumination. The figure is drawn with a diagonal to separate the graphic notation used on the left, and associated with the light adaptation portion of the characteristic, and that used on the right to describe the dark adaptation portion of the characteristic. The time of illumination is shown at the bottom. Prior to the diagonal the time is in milliseconds (the peaks of the three waveforms usually occuring after less than 10 milliseconds). After the diagonal, the time scale is in minutes (the time between sinusoidal crossings of the exponential of the Class B waveform is typically 8-11 minutes). On the left, the solid line represents the temporal response of the P/D process within the chromophores. The shape shown is the nominal current response associated with this process. Any saturation in this waveform, labeled A, due to inversion of the exciton population relative to the n-electron population is ignored at this level of detail. The delay is the nominal case associated with this Class A waveform. The Class B waveform describes the emitter current of the adaptation amplifier and shows the excellent but limited ability of this amplifier to track the Class A waveform faithfully. During the rising portion of the waveform, this inability is associated with the capacitance C_A and the finite current capability of the Activa within the amplifier. It is also associated with the rapid decrease in the amplification of the circuit as the collector voltage falls only marginally. This accounts for the apparent rounding of the Class B waveform. Under extreme conditions, this waveform may also exhibit an absolute maximum amplitude, that could be described by the term “hard

---

[18]Hay, G. & chesters, M. (1972) Signal-transfer functions in threshold and suprathreshold vision. *J. Opt. Soc. Am. vol*. 62, no. 8, pp 990-998

limiting." This limiting occurs if the collector voltage is actually reduced to the level of the base voltage. Any further reduction is not compatible with transistor action. The Class D waveform, representing the output voltage at the pedicel of the photoreceptor. This waveform attempts to faithfully reproduce all of the features of the Class B waveform while performing a logarithmic current to voltage transformation. It shows the characteristic saturation in the amplitude of this waveform due to this logarithmic relationship at this node. Exaggerated delays are shown in the region of the peaks in the B & D waveforms for clarity. Following the peaks in these waveforms, all three waveforms return asymptotically to the steady state value associated with the steady value of the illumination. Note: the Class C waveform associated with the total current passing between the dendroplasm of the photoreceptor Outer Segment and the IPM is not a waveform directly involved in signaling and is not shown in this figure.

Following cessation of illumination, there is a slight delay before the current associated with the Class A waveform goes to zero exponentially. The magnitude of this delay is determined by the average illumination level during excitation. This time constant of the exponential is very short relative to the other time constants associated with the dark adaptation characteristic, about 1.5 seconds. Only a portion of this Class A waveform is shown by the short straight line falling rapidly toward zero. The primary features of the dark adaptation characteristic are seen in the Class B waveform.

As soon as the current associated with the Class A waveform goes to zero, the current through the adaptation amplifier goes to zero. The output impedance of the Activa associated with the adaptation amplifier becomes nominally infinite. Therefore, the collector potential is now determined by the capacitance C_A and the impedance of the electrostenolytic-vascular network. As shown in **[Figure 16.3.5-8]**, this circuit is complex. In general, it is a n-th order system where n can be as high as three. Fortunately, in non-pathological situations, n is only two and under specific laboratory conditions, it can be effectively one. As a result, it is possible to compute the transient response of the system and determine at least the time constants of the various mathematical terms. It is also possible to determine at least the ratio between some of the conductive impedances and the ratio between some of the capacitive impedances. Conductive and capacitive in this sense refer to both the electrical and the hydraulic properties of the various elements of the vascular-electrostenolytic-electronic system of the adaptation mechanism. These ratios will not be defined here because, as a group, they are highly variable and highly dependent on the experimental design of the experiment used to acquire the test data. This is a fertile area of future laboratory work.

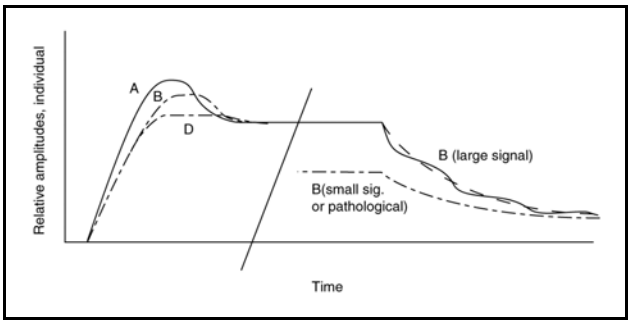

Figure 17.5.2-1 Complete conceptual adaptation characteristic drawn to highlight all of the individual processes involved. The diagonal line separates the line notation. On the left, the principle waveforms are shown. On the right, two different situations involving the Class B waveform is shown under two distinctly different conditions. See text.

The unfortunate aspect of the above network is that in the real case, the voltages on C_2 & C_3 are shared with other photoreceptors. As a result, the transient characteristics of an individual photoreceptor or group of chromatically similar photoreceptors, depends on the state of the surrounding photoreceptors. This situation will be addressed in the next Section.

In the ideal case, the total transfer characteristic of an isolated photoreceptor is seen to exhibit a single significant time delay. This delay can be traced directly to the P/D process. It exhibits two time constants during the rise of the waveform in response to an increase in illumination, and one simple time constant and a complex arrangement that can appear as two additional time constants related to a decrease in illumination. This is not an unusual situation when dealing with electrical circuits under large signal conditions. The complex arrangement depends on the values of the circuit elements. At one extreme, a single short time constant is measured. At the other extreme, a longer time constant is measured. At intermediate values, the circuit is described by the product of an exponential and a sinusoid. Fortunately, under small signal conditions, only a simpler short time constant is measured. This value is only an approximation of the actual value. The actual value can be uniquely determined under impulse excitation conditions. The value of these time constants will be summarized below.

The two time constants related to the transducer have been discussed in detail. The initial signal delay is directly related to the illumination amplitude and is caused by the finite transport velocity of electrons in the excited state of

the liquid crystalline structure of the chromophores. The de-excitation time constant is directly related to the impedance involved in the quantum mechanical transfer of energy from the transducer to the base region of the adaptation amplifier. It is fixed for a given temperature.

The fundamental performance of the adaptation amplifier involves a tradeoff between the signal current generating capability of the Activa in that circuit and the capability of the energy source to maintain the operating potential applied to that Activa while supplying the necessary current. The bioenergetic materials constituting the energy source on the surface of the dendrolemma have a capability of storing a limited amount of charge. This capability is represented by a capacitor in parallel with the energy source. The product of the value of this capacitor and the impedance of the Activa constitutes the pull down phase time constant. The Activa impedance is a direct function of the exciton rate received from the transducer element. Hence, the pull down time constant is relatively short but a distinct function of the illumination level.

As current begins to flow in the collector circuit of the adaptation amplifier, the voltage applied to the collector falls because of the limited amount of bioenergetic material in intimate contact with the dendritic cell outer membrane. This causes diffusion to begin to play a role in re-supplying the bioenergetic material from the IPM. This action causes an additional diffusion process to begin within the IPM itself. This diffusion process eventually impacts the vascular system. However, the impedance of the vascular supply via the optic nerve bundle is low enough that it seldom is a factor in the operation of the human eye. In response to this series of events, the adaptation amplifier establishes a new gain parameter consistent with the steady state capability of the bioenergetic supply. Clearly, there are several time constants associated with this process. However, if any, only the shortest one is ever documented during psychophysical tests. It is labeled the pull down time constant in the following table. Electrophysical tests on animals do document more than one.

Upon the cessation of illumination, the collector impedance of the Activa becomes essentially infinite. Therefore the voltage applied to the collector rises at a rate controlled by the ability of the bioenergy supply to recover through the diffusion processes indicated above.

There is a third time constant related to the vascular system supplying the photodetection function of the photoreceptor cells. Note this portion of the vascular system is not common to the rest of the retina. Only the Outer Segments of the photoreceptor cells are supplied by the choroid arterial system. This time constant is normally not encountered in laboratory testing because only a small portion of the retina is usually subjected to high illumination levels in a given test.

There are two significant practical cases where the vascular supply and the related time constants come into play. One is so-called tunnel vision when the vascular supply becomes inadequate due to fatigue. By whatever mechanism, the vascular supply to the non-foveal portion of the retina is restricted in order to maintain the animals vision in the critical foveal area as long as possible before total blindness occurs. The second is the case of snow blindness. In snow blindness, the high level of illumination applied to the entire retina causes the consumption of all of the available bioenergetic materials at a rate higher than the vascular system of the eye can supply. Complete recovery from snow blindness may require hours.

Upon a reduction in the illumination applied to a given photoreceptor cell, the signal current is reduced and the demand on the energy supply is reduced. The energy supply attempts to re-establish the quiescent operating voltage to the adaptation amplifier. This activity requires the importation of bioenergetic materials as described above. By mapping the recovery time constants of the eye with respect to location in the retina, the health of the choroid arterial system, normally invisible to the clinician, can be ascertained.

A paramount fact related to these time constants is that none of them has ever been related directly to any monochromatic signal channel in the eye. These time constants apply to all of the photoreceptors in a given region of the retina under the same state of adaptation. The data does not support a rod/cone dichotomy in the retina related to the temporal characteristics of the eye.

When recording an ERG, it is possible for it to display an early and late ERP, both Class C waveforms, displayed as a small early version followed by a larger version of an a-wave or as a wrinkle in the leading edge of the a-wave. This occurs when the individual chromatic receptor channels are in different states of adaptation. The same effect is also seen frequently in LERG's where operation under a "dim red light" has led to adaptation of the L-channel. This causes the L-channel Class C waveform to be smaller and occur earlier than that of the other channels.

17.5.2.1.1 Evaluation of the P/D equation parameters

Fulton and Rushton[19] have sought to characterize the transient performance of the human eye using graphical means under impulse conditions. They used a template, developed in 1970 by Rushton's group and labeled H_2 curves, that appeared to define a graph of the logarithm of the slope of the leading edge of the P/D equation transient versus the logarithm of the impulse under scotopic conditions. This graph and template exhibited a constant slope from less than 0 to over 2.0 log td-sec based on an unspecified 500 watt light source with suitable filters, and full field Ganzfeld illumination. Their discussion of the state of adaptation prior to the dark adaptation experiment is meager. The slope of such a curve is the absorption coefficient, σ, according to this theory (this is not the "semi-saturation value" they defined for sigma in their paper). The constant slope was equal to 76% under these conditions for both a "dark background" and a background established by a long wavelength filter (λ>630 nm.). This is a very high absorption coefficient relative to photographic film and completely compatible with the value expected by this work. It approaches the value of the best man-made silicon or gallium-arsenide based sensors.

They performed a similar analysis on what they took to be the b-wave. They used a different definition of the starting point of the b-wave than used in this work and those values will not be discussed in detail here. They found the slope of the b-wave similar to that of the a-wave. This work would interpret such a finding as confirmation of the unity gain of the bipolar and/or lateral neurons of the signal manipulation stage.

In the same papers, they evaluated the same parameter as a function of log backgrounds. Their result suggested that the slope of this relationship was 0.4. If this value were 0.5, it would be completely compatible with the expected value for a stochastic noise limited process where the limit was photon noise. Values lower than 0.5 and approaching zero would be expected as the light level was further reduced. They also noted that the absolute threshold of the dark adaptation characteristic was quite stable in their experiments. Although they took values at lower impulse levels that applied to both graphs, they chose not to plot them. These data points show the slope and noise performance decreasing at lower impulse levels as expected by the P/D equation. At levels considerably above the 2.0 log td-sec value, the adaptation amplifiers should begin lowering the overall circuit gain. That would result in lower overall system sensitivity although the chromophores of the Outer Segment would continue to operate at essentially the same high absorption coefficient.

In an associated paper, they explored the same parameters in the mudpuppy held in tanks at 4 C before dissection, and found similar values. This appears reasonable because the absorption coefficient is not temperature sensitive, although some of the other parameters in the P/D equation are (the delay as an example).

17.5.2.2 Cross-talk characteristics

Mach bands have been widely studied psychophysically because of their obvious presence in normal vision. They constitute the perceived change in brightness associated with the boundary between two large uniformly illuminate fields. They have not been studied in depth from the perspective of the functional characteristics of the eye. The literature has generally associated this phenomena with circuit coupling within the neurons of the retina. Based on the model used here, a simpler explanation for them is available. A sharp edge between two moderately illuminated fields (a moderate contrast situation) is normally perceived as rounded due to the limited frequency response of the photodetection process. However, as the contrast is increased, a band is perceived on each side of the boundary accentuating the contrast in those two areas. There has been no change in the frequency response of the signaling neurons and there has been no significant change in the transducer chromophores. However, there has been a change related to the adaptation amplifier.

[define scale A in pix xxx]
Ignoring the spatial frequency limitation of the eye for the moment, **Figure 17.5.2-2** illustrates how the edge of a large dark field normally appears even darker. On the opposite side of the edge, the nearby light field appears lighter than it actually is. The upper panel shows the incident illumination level. The middle pane can be interpreted as the density of the available bioenergy supply or as the gain of the adaption amplifiers as a function of their position.

[19]Fulton, A. & Rushton, W. (1978) The human rod ERG: correlation with psuchophysical responses in light and dark adaptation. Vision Res. vol. 18, pp. 793-800

It should be obvious that if a large group of photoreceptors are highly illuminated on one side of a line, the cells near the line will have access to the bioenergetic sources immediately across the line. These cells will be able to maintain a higher level of gain in their adaptation amplifiers than cells more distant from the line. The subject will report that the areas near the line appear brighter than the areas farther removed from the line. Conversely, cells near the edge in the lesser illuminated area will see their bioenergetic supplies depleted more than cells more distant from the edge. The cells near the edge will exhibit a lower adaptation amplifier gain than those farther from the line. Consequently, the subject will report that the areas near the line appear darker than the interior areas. This is clearly a case of spatial coupling within the diffusion beds supplying the energy to the photoreceptors via the choroid artery . If careful tests were performed, it would be possible to demonstrate the difference in the recovery process between the cells near the line and those more distant.

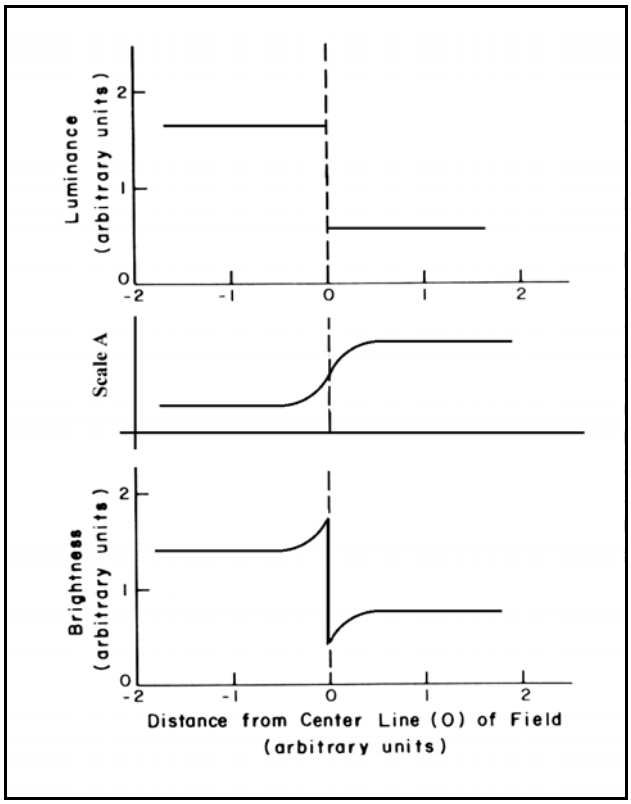

Figure 17.5.2-2 The appearance of Mach bands in relation to a high contrast boundary between two large areas. A light (A) and dark (B) Mach band appears near the points where the luminance of the border changes abruptly. From Wyszecki & Stiles (1982).

Note that as the contrast of the illuminated scene is reduced, the difference in demand on the bioenergy supply drops and the difference in adaptation amplifier gain drops. The bending in the perceived illumination levels is reduced and the Mach bands begin to disappear. When the spatial frequency response of the eye is considered, the composite response is similar to the lower pane, however, the vertical line in that pane becomes a symmetrical arc with a chord that slopes down to the right.

Wyszecki & Stiles[20] make a statement that is in conformance with the above analysis: "The experimental evidence of particular interest to color vision is that Mach bands are, in general, not found near chromatic borders when the two juxtaposed fields have no luminance variation but differ only in chromaticity." A chromatic border, as defined above, is not a border as far as the bioenergetic supply system is concerned. The total input flux per unit area remains the same. The bioenergetic supply must support the demands of the photodetection process that are related to illumination levels. The possible exception would be a border that is carefully matched to the absorption spectrum of the L-channel on one side. In that case and under mesotopic conditions, the square law nature of that channel may place a slightly different demand on the vascular system than on the other side.

The above quotation emphasizes the dominance of the M-channel in luminance channel of normal, and steady state, vision. Besides the above steady state situation, the same underlying process causes significant changes in the transient response of the luminance channel. Because the exponential gain of the adaptation amplifiers is a function of their collector voltage, only small changes in this parameter can have major impact on their performance. A change in the collector voltage of one millivolt is significant. And because of their shared voltage on the equivalent capacitor, C2 and/or C3, the impact on the photoreceptors of one chromatic set by a different chromatic set may be significant. As stated in **Section 16.3.5.2**, this situation greatly complicates the interpretation of laboratory data unless very careful experimental design is employed. This subject will be discussed further in **Section 17.6.1.1.3**.

Figure 17.5.2-3, from Lowry & DePalma, shows one of the few figures of Mach bands in the literature with scales. A more extensive discussion is available in Fiorentini[21].

---

[20]Wyszecki & Stiles, Op. cit. pg. 557

[21]Fiorentini, A. (1973) Mach band phenomena. *In*, Handbook of Sensory Physiology, Vol. VII, No. 4, Jameson, D. & Hurvich, L. *ed.* NY: Springer-Verlag, Chap. 8.

17.5.3 Frequency characteristics of the photodetection system

[xxx frequency response of individual photoreceptor and signaling channels is wider than the variously defined flicker frequencies.]

[xxx see Section 16.4.1 and figure 16.4.1-2]

17.5.3.1 Background

17.5.3.2 XXX

17.5.3.3 XXX

17.5.3.4 XXX

17.5.4 Frequency characteristics of the signal processing system

17.5.5 Frequency characteristics of the signal projection system EMPTY

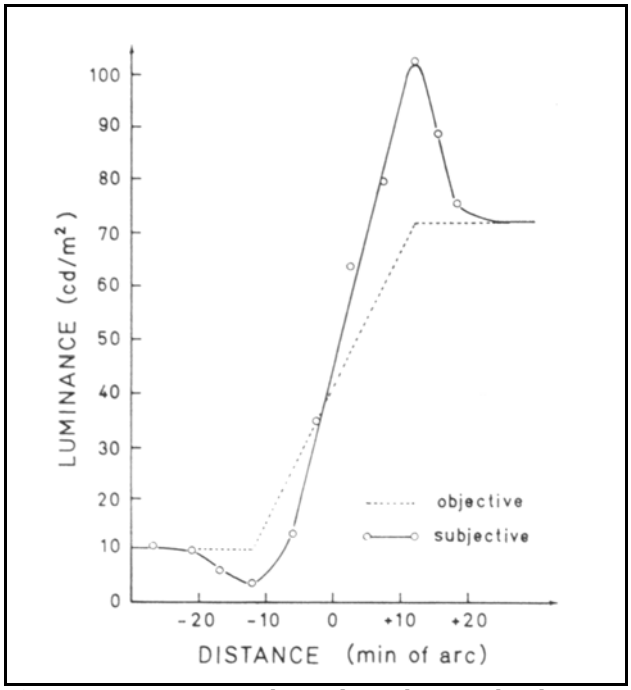

Figure 17.5.2-3 CR Mach Bands. Subjective brightness distribution (open circles) measured across the luminance distribution indicated by the broken line. The characteristics of the source used to produce and the test set used to quantify the luminance distribution were not given. From Lowry & DePalma, 1961.

17.5.6 Time Delay in the visual system EMPTY

There are significant time delays built into the visual system. These delays are found in both the information processing and the servomechanism signal paths. These delays frequently limit the maximum performance of the visual system. The delays are of three main types, delays associated with the tonic signals of the retina (stages 1 & 2), delays associated with the phasic signals of the projections circuits (stage 3), and delays associated with tonic signals within the various feature extraction engines (stage 4). The delays associated with stages 3 and 4 occur in both the information processing channels and the servomechanism channels. This section will provide nominal values for these delays. Because of the variable physical lengths associated with ganglion axons in the retina, the delay associated with these elements will be separated into the delay before reaching the lamina cribosa and the delay associated with the optic nerve.

17.5.6.1 Time delay within the retina

Figure 17.5.6-1 Provides a map for discussing time delay within the retina. Most of the time delays within the retina are due to the slow transport of electrical charge within the electrolytic conduits of the tonic neurons. This transport is largely dependent on the diffusion of charged particles along the conduits in response to relatively small electrical gradients. These gradients are on the order of a few millivolts per hundred microns. The measured velocity of these signals is about 7 mm/sec, but may vary widely. This transport velocity is much slower than the electromagnetic propagation of phasic action potentials along myelinated axons. It is also so slow that the time delay associated with the individual synapse and the internal Activa are negligible. The tonic delays associated with the photoreceptor layer have been developed in **Section 11.1.6** in an introduction to the ERG. They have also been discussed in **Sections 10.4.3.4** and **11.1.8.3**. Those delays will be introduced into the tables below.

The delay associated with the axons of the photoreceptors occur outside the photoreceptor layer. While the length of these axons in the periphery of the retina are relatively short and fixed, those associated with the foveola can be quite long and variable in length. For the periphery, the axon lengths will be taken as 50 microns plus a negligible

variation. For the foveola, the axon lengths can be considerably longer as suggested by Oyster. Lengths at the center of the foveola can be 200 microns or longer as suggested in the figure and shown more clearly in [**Figure 3.2.2-1**].

The delay associated with the bipolar cells is relatively constant. Their length is typically 50 microns and there is no significant delay associated with the Activa or the related synapses. The delay associated with the horizontal and amercine cells is much more variable depending on their level of arborization (and the level of interlinking between lateral cells in the creation of the complete signal to be transmitted over the optic neerve). As a result, the tabular values selected for the lateral cells must contain a much larger variation about the mean. The figure from Oyster would suggest 75 microns or more on average and a variation on the order of 25 microns.

The delay associated with the ganglion cells is complex. In the case of the luminance channels, it consists of a tonic delay associated with its neurite structures, a charging delay associated with the generation of the action potential and a phasic transport delay between the ganglion cell and the lamina cribosa. For the chrominance channels, the computation is somewhat different because the action potentials are generated continuously and the tonic chrominance signals only cause a temporal modulation in the time between the occurrence of these pulses. Therefore, there is no delay associated with the creation of the action potentials.

Not shown in the figure is the length of the ganglion cell axon progressing horizontally within the nerve fiber layer until it reaches the lamina cribosa. This distance is approximately four plus or minus 0.5 millimeters for the signals from the foveola and can reach 18 millimeters for neurons at the extreme periphery of the retina. The travel distance for the signals from the temporal field of vision are considerably less than for the nasal field due to the location of the lamina cribosa. The large variation in the length of these axons with retinal position is used effectively in the LGN's to compute signals associated with stereopsis. Because of the large variation in length of these axons, a feature described as Reyem's Loop in this work, there is a necessity of removing this large variation in time delay following the LGN's. Otherwise, it would be difficult to compute a precise saliency map as a function of time relative to the entire retina. This feature between the LGN's and Area 17 of the cerebral cortex is known as Meyer's Loops. For the signals from the foveola, the variation is much less severe. If compensation is required in these signal paths, it is probably accomplished by appropriate arrangement of the signal axons within the cross-section of the optic nerve.

There is a further complication relative to the phasic portion of the ganglion cell delay. Prior to reaching the lamina cribosa, the axons are generally unmyelinated. This leads to a lower propagation velocity along these segments. Further examination is also required to determine if these long axon segments include Nodes of Ranvier. If they do, an additional regeneration delay must be included in the time delays associated with these signal paths.

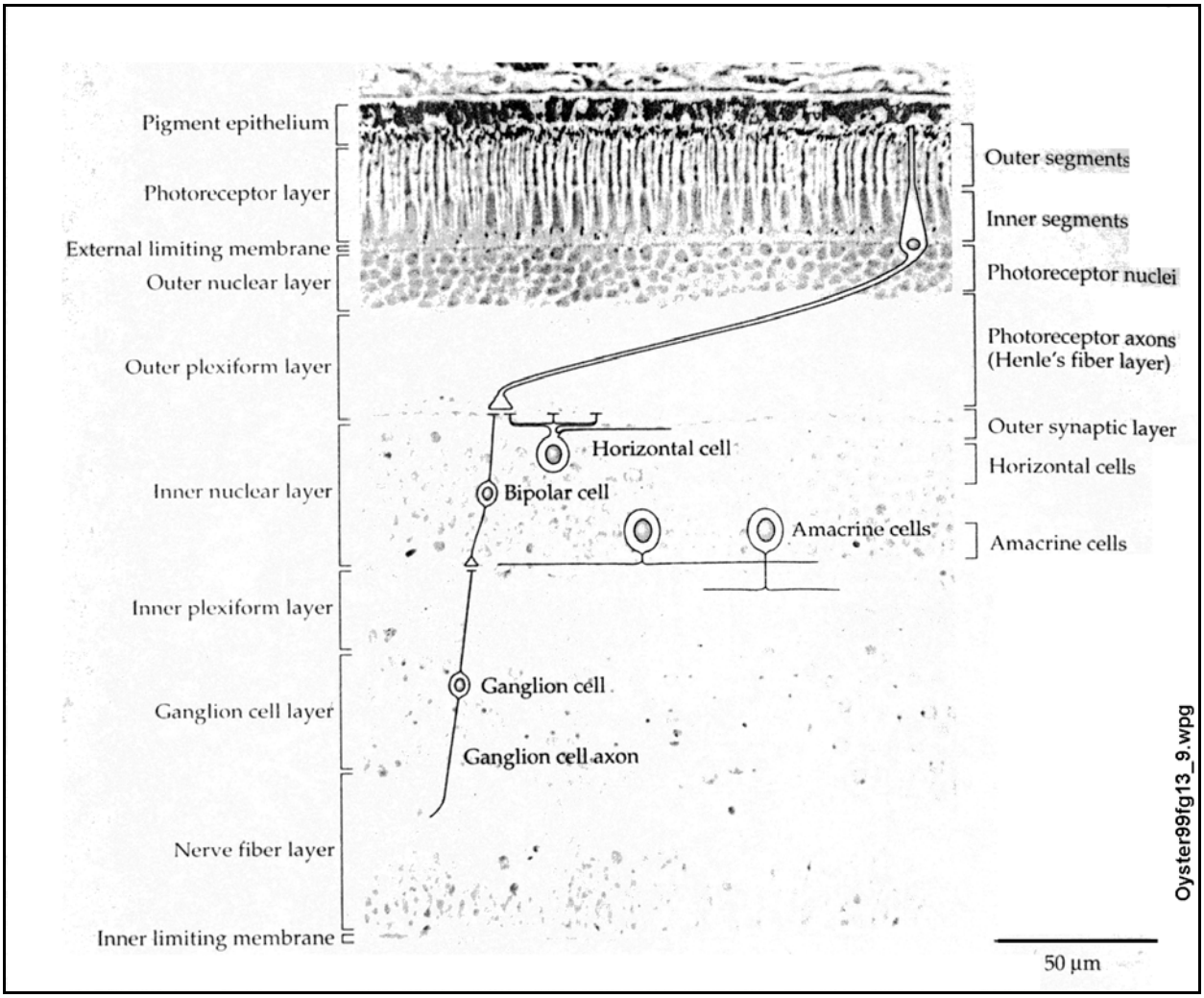

Figure 17.5.6-1 Time Delay in the human retina by path element. From Oyster, 1999.

TABLE 17.5.6-1
TIME DELAYS ENCOUNTERED IN THE RETINA*

NEURAL SEGMENT	NOMINAL LENGTH	VARIATION	TIME DELAY	VARIATION
	(in microns except as noted)		(milliseconds)	
Within the photoreceptors (up to the distr. amp. of inner segm.)	25	4		
Photoreceptor Axons				
Fovea	200		30	
Periphery	50		7	
Bipolar Cells	50		7	
Lateral Cells	75	25	11	4
Typical cumulative time delays			~40	
Ganglion Cells (tonic portion)	30		4	
(charging portion)	—		XXX	
(phasic portion)**				
foveola	4 mm	0.5 mm	0.1	0.01
periphery	up to 18 mm		up to 0.5	
Total cumulative time delay to lamina cribosa			~ 45.0 + XXX	

* Based on 7 millimeters/sec electrolytic transport velocity
** No time delay associated with any Nodes of Ranvier were included here.

17.5.6.2 Time delay orthodromic of the lamina cribosa EMPTY

17.6 The temporal performance of the human eye

The temporal and spatial performance of the human eye are highly entwined and involve a large number of parameters. This section will address the temporal performance and the spatial performance from an incidental perspective. **Section 17.7** will address the contrast performance including the incidenteal temporal aspects. Each section will address many of the individual variables but cannot address them all.

The temporal performance of the human eye has always been difficult to define completely and precisely. Many of the critical performance parameters are difficult to measure accurately because they are short relative to the total of the perception and cognition time. Furthermore, it is often quite difficult to design experiments that adequately distinguish, separate and control all of the variables involved. Because of these problems, the dark adaptation characteristic, in particular, has remained undefined theoretically. Lacking an adequate model of the process has led some investigators in misleading directions. The observation that the first 15-30 seconds of the characteristic are not described at all by an exponential function has led investigators to seek other explanations such as neural adaptation of the external feedback type[22]. This theory has shown that the actual explanation involves three processes; neural adaptation of the *internal* feedback type, the complex contribution of the vascular/electrostenolytic process and the nonlinear (hyperbolic) performance of the chromophores of the outer segment of the photoreceptor. The result is a quasi-exponential function distorted by stretching in the amplitude direction. This function has been labeled an

[22]Dowling, J. (1963) Neural and photochemical mechanisms of visual adaptation in the rat. J. Gen. Physiol. Vol. 60, pp. 1287-1301

expanded damped sinusoid. Here, it will be shown to be an *exposine* function.

The contrast performance of the human eye involves a wide variety of parameters and is very sensitive to the configuration of the task. It depends on the operational aspects of the task, the functional characteristics of the target stimulus, the architecture of the neural system, the performance of the physiological optics, and the topography of the retina.

This work will not address the visual evoked potential and the electroencephalograph. Although finding use in clinical situation, the waveforms involved in these studies have resulted from so much signal processing as to be of only limited utility in this type of investigation.

The temporal performance of the human eye can be divided into three distinct areas; the transient response, the frequency response and the delay response. These areas can be further subdivided into the after-image transient response and the flicker response. These last two will not be treated in detail in this work. The after-image response will be discussed only briefly in **Section 18.7.** A complete discussion of flicker, including the interplay between all of the variables involved, deserves a volume of its own. It will be addressed only briefly in **Section 17.6.6** because of its ubiquity in experiments designed to determine the spatial or temporal characteristics of the visual system.

17.6.1 Transient performance–psychophysical context

[xxx rewrite to eliminate breakdown in collector in favor of bleaching of chromophores – removed breakdown symbol from graphic]
Graham & Hood have provided an extensive paper on adaptation as it is interpreted by the psychophysical community[23]. They describe two conflicting approaches current at that time (1992) and attempt to develop a better conceptual model of the adaptation process based on a variety of rules. They provide considerable data on what can be called the gross dynamics of the adaptation process. They do not address the transient nature of the adaptation process either in the “dark-going” or the ‘light-going” aspect. Nor do they address differential adaptation due to differences in the operation of the individual spectral channels. The competing models they review and their proposed hybrid, although still conceptual, are much more complex than the actual physiological process. Yet, they still do not reflect the broader capabilities of the actual system.

Hecht, et. al. noted that the transient performance of humans was (based on a still small sample size) quite consistent when adequate instrumentation was available to characterize it. Based on the work of Hecht & associates, Spillmann & associates, and Poot et. al[24]. plus the above work on the variable gain capability of the adaptation stage amplifier, it is possible to define the transient performance of the individual photodetection channels of the eye quite precisely. The key to defining the transient performance to this degree is to look at the problem globally and then characterize the individual functions involved.

Section 7.2.4.3 discusses the adaptation process as it relates to the circuit elements of the retina.

Figure 17.6.1-1 provides a physiological map of the photodetection process related to adaptation. This map is developed in greater detail in **Section 16.4.2**. The following points should be recalled from earlier sections in this work:

1. The iris operates over a narrow range of the overall visual range. It operates in the lower photopic and upper mesopic region.

---

[23]Graham, N. & Hood, D. (1992) Modeling the dynamics of light adaptation: the merging of two traditions *Vision Res*. vol. 32, no. l7. pp 1373-1393
[24]Poot, L, Snippe, H. & van Hateren, J. (1997) Dynamics of adaptation at high luminances. J. Opt. Soc. Am. A vol. 14, no. 9, Sept. pp. 2499

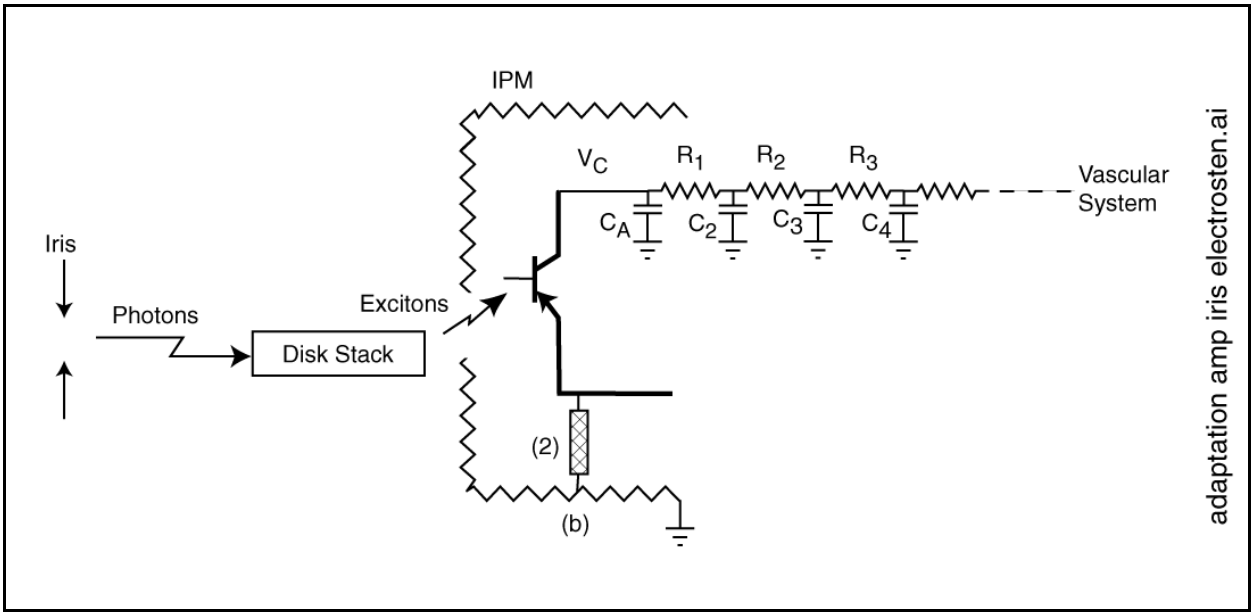

Figure 17.6.1-1 Physiological map of the visual system related to adaptation EDIT. Only the adaptation amplifier of the photoreceptor cell is shown. The load in the collector circuit has been shown explicitly. V_C is the collector potential, C_A is the axon capacitance, and R_1 corresponds to the impedance of the electrostenolytic process. R_2 & C_2, R_3 & C_3, etc. correspond to equivalent impedances related to the diffusion of chemicals to the electrostenolytic site.

2. the chromophores of the Outer Segment act as the photodetectors in vision. They convert photons into excitons. These excitons travel to the microtubule interface rather slowly. A significant delay is introduced into the signal channel as a function of illumination, and also as a function of temperature, particularly in cold blooded animals. The amplitude of the pulse applied to the microtubules is proportional to the integrated flux for intensities above the Hodgkin solution.

3. In the three shorter wave length photodetection channels, individual excitons can interact with the base region of the Activa within the adaptation amplifier circuit to create a electron-hole pair. The electrons are the majority carrier in this “n” type material. They move more rapidly and farther than the holes.

4. In the long wavelength region, represented only by the L-channel, two excitons merge to form a bi-exciton before inducing an electron-hole pair in the Activa base region. This process introduces another functional relationship into the photodetection process.

5. The adaptation amplifier Activa is operated in the open base, common emitter configuration with a collector supply voltage resulting in a *collector to base* voltage near breakdown. This condition provides an amplification factor that is highly sensitive to average current through the Activa.

Since the base is operated without any bias lead attached to it, the current in the collector and emitter leads must be the same.

Whenever there are any electron-hole pairs in the base region, current will flow in the collector circuit. In the absence of any electron-hole pairs in the base region, the collector current is zero.

This last fact is important. It allows the transient performance of the photodetection stage to be evaluated, during dark adaptation, to an arbitrary degree of precision.

The performance of this circuit can be subdivided into four parts;

1. the operation of the iris, with an opening time constant of 1.5 seconds and a closing time constant of six seconds.

2. the response of the chromophores in the disk stack to light. The P/D Equation includes a finite delay related to the intensity of the incident retinal illumination. The amplitude of the response is directly proportional to the incident

illumination for intensities above the Hodgkin Solution, $\sigma \bullet F \bullet \tau = 1.000$.

3. the gain of the adaptation amplifier is an exponential function of the average potential of the collector.

4. the average collector potential is highly dependent on the current through the Activa and the impedance of the electrostenolytic power supply.

The performance of the adaptation circuit changes very rapidly during the initial time of illumination (light adaptation). The illumination causes two changes in the photoreceptor neurons. First, the sensitivity of the chromophoric material is reduced drastically. Second, a rapid rise in current through the collector of the Activa. This current lowers the collector potential rapidly as it discharges the axon capacitance. As a result, the overall sensitivity of the system falls with a time constant measured in fractions of a second.

Operation of the adaptation circuit is different during sensitivity recovery (dark adaptation). As long as the potential on C_3 is equal to the potential on C_4, the load impedance consists of only R_1 and C_A. The circuit shows an exponential recovery following the cessation of illumination. This time constant is measured in minutes (8-16 minutes. However, if the potential on C_3 is not equal to C_4, the overall circuit is represented by a third order differential equation. The solution to a third order equation is the product of an exponential and a sinusoid as will be developed below. The period of the sinusoid is also measured in minutes (12-24 minutes)

Figure 17.6.1-2 presents an early figure from Crawford showing both the short term light adaptation and dark adaptation responses of humans[25]. It did not illustrate or describe all of the parameters discussed above but it has been widely reproduced. Note the small change in the maximum amplitude of the pulse following initial illumination. The light adaptation process has reduced the gain of the Activa significantly within 100 msec.

Crawford made several important observations about this curve;

- It involved one eye of one subject, Crawford himself.
- He noted, "The most striking result is that the liminal test stimulus begins to rise before the conditioning stimulus is applied to the eye, the first appreciable increase occurring nearly 0.1 sec. before exposure of the conditioning field. A substantial increase of about 10 to 1 is found at 0.02 sec. before exposure of the conditioning field. These intervals before exposure of the conditioning field were measured between the end of the test-field exposure and the beginning of the conditioning field exposure and so represent the period of complete darkness intervening between the two exposures. There is thus no doubt as to the reality of the effect." "There seem to be two possible explanations. Either the relatively strong conditioning stimulus overtakes the weaker test stimulus on its way from retina to the brain and interferes with its transmission; or the process of perception of the stimulus, including the receptive processes in the brain, takes an appreciable time, of the order of 0.1 sec., so that the impression of a second (large) stimulus within this time interferes with perception of the first stimulus."
- He further noted, "In the case of the highest conditioning field brightness, a small rise of liminal test stimulus also occurs before the conditioning stimulus is cut off. Thus it would seem that cessation of a stimulus affects the perception mechanism of the brain in the same way as initiation of a stimulus, though to a much smaller degree as measured by the ratio of test stimuli."

[25]Crawford, B. (1947) Visual adaptation in relation to brief conditioning stimuli. *Proc. Roy. Soc. B.* vol. 134, pp 283-302 See also Davson, H. Op. Cit. pg. 201

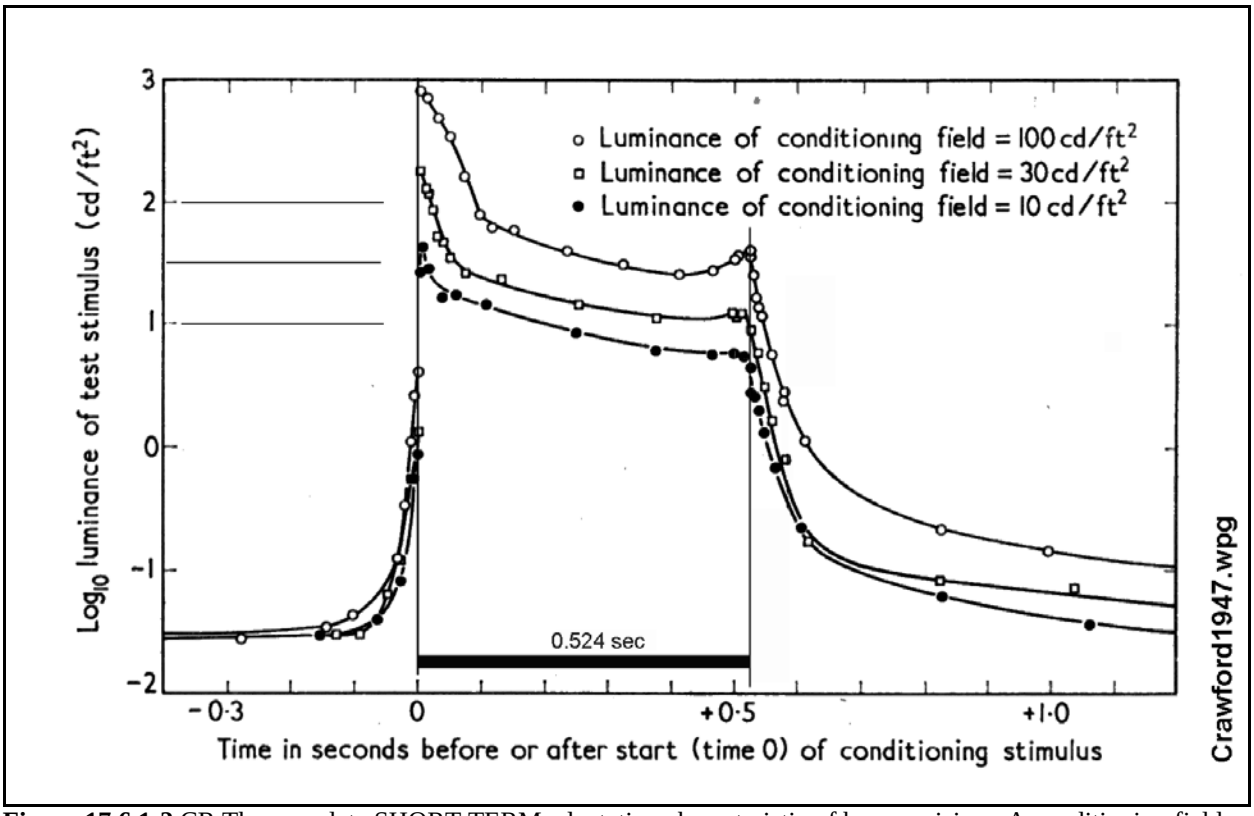

Figure 17.6.1-2 CR The complete SHORT TERM adaptation characteristic of human vision. A conditioning field of 12 degrees diameter and a test field of 0.5 degrees fixated centrally was used. The conditioning field was terminated at +0.524 seconds. The vertical line at zero time, and the length of the stimulus, have been added because of the discussions concerning these data. See text. Both Crawford, Uttal and Davson discusses the idiosyncratic nature of the time line before time zero in this early data. From Crawford, 1947.

100 cd/ft^2 (1000 cd/m^2) is at the low end of the photopic region while 10 cd/ft^2 is below the lower limit of the photopic region (color constancy is not preserved).

Crawford's apparatus and protocol were crude by modern standards. He made no effort to calibrate the delay associated with his biological motor neural path nor the biological recognition delay associated with his protocol. The implication was that the tests were made following adaptation to a given condition. However, in fact, the experiment involved the use of rotating apertures as a shutter with the experiments being presented sequentially every 7.2 sec until the threshold for that level of sequential light and dark adaptation was determined. The test period is so short that the longer time constants of dark adaptation can not be determined from this test protocol. The test interval for determining the threshold was only 10 msec. For this short of evaluation interval, the delay associated with the impulse response of the stage 1 sensory neurons must be considered. No description of the shutter efficiency used in his experiments was provided. The stimulus was clearly not a square pulse. The leading and trailing edges of the light pulse should have been indicated. The shape of his aperture plate (A) and the finite size of the focused image in figure 2 suggests the rise and fall time of his test field as presented to his eye was poorer than for the conditioning field.

Overall, his results must be discounted unless reinterpreted based on the excitation/de-excitation equation. Otherwise a discrepancy of over one order of magnitude must be associated with the figure. The E/D equation does incorporate the delay mechanism required to support his first hypothesis (except the "overtaking" is due to different amounts of time delay within the sensory neurons, not along the way to the brain). It should be noted that the requisite stage 3 analog signal to phasic encoding, and subsequent decoding involve substantial asynchronous time delays not addressed in his protocol or results. The delays Crawford speculates about are given with precision by the E/D equation of **Section 7.2**. The fact that the waveforms are not horizontal at the end of the stimulus phase or the dark phase suggest the Crawford experiments do not result in clearly defined dark adaptation or light

adaptation functions. Dark adaptation is definitely not complete after 7.2 sec.

The comments of Uttal following presentation of Crawford's figure and relating to the delay associated with generation of a neural signal[26] are also addressed explicitly in more modern form using **Section 7.2**.

The dark adaptation process exhibits a clearly exponential form following the cessation of illumination. This indicates the level of illumination was quite low relative to the capacity of the electrostenolytic power source to maintain the potential on the capacitance, C_3. The decay time constant shown, about 40 msec is directly relatable to the time constant of the P/D process. An absolute delay of about 40 msec following the cessation is also directly relatable to the P/D process.

Baker has also questioned the data from Crawford and repeated some of Crawford's experiments in 1963 using updated instrumentation. He explicitly said Crawford's results were not compatible with the chemical theory of the neuron and the putative visual mechanisms of that era. Baker has provided additional waveforms related to the initial stages of dark and light adaptation[27]. He extended their duration to at least 2.0 seconds and then noted, "these curves show the beginning of dark adaptation" rather than the complete function. "There is a rapid drop that flattens abruptly into the regular slow dark adaptation of the classical curves." Baker attempts to de-emphasize the significance of the anticipation recorded before a major change in stimulus level. His arguments are not convincing to this analyst. The initial rapid drop following the cessation of stimulation is clearly due to a separate mechanism (with its own time constant, of less than 0.2 seconds) than that usually associated with dark adaptation.

17.6.1.1 Dark adaptation

[outline show Spillmann and Hecht figures and then a table of values. Show Hecht equivalence data. Then go to light adaptation] [Is the following said well?]
Although dark adaptation is discussed endlessly in the literature, the number of subjects used to collect most of the published data is less than a dozen. The statistical material from Hecht & Mandelbaum covering 110 subjects at 7° from the fixation point being the exception[28]. One of the widely published figures by Hecht, Haig & Wald may be from a single subject with significant disease of the foveal retina. The data in that figure initially appears to be supported by data in Wyszecki & Stiles (1982) from Hecht, et. al. (1937). The caption to their figure claims the data is for the fovea. Unfortunately, the original caption , and the entire Hecht article specifies operation at 30° nasally from the fovea. One of the major problems in analyzing the available dark adaptation data is lack of a reference point for the threshold measurements. Without a threshold measurement during the period of illumination prior to the adaptation process, it is difficult to quantify the change that occurs absolutely. This is particularly true in the "non-exponential" areas of the characteristic. Therefore, it is incumbent upon the vision community to collect additional data in this area to achieve a statistically relevant database. Jimenez-Sierre, et. al. apparently noted the non-exponential characteristic in their data and chose not to plot their data as a continuous line beyond 30 minutes[29]. This measurement should be stressed in future investigations along with a detailed spectral description of all light sources used. Without these parameters, it is difficult to achieve better than 20-30% precision in the required calculations. The importance of adequate control of the pre-adapting illumination cannot be underemphasized.

Nordby, Stabell & Stabell resurfaced Hecht's original thesis (1920) relating dark adaptation to photochemistry in 1984. His position, and creditable at the time was (quoting Nordby, et. al.), "the threshold level of the human rod system, obtained psychophysically at any particular instant during the course of dark adaptation, was a direct measure of the concentration of residual photochemical 'decomposition products' at that moment." As time passed, this thesis was associated with the bleaching of of rhodopsin during adaptation. Based on the concept that bleaching was due to isomerization, "decomposition" was taken to mean the isomerization of rhodopsin. Today, the situation can be discussed in much greater and more precise detail. First, a thesis of this work is that the chromophore is not decomposed or rearranged, it is only excited (for a very brief interval of time). The result is still recognizable as bleaching but the process does not involve decomposition. A second thesis of this work is that the adaptation process is controlled primarily by the change in gain of the adaptation amplifier in response to the average level of

---

[26]Uttal, W. (1981) A taxonomy of visual processes. Hillsdale, NJ: Lawrence Erlbaum Associates, pp 503-504
[27]Baker, H. (1963) Initial stages of dark and light adaptation *JOSA* vol 53(1), pp 98-103
[28]Hecht, S. & Mandelbaum, J. (1939) The relation between vitamin A and dark adaptation. J. Amer. Med. Assoc. vol. 112, pg. 1910. *Also in* Stiles & Wyszecki (1982), pg. 520
[29]Jimenez-Sierra, J. Ogden, T. & Van Boepel, G. (1989) Inherited Retinal Diseases. St. Louis, MO: C. V. Mosby pg 265

illumination. This change is controlled by the ability of the electrostenolytic power source to provide electricity to the amplifier. This electricity is generated via glutamate oxidation in a metabolic pathway (typically or analogous to the α-Ketoglutarate pathway). It is proposed that Hecht's conception of decomposition products is best treated by subdivision into two nominally coincident concepts, the decomposition of the metabolites of glutamate in order to power the adaptation amplifiers and the temporary bleaching of the rhodonines as part of the dynamics of the photoexcitation/de-excitation process. The time course of the metabolic decomposition and resupply of the glutamates is compatible with the time course of adaptation. The Nordby, et. al. article goes into detail concerning the difficulty of relating the bleaching of the chromophores to the dark adaptation characteristic. They list four documented exceptions to the prior simple relationship and finish with the statement that the relationship is not simple, even when plotted on log-log paper.

There are many difficulties in correlating the apparent change in the optical density of the retina to the dark adaptation characteristic. First, the light used to determine this change is not normally correlated to the absorption spectra of the individual chromophores. Second, the percentage of the chromophore bleached under normal conditions is quite small. Third, the color of the materials consumed in the co-located electrostenolytic process is unknown. Fourth, a premise of this theory is that the chromophores are completely de-excited (and therefore unbleached) before the stoppage of current through the base of the Activa and the concurrent start of the dark adaptation transient. There is essentially no physical connection between the "unbleaching" of the chromophores and the dark adaptation characteristic and no relationship between the two associated transients.

17.6.1.1.1 Design of dark adaptation experiments

Past experimental activity in dark adaptation has been primarily exploratory in nature. There was virtually no discussion of the design of the experiment from a theoretical perspective. The selected instrumentation was, viewed in many respects and with hindsight, inadequate. Beginning with the Top Level Schematic of the visual system, it is possible to design a much more defendable experiment. However, the process of design does require some knowledge not explored in this work. For best results, it is important to know the nature of the threshold circuitry of the brain. Although this work has tried to avoid exploring this area, it is clear there are two primary possibilities; a well defined (and noise free) fixed amplitude threshold, or a stochastic threshold set by the noise performance of a specific circuit. Based on the work of Spillmann & Conlon and others, an ultimate threshold that is stochastic and within the cortex will be assumed here. Note in [Figure 17.3 XXX] however, that above this ultimate threshold, the quantum noise associated with the input irradiance plays a significant role. This noise is also stochastic.

In the past, the goal of experiments has been to determine the threshold sensitivity of the visual system in terms of object space performance. This has avoided discussion and determination of the processes involved in determining that performance. With the aid of the Top Level Schematic, it is clear that the threshold performance of the log additive channel (luminance) of the visual system is quite different from the threshold performance of the log difference channels (chrominance, etc.). [Figures 17.2.2-1 & 17.3.2-1] are helpful in visualizing these differences. It is also quite clear that the spectral response of the individual photosensitive channels play a large role in the experiment. Of even greater importance is the performance of the individual adaptation amplifiers associated with those sensing channels. In the first order (operating individually), there is no requirement that these amplifiers track each other during the experiment. In the second order (sharing of a common energy supply) there is such a requirement. The amplifiers share a common energy supply system via the vascular system. This system acts as a poorly regulated common power supply. Recognition of these variables in the problem aids greatly in the design of the experiment.

It has generally been recognized that the visual system needs to be placed in a stable, or quiescent, condition before meaningful data can be obtained. In the past, it has been recognized that the subject must be maintained in a loosely controlled environment for at least 15 minutes before taking data. The norm has been to then present the subject with a controlled irradiance level for two minutes prior to the collection of transient performance data. The data summarized in this Section show that these preparations are inadequate for precise, repeatable experimental results. There are time constants in the visual system that suggest at least one hour of loose control is required (possibly two hours on a bright day with snow on the ground) before the subject is exposed to a pre-adapting exposure level. This level needs to be maintained for at least 20 minutes. Otherwise a more difficult situation must be analyzed.

The conventional procedure is to expose the subject to a specified irradiance covering a significant portion of the retina before data taking and to then use a probe of more limited spatial and temporal extent, and possibly different spectral content, to determine the minimum irradiance required for perception of the probe. The probe is normally coaxial with the center of the larger area. The exact location of the background and probe areas needs to be specified carefully because the retina is highly nonuniform in its response. Many secondary factors are frequently overlooked because of poor choice of location. A simple example is the assumption that the point of fixation is collocated with the optical axis of the eye. It is not. The duration and repetition rate of probe measurements has

varied. However, 0.2 seconds has been a quasi-standard. The impact of the duration of the probe needs to be evaluated. To understand the dynamics of the visual system during dark adaptation measurements, it is absolutely mandatory that the experimenter know the precise properties of the irradiance used in both the pre-exposure and in the probing. Lacking this knowledge results in data that cannot be interpreted optimally and with precision. The actual experiment involves the determination of the transfer characteristic of the visual system between the input irradiance and the perception threshold (for the luminance and chrominance channels separately). The simplicity of the experiment is perturbed by two factors, the parallel signal paths leading to the summing and differencing circuits of the visual manipulation stage and the difficult behavioral task of separating the perceptual responses associated with these two signaling paths (luminance & chrominance). Whereas the summing process may skew the results, the differencing process impacts them significantly. Because of the extensive overlap between the spectral photo-sensing channels of vision, it is difficult to perform dark adaptation experiments on the eye when pre-adapted to a nominally white source, preferably at 7053 K. The data tends to be dominated by the performance of the M-channel adaptation amplifier. By employing highly chromatic pre-adapting irradiance, it is possible to substantially separate the performance of the individual adaptation amplifiers.

As discussed in **Section 16.3.5.2**, under carefully controlled conditions developed from the above discussion, the results of dark adaptation experiments involve the evaluation of the basic relationship between the input irradiance, the transfer function of the visual system between the entrance aperture and the brain and the threshold of the perceptual circuits in the brain. Neglecting the impact of the signal projection system, and the limited amount of saturation that might occur in the transduction process, the transfer characteristic consists of the processes within the signal manipulation stage of vision. Since the circuits proximal to the pedicel of the photoreceptor cells operate at essentially constant gain to the first order, the transfer characteristic is dominated by the performance of the adaptation amplifer(s). The equation of interest becomes:

$$\delta_{sig} = A \cdot \varepsilon_{thresh}[K] \qquad \text{Eq. 17.6.1-a}$$

where δ_{sig} is the amplitude of the probe required to elicit perception by the subject. A is the transfer characteristic of the adaptation amplifier and ε_{thresh} is the stochastic threshold of the appropriate brain circuits. The constant K combines the impact of at least three conditions on the result. It may contain a factor for the variation in optical properties of the eye as a function of field position. It represents an experimental fact that a signal to noise ratio of greater than one is typically found in simple signaling systems similar to the visual system. There is an impact on the result of the spatial size of the probe signal. For probe dimensions larger than the diameter of a single photoreceptor, (normally necessary to achieve adequate signal to noise ratio for perception) the impact of both signal and noise channel integration must be considered. If the noise channel is dominated by stochastic processes, the detectability of a probe signal improves rapidly with size.

The remaining question is, should the bottom line result of the experiment reflect the signal level required in object space to elicit a perceptual response or the signal level at the brain required to elicit the same response. By expressing the result in cortical signal space, it is possible to calculate the value in object space for any arbitrary irradiance profile and any state of one or more adaptation amplifiers. It also allows the signal level required for luminance perception and chrominance perception to be specified separately. Finally, it supports the effective pursuit of the impact of secondary variables on the ultimate results. Although reporting results in cortical space is a change from most of the work before 1972, it is essentially what Spillmann & Conlon attempted to do (with some success). Under steady state conditions, they were able to specify a luminance threshold and a chrominance threshold (and a photochromic interval) as a function of light level. They also described a transient expression for this photochromic interval conceptually. It is defined mathematically below. (See also Section 17.5.1.1.1)

Although not required, it appears desirable to determine the threshold at the end of the pre-adapting irradiance period before the excitation is removed. This provides an experimental method of bridging the interval between the end of pre-adaptation and the first feasible probe measurement.

17.6.1.1.2 Importance of adequate prior adaptation

Making accurate psychophysical adaptation measurements is difficult for the subject and the investigator. The state of the photosensitive channels should be stabilized for at least thirty minutes before attempting to perform this characterization. Hecht, et. al. used a combination of 20 minutes in the dark followed by two minutes of light adaptation before making dark adaptation measurements. Although admirable, this regimen does not insure quiescent conditions. Spillmann & Conlon used a 45 minutes of dark adaptation before establishing the light adaptation state using a two minute exposure. Notice that a two minute light adaptation does effectively establish

the voltage V_A at the collector of the adaptation amplifier. However, it does not insure the equivalent voltage V_1 is at its quiescent value prior to the experiments. The fundamental period of the sinusoid associated with this voltage will be shown to be near 680 seconds (~11 minutes). As a result, at the start of dark adaptation, the voltage on V_1 is still changing. This changes the initial conditions used to evaluate the second order differential equation of Section 16.3.5. The effect of this change is to insure that the phase angle of the sinusoid is not equal to π as assumed in the following discussion. This can cause a shift in the time base between the measured data points and the obtained theoretical curves presented below. The problem associated with the period of pre-adapting illumination can be avoided by using flash illumination. For flashes very short compared to any time constant in any circuit involved in the adaptation process, the situation becomes drastically different. There is minimal change in the quiescent condition of the vascular system but the collector potential of the adaptation amplifier, and hence its amplification factor are changed drastically. Under, these conditions, the dark adaptation characteristic does not exhibit a significant change in slope during adaptation.

17.6.1.1.3 Desirability of using impulse pre-adaptation

To a large extent, the use of impulses to set the pre-adaptation state of the adaptation amplifiers has been overlooked. The dynamics of the adaptation process are such that establishing the initial state is not simple. The state is determined by a complex combination of the intensity and the duration of the pre-adaptation preparation. This complexity can be avoided by using an impulse to determine the intensity-duration product. Although best discussed in **Section 17.6.2**, figure 1 in Bortoff[30] illustrates the significant difference between the response of the same visual system to an impulse (of shorter duration than any time constant in the system by definition) and a relatively long illumination pulse (in this case one second). The trailing edge of the response to the impulse (at a ganglion cell) is completely obscured in the response to a longer duration pulse.

17.6.1.1.4 Theory versus measured data–pulse pre-adaptation

Spillmann & Conlon[31] provided important data on both the transient and steady state threshold performance of the human eye, for both chromatic threshold and achromatic threshold during dark adaptation. The steady state results will be discussed in **XXX [Section 17.8]. Figure 17.6.1-3** presents the transient data from their figure 1 combined with the equation developed in **Section 16.3.5**. That equation described the dark adaptation curve in terms of the variable gain of the outer segment/adaptation amplifier combination and the fixed threshold sensitivity of the brain reflected forward to the pedicel of the photoreceptor cell. This was feasible due to the essentially constant gain of all processes proximal to the pedicel in the luminance channel of vision.

The upper portion of the figure shows the chromatic threshold determined for perception of a green or greenish test stimulus only (as instructed by the test operator). *The test does not involve chromatic discrimination, only chromatic perception of a stimulus.* The chromatic tests employed a Kodak Wratten #61 gelatin filter. Its peak transmission and half-amplitude width was well matched to the M–channel receptor of the eye. As a result, the product of these two spectra exhibited a peak very near 532 nm. They noted the low output capability of their tungsten-iodide light source at 3000° Kelvin. The lower portion of the figure shows the achromatic threshold, perception of a light stimulus without perception of any chromatic aspect. They define the photochromatic interval as the ratio between these two measurements at a given time after the start of the dark adaptation period.

Spillmann & Conlon offered no schematic or model of the visual modality on which to interpret their results. Since the center wavelength of their stimulus was 535 nm and the color temperature of their source was low, it can be concluded that the tests explored only the threshold performance of the M–channel receptors and possibly the R–channel of the visual modality. As a result, their description of their stimulus in terms of foot-candles is probably a poor choice of nomenclature.

---

[30]Bortoff, A. (1964) Localization of slow potential responses in the *Necturus* retina. Vision Res. vol 4, pp. 627-635

[31]Spillman, L. & Conlon, J. (1972) Photochromatic interval during dark adaptation and as a function of background luminance. J. Opt. Soc. Amer. vol. 62, no. 2, pp. 182-185

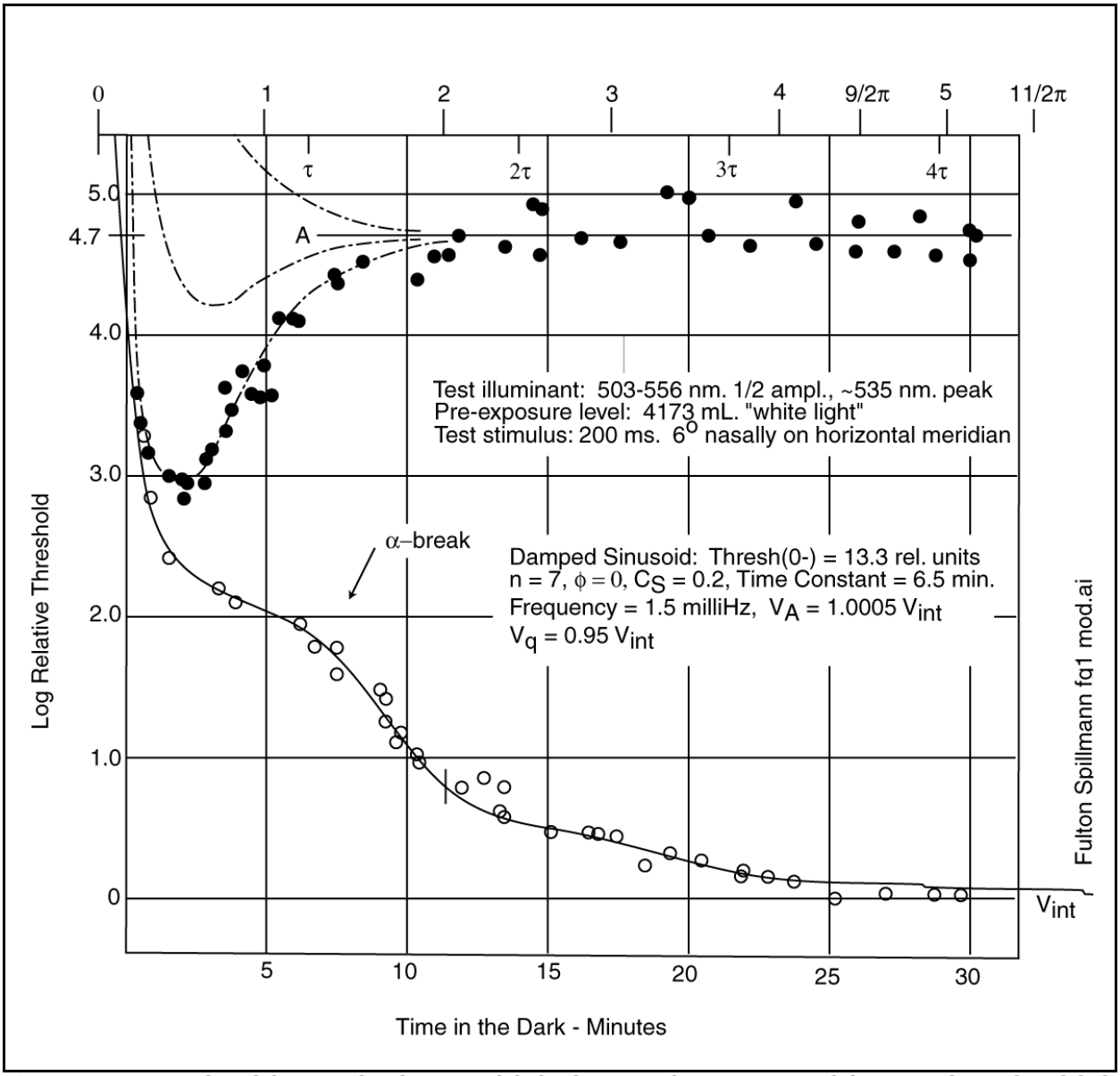

Figure 17.6.1-3 Combined theoretical and measured dark adaptation characteristic. Solid curve is the predicted dark adaptation threshold of the luminance channel for the human eye based on this work. The theoretical curve exhibits several "flats" that aid in determining the interval of the sinusoidal component and the time constant of the exponential component of the curve (See the top time scale). The top time scale is displaced to account for the limited light adaptation period before the start of the experiment. The horizontal line labeled A corresponds to the theoretical asymptote for the dark adaptation threshold of the chrominance channel based on this work. The dash-dot lines form a set of possible chrominance thresholds depending on the detailed spectral characteristics of the irradiance and other second order effects. Data from Spillmann & Conlon (1972).

Looking first at the open circles representing the perceived achromatic dark adaptation characteristic of the subject, Spillmann & Conlon fitted a curve to these data points resembling two distinct but joined exponentials, but without providing the derivation of the equation for such a function. The arrow points to the location of the "α-break" in this curve. Spillmann & Conlon did not provide a threshold value for the irradiance level prior to dark adaptation. This work proposes and shows a damped sinusoid as an alternate curve fitting the data. The α-break is spurious based on this theoretical treatment. An auxiliary time scale is shown along the top of the figure with indices in multiples of the time constant, τ, and the abstract circular function, π. The proposed curve is continuous and does not exhibit an α-break. The damped exponential has the characteristics listed in the figure. The proposed curve, based on n=7 and $\varphi = 0$, has a threshold sensitivity prior to adaptation of 13.3 Log Relative Threshold units when fitted to this figure. However, the best fit to the data points suggests a displacement in the start of the theoretical curve of 1.5 minutes due to unknown variables. Part of this shift may be due to a phase angle of other than zero, in the solution of the required differential equation due to inadequate experimental light adaptation prior to data collection. The available curves were for a phase angle of zero. To accommodate this situation, the theoretical curve is plotted using the top scale and is shown starting at minus 1.5 minutes (a shift in phase of about 45 degrees). The amplitude of the sinusoid was taken as 20% of the initial amplitude of the transient, $C_S = 0.2$. This value results in a nearly horizontal region near 5 minutes and seems to be common to a large number of experimental situations. As it varies, the effect may differ from ones intuitions. Obviously, as C_S increases, the value of the curve near three minutes decreases and the value of the curve near six minutes increases. The more interesting fact is; the portion of the curve between zero and two minutes moves to the left and the portion between six and ten minutes moves to the right. This latter variation was first noted and documented by Hecht, et. al. in 1937, see below. This documentation provides strong support for the theory presented here. This effect does not occur in combinations of simple exponentials. Aurebach & Wald showed a series of dark adaptation characteristics in 1954 that could not possibly be due to two exponentials no matter what the mechanism[32]. They can only be fitted by an exponential sine (exposine) function.

In accordance with the discussion in **Section 16.3.5**, several features in the dark adaptation characteristic can be designated. The most explicit features are the "flat spots" in the tail of the curve corresponding approximately to the peaks in the sinusoidal component of the waveform. These occur near 21.5 ($7/2\pi$) and 26.5 minutes ($9/2\pi$) and would be expected to occur near 35 minutes ($11/2\pi$). They allow one to estimate the frequency as 1.5 milli-Hertz and the time of the zero crossings of the sinusoid. These zero crossings occur at approximately 7, 12, 17, 23, 29 minutes, etc. As Dowling has pointed out, a simple exponential cannot be fitted thru these points. However, the "expanded damped exponential" defined in **Section 16.3.5** fits these points very well and has a time constant of 6-6.5 minutes. The data points only extend to about five time constants of the exponential. Therefore, the data points do not completely characterize the fully dark adapted eye. It is expected that the fully dark adapted eye would reach a threshold value marked by the label, V_{int}, on the right hand scale. This asymptote corresponds to the intrinsic voltage of the electrostenolytic process powering the adaptation amplifier. It is predicted that the data points would have suggested another "flat" at a time of 33 minutes ($11/2\pi$), although it may have been difficult to discern in the absence of a theory.

[xxx edit comments about high internal negative feedback if necessary]
The theory presented in this work suggests that the very high internal negative feedback employed in the adaptation amplifier should maintain the DC output voltage at the collector of the Activa nearly constant. The result of fitting the function prescribed by the theory to the above data confirms this fact. The quiescent collector voltage during light adaptation prior to the test was equal to 95% of the intrinsic voltage. This very small change in the collector to emitter voltage during adaptation, and the relatively constant average current through the Activa makes experimental verification of the operating voltages of the adaptation amplifier very difficult. The average voltage of the dendroplasm of the photoreceptor cell would only be expected to vary by 5-10 millivolts under any illumination conditions compatible with normal vision.

The theoretical curve overlaying the above data represents the performance of a single photoreceptor and is independent of the spectral content of the exciting irradiation. It would be expected that irradiance exciting an L-channel photoreceptor would be different because of the more complex exciton to electron translation. However, because of the high value of n and the very high degree of negative feedback within the amplifier, this effect is swamped out mathematically at any operating level associated with the photopic regime. Secondary effects become important below this level (including the effect of quantum noise on the perceived threshold) in all of the

---

[32]Aurebach, E. & Wald, G. (1954) Identification of a violet receptor in Human color vision, *Science*, vol. 120, pp 401-405

photosensitive channels.

The theory behind the curve is also different from that discussed by Spillmann & Conlon. Several authors have attempted to define a variable "background threshold" based on correlations to observed after images. Such a variable threshold is unnecessary. The variable involved is the gain of the information channel, determined primarily by the adaptation amplifier.

Looking at the filled circles in the above figure, an entirely different situation is recognized based on the nature of the differencing process proposed in this theory. It is still possible to reflect the fixed sensitivity threshold of the brain forward, but only to the output of the 1st lateral cells. Such a threshold would be represented by a horizontal line such as that labeled A in the figure. However, the net input to the Activa of a given lateral cell is the difference between the input from two chromatically different photoreceptor cell types. Since each photoreceptor cell type has a very similar dynamic gain characteristic, to a first order, this subtraction produces a nearly constant residual signal. The actual difference signal depends critically on the spectral content of the exciting irradiance, the spectral absorption characteristic of the individual channels and the state of adaptation of each adaptation amplifier. In theory, if equal currents were injected into each input terminal of the Activa associated with one of the chrominance channels, no output signal would result. The subject would perceive a "white" test signal regardless of its actual spectral irradiance (at least via that chrominance channel). Because of this situation, it is much more difficult to perform chromatic dark adaptation characterization. Furthermore, the differencing process tends to cancel out both the the exponential and the sinusoidal component of each damped sinusoid defining the variation in gain of the adaptation amplifiers. In the above figure, the nominal threshold, taken as the horizontal line, A, is 4.7 log units (50,000:1) higher than the ultimate threshold of the achromatic luminance channel. This shows how effective the signal cancellation process can be. Since both of the individual adaptation signals are damped out as time progresses, the chromatic dark adaptation characteristic quickly assumes its asymptotic value near 4.7 log units in the above figure. The only variation from this threshold occurs early in the waveform where the individual pedicel signals are large and any imbalance in their amplitude is easily seen. This is the case during the time interval from zero to 10 minutes. It is proposed that the deviation from the 4.7 log unit asymptote in the above experiment had an equal probability of being positive or negative based on the particular spectral content of the test irradiance and the prior state of adaptation of the photoreceptors. The envelope associated with these two possibilities is shown by the set of dash-dot lines converging on the 4.7 log unit asymptote. For larger irradiance in the M-channel, the negative swing shown by the data points, with a dash-dot line based on an estimate of the theoretical function passing through them, is to be expected.

The above discussion is based on first order processes only. There may be other as yet undetermined factors involved (See **Section 17.3.XXX**).

Spillmann & Conlon have defined the photochromatic interval conceptually as the ratio between the chromatic threshold level and the achromatic threshold level. They did this after the concept of a variable background threshold failed to meet their needs. Although not stated explicitly, they defined this interval as a function of adaptation time interval and indicated it approached an asymptotic value with time. The asymptotic value is shown as 4.7 log units in the above figure in agreement with their value. As shown in this work, the photochromatic interval is also a function of the spectral content of the test irradiance, the area of the test stimulus and the position in the retinal field. The value of 4.7 corresponds to a 1° square test stimulus at a 6° nasal position relative to the fixation point. The data in figure 2 of Hecht, et. al. (1937) discussed below support a photochromatic interval of about 3.2 for a 5° circular test stimulus at a 30° nasal position relative to the fixation point. Due possibly to stenographic problems, Wyszecki & Stiles (1982) gives this test stimulus as 3°.

17.6.1.1.5 Theory versus measured data–impulse preadaptation

To avoid the problem of long preadaptation intervals in order to stabilize the vascular/electrostenolytic subsystem, an alternative is to use very short pulses of pre-adaptation light. These impulses, are able to impact the voltage on the collector by discharging the capacitor C_A without disturbing the state of the equivalent capacitors, C_2 and C_3. Under this scenario, the solution of the differential equation is a simple exponential. The amplitude of the sinusoidal term is zero. The dark adaptation characteristic is still given by the probe amplitude, δ_{sig}, given by the product of the effective gain of the adaptation amplifier, A, times the threshold level, ε_{thresh}, and a constant. The result is described as an "expanded exponential," due to the exponential gain of the adaptation amplifier, instead of an expanded damped sinusoid. Wachtmeister has provided experimental data demonstrating this point admirably.

Figure 17.6.1-4 shows the dark adaptation characteristic repeatedly changing over a range of 10^5 without any distinct break in the curve. It is also interesting that the threshold at 5 minutes after the last flash of each group only

rises slightly during a one hour experiment, suggesting that the voltage on the capacitor, C_A, is falling only slightly because of the integrated equivalent current through R_2 and concurrent small drop in the equivalent voltage on C_2. This slight drop in C_A causes *A* to drop slightly and the threshold level to rise slightly as expected. Only when the pulses are at one minute interval, or less, is the equivalent voltage on C_2 impacted enough to cause the presence of the sinusoidal term (or the extended exponential term) to become obvious in the characteristics.

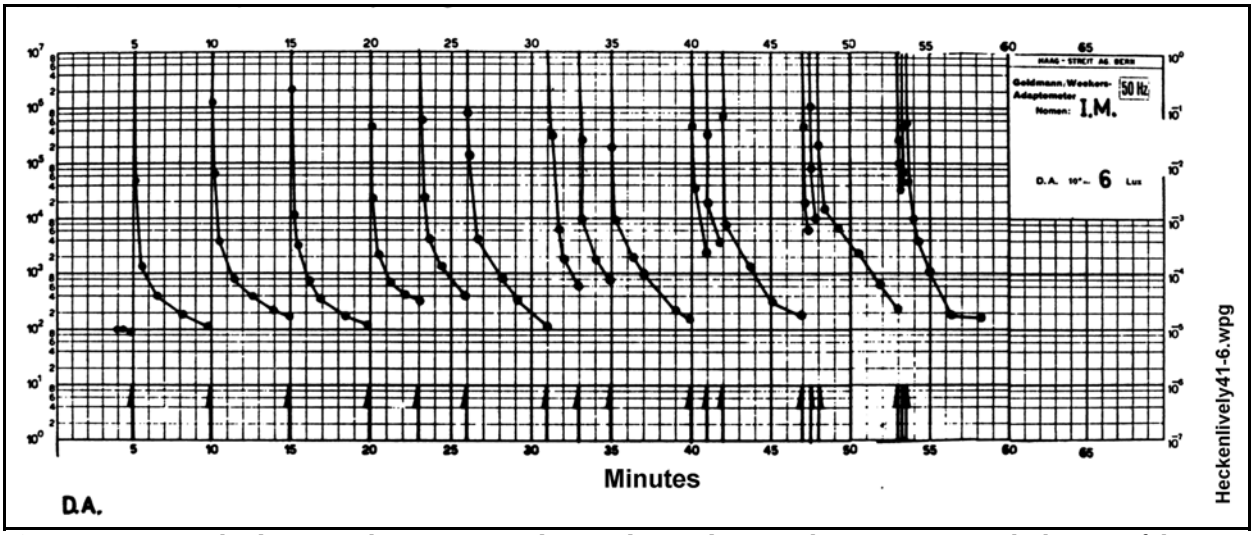

Figure 17.6.1-4 Dark adaptation characteristic under impulse conditions. The "up" arrows at the bottom of the graph show when individual stimulation impulses are generated. The upper traces beginning concurrently with an impulse illustrate the dark adaptation response following this stimulus, or group of stimuli. From Wachtmeister (1973).

Note the ultimate dark threshold shown at 4.5 minutes (before any tests). The curves are returning to this ultimate threshold level without exhibiting a break. It would be interesting to repeat this experiment with longer intervals between pulses to confirm there is no break beyond five minutes. This would demonstrate there are not two separate mechanisms involved, such as rods and cones, in the dark adaptation characteristic under pulse conditions. Alternately, it would be useful to repeat this experiment for a larger number of pulses within an interval ultimately approaching two minutes to explore the changes at levels between 10^2 and 10^5. The goal would be to show that a significant sinusoidal term generates a "break" at a threshold level near 10^4 on the left scale or that the system is either critically or overdamped in this region. If critically damped, the apparent time constant of the exponential exhibits a significant increase. The curve has a significantly different shape, appearing as an almost straight segment due to the exponential being multiplied by $(1+w_n \cdot t)$. This combination will be called an "extended exponential" as it appears to be extended in time. The three right-most curves in the above figure appear to describe this situation. Recall, that the detailed shape observed is actually that of an extended exponential that has been further "expanded" in amplitude due to the exponential gain of the adaptation amplifier.

The time constant of the exponential in the circuit changes as the amplitude of the sinusoid becomes significant. For the left-most curves, it appears to be less than one minute based on the fact the curve approaches its asymptotic value in about 5 minutes. It could be as long as 2 minutes as estimated from Spillmann or as little as ½ minute based on the curve starting at the five minute point.

17.6.1.1.6 Summary of temporal characteristics

Tabulating the time constants involved in the adaptation process is complicated by their changing relationship with each other. The time constants and the frequencies measured in a second order system are not intrinsic parameters. They vary with respect to the damping factor, ζ. There are three distinct relationships and possibly several more of minor importance. The individual time constants are defined loosely and their nominal values summarized in **Table 17.6.1-2.**

TABLE 17.6.1-2

TEMPORAL TIME CONSTANTS OF THE HUMAN EYE*

Time Constant	Nominal Value in Fovea	@ angle	Range in Retina	Comment
TRANSDUCER RELATED				
Transport delay				
De-excitation delay				
Thermal relaxation				
PHOTORECEPTOR RELATED (Adaptation Amplifier)				
Pull down phase (light adaptation)				
Recovery phase (dark adaptation)				
Electrostenolytic supply		~3.0 seconds		R_1C_A product (from Baylor 1984 data
Bioenergy diffusion at cell		~1.0 minutes		R_2C_2 product from Wachmeister 1973 data
Nominal natural frequency		~0.0012 Hz		14 minutes per cycle
Bioenergy IPM/RPE transport**		~6-10 minutes		R_3C_3 product
Choroid artery transport**		**XXX**		
Full body arterial transport		<6 sec.		Normal circulation time
SIGNAL MANIPULATION				None identified
SIGNAL PROJECTION (Fct. of signal levels at Stage 2 output)				
Luminance channel			10-100 ms.	R (summing) channel
Chrominance channel			10-30 ms.	M-channel
			30-100 ms.	L- or S-channel
SIGNAL PERCEPTION				None identified

* Most of these time constants are subject to a wide number of variables. Only nominal values have been stated along with a minimum number of the most important caveats.
** This two parameters appear to be the major contributors to congenital night blindness.

17.6.1.1.7 Clinical measurement of dark adaptation

Goldman-Weekers offers a sophisticated dark adaptometer for recording the transient performance of the human eye under clinical conditions[33]. The instruction manual is quite detailed but does not provide any sample outputs for comparison purposes. Kiser indicates this unit is no long in production. Kiser has provided information on the use of similar instruments and example outputs under more controlled conditions in a psychophysical laboratory[34]. The data included both normal and severely visually impaired patients. The data in their figure 2 is quite extensive and extends out to 45 minutes. The data does not show a characteristic shelf resulting from the two-exponential model proposed in the 1930's and widely reproduced (such as that of Hecht, Haig and Wald (1935).

17.6.1.2 Biophysical measurement of dark adaptation

[33] http://www.iscev.org/varia/Dark%20Adaptatometry/GWDkAdaptometer%20manual.pdf *Also* in my ref. papers

[34] Kiser, A. Mladenovich, D. Eshraghi, F. Bourdeau, D. & Dagnelie G. (2006) Reliability and Consistency of Dark-Adapted Psychophysical Measures in Advanced Eye Disease *Invest Ophthalmol Vis Sci* pp 444-452

The dark adaptation scenario can be discussed in greater detail by combining the quantum physics of the chromophores (the Jablonski Diagram of **Section 5.3.1.3** and **Section 5.4**) and **Figure 17.6.1-1**. [**Figure 17.6.1-2**] shows the excitation illumination, and the generator waveform produced by the Outer Segment.

The transient following cessation of illumination is easiest to explore. The scenario is simple. Following cessation of illumination, no more excitons are created within the chromophore. However, there is a delay in the movement of all of the excitons to the region(s) adjacent to the base region of the Activa within the dendrite. This process has an intrinsic time constant of 1.5 seconds. It is represented by the delay term in the P/D Equation(**Appendix A** and **Section 7.2.6**).

> The delay term is a function of temperature. For endothermic humans, the delay time constant is nominally 3.0 milliseconds. For other animals, the equations as a function of temperature are given in **Section A.2.2.3.2** of Appendix A. Note the delay process does not follow the temperature equation of Arrhenius but follows an equation limited to the biological range, from about zero centigrade to a nominal 48 centigrade. For non-endothermic animals, the delay varies by a factor of 5:1 for a 10° centigrade change. The 48 centigrade number is frequently determined most precisely from enzyme denaturation experiments.

At the end of 15–30 milliseconds in humans, no additional electron-hole pairs are formed in the base of the Activa. Therefore, no current flows in the collector in an attempt to neutralize these charges. From this point on, the voltage on the collector is determined entirely by the power supply characteristics. The diode associated with the power supply is reverse biased and represents a very large impedance that can be neglected. The collector voltage begins to rise back toward the maximum voltage provided by the electrostenolytic process (the power supply) associated with the wall of the dendritic structure. The electrostenolytic process is a diffusion controlled one. It can be represented by an electronic equivalent circuit containing two time constants in series as shown. In this configuration, the initial equivalent voltages on the nodes associated with these two time constants are important in establishing the actual voltage at the collector of the Activa.

As will appear below, the overall dark adaptation characteristic of a photodetection channel depends on the ratio of; the sizes of the equivalent capacitors, the ratio of the equivalent resistive impedances, and the ratio of the initial voltages on the nodes (**Figure 17.6.1-2** in Section **17.6.1**). All of these parameters are parameters of the diffusion channel between the retinal pigment epithelium layer (RPE) and the individual microtubules of the dendrite buried within the grooves of the disks and surrounded by the Inter-photoreceptor matrix (IPM). These parameters vary considerably across the mosaic of the retina, and take on a slightly different character in the foveal region because of the topography of the Outer Segments in that region. For purposes of discussion, this section and the following section will attempt to reproduce the data of Hecht, Haig and Wald[35] for a two degree test field located five degrees from the point of fixation in the fovea. This curve has been widely reproduced over the years. The opening line of their abstract appears to be the source of the often repeated claim that dark adaptation occurred in two distinct phases (with each phase generally described later as exponential functions). No continuous process can be described by the product of two exponentials (such a process generates a new single exponential, $e^{x} \bullet e^{y} = e^{(x+y)}$). The process underlying the dark adaptation phenomenon involves a third order differential equation with a solution known as an exposine function.

- - - -

The signal flow diagram for a visual modality sensory receptor neuron is shown in **Figure 17.6.1-5**. The process begins with the stimulation of a ground state electron within the liquid crystalline chromophore structure coating a outer segment disk by the absorption (A) of a photon. This initial step promotes one of the electrons in the ground state (T_0) of the large number of oxygen atoms in this structure to one of the triplet energy states (T_1) in the liquid crystalline chromophore. There are a great many ($>10^8$) empty T_1 states within a contiguous liquid crystalline coating. Each excited electron is called an exciton. The triplet state of oxygen is a particularly stable state. An exciton can drop into the lowest empty T_1 state by thermal means. However, it will not drop back to the ground state in less than 10^{-3} to 10^{-4} seconds, a long time in quantum mechanics. If it does drop back to the ground state spontaneously, it releases a phosphorescent photon. If the exciton can transfer its energy to another medium in an intersystem crossing (ISC) energy transfer, it will, thereby de-excite itself with a return to the ground state (**Section 5.1.2**). In vision, this opportunity is provided by the adjacent dendritic structure of the PC.

---

[35]Hecht, S. Haig, C. & Wald, G. (1935) The dark adaptation of retinal fields of different size and location Selig Hecht, Charles Haig, and George Wald *Gen Physiol* vol. 19, pg. 321

The dendritic structure usually consists of nine cilia forming a chalice that holds the stack of chromophore coated disks. These cilia are typically present in individual notches around the edge of each disk (**Section 4.3.2** through **4.3.5**).

The result is the excitation of an electron within the dendritic structure from the valence energy band to become a free electron in the conduction band of the conduit forming the base connection to the 1st Activa (adaptation amplifier) of the PC. The summation of all of the free electrons formed per unit time constitute the base current, I_b flowing into the Activa. This current will cause an electron current about 200 times larger to flow from the collector of the Activa (not generally accessible in the laboratory) to the emitter (terminal indicated by the arrowhead). The emitter current, I_e, is usually considered equal to I_b for convenience in routine calculations. The current as observed in the emitter conduit constitutes the output signal of this circuit. By measuring the voltage across the impedance (2), the output voltage associated with this circuit can be measured. These emitter currents and voltages are not easily accessible in the laboratory. However, the signal output voltage is easily measured at the collector output of the following distribution amplifier that constitutes the axon of the PC (**Section xxx**).

In the absence of any stimulation, and after subsequent total dark adaptation, the voltage at the collector terminal of the 1st Activa, V_C, is believed to approach –154 mV, the assumed theoretical voltage produced by the electrostenolytic process that converts glutamic acid to GABA and injects one electron per converted molecule into the axoplasma. During active stimulation, current, I_b, will be injected into the base terminal of the 1st Activa as described above. As the stimulation intensity increases, the injected current will grow up to the saturation current limit of the 1st Activa. This interval constitutes the light adaptation phase of neural sensory receptor operation. As the intensity increases, the collector voltage will decrease due to the increased collector current, I_c, and the impedance of the electrostenolytic process. If the stimulus intensity increases above the supportable base saturation current, the chromophoric material will continue to create additional excitons until the chromophoric material is totally bleached and the outer segment appears transparent to axially applied photons. Under this condition, the ophthalmologist typically sees and reports the material of the RPE behind the active retina as exhibiting a reddish color. Following cessation of stimulation, the current injected into the base terminal of the 1st Activa will continue at a high level as the excitons of the chromophoric material continues to de-excite by producing additional free electrons in the base circuit (dendritic structure). This interval constitutes the dark adaptation or recovery phase of neural sensory receptor operation. Upon total dark adaptation, the chromophoric material of any individual outer segment will absorb all of the photons presented at a reasonable rate and each outer segment will appear totally black, except for a small number of photons reflected from the surface of the outer segment shared with the inner segment. **Section xxx** presents a broader discussion of these mechanisms and a comprehensive serape presentation of these features of operation. The underlying mechanisms related to the electrostenolytic circuit supplying electricity to the Activa is described in **Figure 17.6.1-1** and in **Sections 8.1.3** & **8.6**).

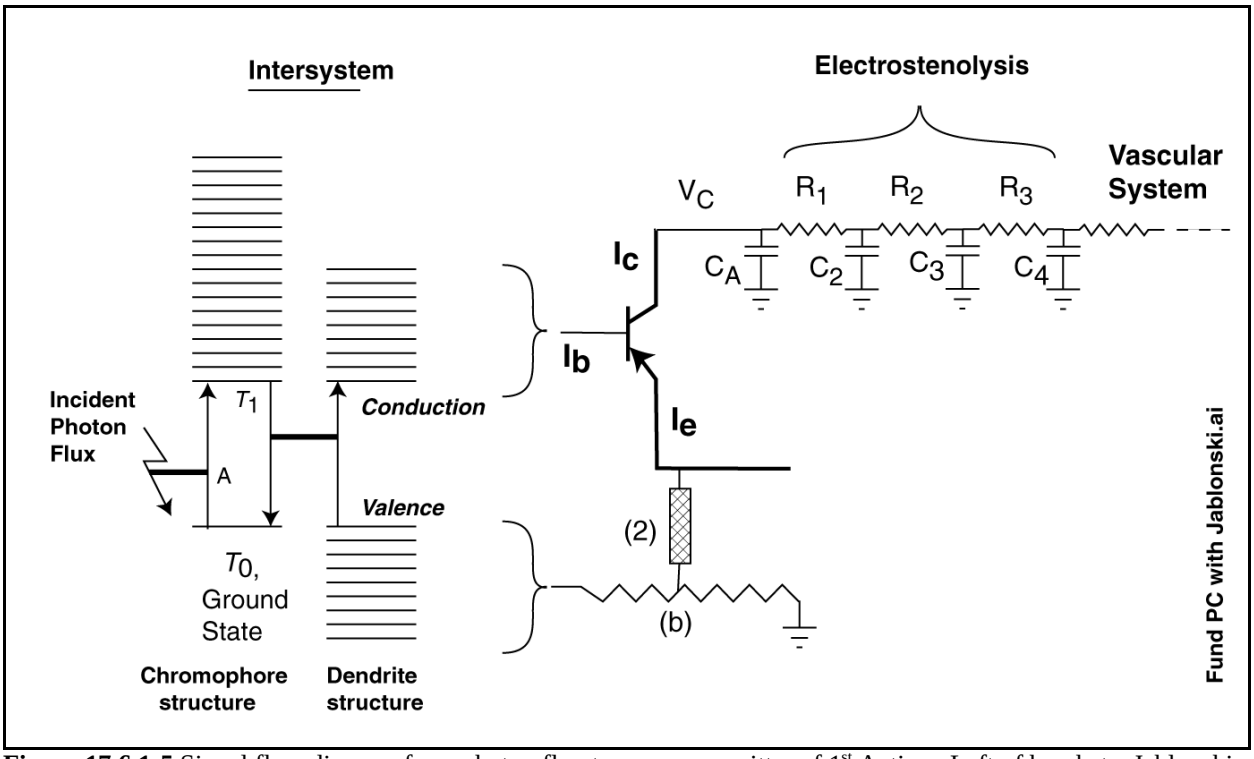

Figure 17.6.1-5 Signal flow diagram from photon flux to common emitter of 1st Activa. Left of brackets; Jablonski diagram for the oxygen atoms associated with the liquid crystalline chromophore structure. Right of brackets; the circuit diagram of the 1st Activa (adaptation amplifier) of a photoreceptor neuron. See text.

[

The papers of Hecht & associates have been mentioned many times. The data points shown in **Figure 17.6.1-6** are reproduced from one of the most widely published graphs of Hecht, et. al[36]. Solving the above expressions for the required threshold illumination, and plotting them on the same logarithmic scale, results in the two smooth curves shown. The solid curve represents only the exponential component of the solution to the third order differential equation. It clearly shows the unique shape of the reciprocal of an exponential function with a time constant of thirty minutes. The dashed curve shows the complete solution to the differential equation. It shows the product of the damped sinusoid and the exponential, called hereafter the *exposine* function. By selecting the time constant and period of the waveforms, the data points can be matched very well. The precision of the model is sufficient to highlight the unexpected decrease in sensitivity (upward excursion of the data points) in the recorded data near 35 minutes. For the conditions Hecht defined, the time constant of the exponential function is 30minutes. The period of the sinusoidal function is 12 minutes. The modulation, b, is approximately 25%. This modulation suggests a significant involvement of the diffusion mechanism in supporting the electrostenolytic process at 400,000 trolands.

[36] Hecht, S. Haig, C. & Chase, A. (1937) The influence of light adaptation on subsequent dark adaptation of the eye. *J Gen Physiol* Vol. 20, pp. 831-850

Hecht et al. have provided many individual dark adaptation characteristics based on many pre-adaptation illumination levels and different positions in the retina. The amplitude parameters associated with the more precise characterizations can be determined exactly as for the above data. Unfortunately, some of their data suffers from test set limitations. Much of it suffers from inadequate spectral calibration and the use of photometry instead of more precise radiometry. Their famous figure 2 of 1937 [**no callout, same as fig 17.6.1-9]** appears initially to be limited to a floor of about 3 microtrolands. Although this floor makes it difficult to detect the sinusoidal variations in parts the right part of the figure, the data does extend to six time constants for the lower luminance values. However, estimates can be made from the left portion of the figure based on the parameters of the highest intensity curve. Some of the resulting data is summarized in **TABLE 17.6.1-1.** A clear conclusion from the data of Hecht shown in this table is the fact that as the illumination level prior to dark adaptation is lowered, the impact of the vascular system becomes much less and the sinusoidal component in the response becomes correspondingly much less (although a discerning eye can still trace its impact in the data points). Additional dark adaptation data of a pathological nature appears in Adler and will be reviewed in **Section 18.8.2.** The general conclusion is that if the impedance of either the electrostenolytic process or the vascular supply network increases, the rate and depth of dark adaptation of the eye is impeded at low light level. This is to be expected since the collector voltage takes an exceedingly long time, if ever, to approach its ultimate quiescent voltage.

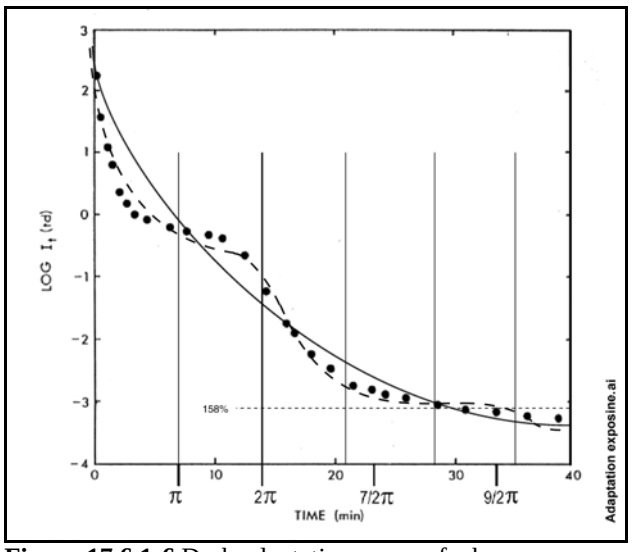

Figure 17.6.1-6 Dark adaptation curve of a human observer, following a 2 minute exposure to an adapting light of 4 x 10^5 td. The solid and dashed lines are from this theory. The dotted line indicates the value of the time constant of an exponential plotted as a reciprocal. The data points are from Hecht, et. al, 1937. The test spot was violet, had a diameter of 3 degrees, a duration of 200 ms, and fell 30 degrees from the fovea.

Figure 17.6.1-7 from Hecht, Haig & Wald in 1935[37] displays threshold data for a two degree test field as a function of field position in object space. **[give subjects identification]** The data is more difficult to interpret because of the paucity of data points in each data set. The data points have nearly the same pitch as the expected sinusoidal component. Here again, the data shows the normal familial form and estimates can be made based on the first fifteen minutes of data. Only the test field centered on the fixation point is clearly different. It shows no oscillatory component, a very short time constant and a high ultimate threshold. These features clearly indicate a different vascular environment for the foveal area of the retina. The data is from one person who may have suffered from significant disease of the foveal retina. This figure is one source of the premise that the human eye exhibits very poor on-axis threshold sensitivity when dark adapted. It suggests the on-axis performance is at least 60 times poorer than a similar position in the periphery. However, only two data points, 25 minutes apart, are presented to support this conclusion. This author has been unable to perceive a change in personal threshold of more than a factor of two between his fovea and 2 1/2° from the fovea after adaptation to starlight conditions.

The dash-dot curves in the figure represent the exponential term in the "expanded damped sinusoid" proposed in this work as the theoretical function describing the complete dark adaptation characteristic. Hecht, et. al. did not describe a complete curve for the dark adaptation characteristic for the 2 1/2° field position. A set of complete curves has been added based on this theory. The curves were drawn freehand because of the lack of adequate parametric data and the paucity of data points. Note the compatibility of the off-axis data points to the expanded damped sinusoid curves proposed in this work.

Based on the theory of **Section 16.3.5.2**, all of the curves should eventually reach an asymptotic value corresponding to the intrinsic voltage of the electrostenolytic process (assuming adequate vascular performance). Beyond the

[37]Hecht, S. Haig, C. & Wald, G. (1935) The dark adaptation of retinal fields of different size and location, *J Gen Physiol* Vol. 19, pg. 321

fovea, the data appears consistent with minor changes in the time constant of the exponential term and minimal change in the frequency associated with the sinusoidal term. Note the 2 1/2° data has only reached three time constants in time before the end of the graph. The 10° data has reached 6 time constants and its threshold value should correspond closely to a collector voltage equal to the intrinsic electrostenolytic voltage level. The discussion of the significance of these changes is beyond the scope of this work.

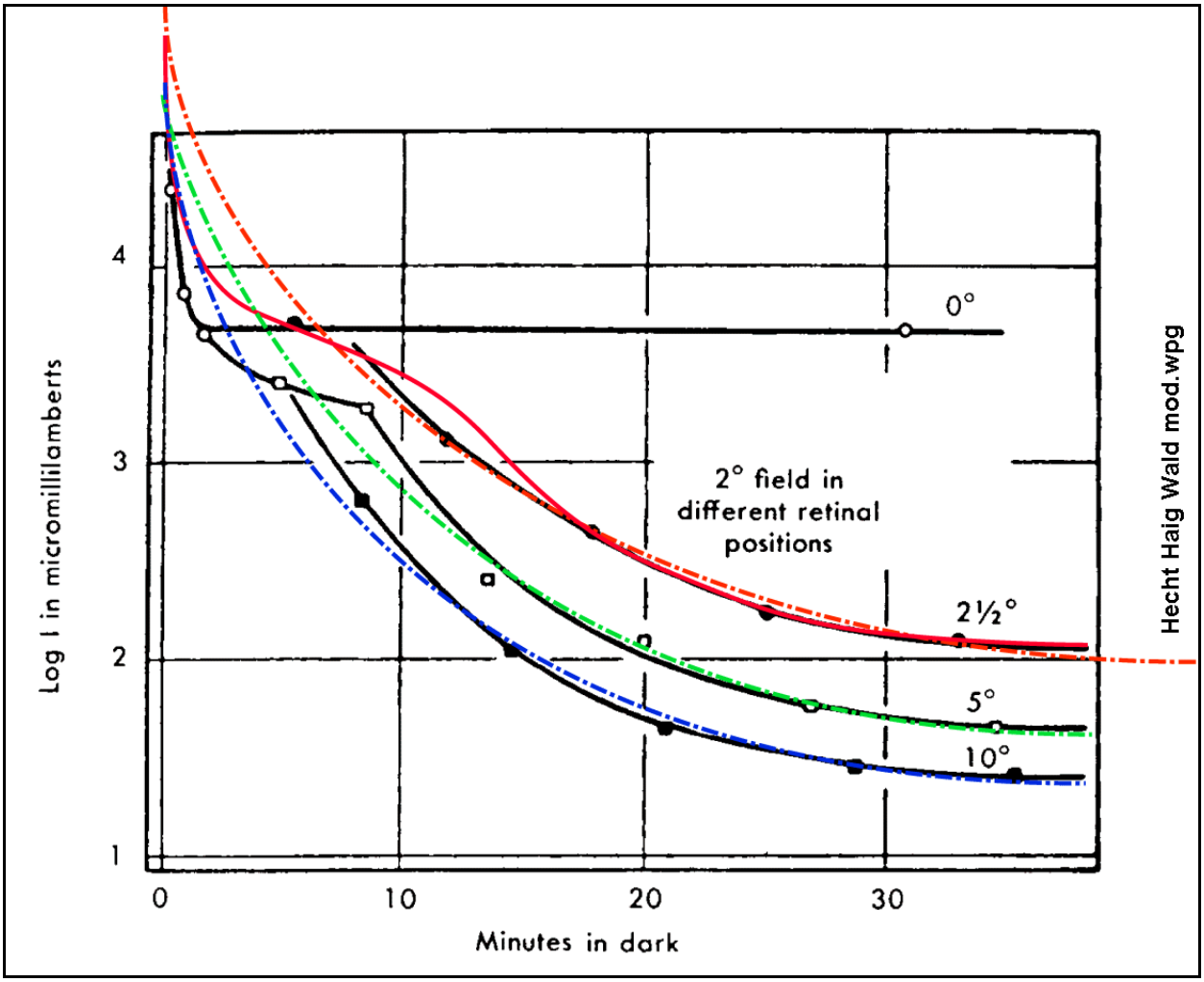

Figure 17.6.1-7 Relative threshold sensitivity for one possibly pathological subject as a function of field position. The 0° line is highly suspect. It shows a foeveal sensitivity 100 times less sensitive than at 2 ½° eccentricity. Dash-dot lines are simple exponentials. Solid lines (except as noted) represent exposine functions. Data points from Hecht, Haig & Wald (1935).

TABLE 17.6.1-1
PARAMETERS ASSOCIATED WITH DARK ADAPTATION IN HUMAN
Estimated values awaiting significant mathematical backup by "students"

Subjects	Prior Conditions			Dark Adaptation Conditions						Source of Data
	"Color"	Level mL.	Time min.	Test Loca.	Test "color"	τ min.	ω milliHz	φ angle, °	C_S	
	White	4173	2	6°N	Green	6.5	1.5	45	0.2	Spillmann, fg. 1
Versus light adaptation level										
S. H(echt).	White	400*	2	30°N	Violet	10	0.9		0.25	Hecht '37, fg. 2
	"	38.9	2			7	1.2		0.2	
	"	19.5	2			4	1.5		0.1	
	"	3.8	2			3	2.4		<0.05	
	"	0.263	2			<2	2.8		<0.02	
Versus retinal position										
				10°		5	1.2			Hecht '35, fg. X
				5°		7	1.3			
				2.5°		11	0.9			
				0°		<1	—		—	

Test locations are given relative to the fixation point. N indicates in the nasal direction of the horizontal plane.

* Hecht & associates worked in an archaic unit, photons, a measure of retinal illumination. This unit was renamed the troland after an early pioneer in this area, Dr. L. T. Troland. The term has recently been expanded to include both scotopic and photopic trolands. One troland is produced when the eye, suitably adapted, observes a surface of π/10 millilambert brightness through a 1 sq. mm. pupil. The values shown are in thousands of trolands (photons).

Newell has provided a highly stylized dark adaptation characteristic based on the conventional wisdom[38]. It does not reflect the true character of the response as illustrated in [**Figure 17.6.1-3**] and it indicates the visual system is non-functional at light levels only slightly below full moon. It is archaic and should not be relied upon.

With the actual dark adaptation characteristic being dependent on the initial conditions of both the voltage on the collector of the Activa and at the nodes of the electrical equivalent of the electrostenolytic system, it becomes possible to understand the additional data in the literature. **Figure 17.6.1-8** is an expansion of Hecht, Haig & Chase[39]. It provides a dramatic demonstration of the exposine function predicted by this work as the level of light adaptation, prior to dark adaptation, is varied. At 263 Trolands, the response is a simple exponential. As the level of photon flux is increased during light adaptation, the sinusoidal component of the exposine function makes a dramatic appearance althought the second repitition of the sinusoid in the time interval of 18 to 40 minutes.

They sought to demonstrate that "The course of dark adaptation of the human eye varies with the intensity used for the light adaptation which precedes it." It has been redrawn to show the initial condition in terms of illumination and to a transient not normally displayed. This is the transient associated with the opening of the iris (six second time constant). This transient has an amplitude range of about 16:1.

The target used by Hecht, Haig & Wald in the 1937 paper was unusual. It was a large cross extending across the entire background field formed by two orthogonal 30 arc minutes wide stripes. Such a pattern has a much lower threshold sensitivity than a simple filled circle of 30 arc minutes or a square 30 arc minutes on a side due to the

[38]Newell, F. (1986) Ophthalmology, 6th ed. St. Louis, MO: C. V. Mosby, pg 97
[39]Hecht, S. Haig, C. & Chase, A. (1937) The influence of light adaptation on subsequent dark adaptation of the eye *J. Gen Physiol* page 831-850

spatial integration performed within the visual system.

As is usual in the literature, a poorly defined "white light" was used as a stimulus. In this case, the test stimulus was also defined less than specifically. Note also the original authors highly unorthodox use of the Troland. At 30 degrees off the fixation axis, the image of the test stimulus would be aberrated to a larger area than anticipated on the retina.

In the upper left of the figure, each curve exhibits essentially the same initial transient, dropping to 5% of its initial value in about five seconds and to 1.0% in about seven seconds. These values correlate with other values in the literature. The complete curve is shown for the 400,000 Troland test. Note how this curve drops precipitously initially because of the short time constant associated with the chromophore. The curve then blends into the original authors curve at a level between 10^9 and 10^{10}. The result is a curve with two shoulders. Each of the curves will exhibit a similar initial decay. However, they will vary slightly in size because of the variation in adaptation amplifier gain as a function of illumination.

Note in the lower left how the 263 Troland initial condition has not impacted the voltage at the second node of the electrical equivalent of the diffusion process. The original curve exhibits only one time constant of approximately four minutes. As the light level is raised during the adapting period, the voltage at the second equivalent node of the electrostenolytic process is impacted and the resulting transient develops the familiar two stage form. Note carefully in this figure, the variation in when the subject reported the test stimulus became achromatic . Based on the absence of a solid triangle associated with the 263 Troland level, the bottom curve does not display any "cone to rod transition," even though it starts above the level of chromaticity and ends at a much lower threshold level than the other curves. This is another clear example that "the Emperor has no clothes," i. e., the less than precise morphological feature distinguishing photoreceptors has no place in the electrophysiology of the eye.

Heckenlively[40] has presented a dark adaptation curve that appears to show a third break in the curve at approximately 25 minutes. The curve is for a two degree test field at an unspecified position and illuminance. This may be indicative of an additional node in the normal vascular system or it may be a pathological situation in the subject.

---

[40]Heckenlively, J. (1988) Retinitis Pigmentosa, NY: J. P. Lippincott, pg 12

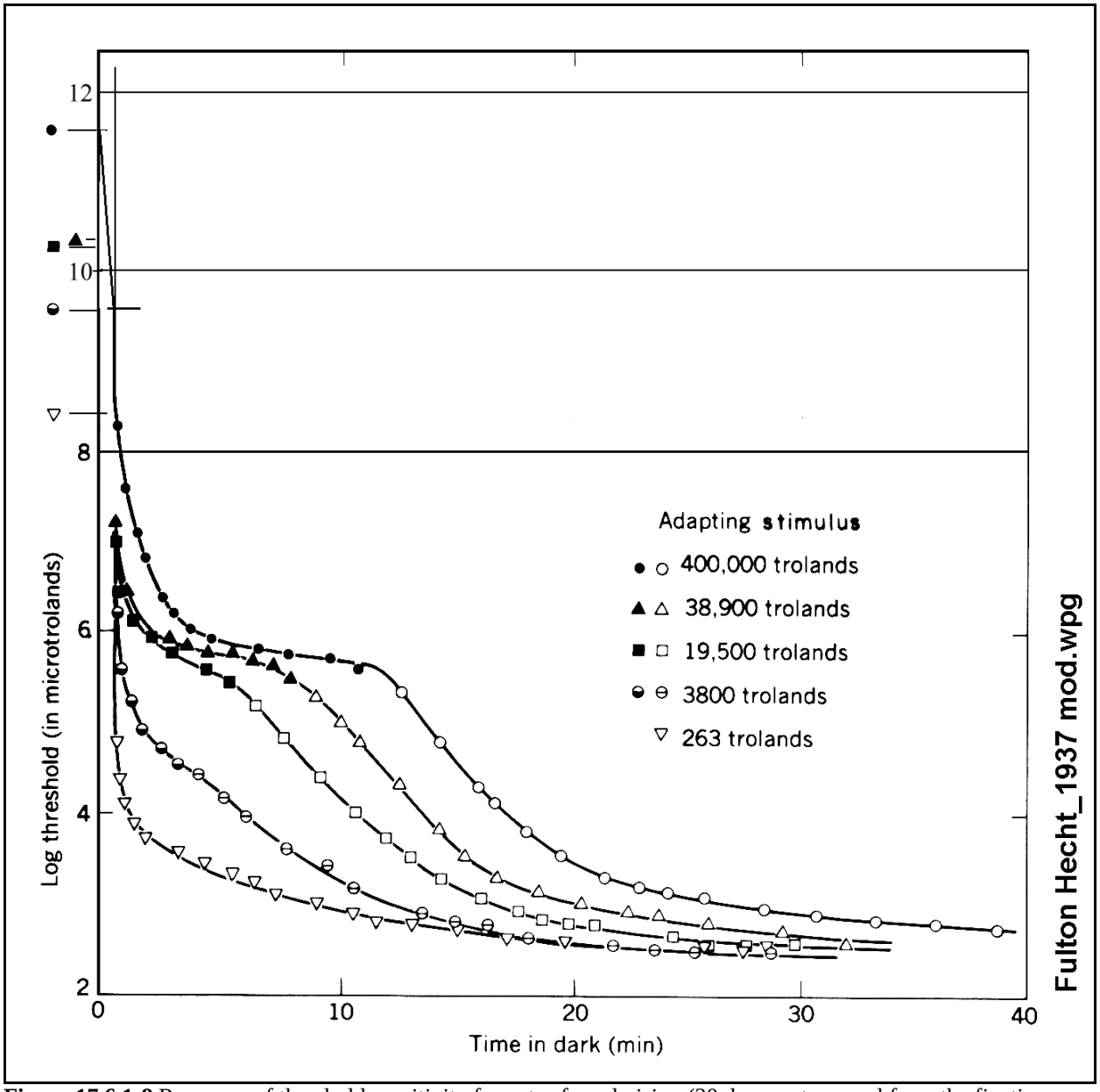

Figure 17.6.1-8 Recovery of threshold sensitivity for extra-foveal vision (30 degrees temporal from the fixation point). The eye was first adapted to "white" light for 2 min at the fixed retinal illuminance shown using a 30 degree diameter field. The "violet" test stimulus (wavelengths below 480 nm) consisted of a cross (each arm of 30 minutes of arc width) presented in 0.2 sec pulses against a background field of 5 degrees diameter. Both target and background field were presented in Maxwellian view. For the test stimulus to be treated as visible, the observer had to recognize it against the uniform background field. Filled in symbols indicate that a violet color was apparent at that threshold. Empty symbols indicate a colorless sensation. Original authors estimated the threshold was approximately three times the absolute threshold. Expanded from Hecht, Haig & Chase, 1937. See text.

[rewrite]
Based on the above discussion, it is now possible to interpret **Figure 17.6.1-9** properly. Although the graphic style is difficult to evaluate, it is by the same team and uses the same illumination levels. However, it is for foveal vision and the test stimulus was changes to a three degree "red" light. As the caption indicates, "this was to reduce interference from rod vision." The assumption can be made that the curves were only meant to present data on

“cone” vision. Note initially, the fovea is considerably smaller than the three degree test stimulus. Thus the data contains some unspecified and unsought physiological signal manipulation. “Red” and blue, also present in the “violet” source, are both awkward to use in a pulse stimulus because of the low bandwidth of the chrominance channels for these colors. Although the data from this time period is very useful from an exploratory perspective, it would be useful to repeat this experiment using the 46 arcminutes of Poot et. al. and more tailored light sources in order to remove some uncontrolled variables from the data.

There is very little sign of the second node of the vascular system in this figure. However, other authors have found multiple branches at still higher levels of illumination[41]. The important conclusions to be drawn are three:

Regardless of the adapting light level, the threshold sensitivity of the human eye for a three degree test stimulus of short “red” pulses on the line of fixation is at approximately 5.5 log units in micro-Trolands, all parameters as defined in the late 1930's.

The experiments need to be repeated under conditions where there is more control of and less cross coupling between the parameters within the visual system. This can best be achieved using narrow spectral band adapting radiation and narrow band test stimuli.

The vascular supply to the Outer Segments in the fovea appears abundant. At adaptation levels up to 400,000 Trolands, only diffusion within the IPM limits the dark adaptation recovery time.

A more detailed study of the vascular system in the vicinity of the fovea on the RPE side of the retina is warranted. With better data and more knowledge of the vascular system in this area, more substantive conclusions can be drawn which may lead to important progress in the clinical treatment of the retina.

---

[41]Du Croz, J. & Rushton, W. (1966) The separation of cone mechanisms in dark adaptation, J. Physiol. Vol 183, pg. 481

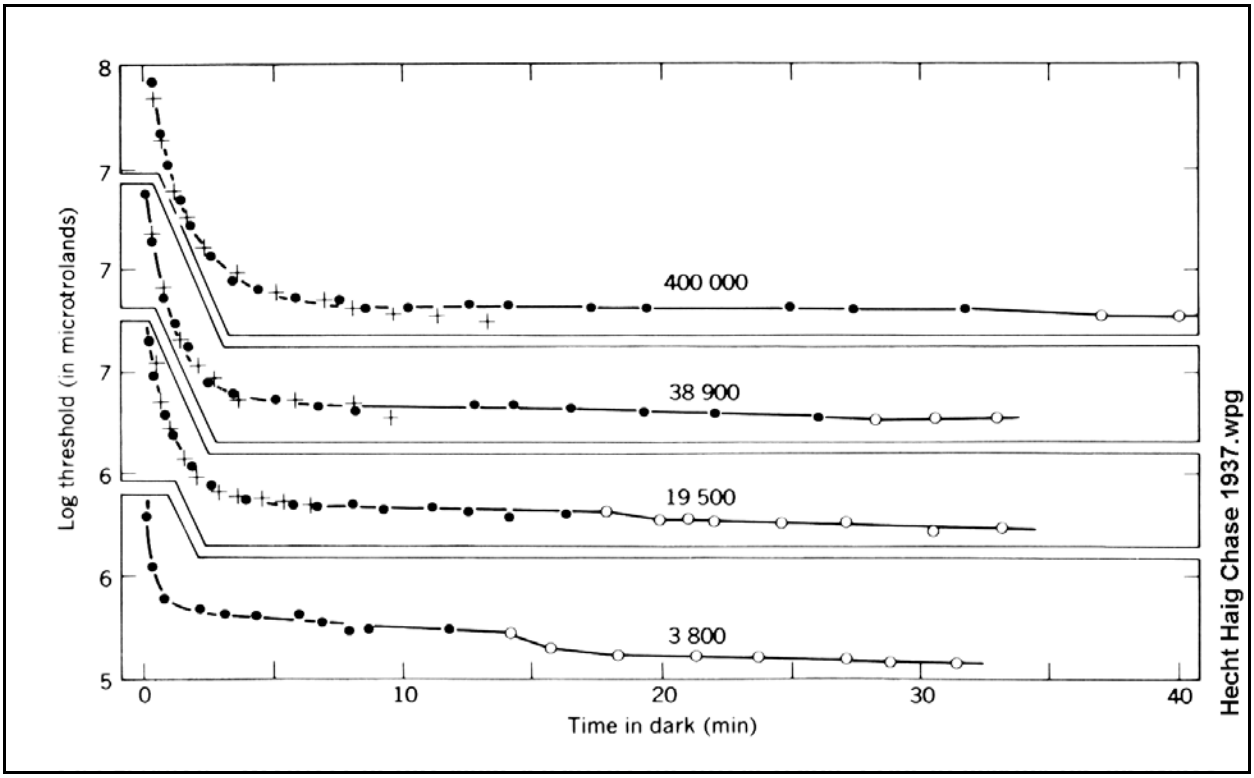

Figure 17.6.1-9 Recovery of threshold sensitivity for vision 30° from the fovea. A 2 min. Adaption to "white" light was provided at the levels indicated. A red (λ>690 nm.) 3 degree test stimulus was presented in 0.2-sec. pulses. The red color was used to reduce interference from rod vision. For the test stimulus to be treated as visible, the observer had to detect it in a broad black cross. The filled circles indicate the subject perceived the test image as red. The open circles indicate perception of an achromatic test image. The + symbols represent similar tests using violet (l < 480 nm.). From Hecht, Haig, and Chase (1937). **[xxx New fig without** +'s]

Glezer has provided further confirmation of the exposine characteristic of the dark adaptation characteristic in humans as shown in **Figure 17.6.1-10**[42]. His experiments clearly show the effect of target size and the distinct difference in performance as a function of position on the retina. All of the curves show the signature of the exposine function rather than the distinct break commonly associated with the two-exponential hypothesis. No abrupt change in slope appears in any of the responses.

[42]Glezer, V. (1965) The receptive fields of the retina *Vision Res* vol 5, pp 497-525

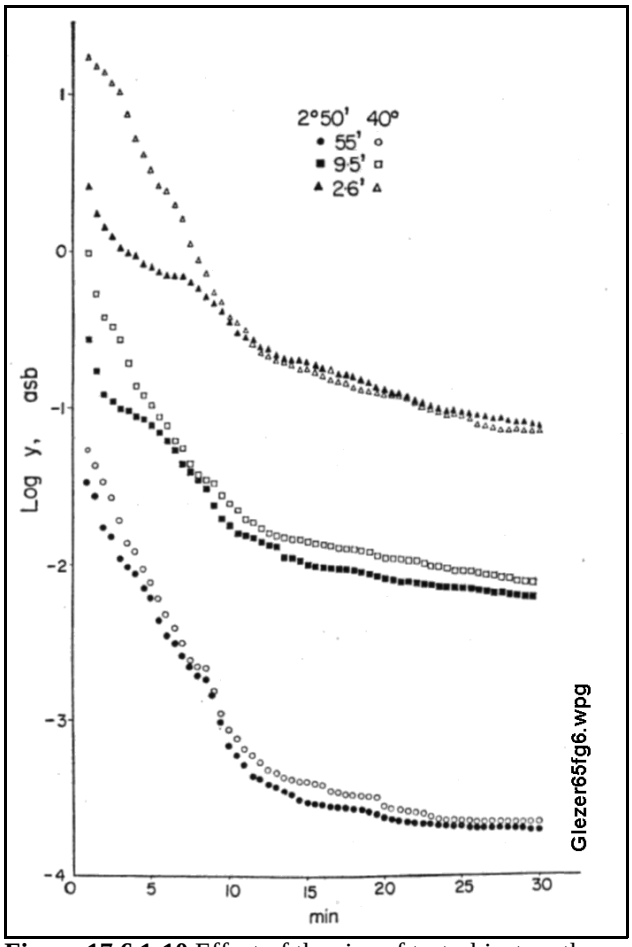

Figure 17.6.1-10 Effect of the size of test-object on the dark-adaptation curve and its localization on the retina. Tests were performed at 2°50' and 40° from the fixation point using test-objects of three different angular diameters. Subject A.A. From Glezer, 1965.

17.6.1.2.1 Further falsification of the conventional wisdom

Figure 17.6.1-11 presents data from Spillmann & Fuld from 1979 showing clearly that the conventional wisdom that the dark adaptation characteristic is founded on two exponential functions can not be correct[43]. Their goal was to find whether a single equivalent background curve could be obtained if retinal eccentricity were used as a parameter. They collected data for both a 2° test stimulus applied for 175 msec and a 0.5° test stimulus for 40 msec. Although no data points are shown, they noted, "The number of data points was so large and the day-to-day variability so small, that any error introduced by fitting the curves by eye was considered to be minimal."

Their data at multiple eccentricities show a consistent up turn in the responses prior to the expected a-break. Such a feature is not compatible with the concept of two concatenated exponential functions. All of the individual functions are compatible with the exposine waveform proposed in this work (**Section 17.6.1.2**) and displayed in previous figures. ***By treating the amplitude of the sine function within the exposine function as a function of the eccentricity, the goal sought by Spillmann & Fuld is realized and defined.***

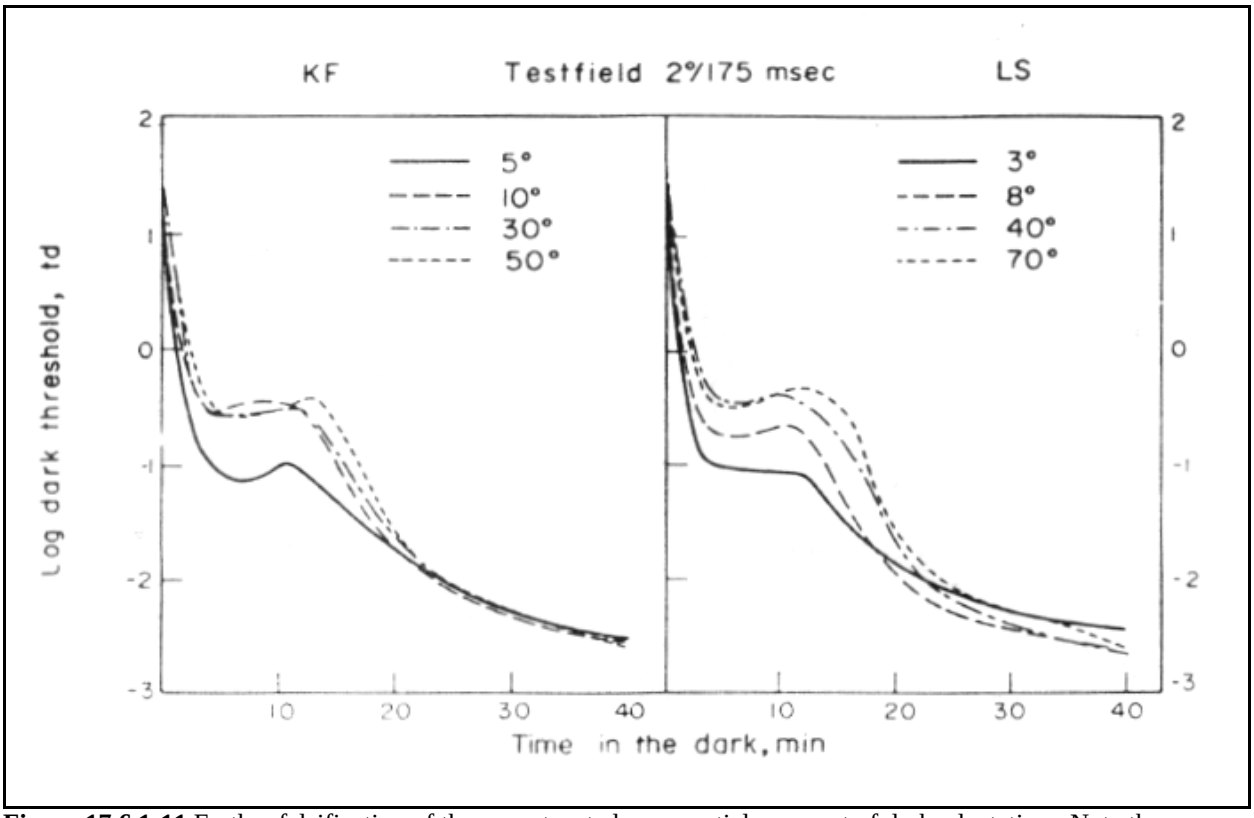

Figure 17.6.1-11 Further falsification of the concatenated exponentials concept of dark adaptation. Note the systemic rise in the initial dark adaptation function near 10 minutes, prior to its additional drop to ultimate threshold sensitivity on the right. A white light of 300,000 photopic td at a color temperature of 6740° Kelvin, was used as a stimulus prior to determining the individual dark adaptation characteristics. See text. From Spillman & Fuld, 1979.

17.6.1.3 Light Adaptation, from dark adaptation

[43]Spillmann, L. & Fuld, K. (1979) The equivalent background and retinal eccentricity *Vision Res* vol 19, pp 117-122

With the parameters of the vascular supply system in hand, it is possible to refer again to the schematics in **Section 17.6.1** and examine the operation of the photodetection system following an increase in illumination, whether large or small.

17.6.1.2 Light Adaptation, incremental change

Poot et. al. Provide excellent data for the incremental case starting from a high adaptation level.
Both the ON and OFF transients in human have been described by Poot, et. al. based on psychophysical experiments using radiation at 563 nm. (FWHM of 30 nm.)[44]. They employed a Maxwellian illuminator and concentrated on the transient performance of the eye over the time interval of less than one second. This time interval is in contrast to the older, but widely referenced, data of Hecht[45] showing the performance over periods of minutes. They did not control the size of the pupil except via the illuminator.

Poot completed her Doctoral thesis in 2000 with a significant discussion of her understanding of adaptation and providing a block diagram (figure 2) of the adaptation process[46]. Unfortunately, her model continues to assume a symmetrical temporal response related to both light adaptation and dark adaptation. Otherwise her paper is a significant contribution. The work is focused on the initial stages of the neural system of the visual modality but it provides no circuit diagram supporting her conceptual block diagram.. She does introduce the difference between luminance and brightness in her explanation of how the large range of luminance is converted into a narrower brightness range but provides no quantifiable particulars. In this regard, she does continue to describe the obligatory but archaic concept of the difference in performance between the putative rods and cones. As a result of her underlying assumptions, her figure 2 includes a profusion of individual blocks in a single block diagram. The diagram relates more to satisfying an underlying thought experiment than it does to a minimalist diagram satisfying the Razor of Occam. By recognizing the asymmetry involved in the operation of the first Activa (acting as the adaptation amplifier) of each visual sensory neuron, a much simpler overall block diagram becomes available that is consistent with the actual circuit diagram of this amplifier. The title of her first chapter recognizes this asymmetry but does not account for it in her model.

---

[44]Poot, L. Snippe, H. & Hateren, J. (1997) Dynamics of adaptation at high luminances: adaptation is faster after luminance decrements than after luminance increments. J. Opt. Soc. Am. A vol. 14, pp. 2499-2508
[45]Hecht, S. XXX (1937) rods, cones and the chemical basis of vision. Physiol. Rev. vol. 17, pp. 239-290
[46]Poot, L. (2000) Light Adaptation and Early Processing in the Human Visual System. Netherlands: U. Groningen Thesis

17.6.1.2 Dark adaptation as a function of aging

Jackson, Owsley & McGwin have provided an excellent study of the effect of aging on dark adaptation[47]. Although their discussion makes the conventional assumption concerning the "rod-cone break," they do note the existence of an undefined second break in the 20-30 minute region as predicted and explained by this theory. **Figure 17.6.1-12** shows their data. Between eight and twenty-one subjects were used in each ten-year wide age group. While they speak of a four-segment linear analysis, their labeling only speaks of the second and third component and the rod-cone break. Using the exposine theory of this work, a single mathematical function passes through all of the segments of each curve as a function of age. The exposine is shown in blue for the 20-year old class. No segmented linear analysis is required. A larger statistical group would be needed before a more accurate overlay could be calculated.

It is clear that the change in the amplitude of the sinusoidal component of the overall response is small compared to the change in the exponential component. It is also clear that the ultimate dark adapted sensitivity decreases considerably with age (possibly an order of magnitude loss). Both of these effects can be explained by a decrease in the performance of the hydraulic system supplying the retina (hardening and clogging of the optic arteries). [xxx should I overlay the exposine on this figure ?]

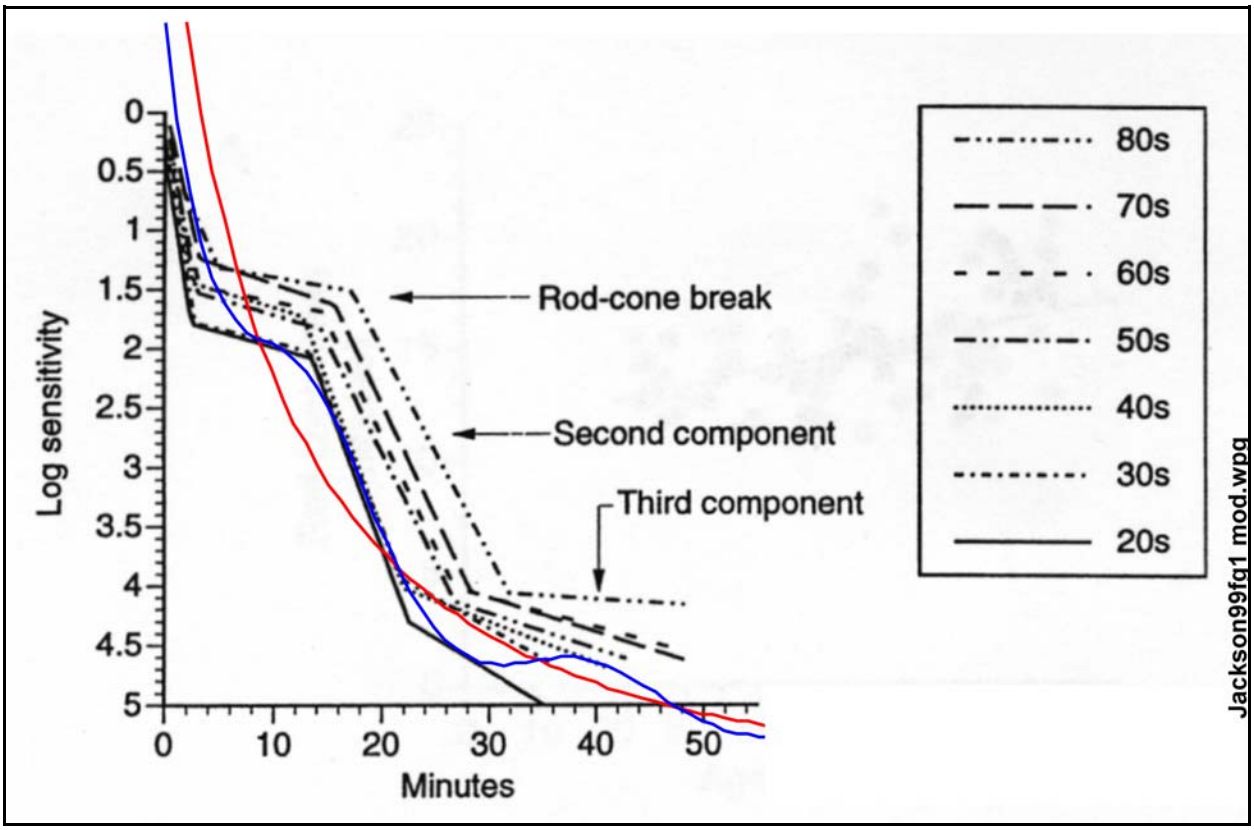

Figure 17.6.1-12 Dark adaptation as a function of age. The blue line shows the exposine overlaying the response of the 20-year olds well within a ratio of 3:1. The red line shows a best fit exponential without the sinusoidal component. The label "Rod-cone break" is extraneous. Each of the responses is better fit by an exposine function. See text. From Jackson, Owsley & McGwin, 1999.

[47]Jackson, G. Owsley, C. & McGwin, G. (1999) Aging and dark adaptation *Vision Res* vol 39, pp 3975-3982

17.6.1.3 Chromatic Adaptation as a parameter in the Luminous Efficiency Function

Wooten, Fuld & Spillmann[48] have provided some interesting data on off-axis spectral sensitivity as a function of dark adaptation recovery time. It is only interesting in the light of the model available from this work. Otherwise the complexity is overwhelming. Although described as luminous efficiency functions obtained for an observer at 30° retinal eccentricity, the curves demonstrate several additional characteristics. First, the light source used for preadaptation was "similar" to C.I.E Illuminant A. The source was deficient in the blue compared to a 7053°K source and has significantly adapted the subject chromatically. The apparent sensitivity of the S-channel has been enhanced by at least 10:1 relative to normal. In fact, the M- and L-channels were suppressed. Thus, a more appropriate title would be "Recovery of normal luminous efficiency after chromatic adaptation." Second, the data in the upper traces has relied upon other dark adaptation curves obtained after abrupt extinguishing of the background stimulus for calibration purposes. No details were given of how long the light was on before it was extinguished. The traces as a group do give a clear idea of the time required for the M- and L-channels to return to normal sensitivity. In this case, about three minutes. Notice that both channels recovered in parallel due to their similar time constant, R_1C_A. The peak on the left of the lower trace correctly determines the peak sensitivity of the S-channel. Unfortunately, the spectral resolution of the equipment did not determine the half amplitude points of the spectrum as well as it could have. The trace is similar to the curve of Wald (1964).

The luminous efficiency function is significantly impacted by differential adaptation ("bleaching" with various narrow band lights). This sensitivity can only be documented based on a visual luminous efficiency function developed from a detailed model of the visual system. **Figure 17.6.1-13** presents a composite of the predicted human visual system as a function of several states of differential adaptation designed to isolate both the L-channel photoreceptor response and the Purkinje Peak described in Section xxx.

As noted earlier, the visual luminous efficiency function is very sensitive to both the diameter and the length of the individual photoreceptor outer segments. A very slight increase in the diameter can increase the absorption width of the particular spectral channel due to the Pauly Exclusion Principle (**Section 5.xxx**). A change in the length of the outer segment can change the absolute maximum absorption that a particular photoreceptor can achieve. When these two factors are considered, the visual luminous efficiency function of an individual can differ significantly at the research level, although it is doubtful the difference could be noticed by two individuals during normal daily activity, even if they knew of the potential difference[49].

The sensitivity of the visual luminous efficiency function to differential adaptation has caused a serious problem in vision research. The problem centers on the inadequacy of earlier test protocols designed to determine the spectral response of the long wavelength photoreceptors. The protocol used by Wald was demonstrably inadequate for two reasons. Unfortunately, that protocol has been adopted as a standard by many psychophysical laboratories since he introduced it. The primary problem was the level to which the M-channel was bleached in order to isolate the L-channel. The secondary problem was the limited bandwidth of the filters used to measure the spectral response after bleaching. His filters appear to have been about 30 nm wide, the nominal type available in his time. Such filters result in a significant smoothing of the overall response relative to the actual performance of the eye being measured.

The top pair of heavy lines in the figure represent the nominal visual luminous efficiency function of the eye based on the theory of this work. The solid line represents the theoretical response in the absence of any smoothing. The dashed line represents the theoretical data smoothed with a 20 nm filter. While the theoretical curve peaks at the expected 532 nm, the smoothed version peaks farther toward the red by an amount determined by the width of the smoothing filter. In this case, the smoothed curve peaks near 550 nm, the widely accepted value in the general literature. No sign of a peak in the vicinity of 565-575 nm appears in these plots.

---

[48]Wooten, B. Fuld, K. & Spillmann, L. (1975) Photopic spectral sensitivity of the peripheral retina. J. Opt. Soc. Am. vol. 65, pp. 334-342. *also in* Wyszscki & Stiles pg. 407

[49]—, (1963) The Science of Color. Washington, DC: Optical Society of America pp 226

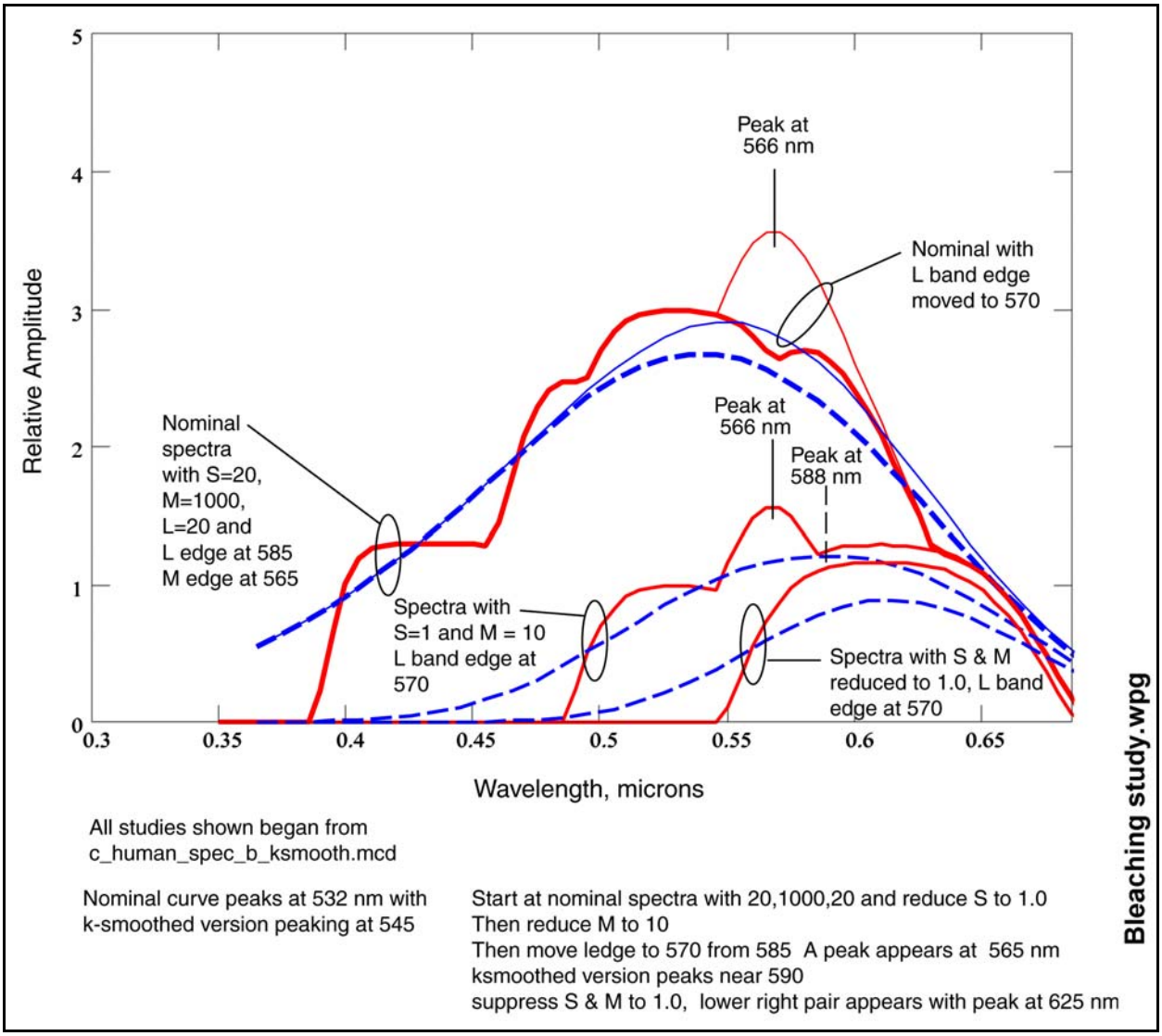

Figure 17.6.1-13 The sensitivity of the human visual luminous efficiency function, V(lambda), to differential adaptation. The upper pair of graphs were based on relative sensitivities of S:20::M:1000::L:20 at the point where the luminous efficiency function was produced as a generator waveform within the retina. The other curves show the effects of changing the distance between the edges of the M-channel and L- channel responses, or of suppressing the M-channel response in order to isolate the performance of the L-channel. See text.

The nominal curve was drawn with the long wavelength edge of the M-channel at 565 nm and the short wavelength edge of the L-channel at 585 nm. The overall luminous efficiency function is very sensitive to the distance between these two edges. The pair of light lines at the upper right, that merge with the previously described heavy lines, display the effect of changing the effective distance between these two edges. By moving the short wavelength edge of the L-channel to 570 nm, a Purkinje peak is introduced into the theoretical luminous efficiency function that peaks at 566 nm (even though there are no photoreceptors present at or near that wavelength. The peak in the smoothed response has moved to about 565 nm. This sensitivity to the width between these edges was obtained without any differential adaptation (bleaching). This change shows the sensitivity of the distance between these edges in human vision. Minor differences in growth of the photoreceptors can cause differences in this dimension.

The middle set of curves were obtained by reducing the sensitivity of the S-channel by 20:1 and the M-channel by 100:1 (a significant level of bleaching). The resulting luminous efficiency function now exhibits a maximum at 568

nm for the theoretical curve and 588 nm for the smoothed curve. No photoreceptor is located at either of these wavelengths!!! This enhanced sensitivity in the region of 565-575 nm was first reported in xxx and has come to be known as the Purkinje Effect. It is commonly noticed by all humans during the approach of sunset when the light level in the S-channel and M-channel regions of the spectrum falls faster than it does in the L-channel region. The result is an increase in sensitivity in the 565-575 nm region[50]. The smoothed curve in the middle set of curves closely matches the spectrum published by Wald in 1964, and assigned to the L-channel photoreceptor, but without any description of the level of M-channel suppression used[51,52]. A wide variety of Investigators have relied upon the Wald data or protocol for many years. Stockman & Sharpe have recently presented a composite of the estimates of many of these investigators[53]. Their proposed L-channel photoreceptor response is quite broad. The peak is somewhere between 550 nm and 560 nm. Their composite is bracketed very nicely by the smoothed curves in the upper two pairs of curves in the above figure.

By increasing the adaptation level, in order to reduce the sensitivity of the M-channel by 1000:1, an entirely different situation is encountered. The third set of curves in the figure illustrate this condition. Both the theoretical and the smoothed responses have moved to 625 nm, the location of the true L-channel photoreceptor absorption spectra. There is no indication of any photoreceptor response in the 565-575 nm region in these responses.

This discussion has shown that previous protocols have not been adequate for isolating the L-channel spectral response. Suppressing the M-channel response by 100:1 results in a measured peak luminosity response in the 565-575 nm region that has generally been assigned (erroneously) to the L-channel receptor in the literature. Suppressing the M-channel response by only 10:1 results in a smoothed response with a peak in the 555-565 nm region as illustrated by Stockman & Sharpe. Suppression of the M-channel response by a factor of 1000:1 or greater is necessary to isolate the L-channel photoreceptor response. At this level of differential adaptation, the L-channel's peak response is found to be at 625 nm. This wavelength is in consonance with the long wavelength phosphor typically used in kinescope displays and is in general agreement with the absorption spectrum of the dyes used in process color printing. The location of the L-channel response at 625 nm places much more distance between the peaks in the M-channel and L-channel responses than generally discussed in the literature. As shown in Chapter 5 of this work, the theoretical peaks of all of the photoreceptor spectra form a linear array with a spacing of 95 +/-2 nm.

Any psychophysical protocol that does not suppress the normally dominant, M-channel photoreceptors by **more** than 1000:1 cannot be used to isolate the L-channel photoreceptor spectral response!

17.6.1.4 Noise performance in the transient case

[xxx figure is very similar to or duplicates 17.6.1-3 that incorporates the exposine function]
Figure 17.6.1-14 shows threshold data for the transient case following pre-exposure to a 4173 mL. luminance for XXX **[update callout to show theoretical aspects or refer to other Section]**. As in the previous case, a theoretical curve from this theory can be provided to correlate with the data points labeled achromatic (open circles) by Spillmann & Conlon (See **Section 17.3.3.6.4**). The match is quite satisfactory. The theoretical curve has the time constants of XXX and XXX and the exponent of the adaptation amplifier is XXX in the XXX region. The theoretical curve assumes only one type of photoreceptor. The α–break is presumed due to the vascular supply system. The ultimate threshold value should agree with the value in the previous figure for the internal threshold limit. It corresponds to the zero log relative threshold in the figure. On an expanded scale, the achromatic data points would be expected to start at approximately 47 Db above the ultimate threshold based on the data in the previous figure for 4173 mL. steady state exposure. Based on the logic used above, the chromatic threshold level should be at the 47 dB level above the achromatic level. Such a line passes directly through the data points of Spillman & Conlon. This would suggest that the subject was very near the threshold of his chromatic capability at the start of the transient threshold measurement experiment. It would also suggest that the asymptote labeled A could be extended to it intersection with the theoretical achromatic dark adaptation curve. The nature of the 17 dB dip in the chromatic threshold near 2 minutes into dark adaptation is of the same order of magnitude as in the previous figure.

[theoretical overlay is missing from figure, change time constant values in standard eye based on curve used]

---

[50]Wyszecki, G. & Stiles, W. (1982) Color Science, 2nd Ed. NY: John Wiley & Sons pp 252 & 406
[51]Wald, G. (1964) xxx
[52]Wald, G. (1966) xxx Proc Nat Adad Sci USA.
[53]Stockman, A. & Sharpe, L. (1999) Cone spectral sensitivities and color matching *In* Gegenfurtner, K. & Sharpe, L. *ed*. Color Vision: From Genes to Perception Cambridge: Cambridge University Press

Since the 17 dB dips in the chromatic curve of both of the above figures have been reported by other researchers, it is worthy of further theoretical investigation. The problem is that there are many conflicting processes in the signal chain that are operating in the regime occupied by this dip. First, the shape of the 200 ms. test exposure may be impacted by the 0.1 Hz. edge of the high pass filter represented by the adaptation amplifier. Second, each of the photoreceptor channels exhibits a dark adaptation characteristic, with an α-break in it **[take this out XXX]**. When the difference between each pair of chromatic photoreceptors is calculated, these dark adaptation characteristics should cancel out if the gain in the two channels, at the input to the lateral cell, are equal. If this condition is not met, a low frequency residual signal may impact the signal applied to the midget ganglion cell. Third, the amplitude of the signal output from the lateral cell is a function of the median wavelength of the input irradiance relative to 580 nm. The output is positive for shorter wavelengths and negative for longer wavelengths. This would lead to the conclusion that the chromatic threshold is not only a simple function of wavelength but that the dip may be a more complex function of a number of parameters. In any future experiments, it should also be noted that the adaptation state of the eye prior to the start of the steady state measurements is more critical than assumed by Spillmann & Conlon. The two-minute "pre-exposure" after a 45 minute dark adaptation is long enough to stabilize the "light adaptation" of the eye but it is not long enough to stabilize the vascular system which has time constants of about

A feature obvious in both of the graphs is the gross difference in the threshold characteristic in the two channels for both the transient versus time and the steady state versus illumination condition. This condition was discussed briefly in relation to the steady state situation.

This characteristic, labeled the photochromatic interval, provides the explanation of why one set of spectrally selective photoreceptors can support a dual channel visual system resulting in chromatic vision above a certain irradiance level and achromatic vision below that level. It is proposed here that the photochromatic interval is a function of wavelength and the specific spectral characteristics of the illuminant(s) used to determine it.

The feature known as the α-break in the achromatic dark adaptation characteristic plays no role in the transition between or merging of the achromatic and chromatic threshold functions. It is an artifact not present when the theoretical exposine overlay is provided to the dark adaptation function.

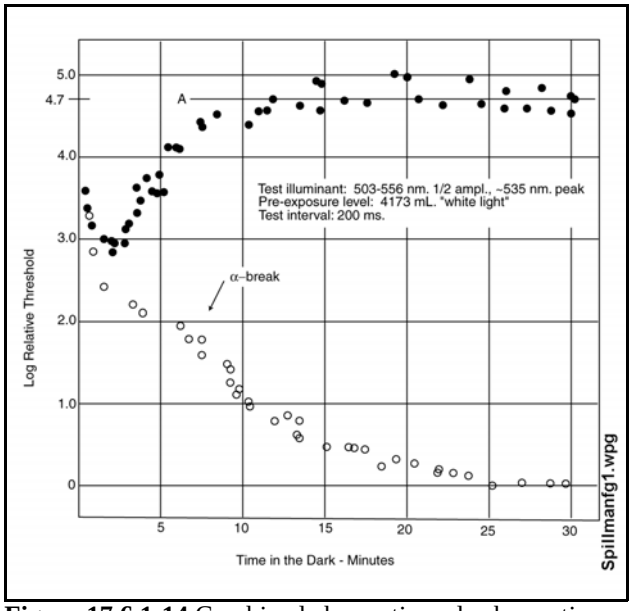

Figure 17.6.1-14 Combined chromatic and achromatic thresholds for the transient case. Data from Spillmann & Conlon (1972)

17.6.1A Equivalence of "Rod" and "Cone" data with this theory XXX

[talk about how perceived chromaticity is lost in both Spillmann's and Hecht's data by the same mechanisms. However, Spillmann presented the two thresholds in separate data sets. Hecht did a similar thing by coding his data points. Both methods agree with this theory. However, the conclusions to be drawn are different. May not need next g raph.]

[Talk about papers of MacLeod, Williams & Makous (1992) confirming outer segment level focus of the nonlinearity. Talk about MacLeod, Chen & Crognale (1989) on same subject.

[photochromatic interval defined in 17.3.XXX]

Figure 5 of Hecht, et. al[54]. is of importance and is reproduced as **Figure 17.6.1-15**. It plots data for the dark adaptation characteristic of the right eye of one subject under both long and short wavelength irradiance, with the intent of emphasizing the putative difference between the performance of rods and cones. The curve is widely reproduced–but generally without reference to the text associated with it. Stiles & Wyszecki (1982) indicate the data relates to the fovea and a 3° test stimulus when it actually applies to 30° nasally from the fixation point and a 5° stimulus. They did not note the "red" irradiance had a short wavelength cutoff of 690 nm. or mention the + symbols at all. Whereas the original caption only mentions "red light following different degrees of light adaptation", the text points out that the + symbols represent the dark adaptation performance of one of the same subjects (A. M. C.) to violet illumination instead of red (at only the three higher levels of the previous figure due to test set limitations). Several points are important; the *single* subject (A. M. C.) had normal color vision, the test stimulus lasted for 0.2 seconds, the light adaptation was by "white" light, the sensitivity of even the long wavelength photoreceptors to light with $\lambda > 690$ nm. is distinctly limited, the differential chromatic sensitivity of the long wave chrominance channel is near maximum at this wavelength, and the individual frames have been displaced for clarity without changing their common scale.

The data is reproduced here with the vertical scale expanded by 2:1 to allow better correlation of the data points and the proposed theoretical adaptation characteristics. In all four of the individual frames, the data points are approaching an asymptote of 5.16 log micro-Trolands that describes the achromatic threshold. The locus of the data points for each initial adaptation level is well described by the theoretical adaptation characteristic (solid lines) of this work. However, because of the minimal absorption of the "red" light compared to the "white" preliminary adaptation light, the sensitivity of the test technique to small amplitude sinusoidal components is quite low. The chromatic threshold in all four frames is nearly a constant at approximately 5.6 log micro-Trolands. Diagonal lines are used in the figure to delineate these values. These lines, representing thresholds, should be horizontal according to this work and essentially vertical according to the literature.

In the context of the scales provided, it could be assumed that the threshold levels shown were significantly higher than in Figure 2 of the same paper. However, The equation for the determining the achromatic threshold includes the spectral sensitivity of the chromophores involved. In this case, the apparent threshold is raised about two and one half log units because of the loss in gain in the phototransduction process. The actual internal threshold appears to remain unchanged at about 2.6 log micro-Trolands for a 5° field 30° nasally from the fixation point.

From the perspective of this work, there is no statistical difference between the data points related to the "red" and "violet" test stimulus in the first 15 minutes of the three frames. Clearly, there is no functional distinction between "rods" and "cones" in this region based on spectral sensitivity as assumed by Hecht's original premise. **[curves must include +'s]**

[54]Hecht, S. Haig, C. & Chase, A. (1937) Op. Cit. pg. 846

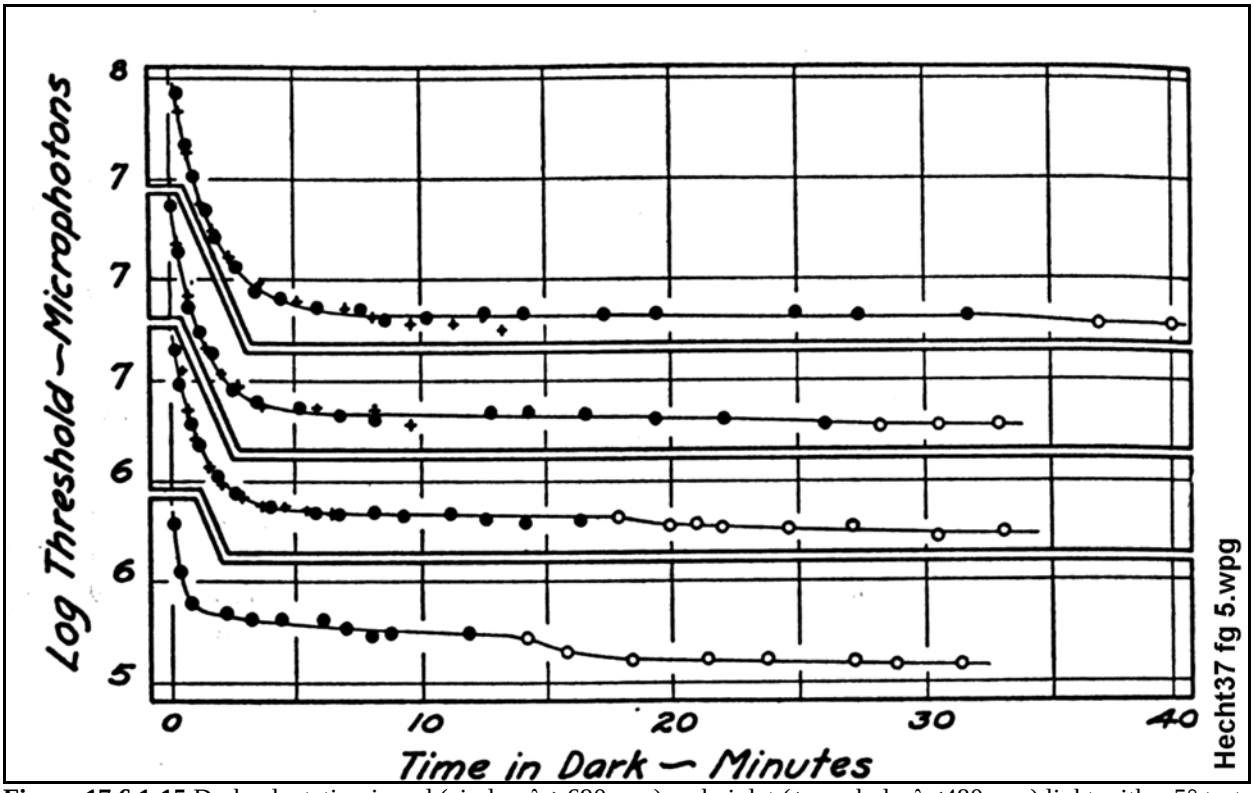

Figure 17.6.1-15 Dark adaptation in red (circles, λ >690 nm.) and violet (+ symbols, λ<480 nm.) light with a 5° test stimulus presented 30° nasally from the fixation point. Filled circles indicate a chromatic content was perceived by the subject. The threshold levels are with respect to object space and do not correct for the change in spectral sensitivity between the preliminary "white' adaptation light and the test stimulus. The curves have been displaced for clarity. From Hecht, Haig & Chase, (1937). **[New figure with o & +'s expand caption to define diagonals. Show color quits at same levels in violet and red**]

17.6.2 Transient performance–electro-physiological context

There are a variety of techniques for recording electrical activity associated with vision. Except for the local electroretinogram, LERG, (and very recently, the cortical visual evoked potential, CVEP, technique) these techniques are designed to be non-invasive. The local electroretinogram is actually a record of the signals at a given point, usually within the retina, accessed by a probe. The CVEP is a similar technique applied to the cortex. **Section 11.1.6** provides an introduction to the ERG.

The conventional visual evoked potential, VEP, employs a measurement of the potential at one or more

Figure 17.6.1-16 XXX EMPTY

points on the surface of the head in response to a specified illumination, and/or scene, profile. The result is a very gross signal, relatively Gaussian in shape, peaking about 100 ms after excitation. More complex stimuli and more complex recording techniques result in very complex waveforms. Desmedt provides considerable background related to the VEP as of 1977[55]. All of the VEP experiments using excitation of different colors have failed to correlate the illumination used with the absorption spectrum of the chromophores of vision. This has introduced spectral crosstalk and degraded the quality of the experiments considerably.

The ERG recorded in the clinical situation does not rely upon calibration of the intensity of the flash. As discussed in Jimenez-Sierra, Ogden & Van Boemel[56], the intensity of the light source may vary over more than 100,000:1. In fact, the precise amplitude and shape of the ERG can vary drastically based on these intensity levels. Greater care is needed in describing the intensity of the light source and the state of adaptation of the subject when reporting ERG results in the literature.

There are several specialized forms of the ERG, such as the pattern ERG, or P-ERG. In this technique, a technically very complex scene is used as part of the stimulus of the visual system. The recordings from the summation of the resulting individual waveforms are so complex, they approach a Gaussian or series of delayed Gaussian, waveforms. They will not be discussed here.

Recently, variations of both the LERG and CVEP have been introduced where complex scenes, patterns, are used as part of the stimulus. These can be redefined as P-LERG and P-CVEP techniques. They have frequently involved probing a two or three dimensional area of the retina or brain in order to ascertain a pattern to the recorded signals. These techniques are primarily exploratory at this time.

A multi-focal ERG is available to evaluate the performance on individual areas of the retina.

Other than for the LERG and the CVEP, all of these techniques involve signals of great underlying complexity. Some of the techniques produce an essentially Gaussian output waveform because of the number of individual signals summed into the resulting signal (a manifestation of the Central Limit Theorem). The LERG, on the other hand, can be used to search for and identify individual waveforms at different locations within the retina, the optic nerve and the brain. The individual waveforms predicted for the individual circuits in the signal detection, signal manipulation, signal projection and signal recovery stages of the visual process can be measured using this technique. These waveforms have been discussed individually in this work and there is no need to discuss them further here. The majority of the signals recorded by the CVEP are outside the scope of this work.

The electro-oculogram is similar to the ERG in technique. It attempts to record a wider range of signals from multiple sources. No contact is made with the eye ball. The sensitivity of this approach is less than that of a conventional ERG. However, it is used in clinical situations.

Because of the complexity of the waveforms recorded by the other techniques, only the waveforms associated with the ERG and LERG will be discussed here.

17.6.2.1 Topology and sources of the ERG

While the ERG is widely used and discussed, <u>no theoretical foundation</u> for it has appeared in the literature and an initial standard protocol for its clinical use has only recently appeared. This situation is at least partly due to the extreme complexity of the composite waveform usually recorded and its variability between laboratories. The elementary nature of the instrumentation used in the ERG is the source of this complexity. The illumination source is usually not well defined. One electrode is placed against an external surface of a highly complex electronic (electrolytic) system and a second electrode is placed *somewhere else*. An attempt is then made to record the current passing through the test circuit connected between these two electrodes and then to interpret the resulting complex waveforms as a function of time without significant attention to the spectral content of the illumination. Only under highly tailored conditions have waveforms been recorded that appear simple enough to analyze.

It should be noted that this process is similar to one used by the NSA and the KGB to steal enemy secrets. However, they are usually able to insure that the second electrode is truly benign relative to the desired signal, they usually use more sophisticated frequency selection criteria than in the typical ERG, they usually know something about the

---

[55]Desmedt, J. (1977) Visual evoked potentials in man Oxford: Clarendon Press

[56]Jimenez-Sierra, J. Ogden, T. & Van Boemel, G. (1989) Inherited Retinal Diseases. St Louis, MO: C. V. Mosby, Appendix A

fundamental nature of the information they are trying to capture, and they frequently are highly versed in the exact circuitry of the typewriter or computer terminal they are attempting to interrogate.

As will be discussed below, there is a significant possibility that the second electrode used in the ERG is not connected to an indifferent area of the subjects skin. This possibility involves signals from the initial circuits of the cortex entering the return electrode, especially when placed near the ear, and exiting via the signal electrode attached to the cornea.
[This all belongs in Chap 17.]
[[see also Brindley (1956) and comment by Dowling & Wald (1960) as follows:]]

17.6.2.1.1 Conventional mathematical description

Although the ERG was first recorded and interpreted crudely in 1865, Ottoson[57] noted as late as 1983 that the measurement of ERG's has contributed little to the understanding of the signal processing in the retina. The present conventional wisdom relies upon the concept promulgated by Granit[58]. Granit described the ERG as due to signals from two physically different regions of the retina. He suggested that the initial portion of the ERG originated in the photoreceptor layer and that later portions originated in the inner nuclear layer (INL). As the title of his 1933 paper indicates, Granit was thinking of the process primarily in terms of action potentials, not analog signaling. He also thought of the signal generated in the INL to be largely independent of the signal generated by the photoreceptors. Hood & Birch give a recent summary of the approach of Granit[59]. Figure 2 of Hood & Birch illustrate the fundamental problem with the conventional wisdom. The negative going signal called P3, presumed to originate in the photoreceptors, has a slow risetime (nominally 20 milliseconds) and achieves a constant value lasting for a long period of time (greater than 100 milliseconds). The positive going signal from the INL has a complex shape beginning after about 20 milliseconds. The net result is a waveform largely dominated by the P2 component. While this conceptualization may be reasonable for stimulation by a rectangular pulse, it is grossly oversimplified and does not characterize the ERG well. **Figure 17.6.2-1** illustrates the conventional concept by reproducing a variant of Figures 1 and 2 of Hood & Birch. It suggests the P3 signal is monotonic and negative going. The composite ERG reflects this P3 signal until the positive P2 component overwhelms the contribution of the P3 signal. Using this analogy, the *a*- wave and *b*-waves are defined more as edges than the common concept of a wave. The *a*-wave is defined as the negative going portion of the ERG prior to the impact of the P3 component. The *b*-wave is defined as the bulk of the positive going portion of the ERG. The papers of Lamb have reflected this view since 1974. When a more detailed model of the retina is considered, the description of the demarcation between the a–waves and b–waves fails. The failure is primarily due to the lack of understanding of the operation of the retina under impulse conditions. Observation of the retina operating in this mode quickly redefines the features of the ERG. This interpretation will be developed in the following sections.

Granit also defined a P1 waveform that was believed to originate in the IPM. In the context of this work, P1 approximates the Class C waveform, P3 approximates the Class D waveform and P2 is a general designation for a composite of the Class E waveforms. However, except under the weakest of stimuli, neither the Class C or Class D waveforms are monotonic during the first 30 ms following the stimulus in humans at 37 Celsius. This is true for both impulse and rectangular pulse stimuli (See **Section 16.4** or **A.2** in **Appendix A**).

Hood & Birch have analyzed the ERG based on the concepts presented in their 1990 paper[60]. They relied upon the mathematical model for the photoreceptor of Baylor, Nunn & Schnapf which relied upon the model of Baylor, Hodgkin & Lamb. The result is a bit of circular reasoning. Lamb adopted the practice of only addressing the leading edge of the photoreceptor response after Hodgkin had failed to solve the necessary differential equation describing the complete response of a photoreceptor to the photosensing process. (See **Section 16.3** and **Appendix A**). Hood & Birch did not repeat the admonition in the Baylor, Hodgkin & Lamb paper that using their simplified equation for a multistage RC filter requires that each stage of the filter be completely isolated from the others. While adopting the mathematics of a multistage filter, Hood & Birch offered no physical model that provided this isolation. Lacking this isolation, a multistage RC filter exhibits a much more complex higher-order response function than the

---

[57]Ottoson, D. (1983) Physiology of the nervous system. NY: Oxford University Press, pp. 364-365
[58]Granit, R. (1933) The components of the retinal action potential in mammals and their relationship to the discharge in the optic nerve. J. Physiol. vol. 77, pp 207-239
[59]Hood, D. & Birch, D. (1992) A computational model of the amplitude and implicit time of the b-wave of the human ERFG. Visual Neurosci. vol. 8, pp 107-126
[60]Hood, D. & Birch, D. (1990) A quantitative measure of the electrical activity of human rod photoreceptors using electroretinography. *Visual Neurosci*. vol. 5, pp 379-387

equation they provide.

The photoexcitation/de-excitation equation (P/D Equation) derived in the referenced sections of this work, does not require a putative multistage filter. The 1990 Hood & Birch paper also relied upon a set of assumptions concerning the response of a photoreceptor to stimulation. Although sophisticated and comprehensive, they are not quite correct. They caveat this possibility by accepting some variations in the context suggested by Penn & Hagins[61]. The diode load of the pedicle does provide the static nonlinearity envisioned by Hood & Birch.

17.6.2.1.2 Conventional instrumentation

The ERG is usually recorded using two signal related electrical contacts between the subject and a sensitive recording voltmeter. There is frequently a third contact that is safety related and intended to be entirely non-functional. Because of the need for high amplification in the instrumentation, it is normal to use only high gain AC coupled amplifiers in the instrumentation. Recently, some experiments have been made with high gain DC amplifiers. The signal input contact is usually made with the outer surface of the eyeball, the sclera, taking advantage of the low electrical impedance associated with the tears covering the eyeball. The signal return contact is usually established at some point on the surface of the skin described as an indifferent location. The contact is usually either on the temple near the eye being recorded, near the ear, or occasionally at another location. These locations have little technical significance and do not constitute indifferent locations. They frequently allow unwanted signals to enter the instrumentation.

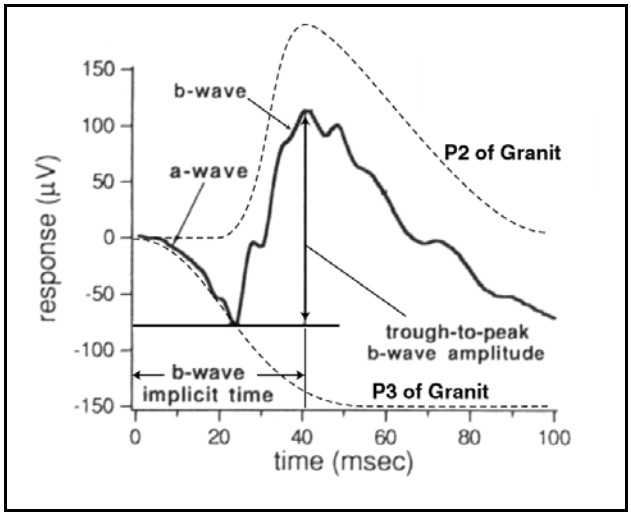

Figure 17.6.2-1 The ERG as defined within the conventional wisdom. The assumptions are that the P2 waveform begins well after P3 and the P3 waveform has a rise time long with respect to the time to peak (implicit time) of the b–wave. The second assumption is not generally true.

Electroretinography (ERG) is a hybrid technique that attempts to record a highly localized *in-vivo* electrical signal from a remote location. On preliminary examination of the signals related to the photoreceptor cell, it is difficult to understand how a signal loop related to one photoreceptor, with dimensions measured in hundreds of microns, could be measured effectively from a distance of at least a centimeter. In fact, it cannot. As indicated indirectly in the previous section, and presented in **Figure 17.6.2-2**, the key to the ERG is the presence of various Limiting Membranes within the eye[62]. These structures introduces insulating surfaces that isolate the various conducting matrices of the retina. These insulating surfaces generally merge at the extreme circumference of the retina. As a result, the retina consists electrically of a group of concentric spherical conducting shells (actually relatively poorly conducting matrices) interdigitated with a similar group of concentric spherical dielectric shells. The conducting shells have a large number of individual electrical sources and sinks imbedded within them.. They also are connected to each other by finite, but unusual, resistances. The resulting composite electrical structure is shown in the lower left.

17.6.2.1.3 The topography and topology of the retina

The highly tailored topography of the retina introduces some unusual properties to its overall electrical topology. Both of these arrangements impact the signals recorded by the ERG. First, the thinness of the individual shells, the general flow of individual signal currents along radials, and the low transport velocity of the signal currents in electrolytic media introduce some very important asymmetries into the electrical performance of the circuit. At the high frequencies associated with the transient performance of the eye to light, the series connected capacitors transfer the voltage related to the charge created within a given matrix to the surface electrode essentially instantaneously (some might say near the speed of light). This is not true of the currents resulting from these

---

[61]Penn, R. & Hagins, W. (1972) Kinetics of the photocurrent of retinal rods. *Biophysical J.* vol. 12, pp 1073-1094

[62]This is a considerably more precise rendition than the resistor-only variant in Steinberg, Linsenmeier & Griff *in* Chapter 2 of Osborne, N. & Chader, G. eds. (1985) *Progress in Retinal Research*, vol. 4.

differences in voltage. Most of these currents are transported at a much slower velocity controlled by the electrolytic properties of the matrices (velocities typically near 4400 m/sec). The loop currents associated with individual neurons only travel distances measured in tens of microns resulting in travel times measured in microseconds. However, the currents associated with the resistive impedance between the conducting shells can be several centimeters long. The delay associated with the electrolytic transport velocities can be long, especially at the low voltage differences involved. As a result, the transient response of networks containing these impedances are not described fully by the simple exponential relationship of ordinary resistor-capacitor networks.

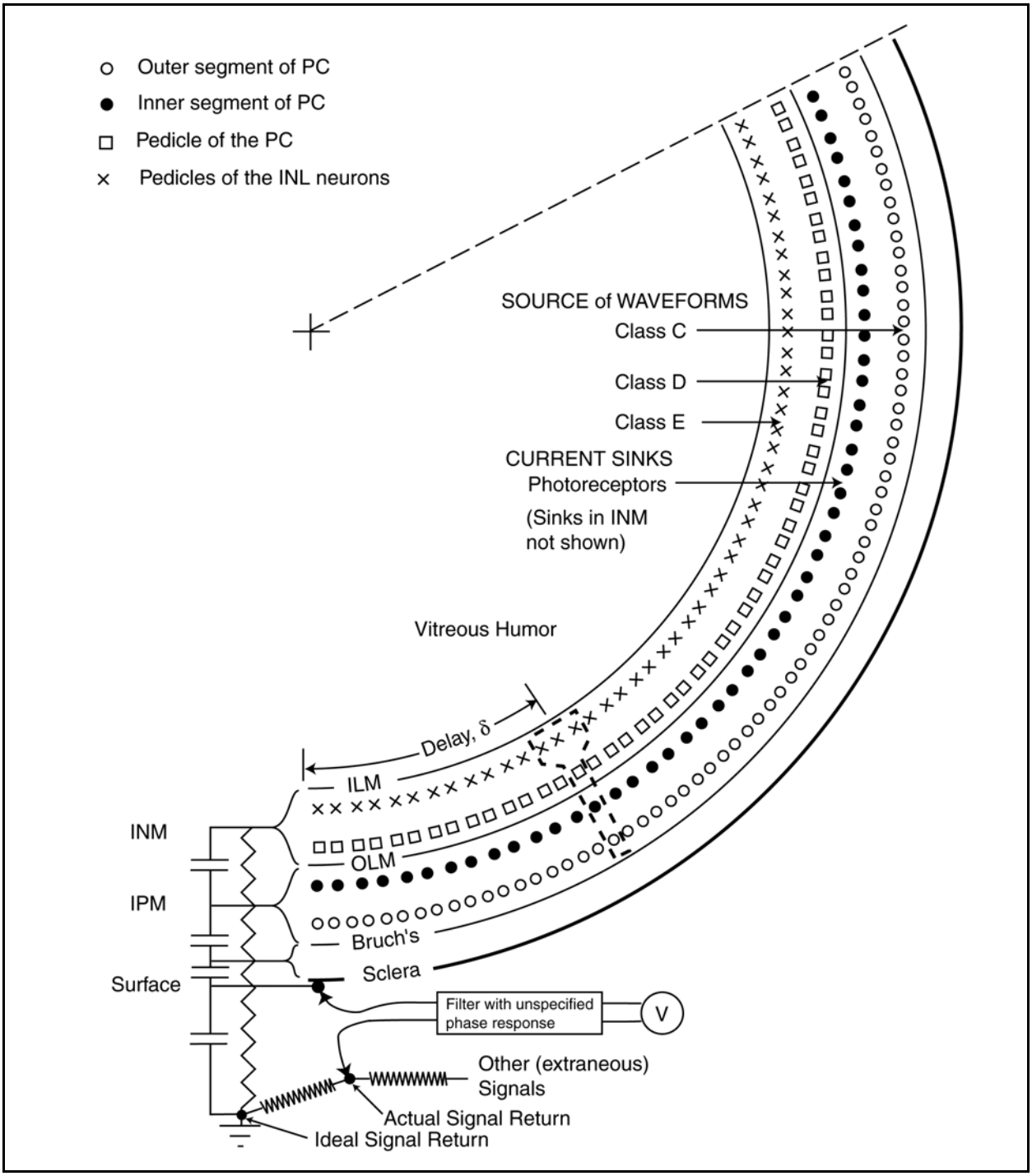

Figure 17.6.2-2 Caricature of the test situation when obtaining an ERG recording. A section of a retina is portrayed topologically on the right without considering the orientation of the individual photoreceptor cells. The equivalent circuit is shown in lower left. The current from a large group of sources is collected and contributes to the charge on each capacitor. The resistive elements are electrolytic in nature and introduce significant time delays. See Text.

Within the two inner conduction shells, there are a large number of individual electrical circuits. Between Bruch's

membrane and the Outer Limiting Membrane, OLM, are all of the neurons called photoreceptor cells. Between the OLM and the Inner Limiting Membrane, ILM, are the rest of the neurons associated with the retina. Each of these neurons exhibits at least one output signal source and several current sinks associated with it. The ERG is concerned with the differences in current flow between these different sources and sinks as a function of time. It is the algebraic sum of these currents that create voltages between the various conductive shells. The DC components of the currents from many of the individual neurons, especially within a single matrix, tend to cancel. However, this is not true of the neurons within each photoreceptor cell. These neurons have axons that traverse the OLM.

The conditions regarding the photoreceptor cells is the most important. The dendrites within the Outer Segments, shown here as open circles, act as sources of current upon the application of light. If a large number of photoreceptors are illuminated simultaneously, the total source current produced by the dendritic terminals of the cells can change considerably. Brindley[63] has noted that the size of the ERG in frogs to be roughly proportional to the area of retina illuminated. The total current exhibits a leading edge transient and a sustained value if step illumination is used. This total current is described by the Class C waveform described above. There are a series of current sinks associated with each photoreceptor cell. The most important sink is located within the Inner Segment. The Inner Segment is in turn located within the IPM along with the rest of the dendritic structure of each cell. The sinks associated with the photoreceptor cells are represented by the filled circles. These current sinks are designed to be of constant amplitude and do not contribute significantly to the ERG. Each photoreceptor cell also exhibits a signal current source at its pedicel. This signal source can be described by the Class D waveform described above. Because of the internal circuits of each photoreceptor cell, the currents associated with the Class C and Class D waveforms of each photoreceptor cell are nearly identical in shape but not in time. They differ in time because of the finite current velocity within the conduits of the neuron. As a result, the total source current due to the illumination of the photoreceptors appears first as a voltage, Class C waveform, between the IPM and ground followed by a similar voltage, Class D waveform, about 8 ms later between the INM and ground. These are the two main voltages sensed initially by the ERG.

The Class D waveform at the output of the photoreceptors is passed to other signal processing neurons, primarily the horizontal cells in humans. These neurons create the Class E waveforms described above. The total source current from all of the cells contributing to this waveform, and represented in the figure by the X's, create an additional voltage between the INM and ground. The peak current associated with this waveform occurs approximately seven XXX ms after the peak in the Class D waveform. These neurons also display slowly varying sink currents that are required to maintain the electrical integrity of the neurons. These sink currents are not shown in the figure. The rapidly varying Class E waveforms and the slowly varying sink currents both contribute to the recorded ERG.

Although described above in terms of currents deposited on a capacitor resulting in a voltage with respect to ground, there is no unique ground in the visual system and the capacitors of the retina are concentric. As a result, the net value of the various capacitors can be described in terms of the group of capacitors in series shown in the lower left. Each of these capacitors is shunted by a resistive impedance.

The signal and signal return leads of the electroretinograph are usually connected as shown. The net fast changing voltage measured by the ERG are derived from the capacitors acting as voltage dividers. Over the longer term, the measured signal is a more complex waveform resulting from the flow of various source and sink currents within each matrix as well as the currents through the resistors shunting the capacitors. Note the opportunity of other signals to enter the ERG sensing circuit due to the inadequacy of the actual signal return terminal. This problem cannot be completely avoided. It illustrates why even the commands to the muscles of the eyelid can cause a feature in the recorded ERG. It also suggests why connection of the signal return lead to an area near the ear may cause signals from the cortex to be included within the composite waveform.

Although the voltage changes within the plasmas of the signaling neurons is usually measured in terms of a few millivolts to tens of millivolts, the ERG is typically recorded at the 500 microvolt level or (less).

The relationship between the response of the individual photoreceptors and the overall ERG is addressed in Ogden & Hinton[64]. Note however the lack of capacitances in their figure. This is a significant shortcoming.

---

[63]Brindley, G. (1956) The passive electrical properties of the frog's retina, choroid and sclera for radial fields and currents. *J. Physiol*. vol. 134, pp 339-352

[64]Ogden, T. & Hinton, D. ed. (2001) Retina. 3rd Ed. Vol. 1 St. Louis, MO: Mosby pg 318

Heckenlively[65] has discussed the fact that the shape of the ERG composite waveforms change with test conditions. Unfortunately, he does not define the spectral characteristics of the illumination used to acquire his data. His presentation does not explicitly address the absolute latency of the signals relative to the time of illumination. His figures note the relative latency, or implicit time, of a feature relative to the time the waveform initially departs from the baseline. This approach obscures the temporal aspects of the a- and b- wave for different peak illumination conditions. Instead of recognizing that the entire waveform is delayed as the illumination level is reduced, he notes that the a-wave is reduced in amplitude at lower illumination levels. In fact, the a-wave occurs later in absolute time and has both a lower amplitude and a lower slope. Because of these features, it tends to disappear into the portion of the composite waveform dominated by the b-wave. More precisely, it is the Class C waveform that is delayed with respect to the illumination and exhibits a lower amplitude and slope. The Class D waveform, which cannot be ignored and is of the same polarity as the Class C waveform and of similar shape, exhibits a fixed delay relative to the Class C waveform. Similarly, the Class E waveform, that is of opposite polarity, exhibits a fixed delay relative to the Class D waveform. He indirectly recognizes the longer absolute delay and lower slopes when he notes that the response to a flickering test source is limited to about 70 Hz at high illumination but to about 8 Hz at low illuminaton. His implicit times must be differentiated from the absolute times relative to the impulse of illumination.

Heckenlively also provides brief data on the ERG amplitude as a function of age and gender. The a-wave data shows some loss in amplitude (~15%) beginning with the 41-50 year range. The loss appears compatible with the loss in transmission of the outer lens group. He shows a larger loss in the b-wave beginning with the same age group. The predominant component of the b-wave is the Class E waveform. This waveform is a difference between two spectrally different Class D waveforms. Because of this differencing, it exhibits an increase in sensitivity to the greater loss in transmission which is spectrally selective.

Heckenlively speaks of the oscillatory potentials occurring in his data during the first 25 ms of the composite waveform. It appears that these intermediate peaks are actually due to the presence of two spectrally separate pairs of Class C and Class D waveforms. Such an assumption is compatible with the change in inflection near 60-70 ms that suggests the presence of a time delay in the Class E waveform related to these pairs.

He also notes that the so-called early receptor potential, the manifestation of the Class C waveform in the ERG can occur with an absolute latency of only 2 ms for the dark adapted eye under very high peak illumination.

When making an LERG measurement, the circuit explains why different composite voltage waveforms and timing relationships can occur for different locations of the signal probe and signal return probe connections. The timing relationships cannot be easily and adequately displayed in a two dimensional circuit topography.

[in the electrical path between the output current of the individual photoreceptor cell and its return current terminal, the poda. When exciting an individual photoreceptor or a group of photoreceptors, the total output current from the axon(s) is forced to circumnavigate the extent of the outer limiting membrane in order to return to the poda. There is a finite voltage drop along this current path due to the impedance of the materials involved. The ERG measures this voltage drop. Several parameters can effect the amplitude of the ERG signal. Obviously, the illumination level and spectral content will affect the signal as will the state of adaptation of the channels illuminated. The size and position of the illumination on the retina will also have an impact. The placement of the leads of the ERG can have a significant impact on the amplitude of the ERG signal. Normally, the D.C. value of the voltage is ignored and the major concern is the relative value of the A.C. voltage. Under these conditions, the location of the “indifferent electrode” is of little consequence. However, it may collect stray signals emanating from the initial circuits of the cortex. These signals are characterized by their transient nature and their occurrance at least 22 ms after the initial impulse or step illumination. In the case of square wave illumination, they are not directly related to the termination of illumination.]

17.6.2.2 Interpretation of the conventional ERG

As frequently noted, there are two major categories of ERG. The most informative theoretically is the ERG in response to impulse illumination. A less demanding technique, generally used clinically, is to use long duration square wave illumination under the same conditions. These two techniques provide drastically different information about the visual system in humans. Within the first category, the use of a broad field of illumination, typically

[65]Heckenlively, J. (1988) Retinitis Pigmentosa, NY: J. P. Lippincott, pg 8

Ganzfeld illumination, leads the the averaging of the responses of millions of photoreceptors and neurons of the INL. The overall response is necessarily less than precise. The alternative is to illuminate only a small region of the retina. While giving more precise results, it places higher requirements on the instrumentation unless an invasive probe is used to acquire the signal.

It is important to note that there are actually three types of simple illumination regimes. The long duration pulse is a hybrid. From a mathematical perspective, the impulse has unique characteristics. The complete, and accurately recorded, response of a system to an impulse completely describes the performance of the system. The integral of an impulse is a step function. The response of a system to a step change in illumination can provide nearly all of the information about a system that can be obtained by exposure to an impulse. However, the data reduction process is more difficult. A long duration pulse is actually two step functions in time series from a mathematical perspective. Use of long duration pulse illumination complicates the data reduction considerably if the time between the two steps is similar to the time constants of the system being evaluated. This is frequently the case in vision experiments.

A common complaint about the impulse ERG is that, unless small signal excitation is used, the non-linearities in the system make analysis of the data difficult. This statement applies equally to the long duration pulse ERG, however the impact of the non-linearites is obscured by other factors. The number of variables involved in the signal recorded by any ERG is quite large. They must be controlled. A major problem in the literature is the number of unique ERG recordings presented. In general, these recordings cannot be correlated with each other because of the lack of control of the variables at the time of recording. The spectral characteristics of the illumination employed usually represents the largest uncontrolled (or poorly controlled) variable. As will be seen in the next Section, the shape of the resulting ERG waveform can be changed drastically by a minor change in the spectral composition of the illumination.

In the context of this work, the ERG presents another complication. Whereas use of a small signal impulse illuminant provides a response that only relates to the signaling system and is easily analyzed, this is not true of the long duration step or pulse scenario. The typical long step or pulse illuminant, even if small in amplitude, impacts both the signaling and power supply channels of the visual system. This is typical of any DC-coupled signaling system like the visual system. As will be seen below, the signal resulting from a long duration illuminant is primarily a representation of the state, and therefore the health, of the power supply system of vision. It can be analyzed in terms of the quiescent condition as well as the transient performance of that system. In that context, it is a measure of the metabolic condition of the subject more than it is a measure of the performance of his visual system (except in the case of substantial abnormalities in the system).

The primary difficulty in analyzing an ERG is the variety of waveforms present in the composite recording and the underlying mechanism associated with each individual waveform. Many of these can be envisioned by studying the Top Level Schematic of Vision and the individual circuits supporting the Schematic. However, it is also necessary to understand the topology of the visual system. This is particularly important when using long duration illuminants as will be shown below. Griff[66] shows a "vitreal" ERG waveform in his figure 9-4 with a feature labeled "b." It can be assumed that it is the feature usually labeled the b-wave. It is not. It is actually the result of subtracting two waveforms that are normally separated by about 13 ms. in time (The Class C and Class D waveforms of this work). This short interval is not shown clearly in the figure, but the difference waveform is obvious.

To aid in developing an ERG based descriptor of the performance of the visual system, the next Section will assemble a synthetic ERG based on a controlled set of parameters. This synthesized ERG can be compared to the conventional ERG's of the literature[67,68]. It has not been generally recognized that the ERG is sensitive to the spectral distribution of the light used as a stimulus (Krill, 1972, pp 227-246). This variable provides another degree of information in a number of clinical situations.

---

[66]Griff, E. (1991) Electroretinographic components arising in the distal retina. *In* Heckenlively, J. & Arden, G. *ed*., Principles and practice of clinical electrophysiology of vision. St. Louis, MO: Mosby Year Book, pg. 95.

[67]Krill, A. et. al. (vol. 1, 1972 & vol. 2, 1977) Hereditary Retinal and Choroidal Diseases. NY: Harper & Row

[68]Krill, A. (1959) "Clinical Electroretinography" in Hughes, W. Year Book of Ophthalmology, Chicago, IL: Year Book Publishers

17.6.2.2.1 Synthesis of the fundamental (Impulse) ERG

Using this work, it is possible to prepare a set of specifications for an ERG waveform of minimal complexity. With this foundation, it becomes possible to interpret more complex ERG recordings in response to less controlled conditions. The fundamental ERG can be defined as the ERG obtained under the above set of conditions and in response to an impulse luminant. These conditions are based on a review of the signal paths of the top level schematic of the visual process. Since the ERG acquires an ensemble of electrical inputs from any and/or all circuits of the visual system simultaneously, it is advantages to minimize the number of these signals in the fundamental ERG. At least two avenues of attack are immediately obvious, employ only one spectral channel of the signal detection stage and minimize or control the signals produced in the signal manipulation stage. A third approach is to use low levels of illumination in order to approach linear system performance, particularly with respect to the signal manipulation processes within the photoreceptor cells. This was the approach used in Section 16.7.2 to decompose the ERG recorded by Smith & Lamb. The same approach can be used to synthesize a fundamental ERG based on the nominal waveforms of the different classes of waveforms defined here. Several findings are important in this synthesis. First, the voltage signal at the pedicel of a photoreceptor cells is of the same polarity as the voltage signal created by current exiting the disk stack of the Outer Segments. Second, the voltage at the output of the bipolar cell is of the same polarity as its input signal received from the pedicel. Only the lateral cells contribute signals that may be of either polarity relative to the pedicel voltage. This situation introduces an additional choice in experiment design. The data in the literature is heavily weighted toward the position that the signal from the M-channel pedicels is applied to the non-inverting input to the lateral cells of the 1st lateral processing (color) matrix. The signals from the S- and L-channel pedicels are applied to the inverting inputs of their respective lateral cells. Accepting this premise allows the removal of another uncontrolled variable from the fundamental ERG. The use of illumination that is highly filtered spectrally can predetermine the nature of the signal at the output of the lateral cells of the 1st lateral processing matrix.

Since there are two separate and distinct chrominance channels in human vision, it is important to review the options for tailoring the signals from these channels in a multidimensional context. One approach would be to attempt to force the output of the lateral cells of both chrominance channels to a null condition simultaneously. This can be done based on the New Chromaticity Diagram for Research but it requires careful control of the flux applied to each of the chromatically sensitive signaling channels. An alternative approach is to attempt to insure that all of the lateral cell signals are of the same polarity. This can be done most easily by limiting the applied illumination to the extremes of the visual spectrum, either the far red or the far violet (or the combination of both since they provide the same polarity signal at the output of the lateral cells). **Figure 17.6.2-3** shows the synthesized human ERG under the conditions of;

+ total dark adaptation of the subject

+ signal and return electrode both located on the corneal fixture

+ small signal input via the violet portion of the spectrum (λ< 460 nm.)–*modified in frame (B)*

+ flash illumination used to simulate a mathematical impulse (duration less than 0.5 ms.)

Frame (A) is plotted with negative voltage upward for consistent graphical appearance with most of the other graphs in this work. Frame (B) will be discussed below and shows the same fundamental ERG inverted (the normal presentation among electrophysiologists). The interpretation of frame (A) is straightforward. There is a significant delay between the illumination impulse and the initial response recorded by the ERG. This delay is the pure delay specified by the P/D equation plus any transport delay within the IPM and the structures of the choroid as the signal travels to the ERG signal electrode. The initial deviation of the ERG signal from the baseline is abrupt. It is due to the first order process representing the excitation and de-excitation of the chromophore molecules in the liquid crystalline state. The signal is due to the current passing into the IPM from the dendritic structure of the

photoreceptor cells within the Outer Segments (the Class C waveform). The transport delays within the IPM and INM cannot be quantified at this time and will be ignored. All times will be recorded relative to the location of the signal probe and the absolute delay due to the P/D process. Therefore, only the P/D delay is shown on the left of the figure. The initial response is represented precisely by the nominal Class C waveform, also known as the early receptor potential, presented in this work. It exhibits two exponential segments, one forming the leading edge and the second the trailing edge. A signal similar in shape to the early receptor potential is recorded beginning approximately 13 milliseconds after the beginning of the Class C waveform. This is the signal (Class D waveform) primarily from the pedicels of the photoreceptors of the S-channel. Because the system is operating under small signal conditions, this waveform is identical to that of the Class C waveform. It has been amplified by the adaptation amplifier but not distorted. It has also been processed by the distribution amplifier but not limited. The composite of these two waveforms is shown by the solid line. The contribution of the Class C waveform is shown by the series of long dashes proceeding toward the axis and the contribution of the Class D waveform is shown by the line using slightly shorter dashes. The signals from the pedicels branche and travel into both the luminance channel (channel R) and one of the chrominance channels (channel P because of the choice of illumination). The signal reaches the low impedance output at the axons of the lateral cells of the chrominance channel (1st lateral processing matrix) first. This channel processes the signal linearly but inverts it. As a result, the Class E_2 waveform starting at 16 ms. drives the composite waveform of the ERG in the negative direction.

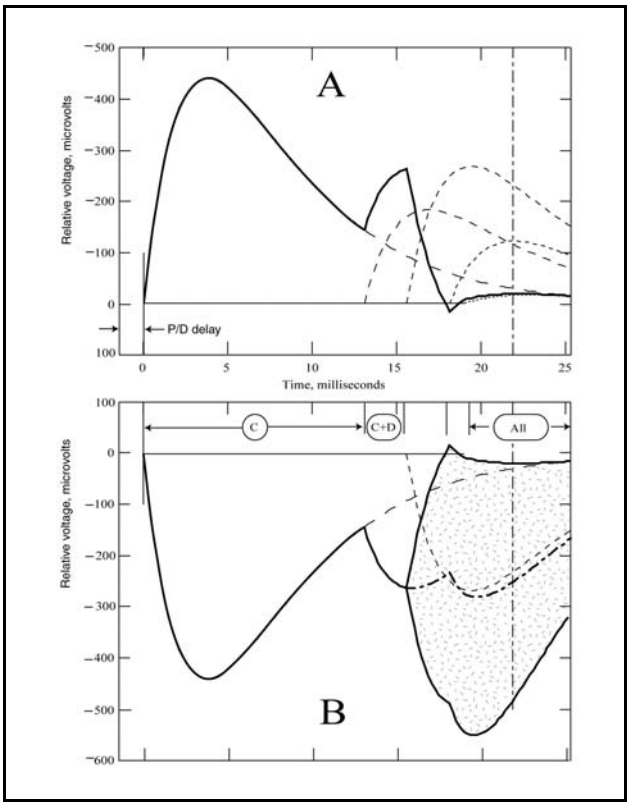

Figure 17.6.2-3 The fundamental human ERG as synthesized. Frame A (negative voltage is up), employing violet light (λ<460 nm) under small signal, mesotopic or lower illumination levels, to maintain linearity. Frame B (negative voltage is down), allowing for a variety of illumination sources. Vertical line at 22 ms. indicates earliest expected occurrence of an action potential. See text for details.

Since all of these waveforms are faithful copies of the original Class A waveform due to the P/D process, they all introduce abrupt discontinuities into the composite waveform. These are usually masked by test set noise, even using Ganzfeld illumination to stimulate all of the photoreceptors simultaneously, under small signal conditions. Under larger signal conditions, a variety of additional waveform features tend to make these changes difficult to recognize. The notch between 13 and 16 ms. is frequently seen in clinical ERG recordings and is portrayed in the sample imagery of the proposed ISCERG Standard (Described in 1999 as the ISCEV, International Society for Clinical Electrophysiology of Vision and documented in Marmor & Zrenner[69]).

The composite waveform continues in a negative direction until 18 ms. At this time, the original signal traveling along the luminance channel has reached the low impedance output axons of the bipolar cells. An additional signal is now generated (Class E_1 waveform) that is of the same polarity as the Class C and D waveforms. It is shown by the dashed line leaving the baseline at at 18 ms. This signal begins to drive the composite waveform positive again. This signal at the output terminal of the bipolar cell also branches. The signal proceeds along the fundamental path to the ganglion cells and is also applied to the lateral cells of the 2nd processing matrix. The 2nd processing matrix is not important in human. However, an output from this matrix does appear in the fundamental composite ERG. Since the amercine cells of this matrix are physically quite close to the output terminals of the bipolar cells, there is only a short delay before an output signal appears. The mathematical manipulations associated with this matrix are currently unknown. However, based on the Smith & Lamb ERG used in Chapter 16, the output of this matrix under

[69]Marmor, M. & Zrenner, E. (1995) Standard for clinical electroretinography *Doc. Ophthal*. vol. 89, pp 199-210

the prescribe test conditions appears to be significant. This additional Class E waveform (Class E_2' waveform for tabulation purposes) appears at 19 ms. and contributes a negative going component to the composite ERG waveform. In this case, and using the relative amplitudes suggested by the decomposition of the ERG of Smith & Lamb, this last waveform causes the overall composite ERG to become essentially horizontal at a voltage very close to the original quiescent condition. Unfortunately, the Smith & Lamb ERG ended at about 22 ms.

The above synthesis of the fundamental ERG under the specified conditions reproduces the Smith & Lamb ERG nearly perfectly except for a deviation between 12 and 13 m. which may be due to test set noise. It also offers a prediction concerning the appearance of the first action potential at the output of the ganglion cells. Using the dimensions shown in Boycott and Dowling for the human retina, it can be expected that the output of the bipolar cells will arrive at the input terminals of the Activas within the ganglion cells at about 22 ms. This is based on the assumption that the input terminals of the Activas are all located along the centerline of the ganglion cell layer. Since small signal conditions were postulated for this synthesis, it is possible that the first action potential will occur slightly later due to the necessity of the signal level rising above the threshold of the cell. However, it is not likely to occur earlier based on the assumed geometry. The amplitude of any recorded action potentials is difficult to predict because of the nature of the test circuit involved in ERG recordings. The original signal from each cell is capacitively coupled from the electrolyte of the appropriate axon (or possibly dendrite in the case of the ganglion cells) to the impedance associated with the surrounding matrix. The signal is then applied to a voltage divider from which the signal probe extracts a variant of it. The fact that the capacitor causes the formation of a high pass filter structure is what makes the estimate difficult. Each action potential will be about 0.15 ms. wide and hard to see at the scale of this frame.

A descriptor line has been added between frame (A) and (B) of this figure to describe the waveform classes participating in that portion of the waveform. Between 16 ms and 19 ms, the descriptors are too complex to appear in the space available. Between 16 and 18 ms, the composite waveform consists of the $C + D \pm E_2$ waveform classes . The negative sign applies to frame (A). The sign and magnitude of the E_2 expression may take any value in frame (B) as discussed below. Between 18 and 19 ms, a similar set of conditions applies except the class E_1 is added to the composite in all cases. Beyond 19 ms, the class E_2' component due to the 2nd processing matrix is added to all composites. The sign of this component could also change depending on the precise test configuration.

Frame (B) shows the same component waveforms in the fundamental composite ERG but inverted per standard practice in the ERG field. However, it explores the alternatives available with respect to the choice of spectral composition in the initial illumination. The sections of the composite waveform during the first 16 ms. are unchanged. At approximately 16 ms., the waveform takes different paths depending on the output of the signals from the 1st processing matrix, specifically the lateral cells creating the Class E_2 waveforms. If the illumination continues to be dominated by very short wavelengths, the composite waveform returns to the baseline as in (A). However, if the illumination were changed to consist of radiation primarily exciting the M-channel (even to the extent of using differential chromatic adaptation prior to the experiment), the amplitude of the Class E_2 waveform would remain high but its polarity would be reversed. The resulting composite waveform would exhibit a larger absolute magnitude in the 16-25 ms. region, possibly even exceeding its amplitude during the first sixteen milliseconds. A third alternative is to tailor the illumination so that the radiation applied to the S-, M- & L-channels appears equal in voltage and of opposite polarity at the output of the chromatic lateral cells (in both chrominance channels). Under this condition, there is no contribution to the composite ERG from these channels and the composite waveform would be expected to follow the dash-dot line after the 16 ms. point.

The shaded area in this frame shows the extent of variation that can be expected from different experimenters that do not control their illumination source precisely. Such a large variation makes comparison of results very difficult. Furthermore, note the confusion possible in labeling the features, particularly the b-wave. Whereas the a-wave can be unequivocally defined by the distance from the quiescent state, the horizontal axis, to the peak of the signal due to the Class C waveform. The b-waveform is usually defined by the voltage from this peak to the most positive voltage of the waveform. Under this definition, the magnitude of the b-wave is ambiguous and depends on the illumination employed in the experiment. It may occur near 13 ms. or near 17 ms. for the low illumination levels used here to maintain small signal conditions.

17.6.2.2.2 Correlation of the a-wave and b-wave with theory

Traditionally, the a-wave has been defined as the first major feature of the ERG. By convention it is a negative going voltage when measured by a signal electrode attached to the external corneal surface with a return electrode, often labeled an indifferent electrode, attached to either the temple or the earlobe. In recent times, the return electrode often makes contact with the conjunctiva of the eye. The time at which this first peak is reached is considered the implicit time of this feature. In the context of this work, the a-wave corresponds to the Class C waveform, also known as the early potential waveform.

The b-wave is less precisely defined. Traditionally, it has been taken as the next major feature exhibiting a maximum potential difference relative to the peak of the a-wave. Any intermediate peaks are ignored[70]. Based on this work, such a definition can apply to a variety of locations relative to the underlying processes, depending on the illumination used in the experiment. Comparing the synthesized ERG of this work to the informal figures presented in the ISCERG Standard, the b-wave would be defined based on the introduction of the signal from the 1st processing matrix, i. e., the input of the signal from the chrominance channels and defined as the Class E_2 waveform, into the composite ERG waveform. By this definition, the intermediate peak associated with the introduction of the component from the pedicels of the photoreceptors, the Class D waveform or the so-called generator potential, would be ignored. It is probable that time has come for new terminology to replace the traditional and recognize the significance of the Class D waveform as a component of the overall ERG.

Although based on short flash (impulse) illumination, the definition of the a-wave and b-wave are frequently discussed as if they were due to a step change in illumination or due to a "latching" mechanism. In Heckenlively, the a-wave is described as a repolarization of the photoreceptor cells. Under these interpretations, the amplitude of the a-wave remains a constant after reaching its peak. The amplitude of the b-wave is measured from the a-wave value. These interpretations are not consistent with this work.

The above statements are not compatible with the position summarized by Anne B. Fulton[71]. They differ in detail with regard to the a-wave and in concept with regard to the b-wave. The photoreceptor cell is intimately related to both the so-called early receptor potential, the Class C waveform, and the so-called generator potential, the Class D waveform. Only the Class C waveform is related to the a-wave, the Class D waveform is a component of the b-wave. The Class D waveform is found after the adaptation process. It normally increases in amplitude as a function of illumination intensity only in the scotopic and mesotopic regimes. At higher levels, it distorts considerably due to limiting in the adaptation amplifier and or logarithmic conversion at the node of the photoreceptor, the pedicel. This work does not find an active role for glial cells in the generation of the b-wave or in any other signaling process related to vision.

Biel has discussed the components of the ERG[72]. He quotes Penn & Hagins as saying the a-wave is due to the photoreceptor cells. He also quotes Stockton that the b-wave is due to bipolar cells. His analyses follows closely the analysis of this work although his b-waves appear to include inputs from the horizontal cells as well. His a-wave shows gain related to the intensity level. His b-wave is a composite of the output of the distribution amplifier and the signal processing. It shows saturation in the distribution amplifiers above 10^{-2} cds/m^2. He also showed Lakowski-type saturation (See **Section 18.1.5.6.4**) by very high backgrounds (30 cd/m^2) before a flash.

17.6.2.2.3 Synthesis of an ERG responding to a long duration step

[address both step and square wave in this section]

It is important to note that the droop(s), whether up or down, associated with a long duration ERG is primarily a representation of the time constants of the electrostenolytic and metabolic portions of the visual system.

17.6.2.2.4 A composite reference ERG

It is not possible to present a single fundamental ERG covering all possible test conditions because of the complexity of the waveforms involved. The problem is particularly difficult because of the length of the various time constants of the visual system and the duration of the excitation illumination. If these two characteristics are nearly equal, the response of the system becomes very complex. The nominal time constants of the HVS tabulated in the Standardized Human Eye, are 0.5 ms, three seconds, two minutes and ten minutes. In addition, there are the 1.2 and 6.0 second time constants of the iris.

Therefore, **Figure 17.6.2-4** presents two typical situations, the impulse and long duration step responses. The figure is meant to be illustrative and uses an unorthodox logarithmic horizontal time scale. The responses shown are not meant to be shown in correct proportion with respect to time. The responses are to an impulse or a step occurring at

---

[70]Heckenlively, J. (1988) Retinitis Pigmentosa, NY: J. P. Lippincott, pg. 7-8

[71]Fulton, A. (1991) Intensity relations and their significance. In Heckenlively & Arden, Chap 31, pp. 260-263

[72]Biel, xxx. et. al. (1999) xxx

time zero (which cannot be shown on a logarithmic presentation). The impulse response is best suited to showing the temporal characteristics of the signal related mechanisms with time constants short with respect to one second. The step response is best suited to illustrating the temporal characteristic for the longer, non-signal related mechanisms.

The figure illustrates a variety of important features related to each excitation situation. It also highlights the difficulties associated with using the feature names developed by the early electrophysiologists.

The transient situation.

In frame (A), the feature marked a- corresponds to the a-wave of the literature. Within this work, it is the initial portion of the Class C waveform as discussed above. This waveform originates at the dendritic terminal of the photoreceptor cells located in the IPM. After a short period, the composite waveform also displays the contribution of the Class D waveform. This waveform originates at the pedicels of the photoreceptor cells located in the INM. It exhibits a time delay due to the phase velocity of the signal within the photoreceptor cells.

After about 13 ms., the Class E waveform contributes to the composite waveform. This contribution can be positive or negative depending on the chromatic content of the illumination. Its envelope is shown by the shaded area of the figure. The polarity of this contribution has a major impact on the feature labeled the b-wave since the b-wave is normally defined as the maximum amplitude signal following the peak of the a-wave. Such a definition is clearly imprecise.

In frame (A), the overall response is shown decaying to the baseline after about 100 ms. This is an idealized case. In the actual case, the transient would overshoot zero amplitude slightly due to a small change in the output of the relevant power supplies. It would then return to the baseline after an extended period related to the time constants of the power supplies.

In general, after a period of less than 100 ms. (nominally 22 ms. as shown by the vertical dash-dot line), the signals caused by the illuminant have reached the ganglion cells and been translated into one or more pulse streams. The *signal related* transient portion of the composite waveform dies out after this time interval. The remaining signal reflects the restoration of the quiescent condition through actions of the power supplies. The pulse streams associated with the signal proceed down the optic nerve to the brain. These signals, and their return path signals, are quite well contained within the optic nerve. Even at the Nodes of Ranvier, the electrical currents related to the re-generation of the signals are quite localized and contained.

The observed transient ERG (as well as the step response ERG discussed below) are not as “clean” as the figure suggests because of the presence of signals in more than one spectrally sensitive detection channel. In this case, the shape of the a-wave is corrupted by the presence of two Class C waveforms that exhibit different time delays. Two Class D waveforms also appear with a delay between them. And then a complex Class E waveform appears that exhibits the temporal features of both of the Class D waveforms following a subtraction.

The observed transient ERG waveforms (more often transient LERG waveforms) are occasionally perturbed by one or more pulse waveforms, usually after the nominal 22 ms. interval from the start of the Class C waveform(s) in humans. The obvious source of these perturbations is capacitive pickup of the action potentials generated by the ganglion cells. There may also be a less obvious source of such perturbations. Under abnormal illumination or operating conditions, most of the neurons of the visual system are subject to spontaneous oscillation. They all contain an Activa that is critically biased to perform its normal role. The Activa normally represents a source of negative impedance. Only small changes in the impedances associated with such an amplifier, such as capacitive loading by an extraneous electrical probe, can cause it to oscillate.

The step illumination situation

In frame (B), the excitation illuminant exists to infinity on the right. Under truly small signal conditions, the composite ERG waveform would remain at a constant level after about 100 ms. However, it is important to note that even under small signal conditions, the purpose of the adaptation amplifiers is to maintain large signal conditions within the signal manipulation and later stages of the visual system. Therefore, some degree of droop, either positive or negative depending on its circuit of origin, can be expected in the signal manipulation circuits under sustained illumination. The time constant(s) of the mechanism causing these droops is normally several minutes long.

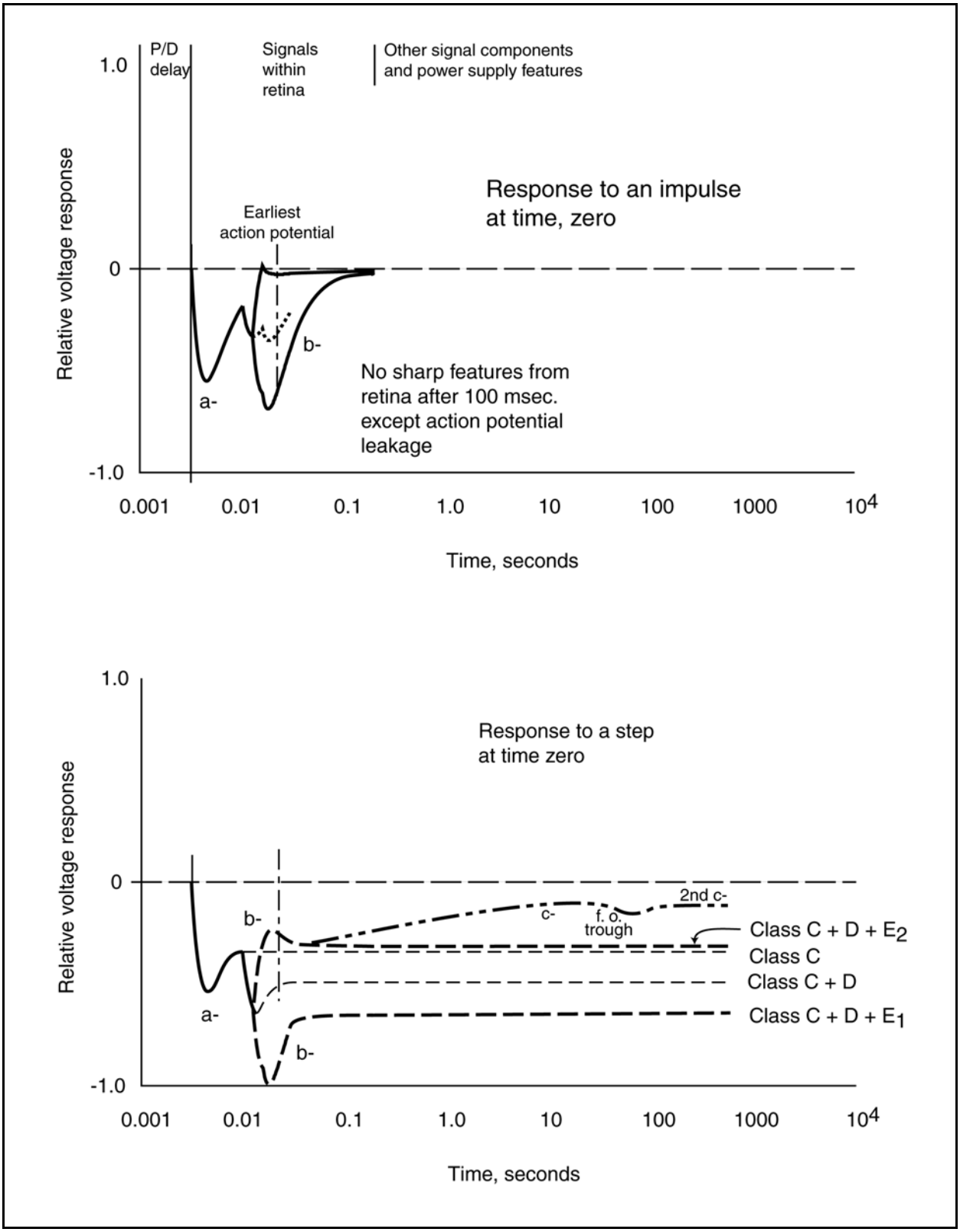

Figure 17.6.2-4 A synthetic ERG based on either impulse or long duration excitation. XXX XXX

The initial waveform (Class C) in the figure shows a distinct overshoot before assuming a constant value. The magnitude of the overshoot is determined by the initial state of the chromophores of the Outer Segment. Only a single Class C waveform is shown. Under some circumstances, the recorded waveform may be perturbed by a second Class C waveform due to the excitation of a second spectral class of photoreceptors (See next Section). This second waveform may exhibit a different time delay than the first due a different set of initial conditions in the relevant chromophores or adaptation amplifiers. In the absence of a second Class C waveform, the only Class C waveform would settle to a constant value given by the upper light dashed line labeled Class C. The delayed copy (Class D waveform) of the initial waveform is of the same polarity as that waveform but may be of a different amplitude. The composite waveform is therefore the sum of these two individual waveforms and is shown by the lower light dashed line labeled Class C + D. Note that the sum of the Class C and Class D waveforms can have a highly variable initial shape depending on their relative amplitudes. The specific shape of the sum of these two waveforms can have a significant impact on the definition of the “a-wave.”

After an additional delay, a component due to either one or two Class E waveforms will appear. Each of these waveforms are generated by the lateral cells of the 1st processing matrix (usually labeled horizontal cells). Each Class E waveform may be of either polarity and of any amplitude. It will generally exhibit an initial overshoot due to its derivation from two Class D waveforms. The overshoot may be followed by a recognizable undershoot because of the difference in time delay between the original Class D signals. The two heavy dashed lines indicate the envelope of the composite waveform due to all of the waveforms of Class C, D and E. The upper heavy dashed line represents Class C + D - E. The lower heavy dashed line represents Class C + D + E.

Note the difficulty in defining the “b-wave” precisely. Two individual labels are shown for the b-wave. The upper label corresponds to the case where the Class E waveform is highly negative relative to the Class C and Class D waveforms. In this case the a-wave is relatively small and the b-wave is relatively large. If the Class E waveform is of the same polarity as the Class C and Class D waveforms, the situation is quite different. The a-wave is now very large and extends to a magnitude of -1.0. The amplitude of the b-wave is now defined by the trailing edge of the Class E waveform.

Droop in the response to step illumination

As in the case of the impulse waveforms, the composite signal resulting from a step input will not show any variation due to the input excitation after 22 to 100 ms. Variations after this time are due primarily to the limited capabilities of the power supplies. There may be some variations due to signals received from the initial circuits of the brain, depending on the location of the signal return lead of the ERG instrumentation. The most notable features are the slowly changing amplitude of the composite response. This change is usually defined as "droop." There is a droop associated with each neural amplifier. For the Class C and Class D waveforms, this droop is conventionally shown as slowly approaching the quiescent baseline with a characteristic defined by the second order parameters of the power supplies. It actually approaches the ultimate steady state value for the specified illumination and the capacity of the metabolic system. In the case of the Class C and Class D waveforms these droops exhibit time constants of about two and ten minutes for healthy humans. The droop associated with the Class E waveform component can approach the quiescent baseline or converge to a different value because of its mathematical origin. If a broadband source of illumination is used, there may be two distinct Class E waveforms. However, they may not be distinguishable using ERG techniques. When combining all of the components of the droop feature, a very complex but slowly changing waveform may result.

As in the transient case above, after about 100 ms, the transient portion of the response has died out. The subsequent waveform is due to the steady state response of the signaling system perturbed by the performance of the power supplies. These power supplies are metabolic and electrostenolytic. They frequently exhibit a droop related to the time constants of the vascular system. Each underlying waveform can exhibit an individual droop. As in the case of the waveforms, the droops can be either positive or negative going. Hence, the composite droop can be positive or negative going. A positive going droop is frequently labeled the c-wave in the literature. The composite droop can also change direction as a result of the subtraction of two signals of different time constant. In one case, probably involving three signals, the resulting waveform may exhibit three features, the initial c-wave, a “fast-oscillation trough”, and a “2nd c-wave.” The so-called “fast-oscillation trough” frequently extends over an interval of 30 seconds. Note that it may appear as a relatively narrow, “fast,” trough if it appears out near 1000 seconds. However, if it occurs nearer 60 seconds, it appears distinctly broader.

Response to two step changes in illumination

There is no requirement that the response to a step input must return to zero. If a second step input is used to

complete a long duration pulse, the individual waveforms forming the subsequent composite waveform must be re-examined in detail. Some of these waveforms are state variable dependent. The smaller the excitation level, the less droop observed in the laboratory. However, the signal level is also lower and frequently lost in the noise.

To display a square wave response in frame (B), a second excitation step of opposite magnitude must be introduced at a finite time. The resulting response is not a mirror image of the first response because of the state variable characteristics of the photoreceptor cells. The actual Class C and Class D waveforms appropriate to the change in illumination must be computed (with their appropriate time delays) in order to describe the complete waveform. The resulting transient associated with this change in illumination is normally defined as the d-wave. Its polarity is normally opposite that of the a-wave. It is actually the result of the summation of a Class C, a Class D, and one or two Class E waveforms. The sum of these waveforms dies out completely if the net illumination is now zero. However, the composite ERG may not be zero for many minutes because of the action of the power supplies in returning the visual system to its quiescent condition. Figure 9-2 of Griff shows this transient clearly in the upper two traces. These traces also clearly show the first time constant of the power supplies of the photoreceptor cells for the cat (slightly less than one minute). The top trace can be related to the Class C waveform and the middle trace to the Class D waveform. The feature labeled the "light peak" in the third trace is the result of subtracting two transient waveforms exhibiting distinctly different time delays. These time delays are to small to appear in the figures but their cumulative effect on the amplitude of the composite waveform is not.

17.6.2.2.5 A baseline ERG with definition of "wave" features

Figure 17.6.2-5 will be used to graphically define the "waves," and not the "waveforms," defined in detail semantically in **Section 11.1.3.** The "waveforms" have been defined graphically above. As above, a logarithmic time scale is used in the figure to help span the time intervals of interest in ERG's and LERG's. Thus, the start of a square wave pulse of illumination beginning at zero time occurs at a point infinitely distant to the left. The termination of the pulse is shown with ease on the logarithmic scale. For the sake of simplicity, the illumination is taken to be a poorly defined "white" from an incandescent source and the eye is assumed to be fully dark adapted (no safe-light used in the experiments, no pilot lights visible to the subject). Let the color temperature of the source be less than 3000°K and let the integrated photon flux be equal between the S- and M-channel. As a result, only one chrominance channel, represented by a Class E waveform need be considered. The magnitude and polarity of the signal in that chrominance channel will depend on the relative amount of flux in the M- and L-channels. The nominal ERG still exhibits a variable related to the location of the signal return lead. Depending on this location, the initial delay before the composite waveform leaves the baseline can also vary in duration. It can exhibit a delay due to two distinct factors. The first factor involves the intrinsic delay in the photoexcitation/de-excitation process. The second delay involves the distance from the IPM layer of the retina to the point of signal collection on the surface of the eyeball. While this latter delay is usually fixed in a given experiment, the P/D delay is a function of the amplitude of the illumination and the temperature of the subject. The portion of the recorded composite waveform represented by the solid line after it leaves the baseline can also vary. The definition of the a-wave, usually defined as that portion of the ERG between the baseline and the most negative excursion of the composite waveform, can also vary. It can terminate at the time directly under the symbol, a-, or it can terminate to the right of that symbol. It can terminate at the end of the solid line or it can extend to the most negative excursion of the dashed segment. Care is required to avoid ambiguity in the definition of the a-wave. The b-wave is conventionally defined as that part of the composite waveform extending from the peak negative excursion of the a-wave to the most positive excursion of the composite waveform (within less than 22-50 ms). Clearly, this definition makes the b-wave a function of the amplitude of the amplitude and polarity of the Class E signal in the chrominance channel. The b- wave can extend to the first peak in the upper dashed line or to the break in the lower dashed line where it transitions to the dashed-double-dot line. Beyond 22-50 ms, both of the composite waveforms shown "droop" toward a more positive value. This waveform is commonly defined as the c-wave. Since this portion of the composite waveform represents the sum of voltages due to several possible metabolic processes, it can be complex. If it shows an intermediate negative going dip (extending for up to thirty seconds, this dip is frequently labeled a "fast oscillation trough." This label is less than descriptive when compared to the earlier features. The slowly varying section of the composite waveform following any trough is labeled the 2nd c-wave. Upon termination of the illumination, the composite waveform exhibits a positive going transient. This feature is usually labeled the d-wave but some authors have labeled it the "light peak." It is a response by the same mechanism that caused the initial portion of the a-wave but as a result of different initial conditions.

17.6.2.3 Source location via the LERG

The local ERG, or LERG, offers a capability not found in the basic ERG. It is able to determine the location of the source of the individual component waveforms. The LERG often provide more distinct recordings of the composite waveform than obtainable with an ERG. While the composite waveforms obtained by this technique are still complex, they show systematic changes with probe location. By using a probe to explore the depth of the retina, it is possible to localize these sources to within about ±15 nm. This is sufficiently accurate to correlate the signals with the individual layers and features in the cross section of the retina.

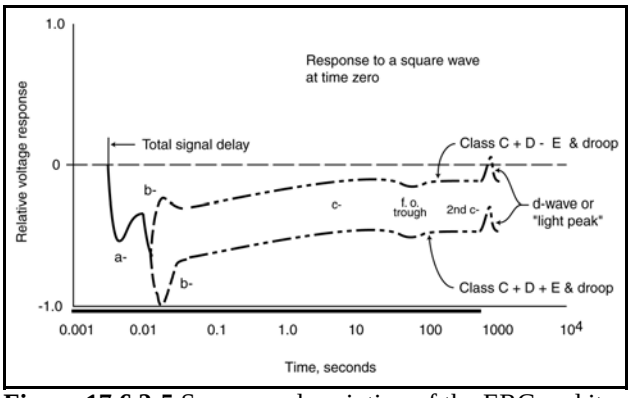

Figure 17.6.2-5 Summary description of the ERG and its "wave" nomenclature. Drawing is conceptual and scales are distorted. Dark bar represents illumination beginning at zero time. Difficulty in defining the a- and b- wave are illustrated.

The LERG provides higher sensitivity to voltages than can be obtained with the basic ERG. However, it introduces at least one additional variable, the variable impedance of the background medium and the variation in the amount of capacitive coupling between the probe and the various structures it approaches. The composite waveform obtained with the LERG technique frequently exhibits oscillatory components, particularly after the nominal 22 ms. following the beginning of the Class C waveform in humans. These are generally labeled oscillatory potentials. Bortoff[73] shows these pulses occurring after 100 ms. in Necturus at 5°C.

The source of the observed oscillatory potential, OP, features have been studied with mixed results[74]. Their localization, and even observation is complicated by the fact that any OP's related to the chrominance channels are not necessarily synchronous in time with the analog waveforms. Karwoski & Kawasali conclude that the primate OP's occur near one location within the retina. Their figure 16-1, from the retina of a rhesus monkey, clearly shows the oscillations occurring after an initial time interval (nominally 22 ms. as proposed by this work) from onset of the Class C waveform. This would be confirmation that source of the OP's are the action potentials of the ganglion cells. Although not well characterized in that figure, it appears the OP's exhibit a peak amplitude in the waveforms when the probe is close to the dendritic terminals and the Activas of the ganglion cells (waveforms labeled 24 through 40%). Their figure 16-2[75], based on a an isolated frog retina, exhibits very clear components due to the Class C, Class D, and Class E waveforms that must be accounted for before assigning the OP label to the subsequent features.

In this case, the maximum peak positive excursion of the waveform labeled "100%" (intraretinal probe near RPE layer with reference electrode was on the vitreal side of retina) is assigned to the underlying Class E waveform. Before this peak occurs, there are at least three negative going components. Based on this theory, the assumption is that there are four. The first peak due to a Class C waveform is only seen as an inflection point. It starts at 29 ms after the illumination step and the plateau is at 51 ms. The maximum negative peak is predicted to be composed of a Class D waveform, following the above Class C waveform, and a second Class C waveform. This peak is at 68 ms after the step in illumination. The third negative peak represents the second Class D waveform associated with the second Class C waveform. This peak occurs at 103 ms. The time difference between each Class C and Class D pair is 55 ms ± 2 ms as read from the graph. The most positive peak occurs at 126 ms and is followed by a negative going peak at 152 ms. However, there is a kink in the curve between these two points. This kink would suggest a minor peak hidden in the data. In the absence of other waveforms, the last peak would be expected to occur near 152-160 ms.

More information can be gleaned from this data. The presence of two Class C waveforms of different delay would suggest the animal was not dark adapted. The experiment was probably carried out under the notorious red safe

---

[73]Bortoff, A. (1964) Localization of slow potential responses in the *Necturus* retina. Vision Res. vol 4, pp. 627-635

[74]Karwoski, C. & Kawasaki, K. (1991) Oscillatory potentials, *In*, Principles and practice of clinical electrophysiology of vision. Heckenlively, J. & Arden, G. *ed*. St Louis, MO: Mosby Year Book, pp. 125-128

[75]Yanagida, T, Koshimiz, M. Kawasaki, K. et. al. (1988) Doc Ophthalmol, vol. 67, pp. 355-361

light. In this case, the L-channel would exhibit less delay than the M-channel. The long delay, compared to the nominal 22 ms, before the start of the first Class C waveform would suggest the experiment was carried out at room temperature or below. Note also that the amplitude of all of the signals decreases as the signal probe is brought closer to the signal return probe, as expected.

The conclusion is drawn that the first spike in the waveform that might be due to an oscillation potential, OP, occurs at about 165-170 ms. There appear to be only three OP candidates. The variable time interval between the three candidates suggests they could be due to capacitive pickup from the ganglion cells although they die out before the signal probe reaches the ganglion layer. Capacitive pickup would be reduced as the impedance between the two probe terminals due to the INM was reduced.

Bortoff discusses the source of the OP's in detail, using the terminology of the 1960's. He is specific in saying that: the photoreceptor potentials were never recorded together with spike potentials. He also associates the OP's with the bipolar or ganglion cells and notes "In the absence of illumination small oscillatory potentials were obtained from most cells in the bipolar and ganglion cell layers." It will be assumed here that the signals found in the bipolar layer related to the dendritic structures of the ganglion cells. According to this work, Op's normally occur in the absence of illumination in the differencing signal channels. **See Chapter 14**. Bortoff also noted the difficulty of recording full amplitude OP's due to the extremely high impedance of the source circuits and the significant capacitance of his probes (150-200 megohm resistance).

17.6.2.4 Variations in the early receptor potential

The literature contains a variety of reports of separation of the early receptor potential into an early and late component. It is critically important that the test configuration be known in detail before discussing such possible differentiation. Since the early receptor potential recorded by the ERG, and to a lesser extent the LERG, is the summation of signals from an ensemble of photoreceptors, such an occurrence is not unexpected. As an example found commonly in the literature, the experimenter prepares the experiment "under dim red light." However, this is more than enough light to impact the adaptation level of the L-channel photoreceptors. There are two aspects of the result. The higher average flux through the L-channel chromophores reduces the delay inherent in the P/D process for this channel and the adaptation amplifier may reduce the gain of this channel. As a result, the composite ERG obtained using broad spectral band illumination will display two independent Class C waveforms. One relates to the L-channel and the second relates to the M- and/or S-channels. That related to the L-channel will typically be earlier and of lower amplitude. Since the Class D waveform is a faithful copy of the Class C waveform under small signal conditions, the portion of the composite ERG associated with the Class D waveform may also exhibit a distinct separation into two components. However, this separation may not be as apparent since it occurs in the notch between the Class C and the Class C + D components in the composite waveform. This component may well have been present and contributed to the filling of the notch in the experiments of Smith & Lamb[76]. Although not discussed in detail, they used an infra-red sensitive CCD camera to monitor the pupil size, red LED sources below the camera as infra-red sources (880 or 930 nm peak wavelengths) and 1-4 red LED as a fixation reference. Normally, the *uncooled* CCD camera does not exhibit a spectral response (typical cutoff wavelength of 1.1 microns) significantly different at the infra-red wavelengths used than the human eye. The light from the LED's is integrated by the Ganzfeld sphere and effectively illuminates all photoreceptors of the eye to a degree.

Many years ago, the author as a young Air Force lieutenant, would astound visiting dignitaries by using a specialized television camera with an S-1 photosurface to reproduce their picture in "complete darkness." In fact, there was a red pilot light present but not obvious to the subject or the audience. The *steady* red light significantly desensitized the subjects L-channel photoreceptors and aided the television camera immensely.

17.6.2.5 ERG experiment design for research

There is considerable difference between the set of conditions developed above and those found in the ISCERG Standard designed for clinical purposes. The Standard calls for a maximum illumination flash width of 5 ms. and then introduces an asterisk followed by several sentences of caveats. The principle point is that such a long pulse does not represent an impulse to the system, the resulting waveform associated with the P/D process (Class A waveform) does not represent the transfer function of the underlying process, and the subsequent waveforms

---

[76] Smith, N. & Lamb, T. (1997) The a-wave of the human electroretinogram recorded with a minimally invasive technique. Vision Res. vol. 37, pp. 2943-2952

reproduce this distorted waveform. If study of the signal related waveforms of the ERG are to be studied, it is recommended that the pulse width not exceed 0.5 ms.

The Standard recommends a white source of illumination and suggests that most currently available strobe lamps exhibit a color temperature of 7,000 K. Strobe lamps normally do not exhibit a blackbody radiation spectrum. It is critical in research involving the ERG to know the spectrum of the radiation source as outlined above. The Standard also defines illumination in terms of photometric units. As indicated elsewhere, the instrumentation used in photometry does not accurately reflect the amount of light sensed by the eye (the eye is based on the internal photoemissive effect whereas nearly all photometers employ photoconductive detectors behind a filter) to the precision desired in reproducible research. Considerable effort should be expended in characterizing both the radiation source and any attenuating filters if results reproducible by other experimenters are desired. Measuring spectrally filtered illumination with a photometer amounts to an oxymoron.

Although pupil dilation without an artificial pupil is recommended in the clinical situation, an artificial pupil is required unless precision measurement of the pupil diameter is anticipated before and during the research activity.

The Standard recommends a reporting protocol that is strongly supported, including extraction of the critical parameters for presentation along with any waveforms in publications.

The dark adaptation interval should be specified explicitly. A period longer than 20 minutes is recommended, especially for those living in areas of high outdoor brightness. 40 minutes will suffice in all but the worst situations.

The Standard also makes other recommendations. The researcher must coordinate all of these individual recommendations in the context of the desired results.

17.6.2.6 Data from the literature

Iijima[77] has provided preliminary parametric data for the b-wave of the ERG under both photopic and scotopic conditions. The data shows good internal consistency based on the criteria of this work. However, it also illustrates a difficulty. The so-called implicit time, either to the peak of the a-wave or to the peak of the b-wave as shown above, involves a continuous variable, the delay term of the P/D equation. This variable is directly related to the illumination level employed. Therefore, the values given in Iijima should be accompanied by a much more specific characterization of the illumination used. The mean values for the implicit time of the photopic b-wave appear quite long in Iijima compared to that of Smith & Lamb for violet illumination. The conclusion could be drawn that Iijima was operating very near the mesotopic end of the photopic range but no values related to illumination or the test configuration were supplied in the article.

Dawson & Galloway[78] have provided an important figure in understanding the origins of the ERG. In an ERG recording from a man with a detached retina, they show that the Early Receptor Potential, the Class C waveform, is still recorded while the rest of the ERG waveform is not. This would be the expected result if the common emitter impedance of the adaptation amplifier was located within the detached portion of the photoreceptor complex. The photodetection process, up through the output of the adaptation amplifier would remain functional under this condition, although some change in the absolute gain profile might be expected. This impedance is associated with an electrostenolytic process on the surface of a specialized portion of the dendroplasm of the photoreceptor cell. The resulting situation appears compatible with figure 6 in Baylor, Lamb & Yau[79].

Dowling and Wald[80] have provided discussion of the ERG of subjects deprived of dietary vitamin A. The conclusion is that the Outer Segments of the photoreceptor cells fail to regenerate after significant deprivation.

---

[77]Iijima, H. (1991) Distribution of ERG amplitudes, latencies and implicit times. In Heckenlively & Arden. Chap. 37, pp. 289-290

[78]Dawson, W. & Galloway, N. (1991) Early receptor potential: origin and clinical applications. In Heckenlively & Arden, Chap. 40, pp. 317-321

[79]Baylor, D. Lamb, T. & Yau, K.-W. (1979) The membrane current of single rod outer segments. J. Physliol. vol. 288, pp. 589-611

[80]Dowling, J. & Wald, G. (1960) Role of Vitamin A Acid in Vitamins & Hormones. In Vitamins and Hormones, *Edited by* Harris, R. & Ingle, D. NY: Academic Press vol. 18 pp. 536-537

Biel, et. al. have recently presented a series of ERG's for the same eyes over an intensity range of 10^5:1[81]. Although the data is for dark adapted wild mice, it appears representative of *Chordata* and humans. **Figure 17.6.2-6** is an annotated version of their data. They did not specify the duration of their stimuli. Notice the variable latency in the start of the a-wave as a function of illumination level, approximated by the sloping dashed line. This delay is in agreement with the delay expected for warm blooded animals. Note also the delay, δ, of about 17.3 ms between the start of the a-wave, due to the Class C waveform from the collector of the adaptation amplifier of the photoreceptor cell and the start of the b-wave, due to the Class D waveform from the distribution amplifier of the photoreceptor cell. The so-called oscillations are seen begin earlier in time for higher stimulus levels. They may correlate with the start of the a-wave. Note also the significant reduction in the slope of the a-wave at lower light levels in agreement with the P/D Equation of Section xxx.. The Class C waveform would not be expected to reach its peak until about or after the start of the opposite polarity Class D waveform. At the -3 log unit level, the a-wave has hardly begun to rise when the related b-wave begins to oppose it. The net result is that the dominant feature in the response is due to the Class E waveforms related to the signal processing neurons of the retina. At the -4 log unit level, the signal amplitude is near the noise level of the test set.

Biel, et. al. presented similar data for mice suffering an induced mutation in the CNG3 gene. This mutation is directly related to the disease of Achromatopsia. The applicability of the data to this disease will be discussed in **Section 18.8.2.**

17.6.2.6.1 Pharmacology and the ERG

There is a large experimental literature attempting to correlate the impact of various drugs on the ERG. These studies have generally attempted to determine the impact of different drugs on different layers of the retina and sometimes different types of neurons within a layer. They have suffered from the lack of an circuit model. As a result, the data usually refers to the hyperpolarization or the depolarization of a signal due to pharmacological intervention. The results have been most useful when related to the photoreceptor cells, the so-called ON-bipolars and the ganglion cells. These cells all operate in the monopolar mode. When the experiments involve cells operating in the bipolar mode, the results are often confusing. This is because the pharmocological agent usually impacts the electrostenolytic process associated with the cells. This impact does not correlate directly with the signal output of the cell.

Stockton & Slaughter have provided an analysis of the impact of a group of pharmacological agents on what they take to be a discrete b-wave (as opposed to the composite b-wave described above)[82]. They develop the fact that APB (2-amino-4-phosphonobutyrate) is an analog of glutamate (sic). In the context of the electrostenolytic processes of the neural system, it is probably more appropriately described as an analog of GABA, γ-aminobutyric acid. In this context, it is likely that APB interferes with the normal operation of GABA in the glutamate cycle, possibly by occupying the receptor site on the surface of the plasma membrane usually used by GABA.

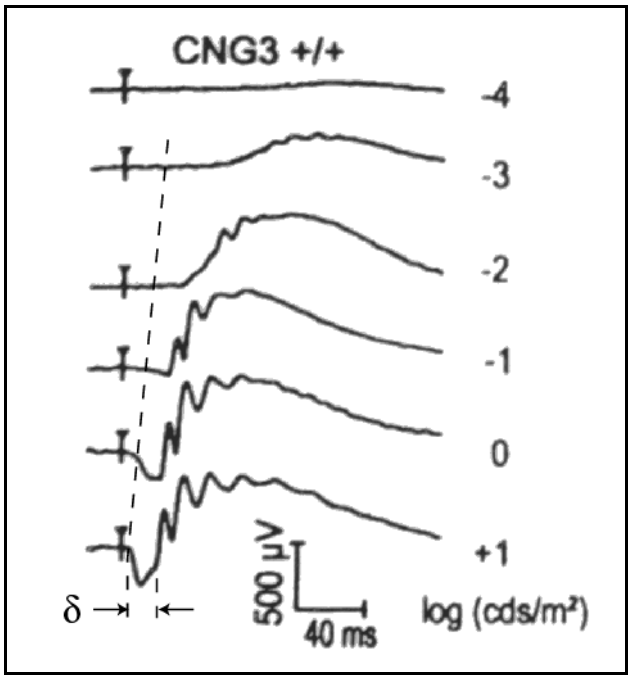

Figure 17.6.2-6 A series of ERGs versus low illumination levels recorded from wild mice. The sloping line illustrates the variable latency in the start of the a-wave as a function of illumination, from about 4.6 ms at maximum stimulus to 23.3 ms at -3 log units. δ represents the approximate delay, 17.3 ms between the Class C waveform generating the leading edge of the a-wave and the Class D waveform initiating the rise of the b-wave. The duration of the stimulus was not specified. Adapted from Biel, et. al. 1999.

[81]Biel, M. et. al. (1999) Selective loss of cone function in mice lacking the cyclic nucleotide-gated channel CNG3 Proc. Natl. Acad. Sci. Vol. 96, pp 7553-7557

[82]Stockton, R. & Slaughter, M. (1989) B-wave of the electroretinogram *J. Gen Physiol* vol. 93, pp 101-122

17.6.3 Temporal (and related spatial) frequency domain performance

The determination of the frequency response of human vision is complicated because of the "optimizations" added to the basic visual system through environmental adaptation. It is also complicated by the difficulty of separately defining the immense potential of the brain to perform temporally related signal processing, including the correlating of current input with data available from long term memory recall. In general, the cerebrum operates in a highly parallel processing regime that does not limit the overall performance of the visual system. However, the time delays that are encountered in signal projection between different cortical engines can introduce limitations. This work will be restricted to the processes and techniques performed in the first three stages of vision. Those performed in Stage 4, intrinsically cerebrum related, will not be addressed except on an ad hoc basis during the remainder of the discussion.

There is a basic signaling capability that is independent of the effects of spatial integration, chromatic integration, the spatial to temporal conversion associated with tremor, and the special techniques (used primarily if not exclusively in *Chordata*) to project the signals to the brain. In the above sentence, the word integration is used in the sense of a complex form of summation. There is, in addition, the signal differencing found in the chromatic, spatial and (potentially) polarization channels of human and other sophisticated animals. A number of specialized encoding techniques are used in vision, similar to some of the techniques found in recent man-made systems, to achieve unique optimizations. The optimal use of all of the above techniques and processes requires the use of a mode switching strategy in support of the overall architecture.

Because of the variety of strategies and implementations available and the absence of some of these in human vision, it must be reiterated that the HVS does not appear to be *the most* sophisticated system in *Chordata*. It may be that it is necessary to recognize a number of systems *as equally sophisticated but significantly different*.

There have been a wide variety of psychophysical studies attempting to understand the organization of the visual system by using various pattern and flicker techniques[83]. These involve more independent variables and thresholds than the investigators can enumerate or control. One of these is the angular size of the overall pattern relative to the size of its finest detail. This ratio has a large impact on the threshold in the psychophysical experiment. They have not provided a clear description of the relationship between the temporal and spatial dimensions in the visual system. In their conclusion, they stress "the need for caution in the use of two-criterion techniques for postulating separate pattern and flicker mechanisms." Although, Harris introduced a concept of velocity (or equivalent velocity) to relate temporal frequency and spatial frequency, he appears to have done it based on a parametric analysis of the equations involved[84]. Cycles/sec divided by cycles per degree equals degrees/sec. This work will take an entirely different approach based on tremor as the physical mechanism that provides the conversion factor, velocity, between spatial and temporal frequency.

This section will be subdivided to address the impact of the processes and techniques enumerated above on the overall frequency response of the resulting system. A final paragraph will attempt to summarize the impact of all of these implementations on the overall frequency response of the visual system.

A first order model will be presented that applies primarily to the analysis signal path associated with the foveola when it is operating in the photopic range. The model will concentrate on the overall modulation transfer function of the system with only a few remarks related to the threshold characteristic required to generate the overall contrast frequency functions. The model will be compared to the data in the literature for the threshold contrast performance of the human eye. The threshold contrast is a function of the threshold level within the signal channel. This level is normally associated with the dynamic range of the system and is constant (deterministic) within the photopic range. Below this level, the threshold level is stochastic. It is determined either by the photon noise associated with the illumination or by the random noise associated with the amplifiers of the signal path. This mechanism introduces an additional function into the contrast temporal frequency (CTF) function that will not be developed here. It only affects the shape of the CTF at very low frequencies and illumination levels.

It is difficult to correlate some of the data in the literature due to the variety of test patterns used by different investigators. Comments concerning these patterns appears in **Section 17.8.2.1**.

---

[83]Panish, S. Swift, D. & Smith, R. (1983) Two-criterion threshold techniques: evidence for separate spatial and temporal mechanisms. *Vision Res*. vol. 23, no. 12, pp 1519-1525

[84]Harris, M. (1980) Velocity specificity of the flicker to pattern sensitivity ratio in humna vision. *Vision Res*. vol. 20, pp 687-691

17.6.3.1 The primary modes and mechanisms affecting the frequency response.

The presence of different operating modes in the visual system has contributed significantly to a low level order of confusion in the literature. This confusion has prevented various investigators from fully exploiting their experimental data base.

Conventional wisdom not withstanding, the fundamental HVS is not an imaging system. It has evolved from and remains fundamentally a change detection sensor. Based on this fact, it is easiest to define the fundamental operating mode of the system as that associated with "staring off into space." The other modes can then be defined relative to this baseline. **Section 15.2.4** illustrates the topology of these modes. When in the awareness mode of vision, the system is optimally configured, even to its state of focus, to sense any change occurring within its total field of view. The specular reflection of sunlight by the smallest object at a great distance will cause a signal to be transmitted to the brain. This signal is transmitted over a different path than the signals of the awareness mode. This path represents the alarm mode of the system.

Upon receipt of a change signal from anywhere in the field of view via the alarm mode, the midbrain will call for a large saccadic motion that brings the line of sight into alignment with that source of change. Normally, several bytes of information will be received by the brain before it has computed the necessary commands to the muscles. It uses this additional information to compute the second and possibly later terms in a serial expansion of the desired command. The result is greater precision in the resulting pointing command. During this saccadic motion, the signal paths to the brain are essentially disconnected, similar to the blanking interval in a television system, and the brain relies on its short term memory of the scene to control other bodily motions. Because of the precision of the overall calculation mentioned above, it is only in rare cases that the visual system fails to bring the source of the change into the desired location relative to the foveola within the required precision.

Following the saccadic motion, the eye will enter the analytical mode. In that mode, an internal signal will be applied to the muscles of the eye in order to create a synthetic motion between the subject of interest and the line of sight. This motion, known as tremor, converts the spatial information imaged on the retina into temporal changes in the signals transmitted to the brain. This conversion allows the specialized portion of the retina, known as the foveola, to extract precise spatial information from the image and the pretectum to perceive this information.

During both the awareness and analytical modes of visual operation, the tremor also affects the operation of the non-foveal portion of the retina. This small artificial spatial motion causes the entire scene to appear to be changing very slightly at a frequency controlled by the tremor generator. As a result, the HVS is able to extract what appears to be a continuous image of the scene on a continuous basis. This is a deception. Most of the information obtained in this way is discarded within the retina and the cortex relies on its short term memory to remember what the external world looks like. The information that is not discarded in the retina is transmitted to the cortex using a high level of encoding to tell the brain that nothing has changed. Changes that occur unrelated to the phase and frequency of the tremor are transmitted to the midbrain separately to indicate a new and possibly threatening change in the scene.

The majority of lower chordates, lower molluscs and probably all arthropods do not employ tremor. As a result, these animals are unable to perceive a continual image of their environment under any conditions in the absence of threatening or self induced physical motion. A similar pathological condition is well documented in humans. The subject only sees "ghostly shadows" moving within its field of view. During the transition between these modes, the effect of tremor is essentially quashed by the larger motions related to the saccadic motion and the blanking process within the visual system.

17.6.3.2 Frequency response based on temporal processes

The basic frequency characteristics of human vision are determined by a number of fundamentally different temporal processes. The first order processes, found in the signal sensing stage, are analog in nature. The second order processes, found in the signal projection stage, involve "sampled data" techniques. A third order of processes involves the amplitude differencing between two analog channels.

Isolation of many of these processes is possible through review of the data from a variety of experimenters. In the course of this work, no sign has appeared suggesting the presence of any lumped constant or sampled data based bandpass filters exist in the biological vision system. On the contrary, a simple serial arrangement of low pass filter elements (with one used in a feedback arrangement and one exhibiting a pole that is a function of the irradiance) account for all of the frequency determining elements in vision.

Since the observed temporal response affects both luminance and chrominance perception, it can be assumed that the

controlling processes occur early in the signaling paths. Such inferences correlate well with the proposed temporal characteristic of the adaptation amplifier proposed in this work. In addition, the spatial frequency performance of the visual system will be shown to be highly dependent on these temporal frequency elements in **Section 17.8.4.** xxx

17.6.3.2.1 The primary temporal frequency limiting processes

There are multiple mechanisms limiting the temporal frequency response of the human eye. These mechanisms contribute to an overall temporal frequency response defined as a bandpass filter. This frequency response can be defined in detail using the rules of electrical network theory and the mathematics of the LaPlace Transform (a simplification of the Fourier Transform that is required to study the spatial frequency response of the visual system).

Figure 17.6.3-1 describes the elements of the visual system involved in determining the temporal frequency response of the luminance channel of vision.

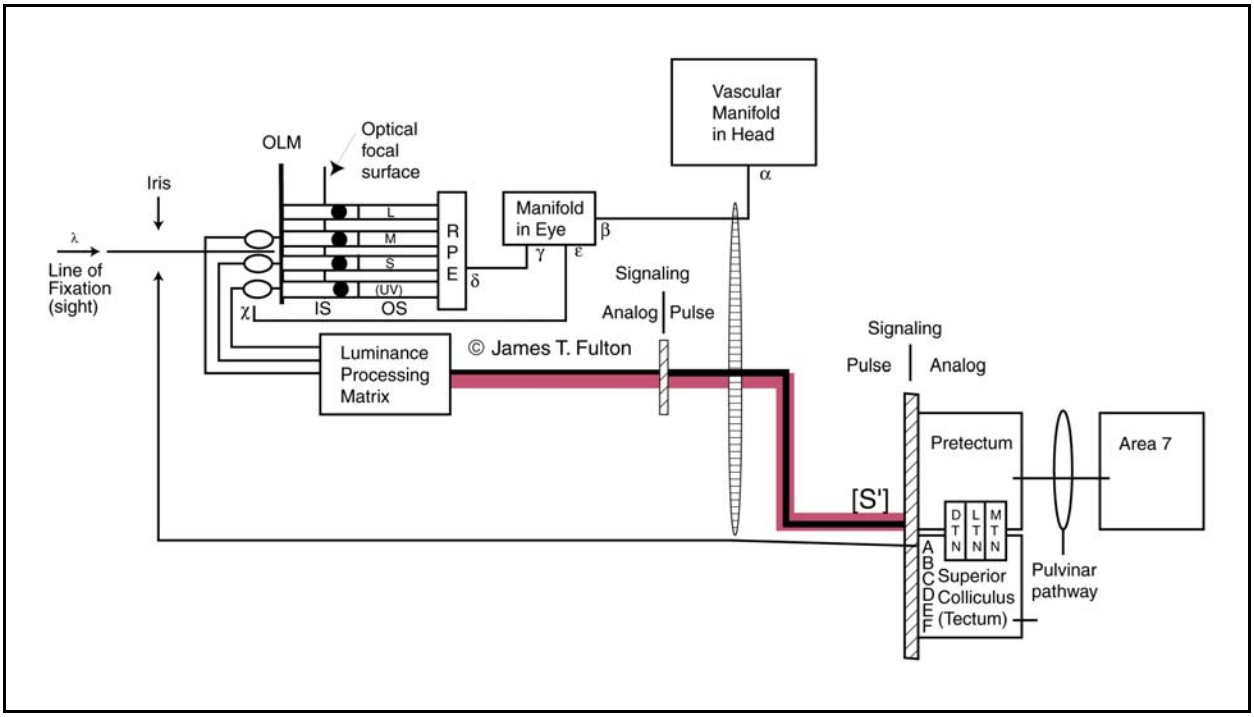

Figure 17.6.3-1 The model of the visual system relevant to the temporal frequency performance of vision. The path shown is for light imaged on the foveola. The light enters the eye through the iris associated with Stage 0 and excites the chromophores within the OS of Stage 1. The chromophores are de-excited in the process of initiating the electrical signal in the dendrite associated with the Activa within the photoreceptor cell. This Activa is the heart of the adaptation amplifier found in Stage 2. After additional signal processing, the signal is encoded by the ganglion cells of Stage 3. The decoding of this signal at the Pretectum involves a low frequency filter. Following additional analog signal processing in the Pretectum, the signal is again encoded, but in vector form, for projection of the signal to Area 7 of the cortex which is part of Stage 4 of vision. As shown, the iris aperture is controlled by a signal generated in the Pretectum and passed through the Superior Colliculus. The manifolds are major factors in the performance of the adaptation amplifiers.

Note the connection between terminal A of the Superior Colliculus and the iris of the eye. This path represents one of the only external feedback paths in the visual system that can effect the signals within the neural system. Because of the polarity of this path, it introduces a high pass filter function into the overall response. However, it occurs at such a low frequency it is hardly ever noted in the laboratory.

[xxx The low frequency limit is essentially fixed, but has not been studied in great detail. The upper frequency limit is variable and has caused great confusion in the experimental literature. Authors have strove to define the upper frequency limit of the visual system by proposing a variety of different multi-stage RC filters as best fitted their data.

This data was usually collected over a limited dynamic signal range in experiments that did not fully document the parametric relationship between the measured variables and this range. The experiments and data must be considered exploratory because of this endemic problem.]

[xxx The most important low frequency limitation on the visual system is due to the load characteristic of the adaptation amplifiers of the photoreceptor cells. The primary role of this load is to remove the sensitivity of the eye to slowly varying changes in illumination so that it can operate successfully over a dynamic range of about 10^7:1. To do this, the signal passband is restricted to frequencies above about $f_{1/2}$ = 0.1Hz (based on a three second time constant and $f_{1/2} \sim 1/\pi T$).]

Figure 17.6.3-2(a) shows the terms in the modulation transfer function of the visual process as they relate to the above stages. Note the use of the imaginary operator, j, in the equation.

The stage 0 term is due to the operation of the iris and the servo loop controlling it. This equation has S, representing frequency, in the numerator. The form of the equation is that of a high-pass filter. It results from the presence of a low-pass filter in the feedback path. This high-pass filter is difficult to model in a first order form because of the data processing associated with the pretectum and superior colliculus portion of the feedback loop. The opening and closing time constants are not equal and normally the iris operates primarily in the mesotopic range of vision. It remains nominally closed (2.0 mm diameter) throughout most of the photopic and hypertopic ranges and therefore can be ignored in tests above about seven Trolands.

The stage 1 term is taken directly from the P/D equation of the visual process and represents the mechanism associated with the chromophores within the outer segment of each photoreceptor cell. It is the Laplace transform of the transient response developed in **Appendix A** and discussed in **Chapter 12.** The denominator contains two terms and one of them is a direct function of the illumination level. A special mathematical case applies when the two time constants are equal. As discussed in **Appendix A**, in this special case, the transient equation reduces to that suggested by Hodgkin many years ago. In that case, the denominator can obviously be expressed as a second power of the single term.

The stage 2 term also has S in the numerator. This is the term associated with the adaptation amplifier within the inner segment of each photoreceptor cell. It is the result of internal feedback within the first Activa circuit of that stage. The time constant associated with this term is affected by the state of adaptation of the eye and the health of the hydraulic manifold shown in the above block diagram at the time of the experiment.

The stage 3 term is that of a low-pass filter. It represents the integrators associated with the stellate cells in the pretectum at the end of the projection circuit that is associated with the ganglion cells of the retina.

Figure 17.6.3-2(b) and **(c)** illustrates the nominal modulation transfer function for each of the elements in the formula of **(a)**. **Figure 17.6.3-2(b)** shows each filter section separately along with their half amplitude points. It highlights the fact that the time constant $S_{P2}(I)$ is a variable and its low pass characteristic varies accordingly. The variation is shown for a ±16% range about the value of 30 candela/meter^2 so it can be related to the current MODELFEST (www.sightresearch.net/files/contrastperf.htm) activity within the community. The actual variation is much larger in the data from Kelly. The two high frequency responses in red are associated with the iris. Two responses are shown because the precise nature of the small signal frequency response of the pupil within the mesotopic range is not reported in the literature.

Figure 17.6.3-2 (c) shows the product of the individual MTF terms forming the overall modulation transfer function of (at least) the portion of the visual system related to the foveola. It is aligned with **(b)** in order to illustrate how some of the time constants become obscured in the overall response, particularly at high frequencies on a logarithmic graph. The vertical scale has been compressed in order to illustrate the range of slopes associated with the asymptotic form of the overall response. The black lines indicate the normal characteristics of the graph with the effect of the iris shown in red on the left. It is useful to note the local slope of the overall modulation transfer function indicates the number of individual filter stages that are actively impacting the operation of the overall signal path at a given frequency.

At very low frequencies and illumination ranges where the iris is active, the slope of the overall MTF becomes +2 and the visual response falls very rapidly with decreasing frequency. At the higher frequencies, the form of the overall MTF is seen to vary considerably with the illumination level due to $S_{P2}(I)$. The form is precisely that measured by Kelly and others for a small field of view centered on the line of fixation. The maximum slope at high frequencies measured in the laboratory is frequently minus three. However, some experimental data has suggested a slope of minus four or even minus five.

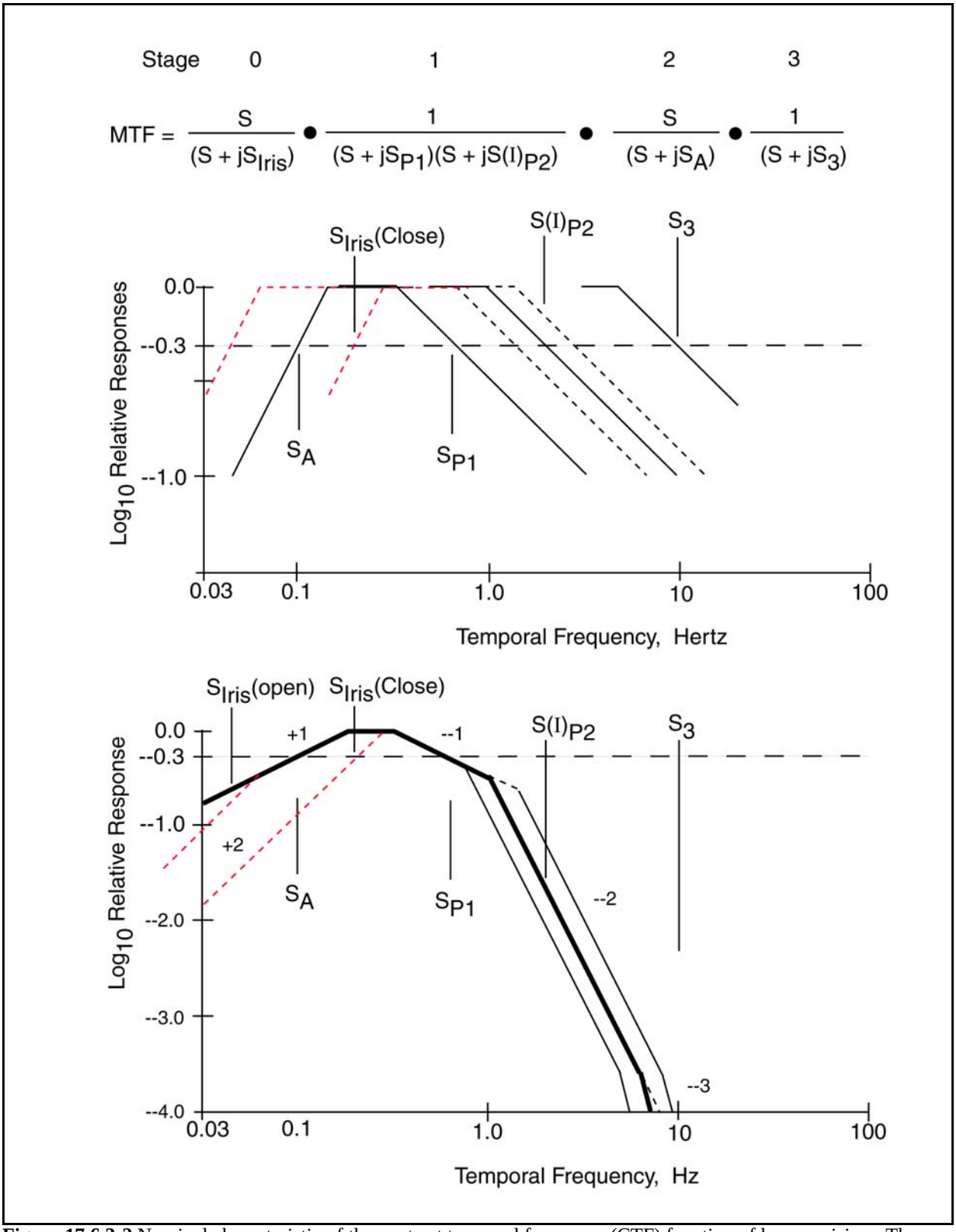

Figure 17.6.3-2 Nominal characteristic of the contrast temporal frequency (CTF) function of human vision. The analysis and diagrams apply specifically to the foveola. Xxx frequencies seem to be too low.

17.6.3.3 Formulation of the CTF, Contrast Temporal Frequency function

The conventional method of displaying the CTF data, collected by the empirical community, can be given a theoretical foundation. The foundation relies upon the fundamental goal of the collection activity, the determination of the minimum contrast threshold required for perception of a given test image for a given illumination environment. For precise work, the illumination environment must be known with precision and should be carefully tailored to only excite one spectral channel of the visual system.

It is important to agree on a definition of the term contrast. Many authors define the contrast as the maximum irradiance minus the minimum irradiance provided by a source divided by the sum of the maximum and minimum irradiance[85]. This is consistent with the description of contrast as a modulation about an average value. However, in many physical configurations, the minimum irradiance viewed by the subject is not the intrinsic level of the dark source. For many CRT based displays, it is the reflection of the ambient illumination by the unexcited phosphor and glass of the faceplate. In those cases, the contrast is defined as the maximum source illuminance minus the ambient illuminance divided by the sum of the maximum and ambient illuminances. In either case, it is important to maintain the surround at the level of the average illuminance and not allow the subject to fixate outside of the surround. Under the above definitions, the range of the contrast is between an absolute maximum of 1.0 and 0.

17.6.3.3.1 The derivation of the contrast threshold frequency functions

The CCF, CSF and CTF defined in **Section 17.1.2.3** are all based on a single underlying architecture. They are all expressions of the equality between the threshold level required for perception and the signal level at the point of perception. This point of perception can generally be described as the point where the visual system transforms the signal information from the temporal domain to the vectorial domain. This point is generally associated with the pretectum for information derived from the foveola and areas 19-22 of the posterior lobe for other retinal information.

The basic expression can be expanded to the equality between the product of the threshold level and the perception criteria (based on the structure of the stimulus) and the product of the input temporal stimulus profile and the MTF of the signaling channel. The input temporal stimulus profile can be expressed as a contrast level that is symmetrical about a mean illumination level. Mathematically, this equality can be expressed as:

$$C_{TH} \bullet S_{AVG}(Ir) = \left(\frac{Crit. \bullet Level}{MTF} \right)$$

Eq. 17.6.3-1

where C_{TH} is the measured threshold contrast, $S_{AVG}(Ir)$ is the average signal level at the point of perception for a given illumination due to a given spectral irradiance, Crit. is the perception criteria required by the perception mechanism to perceive a stimulus with a given structure, Level is the threshold level of the perception mechanism, and MTF is the cumulative <u>absolute</u> modulation transfer function of <u>all</u> mechanisms between the stimulus and the point of perception. The value of Crit. is usually a small value near one. It may be larger or smaller than one. The classic example of a value less than one is that of a long telephone wire in aerial photography. This wire can frequently be perceived in the prints although it is below the normally defined performance limit of the camera system.

Many variables affect the applicable MTF but the simplest is the diameter of the pupil. **Figure 17.6.3-3** shows this basic function along with two other parameters from Cooke et al[86]. All of the functions are obtained from the Fourier transform of their respective optical spread functions. The optical spread functions for tremor and drift did not appear in their cited source. On page 141, they gave a linear drift parameter of 1.5 minutes of arc during the assumed glimpse interval of 333 milliseconds. They gave a "tremor amplitude of typically 1-3 minutes of arc." The tremor range corresponds to three to nine photoreceptor diameters. This work generally assumes the RMS tremor amplitude to be on the order of three photoreceptor diameters with peak excursions to the larger amplitude.

---

[85]Kelly, D. (1961) Op. Cit. pg 423

[86]Cooke, K. Stanley, P. & Hinton, J. (1995) The Oracle approach to target acquisition and search modelling *In* Peli, E. *ed*. Vision Models for Target Detection and Recognition. Singapore: World Scientific page 135

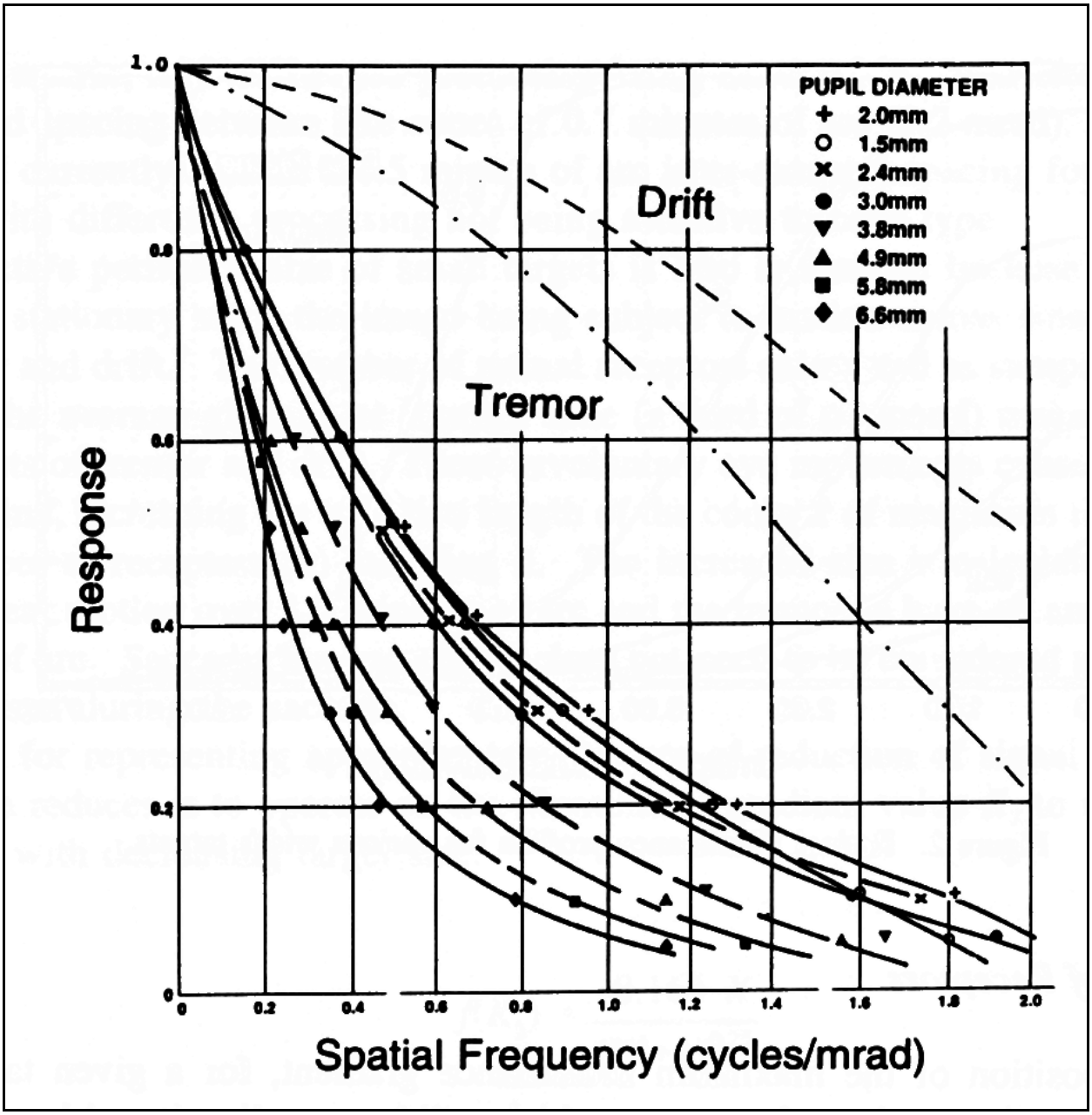

Figure 17.6.3-3 MTF of the eye: optical and motion components. The curves are obtained by Fourier transformation of the appropriate optical spread functions. See text. From Cooke et al., 1995.

Note the goal of the adaptation process within the photoreceptor cells is to maintain the average signal level constant at the point of perception. To the extent, it is able to do this, the equation is modified to:

$$C_{TH} \bullet \left(S_{AVG}(Ir) \bullet G_{ADAPT}\left(\frac{1}{S_{AVG}(Ir)} \right) \right) = \left(\frac{Crit. \bullet Level}{MTF} \right)$$

Eq. 17.6.3-2

where G_{ADAPT} is the gain of the adaptation process (on a per individual spectral channel basis) and this gain is inversely proportional to the input signal, $S_{AVG}(Ir)$, generated by the P/D process (also on a per individual spectral channel basis). Within the capability of the adaptation process, the product of the signal gain and the adaptation gain is equal to a constant. If desired, this constant can be transferred to the other side of the equation.

Watson has recently provided relative data on the criteria level associated with a large group of simple sinewave-based Gabor patches[87].

Figure 17.6.3-4 presents two frames, out of many possibilities, illustrating how the above relationship can be presented. The frame on the right is the form most commonly found in the literature. At low incident stimulus levels, the gain of the adaptation amplifier is unable to maintain this constancy. As a result, all of the elements illustrated in the figure and the threshold contrast begin to move toward the zero log threshold level. In addition, as the incident stimulus becomes less intense, the second and variable time constant in the P/D equation begins to move toward zero frequency as indicated by the dashed line. This movement frequently causes the maximum MTF value to decrease.

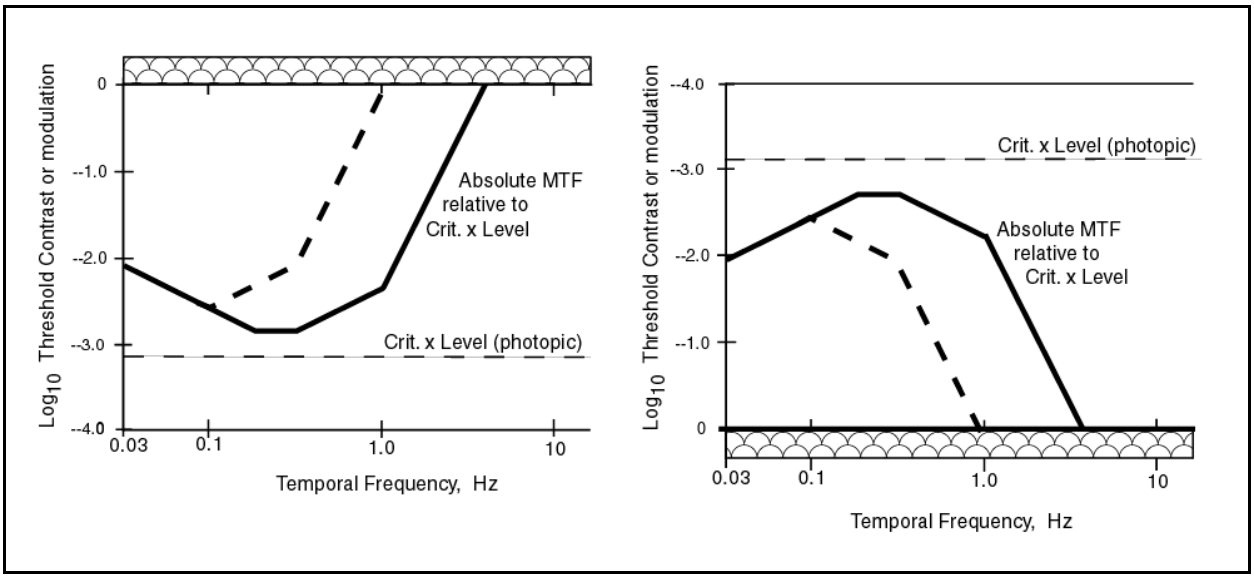

Figure 17.6.3-4 Conceptual forms of CTF presentations assuming a photopic stimulation level. At a lower stimulation level, the product of the criteria and the threshold level moves toward the zero log threshold level. In addition, the overall MTF tends to move toward the dashed line because of the shift in the variable time constant associated with the P/D process. This shift is frequency frequently results in a reduction in the maximum value of the MTF function. These effects tend to raise the threshold contrast value.

The product of the criteria and the level may or may not be a function of frequency based on the design of the experiment. It usually is not. Within the photopic region, this product is determined primarily by the deterministic threshold of the ganglion cells at the input to the projection stage or at the sensing cells following the stellate cells at the output of the projection stage (stage 3). However, when the stimulus level is reduced significantly, the effects of quantum noise begin to change the nature of the signal within the visual channels. The signal itself becomes noisy.

---

[87] http://epubs.osa.org/oearchive/pdf/14103.pdf

Under this condition, the perception circuits make a judgement about a signal containing a stochastic element. As the stimulus is reduced further, the noise performance of the input circuitry of the visual process, either within stage 1 or stage 2, become the limiting stochastic process in the visual system.

[xxx
It is generally a function of the threshold criteria adopted in the laboratory experiments. The following material will discuss each term in this calculation separately starting with the MTF functions. During the early discussions, many references many references will be made to the literature related to the complete functions. These references will be primarily to the shape of the functions with respect to frequency without regard to the absolute value of the vertical scale. Once the form of the MTF's have been determined, it is possible to factor in the static contrast and the threshold level to compute the complete CCF, CSF and CTF. The form of the static contrast function is unique to the environment under test. The threshold level is also unique to the type of test and the region of the luminance range under test. The difference in the threshold level among the terms of these functions and its change in form in the case of chromatic contrast, are important in modeling the overall performance functions and relating them to the laboratory data.]

17.6.3.3.2 Secondary features in the contrast temporal frequency response

To compute and or measure the CTF function for a "white" illumination source, the total signal in the R–channel must be considered rather than just the signal from one spectral channel. The summation of the spectral signals occurs at the input terminal of the first Activa in the luminance signal processing matrix of stage 2. This Activa is generally found within a (morphologically labeled) bipolar cell. To account for the logarithmic conversion of the signals from the current mode in the photoreceptor cells to the voltage mode at the inputs to these Activa, and any adjustments in the individual spectral signal gains due to the electrical coupling network, it is important to refer to the contrasts due to stimulation as they are measured at this point in the system. This involves calculating an equivalent R–channel contrast that incorporates the contrast changes from each spectral channel in proper proportion. The methodology for doing this, while insuring no conflict and cross coupling of data with the chromatic signaling channels is discussed in connection with the CCF in [**Section 17.6.3.6**].

There is some test data in the literature based on a very wide field of illumination (65 degrees)[88]. This field extends well outside of the foveola on which the previous analysis was based. There is a suggestion in this data that the asymptotic slope of the high frequency skirt of the contrast response may reach five. This feature of the data may be due to any of several factors. First is the fact that the signal is processed logarithmically at the output terminal of the photoreceptor cells. Second is the possible presence of additional low-pass filter stages in the signal path. Third is the fact that very high test contrast stimuli necessarily cause large-signal conditions that require more sophisticated modeling because of the nonlinearity of the adaptation circuits. The logarithmic processing may complicate the mathematics of calculating the overall modulation transfer function. If the system includes additional low-pass filters, these can be accounted for by adding additional terms of S_4, S_5, etc. to the model. Determining the precise source of these graphical features may require very careful experimentation.

Although there is little data for frequencies below one Hertz, some of the contrast threshold data in the literature appear to incorporate a horizontal plateau in that region that is statistically relevant but not suggested by the analysis provided above. As noted in Kelly (1958), this effect is most noticeable at scotopic and mesotopic test levels[89]. Under these conditions, the threshold associated with the experiment is becoming a photon noise limit rather than the dynamic range limit usually found in the photopic range. This artifact may also be due to the introduction of chromatic contrast changes into the psychophysical experiments used to collect the data due to inadequate experiment design. This will be discussed in **Section 17.6.3.5**. xxx

[In his 1961 paper, Kelly extended the test illumination up to 9300 trolands. He remarked that this level elicited pain in his eyes and he did not ask other subjects to perform this test. The data clearly shows the effect of saturation in the signaling channel due to the inability of the adaptation amplifiers to process this high signal level. This level is in the hypertopic range of illumination. The peak modulation did not increase with illumination and actually fell in his figure 4.] xxx move to 17.1.2.3

[It is necessary to note that the adaptation amplifiers have a limited range of operation (nominally defining the photopic range of vision. When the illumination falls below about seven Trolands, the transfer function shown for stage 2 is no longer appropriate. The adaptation amplifiers are now operating in a different mode due to their limited

---

[88]Wyszecki & Stiles or original xxx
[89]Kelly, xxx ref 10 on pg 466 of ww 270 P957 '91

amplification capability. This fact reduces the slope of the high-pass filter characteristic associated with them to a more nearly horizontal line. Similarly, the servosystem associated with the iris also reaches the maximum open condition. Its individual response also approaches a more nearly horizontal line. As a result, the overall MTF also becomes a more nearly horizontal frequency function in the lowest frequency range. This is clearly seen in the Kelly data and other data for low illumination levels.]

17.6.3.4 Formulation of the CSF, Contrast Spatial Frequency function

The literature contains experimental data on the achromatic Contrast threshold as a function of spatial frequency for a stationary image, labeled here the CSF, and similar data for a contrast threshold as a function of spatial frequency in the presence of lateral image motion. It also includes some interesting, but dated data from Blakemore & Campbell based on adaptation[90]. Similar data has been collected with regard to the chromatic contrast threshold function, CCF, that will be discussed in the next section.

The test sets used to collect this data have varied significantly over the years as the concepts involved in spatial resolution have moved toward a more sophisticated understanding of the visual process. Originally, the tests employed square wave patterns in object space, then sine wave patterns and more recently Gabor Patches. The latter are designed to avoid sharp transitions in the field unrelated to the test pattern itself which might corrupt the data base. Most recently, interferometric methods of stimulating the retina have been introduced. These will be discussed in **Section 17.6.3.4.2**.

In the presence of lateral motion exceeding about three degrees per second, this type of motion causes the visual system to operate in a continuous ***tracking mode***, frequently referred to as a pursuit mode. This mode was described in **Section 15.2.5**. The tracking mode places significantly different requirements on the visual system and employs different operating protocols than does the perception of images fixed with respect to object space. Performance in this mode is significantly changed through training and experience. Below three degrees per second, the performance of the visual system blends into the normal ***analytical mode*** prior to reaching about 0.1degrees/sec. In this intermediate range of motion, the servomechanism of the oculomotor system operates in a hybrid mode. The tracking and hybrid modes will not be discussed here. Kelly has provided extensive experimental data regarding these modes using image stabilization techniques[91]. In figure 6 of his paper, he shows that the peak in the threshold modulation occurs at a spatial frequency that varies inversely with lateral velocity for frequencies above three degrees/sec. His test set was incapable of sensing the tremor of the visual system. Therefore, his velocity values of 0.15, 0.012 and 0 degrees/sec. must be considered the average values associated with a more complex motion.

Figure 17.6.3-5(a) is similar to the previous figure presented for describing the MTF for the human eye as a function of temporal frequency. However, it includes an initial term related to the MTF of the optical system of the eye multiplied by the conversion factor for angular frequency in object space to temporal frequency in signaling space. This term is shown by the dotted red line. The parameter S_L represents the one half amplitude point in the MTF of the physiological optics. It replaces the term associated with the operation of the iris. Subsequent to this term, the remainder of the equation is identical to the previous one.

> The performance (MTF) of the physiological optics are very complex. This performance is summarized in **Section 2.4.2** to **2.4.7**. The eye is typically aberration limited for iris openings exceeding 2 mm. It is nearly diffraction limited for a 1 mm. iris opening. In a well designed system, the MTF of the physiological optics would be expected to be matched to the MTF of the neural portions of the system. It is shown as a broader MTF here for illustration purposes. The line is also shown as straight for convenience. **Section 17.6.4** will discuss the impact of real physiological optical systems and special test conditions related thereto.

As a result of the introduction of the physiological MTF, it is possible to construct the overall MTF of the visual system in **Figure 17.6.3-5(b)** and **(c)** by multiplying the individual terms together and plotting the composite as done earlier. The result shown in the lower part of the figure shows that once again, the slope of the asymptotes can be used to evaluate the character of an equivalent measured function in the laboratory. As in the previous derivation, the MTF of the optical system is seen to play a minor role in the operation of the eyes for the on-optical-axis condition. A similar situation applies to the foveola at the point of fixation. The spatial performance of the visual

---

[90]Blakemore, C. & Campbell, F. (1969) On the existence of neurones in the human visual system selectively sensitive to the orientation and size of retinal images *J Physiol* vol. 203, pp 237-260

[91]Kelly, D (1979) Op. Cit.

system as a function of frequency is largely independent of the optics of the eye until large angles from the point of fixation are explored. For these conditions, the performance of the optical system falls dramatically.

Figure 17.6.3-5(c) includes two additional lines presenting the data curves obtained by the MODELFEST team during the last few years. The diamonds represent data collected using fixed size Gabor patches. The squares represent data collected using Gabor patches with a fixed number of cycles in a pattern. Note, these two traces can be superimposed by merely moving them vertically. This would suggest the difference between them is in the criteria term in **equation 17.6.3-2** due to the change in the design of the patches. The theory presented is in good agreement with the data from that group at a nominal illumination level of 30 cd/m^2. At this low illumination, the value of $S(I)_{P2}$ is lower than S_{P1}. Kelly has provided a number of figures in part II of the 1979 paper that shows how closely the MTF as a function of temporal frequency and of spatial frequency track each other. Derrington & Lennie[92] have also contributed considerable data for Macaque. Their data was obtained with probes within the LGN and is based on the frequency of action potentials at that location. Unfortunately, all of the curves shown in their paper were obtained by curve fitting a polynomial with four degrees of freedom to a very sparse data set. It is clear that the mathematical model presented in **Figure 17.6.3-5(a)** is compatible with the available data. The question to be resolved is the value of the conversion constant between spatial frequency and temporal frequency in vision. Derrington & Lennie also provided good data on the orientation sensitivity of the magnocellular cells to a grating.

Note the transition from a nominally horizontal slope at the peak in the threshold waveform (its presence depends on the ratio between S_A and the other frequency constants in the fundamental equation) to a slope initially of –1 followed by a slope of –2. It is proposed that this theory is the first work to ever explain the reason for this dip found so frequently in the literature. As noted by Prof. du Buf at the Univ. of Algarve (private communication), this dip has usually been ignored by the computational modelers.

---

[92]Derrington, A. & Lennie, P. (1984) Spatial and temporal contrast sensitivites of neurones in lateral geniculate nucleus of Macaque. *J. Physiol*. vol. 357, pp 219-240

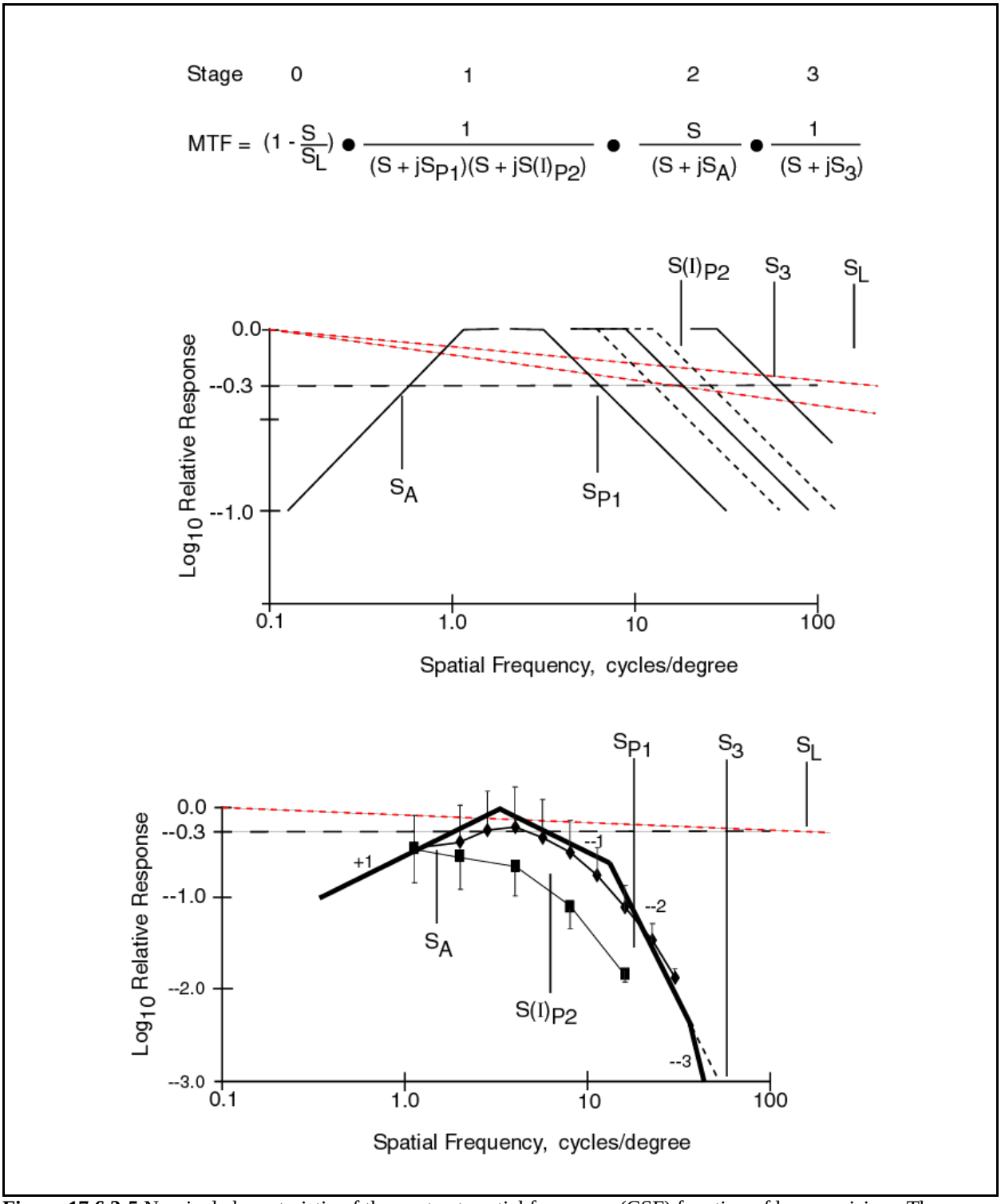

Figure 17.6.3-5 Nominal characteristic of the contrast spatial frequency (CSF) function of human vision. The analysis and diagrams apply specifically to the foveola. Top; equation of the overall MTF. Middle, the graphical form of the individual MTFs. Bottom, the overall MTF (heavy solid line) with the time constants changed to represent a real situation (note vertical scale change from middle figure). Data points and light lines from MODELFEST data (see text).

Smith provides a simple contrast versus angular resolution compatible with the above theory and the material discussed below[93]. He notes performance increases as the light level increases and falls with lower levels.

A largely overlooked figure from Kelly, is shown in **Figure 17.6.3-6**. It concentrates on the lower spatial frequencies. It clearly shows the +1 slope at low frequencies and the – 1 slope at frequencies in the 2-10 Hz range. It also shows that these slopes are independent of the illumination intensities used. The data clearly shows the square root relationship between the illumination intensity and the threshold amplitude. The labels, Weber and D– R (de Vries-Rose) highlight the limited regions of the curves described by these laws.

Burton, using an early full-aperture laser interferometric test bench, also shows the +1 and –1 slopes characteristic of the visual system[94].

Blakemore & Campbell[95] provide data that also clearly shows the +1 and –1 relationships for data taken at 100 cd/m^2 under a variety of adapting conditions.

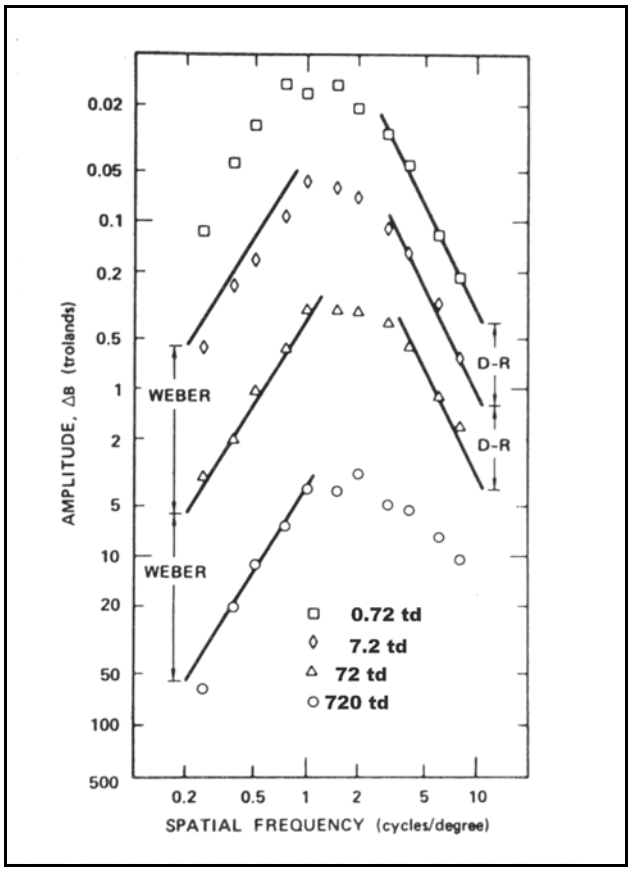

Figure 17.6.3-6 Contrast threshold for low- and mid-frequency sine-wave gratings measured at several background levels. From Kelly, 1972.

[93]Smith, W. (2000) Modern Optical Engineering NY: McGraw-Hill, pg 137
[94]Burton,G. (1973) Evidence for non-linear response processes in the human visual system from measurements on the thresholds of spatial beat frequencies. *Vision Res*. vol. 13, pp 1211-1225
[95]Blakemore, C. & Campbell, F. (1969) Op. Cit. pg 251

Figure 17.6.3-7 provides two curves from other studies by Kelly, et. al. and a set of asymptotic curves from this work. This figure serves two purposes. The dashed black curve is the modulation versus spatial frequency presented for the human at a measured 300 Trolands using a P-24 phosphor and a magenta filter. The solid black curve through the data points represented by circles is the modulation versus temporal frequency for the human at a measured 860 Trolands using a 3400 Kelvin light source. Both of these curves are for illumination levels more than an order of magnitude greater than those of the MODELFEST team. Both of these curves can be fit to the asymptotic curves proposed by this theory to an arbitrary precision that exceeds the accuracy of the data (see colored lines). The laboratory protocol needs to be repeated using a more precise measurement of the incident photon flux and a larger group of subjects to obtain a more calibrated range of values. The ideal illumination source can be selected from the New Chromaticity Diagram for Research. By using a mixture of 494 nm aqua and 572 nm yellow, a white light can be generated that does not excite either of the chromatic channels of vision.

In this figure, the two curves were collected at different light levels and the responses would be expected to be different due to the parameter $S_{P2}(I)$. In this case, the two curves can be overlayed quite well if the function associated with the 300 Troland data is shifted to the right by 0.25 log units. The resulting curves at 300 and 860 Trolands (using clearly different methods of calibration) then overlay each other within the apparent accuracy of the data. The hump in the 860 Troland data near 1.0 Hz is believed to be due to CCF data mixed into the CSF data set because of the spectral profile of the illumination used. It was not selected to minimize perception of a chromatic contrast difference in these experiments. The theoretical model can be made to overlay either or both of these curves well within a factor of two, well within the probable accuracy of the data and without incorporating any term for the MTF of the optics.

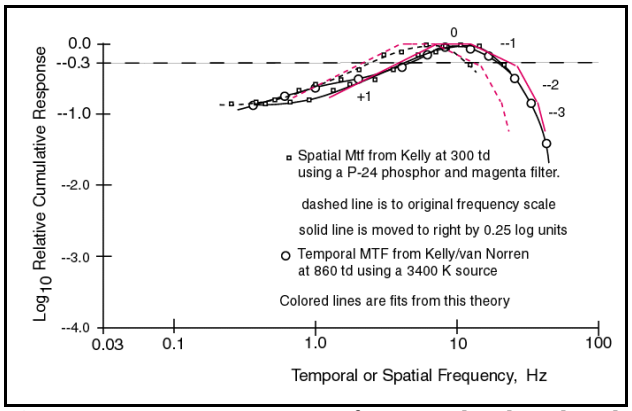

Figure 17.6.3-7 A comparison of measured and predicted MTF for the human eye. The numerics indicated the slope of the asymptotic fit to the experimental data. The hump in the 860 td data near 1.0 Hz is believed to be due to the presence of CCF data mixed into this CSF data set. S_{P1} has a value of about 2 Hz in the 300 td data and about 6 Hz in the 860 Hz data.

The above formulation of the MTF does not include any contribution of the pixelization of the retina. In the absence of any tremor, one would expect this process to introduce a low-pass filter feature with a null near
720 cycles/degree. This frequency limit is similar to that of the optics and is sufficiently high to be negligible.

17.6.3.4.1 Curve fitting to the CSF function

The MODELFEST team has presented a number of empirical equations using modeling techniques akin to the kinetic energy modeling of the chemist. These have attempted to fit a curve to the above CSF functions based on various abstract mathematical relationships[96]. In one case, a parabola in log contrast-log frequency space was fitted to the data base after relocating the measured value at a nominal zero spatial frequency to 0.5 cycles/degree. This modification has obscured the nominal slope of +1 or +2 in the actual data. There has been no mention of the fact that the parabola would have to be truncated at a log contrast of 0.0 to conform to the actual situation. While it is true that the slope of the high spatial frequency component of the data may reach high negative values, this is not true of the low frequency component. An electrophysiologically more appropriate curve to fit the data, omitting the potential flat top and straight segment at a slope of –1.0 which occur at higher illumination levels, would be a hyperbola with a vertical asymptote at high frequency and an asymptote with a slope of +1.0 at low frequency (omitting any impact of the iris at low light level).

An alternate equation that can be fit to the data without modification is the DOG, difference of Gaussians, function. This function exhibits a +1 slope at low spatial frequencies and a very rapidly falling skirt at high frequencies when

[96]http://epubs.osa.org/oearchive/pdf/14103.pdf

plotted using logarithmic scales[97]. By making the difference in standard deviations between the two Gaussians a function of illumination, the peak of the DOG function can be made to move to higher frequency with higher illumination while maintaining the +1 slope of the low frequency skirt.

Ross & Johnstone demonstrated conclusively that the contrast threshold at a given frequency was a function of the amplitude of the impressed signal and not of its signal energy (as opposed to its quantum energy)[98]. They did this using compound gratings consisting of harmonically related components. They reversed the 5th harmonic in a series consisting of the fundamental and the third, fifth, seventh and ninth harmonics. A peak signal amplitude change of +50% due only to the phase shift resulted in a change in threshold of three decibels. Their paper was brief and left several procedural questions unanswered.

17.6.3.5 Formulation of the CCF, Chromatic Contrast Frequency function

Establishing a protocol that will stimulate only the chromatic channels of vision, and avoid stimulating the luminance (R–) channel, is quite difficult. It is also difficult to prepare a protocol that introduces a signal in only the O–, P– or Q– channel of vision. In the absence of such precision, the measured data will not achieve the maximum performance related to the putative test objective. As a result, the measured responses in the literature related to the CCF must be considered exploratory. The New Chromaticity Diagram provides the necessary framework to plane more precise protocols. Based on this Diagram, it is clear that general designations such as red, green or blue are inadequate in the context of CCF measurements. Even using a tri-color display as an uncalibrated source does not provide the necessary precision.

A distinction should be made between contrast measurements made using a single narrow spectral band source designed to stimulate the retina and a more complex stimulus using two spectrally different sources to stimulate the retina sequentially. The first source necessarily excites both the R– channel and at least one chrominance channel. The second arrangement typically excites the R–channel and two different chrominance channels. Only through careful control of the relative amplitudes of the two sources can reliable results related to a single chrominance channel be achieved.

The graphical form of the measured CCF is dramatically different from the CTF and CSF. This is due to the significantly different signal processing involved in its formation. In formulating the mathematical description of the CCF, the difficulty of performing tests to isolate the individual CTF, CSF and CCF responses becomes apparent. Any source of illumination used as a stimulus necessarily excites more than one spectral channel in the visual system. Whereas these excitations are logarithmically summed in order to form the R–channel luminance signal, they are differenced after logarithmic conversion to form the P– and Q–channel chrominance signals.

In any case, at least two separate signals are sent to the brain for perception, interpretation and cognition. It is likely that each signal generates a response reported in psychophysical experiments. Although the chromatic signals are bipolar as transmitted to the brain by stage 3, it is not known whether the initial perception by the brain generates a polarity sensitive response. It is likely that the luminance and chrominance signals are initially interpreted as "changes" without regard to polarity. If this is true, the reported response during contrast threshold measurements are likely to represent the sum of the absolute responses due to both the luminance and chrominance channel responses.

The chromatic signal paths are more complex than the luminance path shown in the abbreviated Overall Block Diagram of [**Figure 17.6.3-1**]. As shown in the Top Level Schematic of [**Figure 11.6.4-4**] and confirmed by Maxwell's Spot, the chrominance information follows two distinctly different signal paths in human vision. The path associated with the ex-foveola retinal is processed in the 2nd matrix. The chrominance information associated with the foveola may also be processed in the 2nd matrix or it may be processed in the pretectum. The observation of Maxwell"s Spot suggests that the chromatic information associated with the foveola is processed separately from the other information.

The general form of the CCF can be derived as in the case of the CTF. Let the magnitude of the transient response of each spectral channel be defined as the product of its electrical response times the average sensitivity of its absorption characteristic to the spectral content of the stimulus. As in the case of the general CTF function for a

---

[97]Regan, D. (1991) Spatial Vision. Vol. 10 of Vision and Visual Dysfunction, Cronly-Dillon, J. *general ed*. Boca Raton, FL: CRC Press pp 22-23

[98]Ross, J. & Johnstone, J. (1980) Phase and detection of compound gratings. *Vision Res*. vol. 20, pp 189-192

"white" illumination source, the summation of the spectral signals occurs at the input terminal of the first Activa in the signal processing stage. In this case, the process involves a differencing operation within the 1st lateral processing (color) matrix. To account for the logarithmic conversion of the signals from the current mode in the photoreceptor cells to the voltage mode at the inputs to these Activa, and any adjustments in the individual signal gains due to the electrical coupling network, it is important to refer to the contrasts due to stimulation as they are measured at this point in the system.

Let the absolute cumulative MTF at the output of the mid wavelength spectral channel be given by the first three terms of the equation in [**Figure 17.6.3-2**] (the product of the MTF's due to stage 0, 1 & 2) and be given a subscript M. Let the absolute cumulative MTF of the long wavelength channel be defined similarly and be given a subscript L. The result of this action is shown in **Figure 17.6.3-8(a)** where $C_M(\lambda_{1-2})$ is the apparent contrast at the output of the photoreceptor cells of the M–channel, $C_L(\lambda_{2-1})$ is the apparent contrast at the output of the photoreceptor cells of the L–channel, and the term containing jS_3 is associated with the integrator at the output of the signal projection stage of the Q–channel.

This formulation is difficult to interpret because of the variety of parameters. However, if the time constants associated with each spectral channel are assumed to be equal, a much simpler form emerges as shown in **Figure 17.6.3-8(b)**. In this case, the term $C_M(\lambda_{1-2}) - C_L(\lambda_{2-1})$ represents an apparent net color contrast between the two signals at the output of the photoreceptor cells.

Figure 17.6.3-8(c) illustrates the resulting predicted CCF based on the photopic level model.(the dashed lines including the red dashed lines due to the iris at mesotopic illumination levels). The predicted CCF is compared to the reported CCF from Kelly and van Norren for a single subject at 860 Trolands, a 1.8 degree image field and a 2.3 mm articial pupil. The light source was a 3400 Kelvin source filtered by Wratten #29 and #61 filters. The one-half amplitude frequencies of the various filter circuits are shown approximately and will be discussed in **Section 17.6.3.7**.

The signaling paths of the chromatic channels of vision are considerably more complex than the luminance channel. As mentioned earlier, they are also asymmetrical in their performance. Thus experiments can be defined that evaluate the chromatic frequency response of the system under a variety of different conditions. The preferred experiments would be those evaluating either the P– or Q–channel independently. This requires careful choice of the illumination employed. In the case of the P–channel, the preferred light sources are two lights well separated but both along the 494 nm value of the New Chromaticity Diagram for Research. Values along this line will not introduce any signal in the Q–channel. Similarly, to evaluate the Q–channel, two light sources well separated along the 572 nm value should be chosen. A residual signal is likely in the R–channel unless the amplitude of the chosen signals are appropriately matched to the luminance function of the system to eliminate any luminance signal. This is difficult to demonstrate since the human observer is not able to distinguish a luminance contrast from a chrominance contrast under threshold conditions.

If it is necessary to employ non-spectral light sources, the experimental protocol becomes much more difficult. The contrast performance of the system will depend in the difference in the mean spectral values of the individual light sources. Further, it is nearly impossible to avoid crosstalk between the P– and Q–channels.

(a)

$$MTF = \left[C_M(\lambda_{1-2}) \bullet \left[\frac{S}{(S + jS_{Iris})} \bullet \frac{1}{(S + jS_{P1})(S + jS(I)_{P2})} \bullet \frac{S}{(S + jS_A)} \right]_M - C_L(\lambda_{2-1}) \bullet \left[\frac{S}{(S + jS_{Iris})} \bullet \frac{1}{(S + jS_{P1})(S + jS(I)_{P2})} \bullet \frac{S}{(S + jS_A)} \right]_L \right] \bullet \frac{1}{(S + jS_3)}$$

(b)

$$MTF = \left[C_M(\lambda_{1-2}) - C_L(\lambda_{2-1}) \right] \bullet \left[\frac{S}{(S + jS_{Iris})} \bullet \frac{1}{(S + jS_{P1})(S + jS(I)_{P2})} \bullet \frac{S}{(S + jS_A)} \right] \bullet \frac{1}{(S + jS_3)}$$

(c)

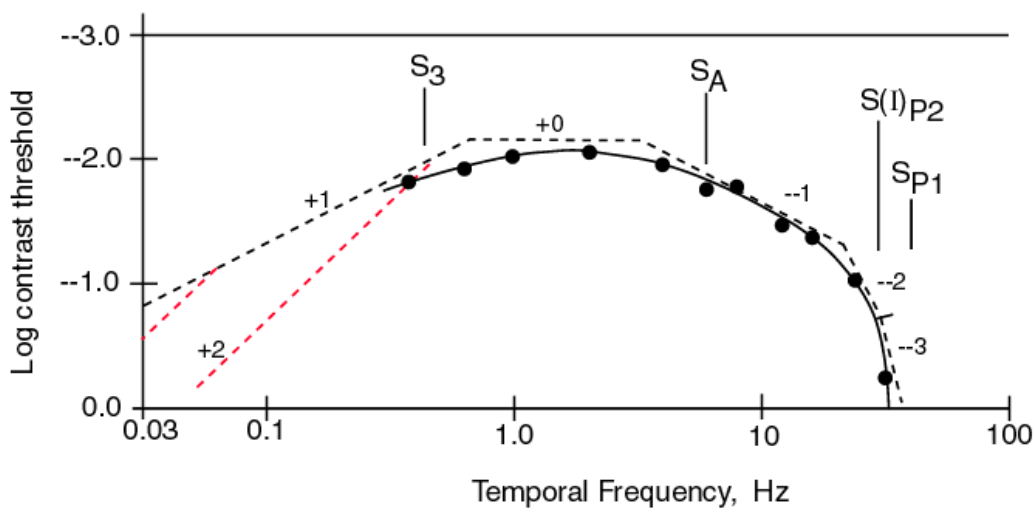

Figure 17.6.3-8 The Chromatic Contrast versus Frequency (CCF) function of vision. (a); the basic mathematical construct. (b); an idealized mathematical construct. (c); the nominal CCF function. The data points and solid line are from Kelly & van Norren (1977). Dashed black line represents predicted CCF. Numerics represent the predicted slopes. Red dashed lines represent iris function at mesotopic light levels. See text.

17.6.3.5.1 Secondary factors related to the CCFs

As developed in Section XXX, the encoding scheme used in stage 3 to project the chromatic signals to the brain is

not symmetrical with respect to the color of the differenced signals. This is the source of many flicker phenomena and it is an irritant in measuring the chromatic frequency response of the visual system. This asymmetry also plays a major role in the frequency response of the CCF functions. The polarity of the two chromatic contrast functions, $C_M(\lambda_{1-2}) - C_L(\lambda_{2-1})$ and $C_M(\lambda_{1-2}) - C_S(\lambda_{2-1})$ presented to the ganglion cells of stage 3 are still uncertain. However, it appears that in both the P– and the Q–channels, the mid wavelength stimulus drives the spacing of the action potentials generated by the cells to shorter times. By this action, the codec (coding-decoding algorithm) associated with the P– and Q–channels provides a faster rise time to the decoded signal at the point of decoding that relates to the M–channel than it does to either the S– or L–channel. The codec introduces another MTF into the CCF function that varies with the mean wavelength, on a photon-flux basis, of the stimulus.

17.6.3.5.2 Variation in CCF's with position of the retina and orientation of the pattern

Derrington, Krauskopf & Lennie have provided valuable data on the response of the Macaque visual system based on probing the LGN[99]. They used a few fixed spatial frequency stimuli while varying their orientation and position within the field of view of the subject. They mapped the response of the animal in both the parvocellular and magnocellular regions of the LGN. They showed the magnocellular pathway supported higher flicker rates than did the parvocellular pathway. They showed that the parvocellular pathway was primarily chrominance oriented and was dominated by two groups of cells. The magnocellular pathway was oriented toward luminance signals and appeared to be effective in extracting information about the movement of objects. This work would suggest they are also effective in determining parallax parameters as well. The magnocellular signals appeared to be monopolar while the parvocellular cells responded in a differential manner.

17.6.3.5.3 Variation in CCF's with temporal frequency from fMRI experiments

Engel, Zhang & Wandell have presented some early color contrast data as a function of stimulus frequency[100]. While the stimulus frequencies were in the one to ten Hz range, the data was collected using a more complex timing arrangement. An fMRI image was obtained at a repetition rate of once every 2.5 to 3 seconds. However, the data was analyzed using a more complex 42 second composite stimulus period. The nomenclature is also complex. They have given the expression for contrast a sign and expressed it over a range of –1 to +1. Their analysis is based on the conventional wisdom as summarized in their introduction. Some of the conflicts they note can probably be resolved by reinterpreting their findings based on the models of this work. They did not use a display mechanism capable of precisely matching the peaks in the absorption spectra of the eye. Nor did they calibrate the performance of that display sufficiently to allow precise interpretation using the model of this work.

17.6.3.6 Experimentally separating the CTF and the CCF functions

The complete CTF includes a contrast term that can be represented by $C=C_S(\lambda) + C_M(\lambda) + C_L(\lambda)$ while the CCF involves two distinct functions. The Q–channel equation includes the contrast term $C_M(\lambda_{1-2}) - C_L(\lambda_{2-1})$ while the P–channel equation includes the contrast term $C_M(\lambda_{1-2}) - C_S(\lambda_{2-1})$. By solving these equations simultaneously, it is theoretically possible to determine these functions for a stimulus of arbitrary spectral content with time. However, it is much easier to design the laboratory program so as to generate the functions directly. This can be done by selecting the spectral content of the stimulus so that it only impacts the CTF or the CCF(s). The simplest approach is to recognize that the CCF's can be eliminated by controlling the mean spectrum (on a quantum-flux basis) of the stimulus. If a mean wavelength of nominally 572 nm is used for the spectral stimulus, the Q–channel signal will equal zero as a function of time and no response due to this channel will be reported by the subject. Alternately, If a mean wavelength of nominally 494 nm is used for the spectral stimulus, the P–channel signal will equal zero as a function of time and no response due to this channel will be reported by the subject.

By carefully selecting a white light formed of three sources where both the P–channel and the Q–channel are not excited, the CTF due only to the luminance or R–channel will be reported.

By carefully selecting a pair of light sources that exhibit a large spectral separation along either the P– or Q– axis and are of the proper amplitude to allow switching of the sources without impacting the apparent brightness (not lightness) of the stimulus, individual CCF functions can be obtained for both the P– and Q–channels.

---

[99]Derrington, A. Krauskopf, J. & Lennie, P. (1984) Chromatic mechanisms in lateral geniculate nucleus of macaque. *J. Physiol*. vol. 357, pp 241-265

[100]Engel, S. Zhang, X. & Wandell, B. (1997) Colour tuning in human visual cortex measured with functional magnetic resonance imaging *Nature* vol. 388, pp 68-71

This experimental rationale can provide independent measurements of the CTF and both CCFs. However, these results cannot be obtained using an off the shelf light source or CRT display. Carefully tailored light sources are required based on the New Chromaticity Diagram for Research and following conformation that 572 and 494 nm are the null wavelengths for the two chrominance channels.

17.6.3.7 Evaluating the time constants based on CTF CSF and CCF data

By following the protocols defined in the previous section, it becomes possible to determine the individual time constants that appear in the above CTF, CSF and CCF functions with good precision.

Even though it represents only one test sequence using one subject, **Figure 17.6.3-9** provides an excellent point of departure for determining the time constants associated with the temporal contrast performance of the visual system as a function of photometric illumination. The data is from Figure 1 of Kelly & van Norren (1977). In line with this work, the label on the ordinate has been made more explicit than in the original figure. By using a pair of "red" and "green" sources, they were able to separate the CCF and CTF functions adequately to demonstrate the concept at a given illumination level. However, the asymptotes suggested by the theory, highlight the likelyhood of cross coupling between the measurements. It is proposed that the slight hump in the CTF below two Hz is due to cross coupling from the CCF response function. Similarly, it is proposed that the extension of the CCF to the right of two Hz is due to cross coupling from the peak in the CTF function. Both of these putative artifacts could be eliminated by more careful selection of the content of the two light sources. It should be noted that neither of these functions approaches the abscissa horizontally. Both are rising with a slope of +1 at low frequencies.

After rising with a slope of +1, the CTF function continues to rise until the vicinity of 10 Hz where the slope changes quickly to -1 under the influence of *two* poles in the vicinity of 16 Hz. The slope increases to -2 due to a pole in the vicinity of 24 Hz. The slope increases further to -3 due to a pole in the vicinity of 48-50 Hz.

After rising with a slope of +1, the CCF function begins to level off due to a pole in the vicinity of 0.3 Hz. It then begins to drop toward a slope of -1 due to a pole near 10 Hz. It then proceeds toward a slope of -2 in the vicinity of 24 Hz, and finally reaches a slope near -3 due to a pole near 48-50 Hz.

Comparing the apparent pole positions between these two curves, it appears the major difference is the location of the poles near 0.3 Hz and 10 Hz in the CCF function. The 10 Hz pole is compatible with the lower frequency pole in the chromatic decoder of stage 3 of the model. The pole at 0.3 Hz may be the result of the codec transmitting a "deep red" signal to the brain. If this is the explanation, it is a variable pole as a function of mean wavelength of the red stimulus relative to 572 nm. The double pole in the CTF is probably due to the S_{P1} and S_{P2} poles occurring at nearly equal frequency for 860 td illumination in the presence of the filters used.

The horizontal line at a contrast level of 0.008 was added to support two points. First, the lowest level contrast in the monotonic functions does not normally represent the actual product of the criteria and the internal threshold level. This condition only prevails if the poles of the waveforms are far enough apart to generate a long horizontal region between the rising and falling portions of the waveform. Second, the fact that the CCF and CTF both show nearly the same minimum threshold contrast is most likely an artifact of the investigators desire to maintain a nominally equal object space illuminance during the tests. If the relative illuminances of the "red" and "green" channel had been adjusted to generate equal signals at the perception location in the R-channel, this similarity in contrast threshold might not have been found and the cross coupling of the CTF into the CCF would have

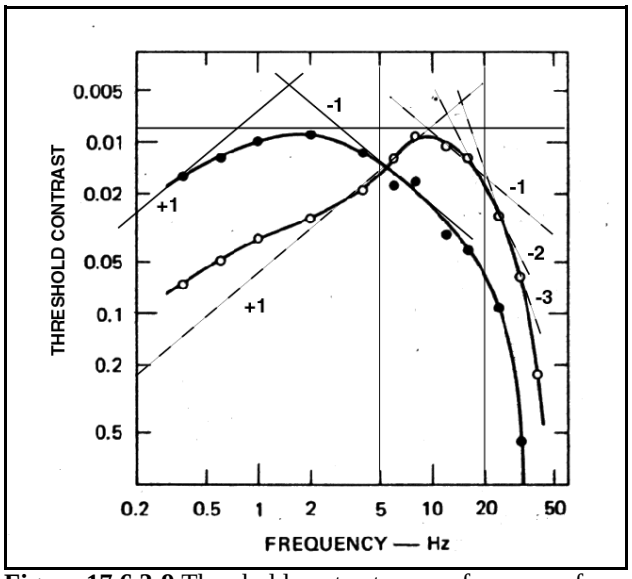

Figure 17.6.3-9 Threshold contrast versus frequency for the CTF and CCF functions. The CTF is represented by the open circles and solid curve obtained using a broad spectral band yellow source ("red" + "green"). The CCF is represented by the filled circles and solid line obtained by alternating between the "red" and "green" sources. Data is for one experiment by one subject at 860 td, 1.8 degree field, no surround, and a 2.3 mm. artificial pupil. Numerics indicate the slope of the asymptotes.

been reduced. Kelly & van Norren discussed the range of ratios between these two sources that they used. They suggest that they could achieve the results similar to those of many other investigators by varying this ratio. This work suggests that only one ratio gives the optimum separation of CTF and CCF data. This ratio should be an anchor point in future laboratory studies.

It is proposed that the concepts of “silent green” and “silent red” flicker, discussed in the Kelly & van Norren as well as other papers, are not required when an adequate model of the visual system is available. These concepts arise because of an artifact of using illumination sources that are not adequately aligned to the absorption spectra of the actual chromophores of vision (and possibly due to a lack of control of the stimulation of the P–channel of vision).

It is not clear that the cross coupling of the total CCF into the CTF would have been eliminated because only the CCF associated with the Q–channel was controlled in this experiment. The CCF of the P-channel due to the repetitive changing of the “green” signal relative to the “blue” signal (which may have had a value of zero in the signal channel) was not investigated.

Note the tendency of the sum of the CCF and CTF functions to exhibit a horizontal trend down to below 1 Hz. This tendency is frequently observed in the literature when care is not taken to isolate the CTF from the CCF. As shown in this figure, the +1 slope will always be observed if the lower experimental frequency is low enough.

Over large illumination ranges, different specific models must be used for the hypertopic, photopic, mesotopic and scotopic regions as discussed above. These models must recognize the different operating modes of the adaptation amplifiers in these regions.

In the case of the hypertopic region, to some extent the 850 Troland curve, and to a large extent the 9300 Troland curve show the effect of saturation in the adaptation amplifier leading to saturation in the stage 2 signaling channel.

In the case of the scotopic region, the 0.06 Troland curve shows the effect of the time constant $S_{P2}(I)$ becoming smaller than the time constant of the adaptation amplifier. In the absence of any problem with the test signal contrast differing from the sensed contrast, this situation alone would generate a horizontal feature in the response at low frequency.

Within the photopic region, it is clearly seen that the time constant associated with $S_{P2}(I)$ becomes very short with a resultant frequency response with a one-half amplitude that is very large and outside the range of interest. Under this condition, it appears that the low-pass characteristic of the adaptation amplifier or of the other amplifiers within stage 2 introduce an additional limit on the overall MTF of the system. The additional low pass filter characteristic will be associated with a frequency labeled S_4. The slope of the 9300 Troland response at high frequencies suggests the presence of an additional low pass filter with a parameter of around 60-80 Hz. However, a clear determination requires analysis of a more specialized model of the hypertopic region.

By determining the slopes of the various portions of each curve, it is possible to establish nominal a nominal one-half amplitude point for the frequency of each of the individual frequency parameters of the photopic model. TABLE 17.6.3-1 tabulates these estimates.

TABLE 17.6.3-1
INITIAL ESTIMATES OF THE FREQUENCY PARAMETERS OF THE HUMAN VISUAL SYSTEM
based on source of poorly characterized color temperature

Region	Test Illumination	High-pass		----------Low-pass----------				
		S_{IRIS}	S_A	S_{P1}	$S_{P2}(I)$	S_3	S_4*	S_5
Scotopic	0.06 td	—	—	16Hz	1.2Hz	24Hz	48-50Hz	
Mesotopic	0.65	<0.3Hz	?	16	12	24	48-50	
Photopic	7.1	<0.3	3-5 Hz	16	120	24	48-50	
	77	—	3-5	16	1200	24	48-50	
	850	—	3-5	16	—	24	48-50	
Hypertopic	9300	—	—	16	—	24	48-50	60-80 Hz

* S_4 may be vary in the chromatic channels due to the codec. It may go as low as 0.5 Hz in the chromatic channels for very deep blues and reds.

In 1979, Kelly provided additional data bearing on the values in the above table. However, it should be noted that his test set was significantly different. He introduced a monitor with a P-24 phosphor and a “magenta” filter which he claimed transformed the color to a neutral gray at an intensity of 300 Trolands. The P-24 phosphor is listed as a fast blue-green phosphor with a peak response at 507 nm and a decay to 10% value of 1.5 microseconds. This source does not qualify as an equal-energy or equal-flux source of illumination. He compared two subjects of different age and generated curves with and without artificial stabilization of the test images. Stabilization had a significant impact of the shape of the curves at frequencies below one Hertz. Age appeared to cause a shift in either S_{P1} or $S_{P2}(I)$, suing the new source of illumination. A larger group of subjects is still needed to obtain statistically relevant range values for the individual intensity curves.

TABLE 17.6.3-2 provides an alternate set of time constants reflecting the data collected by the MODELFEST team.

TABLE 17.6.3-2
TEMPORAL PARAMETERS OF THE VISUAL PROCESS
at 30 cd/m^2 and a free iris

STAGE	PARAMETER	TIME CONSTANT	TEMPORAL FREQUENCY
Stage 0	S_{iris}	6.0 sec. (Open) 1.2 (Close)	0.05 Hz 0.26
Stage 1	S_{P1} $S_{P2}(I)$	0.525 0.175	0.6(est.) 1.8(est.)
Stage 2	S_A	3.0	0.1
Stage 3	S_3	0.033	10

17.6.3.8 Empirical data on the temporal and spatial frequency domain performance

Besides the work referenced above, Rovamo and his team have recently provided new data and voluminous references[101]. Most of the references suffer from the lack of a graphic representation of their model. They frequently assume the visual system exhibits a low-pass rather than a band-pass characteristic. Rovamo, et. al. do present data consistent with this work in their figure 2[102]. They show the spatial response of the luminance channel exhibits a band pass characteristic while a chrominance channel response exhibits a low pass response due to the differencing mechanism involved This data expands on the general premise in their 1998 paper. That paper did not include a graphic of their model and appears to be limited to the luminance channel transfer function.

17.6.3.9 A three dimensional representation of the CSF function

Figure 17.6.3-10 from Daugman[103] provides a two dimension modulation transfer function of the overall visual system of two subjects based on careful psychophysical tests. The tests were designed to determine whether there were separate "filters" in neural space recognizing orientation and spatial frequency separately. His conclusion was that the two functions were not treated separately. The tests used a "signal detection masking paradigm." The graphics are quite informative. However, no data points were included in the paper. This may have been expected since 1024 separate orientation angles were used to create the MTF profiles. Although the subjects were healthy and tested for common optometric performance, the experiments were not rigorously controlled with respect to other parameters related to vision. The test used a P31 phosphor cathode ray tube that measured 22 cd/m^2 mean luminance. This phosphor emits strongly in the middle of the yellow-green region of the spectrum. Its peak emission wavelength is virtually identical with the peak wavelength of the M-channel chromophore. Its relative output is less than 10% at 437 and 625 nm. The subjects viewed a two degree visual field, within a ten by ten degree surround at the same measured luminance from an unspecified source, binocularly at a distance of 2.44 meters. Each set of tests lasted about one hour.

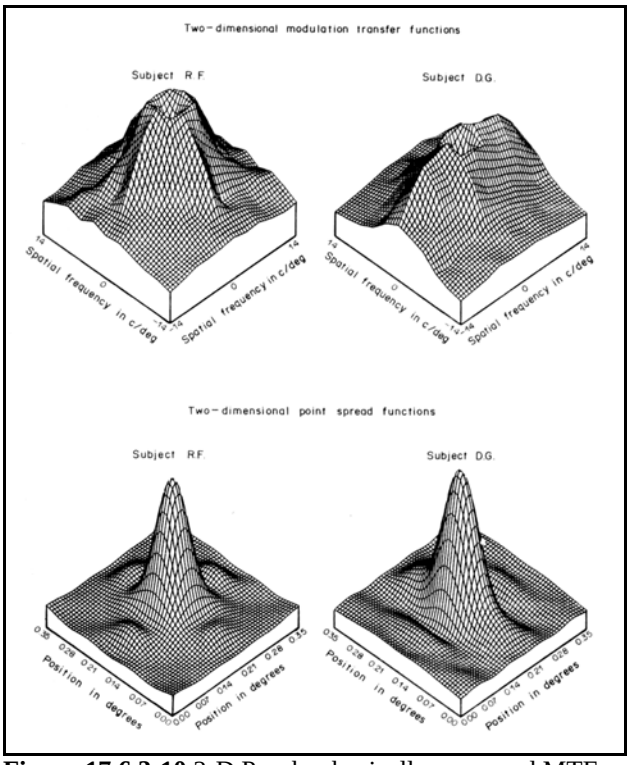

Figure 17.6.3-10 2-D Psychophysically measured MTF and calculated point spread function for two subjects. 2° circular test field from a P31 phosphor within a 10° by 10° surround at a nominal 22 cd/m^2 luminance was viewed binocularly. D. G. was dropped from the study due to his being a meridional amblyope. Position scales appear to be relative in the lower frames. From Daugman (1984).

A given trial consisted of two 500 ms test intervals separated by 200 ms. Thus, the temporal frequency spectrum of the stimulation was concentrated between 0 and 2 Hz. This temporal spectrum in object space may be impacted by the limited low temporal frequency performance of the adaptation amplifiers.

The author provides a sophisticated discussion of the subtle differences between the one dimensional and two dimensional Fourier analysis. In the discussion, he offers the statement that the 2D point spread functions might be considered neural point spread functions because "it has been shown that the transfer function of

[101]Rovamo, J. Kankaanpaa, M. & Hallikainen, J. (2001) Spatial neural modulation transfer function of human foveal visual system for equiluminous chromatic gratings. *Vision Res*. vol. 41, pp 1659-1667
[102]Rovamo, J. Kankaanpaa, M. & Kukkonen, H. (1999) Modeling spatial contrast sensitivity functions for chromatic and luminance-modulated gratings. *Vision Res*. vol. 39, pp 2387-2398
[103]Daugman, J. (1984) Spatial visual channels in the Fourier plane. Vision Res. vol. 24, pp. 891-910

the eye's optics normally has little effect on the kind of measurements" used in the paper. This last assertion does not appear creditable in light of the more detailed model available in this work. The measured spatial resolution appears limited by the relatively low light level used in this study. Under this condition, the iris would be expected to be near maximum aperture. The resultant optical aberrations of the optical system would be significant in this study. Furthermore, the P/D process would exhibit a relatively low high frequency pole under these conditions. Although, this latter condition could be considered of neural origin (this author would rather not), it is not associated with the available passband of the visual system. Repetition of these experiments at a higher luminance level, while observing the pupil size, would probably give distinctly different results.

The author also asserts "The fact that signal detection is a statistical process involving intrinsic stochastic variables which influence threshold estimates has been recognized for a some time, . . ." This is in agreement with the assumptions used here only in the mesotopic and scotopic illumination ranges.

The upper left frame clearly shows a notch at zero frequency. However, it does not show the depth of that notch. For their test regime, the dip occurs for spatial frequencies below 4 cycles/degree. Using different scales, the notch would be seen to go to zero at very low spatial frequencies. The author remarks that the MTF's are asymmetrical, showing prominences related to the horizontal and vertical planes. They label this the "oblique effect." These result in orthogonal secondary features in the reconstituted point spread functions. In this work, these two conditions would suggest some involvement by the muscles of the eye creating tremor. The point spread function of the total visual system referred to object space is estimated by Daugman as about 0.16 degrees at the 1% level.

17.6.4 Extension of the analysis to real optics and new techniques

The analyses of **Sections 17.6 & 17.7** employ very simple expressions for the MTF of the optical system in order to simplify the discussion. In the actual case, the optics is matched well to the neural portion of the visual system. However, the basic mathematics is distinctly different. These differences have been recognized for many years. A concise summary of the MTF pertinent to this section can be found in the IR Handbook[104]. For the more complex situation related to interferometry, explicit theoretical sources are harder to find. Rossi is useful[105].

17.6.4.1 The introduction of real physiological optics

For the aberration free optical system with a circular aperture, typically less than a 2 mm aperture for the human eye, the MTF can be given by a formal version of the expression used above. It includes an expression involving arccosines and is messy. For a slit or rectangular aperture, the MTF perpendicular to the long dimension is simpler.

$$MTF = 1 - S/S_L = 1 - f/f_c = 1 - f \cdot \lambda \cdot (F/\#) = 1 - (f \cdot \lambda)/2NA \qquad \text{Eq 17.6.4-1}$$

For wider aperture physiological optics, or for bundles not entering along the centerline of the optics, the impact of aberration can be considerable. The correct description of the MTF under aberrated conditions involves Bessel Functions. However, an estimate of the MTF can be made by considering f_c in the second form of the equation to be given by $f_c \cdot$(1 – wavefront error) and the wavefront error is expressed in fractions of a wave and is less than 3/4 (Figure 8-26 in the reference). **Figure 17.6.4-1** portrays these conditions graphically. However, the data is plotted relative to the Rayleigh limit of resolution, f_c.

---

[104]Wolfe, W. & Zissis, G. *ed.* (1985) The Infrared Handbook, Washington, DC: US Gov't. Printing Office, Chapter 8

[105]Rossi, B. (1957) Optics. NY: Addison-Wesley, Inc. pp 75-79

Experience shows, and the next section will demonstrate, the on-axis limiting resolution of the human physiological optics in the presence of adequate illumination is well matched to the performance of the remaining neural portion of the visual system. The limiting value for f_c under these conditions is approximately 200-250 cycles per degree depending on wavelength. As the iris opens, the on-axis performance rapidly drops to an effective limit nearer 100 cycles/mm. This performance is the subject of the Stiles-Crawford Effects– of the various kinds (see **Section 17.3.7**). Williams approached the theoretical Rayleigh limit, *in-vivo* using unique test conditions. He uses the number 221 cycles/degree at 632.8 nm as the contrast sensitivity limit for an eye with adequate incident radiation limited to a 7.25 mm diameter pupil centered on the line of fixation (see the next section).

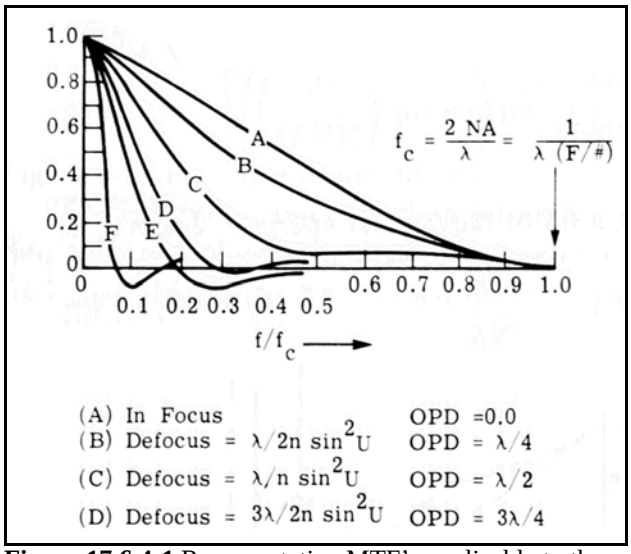

Figure 17.6.4-1 Representative MTF's applicable to the human eye. The OPD, optical path difference, is frequently used to describe the cumulative effect of all individual aberrations present. From Smith, 1966.

17.6.4.2 The introduction of interferometric test methods

Williams prepared a new interferometric optometry bench in 1985[106]. Its stability opened a new level of exploratory research. Unfortunately, the discussion did not include a detailed optical schematic of the test configuration. Since the bench used only two-beam interferometry, the reversal in phase in the various diffraction orders was not reported. If a multi-beam approach were used, the higher finesse ratio (ratio of the width of the individual peak to the cyclic pitch of the waveform in the interferogram) achievable would have made the phase reversal more obvious.

In subsequent papers from Williams' laboratory, the investigators have repeatedly claimed this technique allowed them to measure the response of the human eye out to 221 cycles/degree <u>without encountering diffraction effects or aberrations</u>. After a thorough investigation, this claim is not supported in this work. Interferometry does not provide a method of avoiding either the diffraction limit or aberrations associated with the eye. It is ironic that 221 cycles/degree is the precise resolution limit predicted by Rayleigh diffraction for an 8 mm pupil and 632.8 nm light. A complete analysis and reinterpretation of the Williams test set is presented in an **Addendum** to this work. It is available on request from this author. The addendum is labeled INTERFEROMETRY IN VISION RESEARCH.

Recently, Sekiguchi, et. al. have introduced a new approach to acquiring CSF and CCF, data using the above interferometric test set[107]. Their second paper examines the efficiency of the design[108]. While the test wet is quite sophisticated in concept, the investigators appreciation of it appears to still rely on concepts of Gaussian Optics. They do not address the sophistication (particularly the gradient index properties) of the lens of the human eye.

The papers were not accompanied by a detailed optical schematic or an analysis justifying the operation of the test configuration in the manner they assumed. It is hoped and expected that future papers will amplify on and justify these circumstances and perfect the test configuration. In the mean time, this work will provide an alternate analysis and interpretation of some of the results. It is proposed here that their method is the most accurate method of measuring the spatial contrast function and the MTF of the optics of the eye available.

The interferometer of Sekiguchi, et. al. was extended by Metha & Lennie. Results from this test set are just

---

[106]Williams, D., (1985) Aliasing in human foveal vision. *Vision Res*. vol. 25, no. 2, pp 195-205
[107]Sekiguchi, N. Williams, D. & Brainard, D. (1993) Aberration-free measurements of the visibility of isoluminant gratings. *J. Opt. Soc. Am.* vol. 10, pp 2105-2117
[108]Sekiguchi, N. Williams, D. & Brainard, D. (1993) Efficiency in detection of isoluminant and isochromatic interference fringes. *J. Opt. Soc. Am.* vol. 10, pp 2117-2133

beginning to appear[109,110]. The paper by Metha & Lennie still did not provide an analysis of the test set design, although it did give one reference to a text of general interest. It appears they made a serious misinterpretation of the capability of the instrument-eye combination as they used it.

The Williams instrument can be described as a unequal-path lateral shearing triangular cyclic interferometer of the Twyman-Green type. It produces two laterally spaced converging beams focusing at the entrance aperture of the visual system. When the converging beams have a numerical aperture equal to or better than that of the eye, the system can be made to provide a spatially limited stimulus on the retina that consists of a uniformly illuminated area modulated by a sine-wave pattern. If the wavefront error of the converging optical bundle is less than the wavefront error of the optics of the eye, the measured performance is that of the physiological optics.

The resulting spatial contrast function is shown in **Figure 17.6.4-2**. While the original figure used a logarithmic scale to more precisely define the data points, this version is plotted more conventionally to make it more recognizable to the majority. While one might expect the technique of only using a thin annulus of the lens, to generate each spatial frequency (as shown by the lower scale), might surface additional anomalies in the optics, this does not appear to have occurred (except possibly at 20 cycles/degree). The shape of the solid curve is typical of a lens system suffering from one of a variety of obstructions, aberrations or defocus. It is conventional to define an equivalent spherical aberration to represent these errors. In this figure, the solid line (including the low frequency extension) represents an equivalent spherical aberration of between ½ and 3/4 wavelengths. This degree of aberration confirms the more detailed findings of Liang & Williams using the same subject[111]. See also Liang, et. al. for a detailed discussion of the test set used[112].

---

[109]Williams, D. Sekiguchi, N. & Brainard, D. (1993) Color, contrast sensitivity and the cone mosaic. *Proc. Natl. Acad. Sci. USA*, vol. 90, pp 9770-9777

[110]Metha, A. & Lennie, P. (2001) Transmission of spatial information in S-cone pathways. *Visual Neurosci*. vol. 18, pp 961-972

[111]Liang, J. & Williams, D. (1997) Aberrations and retinal image quality of the normal human eye. *J. Opt. Soc. Am. A.* vol. 14, no. 11, pg 2873-2883

[112]Liang, J. Grimm, B. Goelz, S. & Bille, J. (1994) Objective measurement of wave aberrations on the human eye with the use of a Harmann-Shack wave-front sensor. *J. Opt. Soc. Am. A.* vol. 11, no. 7, pp 1949-1957

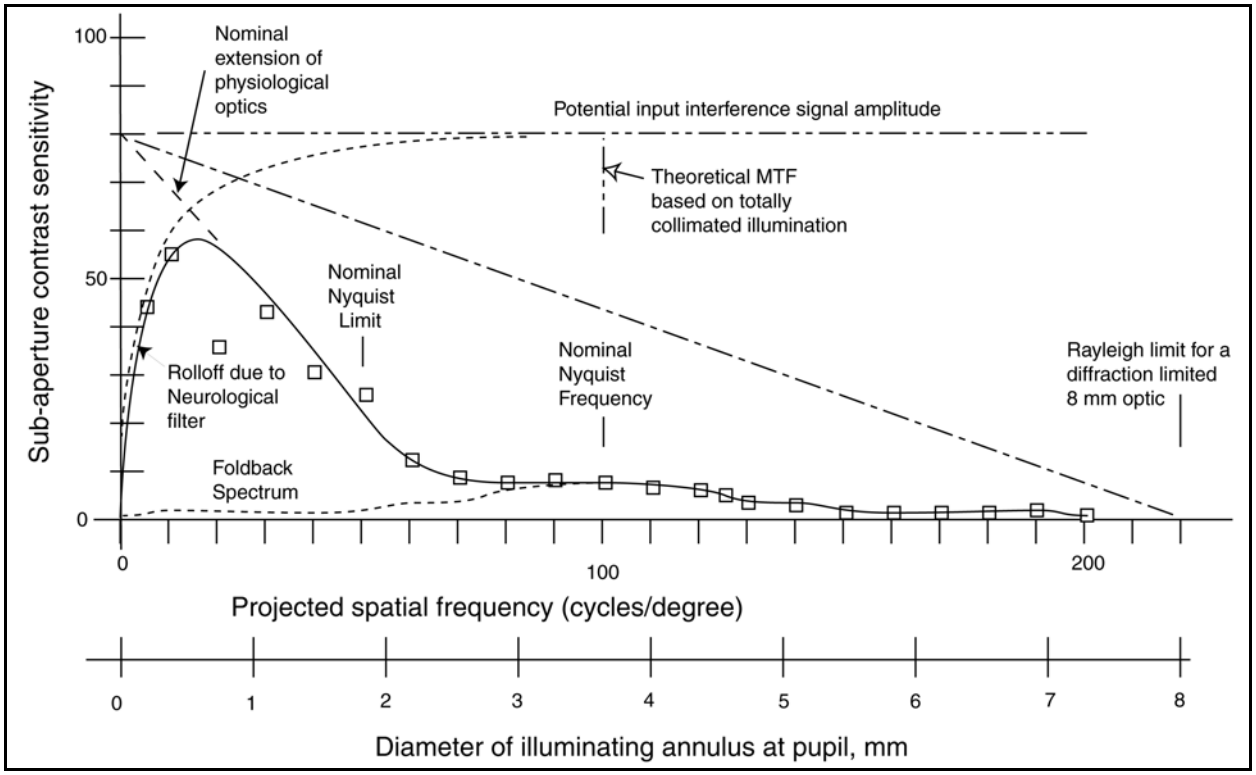

Figure 17.6.4-2 The spatial contrast function of a human eye measured interferometrically. Note the sensitivity adequate to measure the function out to 200 cycles/degree. The data points are a re-plot of the data for D.R.W. The shape of the solid line reflects an equivalent spherical error for the physiological optics of between ½ and 3/4 waves. The Nyquist frequency is estimated from the discussion in the Williams (1985) paper. It is consistent with the Nyquist frequency of 108-128 determined by Yellott using a real retinal photograph attributed to Polyak.

The important features of the contrast function obtained using the interferometric test set is the high signal to noise ratio achieved. This is due to both the quality of the interference pattern and the large size of the patterns (compared to Gabor patches, a Snellen letter or a three-bar test chart). The large pattern size leads to much more effective correlation within the visual system and a lower threshold for detection. The test set can also achieve precise spatial frequencies down to near zero cycles/degree. This low frequency capability allows a precise determination of the low spatial frequency capability of the eye (note the rolloff at low frequencies) that can be directly compared to the equivalent rolloff in the temporal frequency domain. By comparing these values, a precise effective velocity for the tremor of the eye can be computed. The nominal calculated value is 2.5 cm/second. This is associated with a triangular waveform with a fundamental frequency of a nominal 30 Hz. The waveforms applied to the horizontal and vertical oculomotor muscles are assumed to be in quadrature. This subject is discussed more thoroghly in **Section 7.3**.

17.6.5 Delay performance

Tests involving flicker are particularly difficult to define adequately, especially without an adequate model of the visual process. Although all of the conventional time constants, including the time delay term, are essentially independent of the chromatic photodetection channel involved, or the luminance or chrominance channel involved, this is not true of the encoding process used to transmit the data through the projection neurons to the brain. The coding process is highly asymmetrical with respect to its temporal performance. This asymmetry significantly affects the perception time for various colors, and accounts for a majority of the special effects and phenomena related to flicker experiments.

17.6.5.1 Asymmetry in the codec

The coding/decoding (codec) process is a nonlinear process as implemented in vision. It is implemented slightly differently in the luminance and chrominance channels. As indicated in **Section XXX**, it appears that the cortex senses the arrival of the initial action potential in the luminance channel as an indication of change in the scene. It then determines the significance of the change in the scene by the time interval before the next action potential in the luminance channel. Simultaneously, it interrogates the two chrominance channels to determine the chromatic characteristics of the change in the scene. The cortex obtains coarse information as to the coordinates of the change in the scene, in inertial space, from two sources. Its memory of previous commands sent to the muscular-skeletal system and its memory of the previous scene in inertial space. The cortex obtains fine information as to the coordinates of the change in inertial space by interpolating the presumed angular orientation of the ocular in response to its most recent commands controlling tremor. The cortex is also apparently aware of the nominal delays associated with the signal processing in the photodetection, luminance, and probably the chrominance channels. Unusual delays in these channels can lead to misinterpretation (a facet of vertigo).

17.6.5.1.1 Delay in the luminance channel

In the luminance channel, the parasol ganglion cells exhibit an integrating function and a threshold level that must be attained before they generate the first action potential. This typically results in a discernable time delay at low light levels, in addition to the time delay inherent in the P/D process in the Outer Segments. This effect is well documented in lower animals. The two delays can be separated. The P/D delay is sensitive to temperature.

17.6.5.1.2 Delay in the chrominance channel

The codec is implemented differently in the chrominance channels. There is no thresholding. No integration has been observed. However, the system still uses a form of phase modulation, although no longer of the simple time delay class. The codec now calls for the midget ganglion cells to generate a continuous stream of action potentials, in the absence of excitation, at a nominal interpulse period of 33 milli-seconds--equal to a nominal frequency of 30 Hertz. This “carrier” is modulated by a bipolar signal that can cause the interpulse interval to drop to about 15 millisecond or rise to a much larger number. The highest value is unknown but can easily exceed 60 milliseconds. As a result of this bipolar encoding, the time delay associated with a specific monochromatic color can vary significantly depending on the saturation level. If the scene is of low chromatic saturation, no problems arise. However, if the scene is of high chromatic saturation, the chromatic information related to the S- and L-channels can be delayed significantly. The information related to the M-channel arrives relatively early.

17.6.5.2 Elimination of the "Dark Background" as a variable

A group of workers have defined a synthetic "dark background" as accounting for the variable threshold sensitivity of the human eye during dark adaptation and other situations. It appears that this concept is based on the assumption that the eye is a linear system with constant gain. Under this assumption, the background signal level has been assumed to be a variable. This dark background has been expressed as both a "equivalent background luminance" and a "equivalent background brightness" beginning in 1937. Spillman, Wolf & Nowlan provide references to this activity[113]. Based on the proposed model, this work takes the alternate approach. It assumes the background level of both the luminance and other differencing channels are fixed in time and amplitude, and it is the signal manipulation that involves variation under a variety of conditions. Thus, the variation in after images is proposed to be a result of the dynamics of the adaptation amplifiers and their vascular supply system. In the first order, the shape of the after image is primarily a consequence of two elements, the quality and health of the vascular system of the retina and the magnitude of the prior illumination eliciting the afterimage. In the second order, it is the precise state of the adaptation amplifiers that determine the perceived colors oas a function of time. It is not absolutely clear whether the background levels surrounding the after image are fixed, as in the case of a threshold circuit, are the result of a "paint"program within the cortex, or are stochastic, based on a random noise source. Highly specialized tests need to be designed to clarify this point completely.

In the above paper, Spillman, et. al. employ a multi-quadrant graphical presentation. The graph is difficult to interpret because the common vertical axis actually represents two different underlying functions. The left scale is the threshold sensitivity as a function of time in the absence of any background illumination, a transient characteristic. The right scale is the threshold sensitivity as a function of illumination level independent of time, a steady state characteristic. No mathematical relationship was provides correlating these two characteristics. Illustrative correlation lines were only drawn for a few points between the two quadrants. The concept has not been pursued in the literature.

17.6.6 Flicker performance

[xxx probably should separate white light flicker from alternating color flicker]
Flicker tests in the psychophysical environment are beguilingly simple. The instrumentation appears simple, the tests images are easy to create, and a simple threshold criteria is employed. However, the combination of the multiple signal channels of the visual system prior to cognition and cognition itself introduce formidable complications. Kelly[114] has briefly discussed some of these challenges. Working only with "white light" that he did not further define, and employing a modified Ganzfeld illumination that he took care to define he acquired considerable data. He noted a variety of difficulties: "Other subjective phenomena included sensations of *motion* at very large amplitudes (10-100 times threshold at frequencies of 8-20 Hz); some observers saw bright fringes crawling across the entire field. Several observers reported that occasionally during a session large areas of their retinas would 'blank out' (as in stabilized-image experiments and perhaps for similar reasons). No data were taken in this condition; it could be dispelled by blinking or momentarily increasing the stimulus amplitude." When one introduces a multicolored test environment, the complications increase exponentially. At the conclusion of the above paper (one of an extensive series), he noted: ". . . the amplitude sensitivity data of Table I present a two-fold challenge: (a) to find the simplest realistic model of the visual mechanism which can account for this behavior, and (b) to explore other variations of the sinusoidal stimulus (e.g., spatial, chromatic, individual differences), in the hope of unifying still other visual phenomena."

The fundamental problem is to define more unique test conditions that control or quantify all of the variables involved. While recognizing the hypertopic regime in his test results (he encountered visual pain at 9300 trolands and truncated his test protocol below this level for other subjects), and recognizing the result of uncontrolled tremor but not understanding the inability of the system to quantify a constant intensity scene, Kelly acquired data that clearly records the variable bandwidth nature of the signals generated in the different visual channels. Interpretation of this data becomes difficult because of the number of uncontrolled variables. An equally important problem is in training subjects in preparation for the tests. It is not clear that one is able to define the training required based on the current state of the art. Such training clearly involves preparing the subject to recognize and ignore cognitive

---

[113]Spillman, L. Wolf, E. & Nowlan, A. (1971) Dark and light adaptation with opposite time courses. J. Opt. Soc. Am. XXX vol. 61, pp. 1122-1123

[114]Kelly, D. (1961) Visual responses to time-dependent stimuli. I. Amplitude sensitivity measurements. J. Opt. Soc. Am. vol. 51, no. 4, pp. 422-429

processes that are not understood (e. g., ignoring apparent perceived motion in an obviously stationary object field).

Kelly & van Norren[115] expanded their studies into the heterochromatic flicker arena. Burr also provides useful insights[116].

The above two problems illustrate some of the problems endemic to psychophysical flicker phenomena testing and why this area of research will be left to other investigators. When the additional area of electrophysiological flicker testing is also addressed, the number of variables that must be controlled and the detailed knowledge of the visual system architecture required further complicate this area. Baron , Boynton & van Norren have provided data in this area[117]. They worked only with the LERG of monkeys and drew few conclusions. Completely correlating their data with the more complex psychophysical data may be difficult.

Fukada, et. al have provided some very interesting data on flicker phenomena in cat using only a "white" light source[118]. While their experiments did not separate all of the variables adequately, additional mining of their data is feasible (see Section **14.6.3.4**). They did offer definitions related to flicker frequencies that are electrophysiologically based rather than the looser definitions associated with psychophysical tests.

Conner has provided a paper based on conventional psychophysical testing that includes considerable data relating flicker frequency parameters to background and field illumination[119]. He offered no model of the visual system he was attempting to describe. The data clearly shows the impact of the transient performance of the adaptation amplifiers in human vision. Much of the discussion is involved in conceptual matters related to (putative) rods and cones.

The variety of situations involving flicker that can be defined is large. Livingstone & Hubel[120] have provided a discussion of many of these (the latter part of the paper). There experiments appear to be primarily exploratory. No effort was made to associate them with a comprehensive model of the visual system. This situation is recognized in their concluding discussion.

Stockman, MacLeod & Lebrun have explored chromatic flicker showing how the performance of the high bandwidth luminance channel could be separated from the low bandwidth chrominance channels (See reference in **Section 17.5.1.1.3**). Their material is discussed **in Section 17.6.6.5**.

17.6.6.1 Review of Kelly papers

The 1961 Kelly paper referenced above does show obvious correlation to this work. The fact that pain was experienced near 9300 trolands is in agreement with the hypertopic illumination regime defined in this work. He also recognized the onset of the scotopic regime near 0.06 trolands. The distinct linear change in maximum signal bandwidth with illumination level is in agreement with the term $\omega = \sigma F \tau$ of this work. Although less obvious, the form of the threshold amplitude as a function of frequency is represented by the difference in signal amplitude between two photodetection channels of different bandwidth because of the above relationship. This is a critical distinction. Although the experiments were designed within the concept of a brightness change as opposed to a chromatic change within the modern zone theory of 1961, the data does not relate well to a brightness change within the extended zone theory proposed in this work. Based on the concepts of this work, the data appears to correlate better with a change in the chrominance channels of vision. The above statement is based on the fact that the illumination is partitioned into multiple, chromatically independent, signaling channels before any other process takes place. These channels exhibit independent photodetection and adaptation characteristics that are both time and illumination level sensitive. Within the signal manipulation stage following the signal detection stage, these signals are processed in both luminance and chrominance sensitive channels. The luminace channel incorporates a

---

[115]Kelly, D. & van Norren, D. (1977) Two-band model of heterochromatic flicker. J. Opt. Soc. Am. vol. 67, no. 8, pp. 1081-1091

[116]Burr, D. (xxx) Human sensitivity to flicker and motion, *In* Kulikowski, J, Walsh, V. & Murray, I. *eds*, Vision and Visual Dysfunction, Volume 5, Boca Raton, FL: CRC Press, Inc. Chapter 12

[117]Baron, W. Boynton, R. & van Norren, D. (1979) Primate cone sensitivity to flicker during light and dark adaptation as indicated by the foveal local electroretinogram. Vision Res. vol. 19, pp. 109-116

[118]Fukada, Y. Motokawa, K. Norton, A. & Tasaki, K. (1966) Functional significance of conduction velocity in the transfer of flicker information in the optic nerve of the cat. *J. Neurophysiol*. vol. 29, pp 698-714

[119]Conner, J. (1982) The temporal properties of rod vision. *J. Physiol*. vol. 332, pp 139-155

[120]Livingstone, M. & Hubel, D. (1987) Psychophysical evidence for separate channels for the perception of form, color, movement and depth. J. Neorosci. vol. 7(11), pp. 3416-3468

summation of logarithms, while the chrominance channels incorporate a difference of logarithms. Under the conditions of the experiments, it appears the chrominance channels that are perceived by the cortex as most important and it is the signal from those channels that is reported in the above psychophysical experiments.

For the moment, the high pass filter characteristic of the adaptation amplifiers will be ignored. The impact of this characteristic is only important for signaling frequencies below 0.3 Hz. Only the low pass filter characteristic of the P/D process will be considered. The amplitude response of this difference for two simple low pass filters is given by an equation of the form:

$$A = \frac{A_x}{s+x} - \frac{A_y}{s+y} = \frac{(A_x - A_y)s + A_x \cdot y - A_y \cdot x}{(s+x)\cdot(s+y)}$$

Eq: 17.6.5 -z

where y and x are separate expressions of the form σFτ relating to the P/D equation for the individual photodetection channels, probably the M- and L-channels, as indicated above. The subscripted A's are the gain coefficients associated with each of these channels. Their precise value is determined by the spectral content of the "white" illumination used and the state of adaptation of each of the channels. Because of the dependence on spectral content, the amplitude and frequency parameters vary in a coordinated manner as shown in figure 4 & 5 of Kelly. This correlation will be explored in more detail in the next Section. Since the experiments were designed to be achromatic, no comments appeared in the Kelly paper concerning the chromatic appearance of the light used as a function of the illumination level. It would have changed significantly to the discerning experimenter (probably from a "warm white," as the term is used in the lighting industry and assuming a color temperature of 2400-2800 Kelvin, to neutral gray) as the scotopic level was approached. It is this change that becomes more important in the response of the subject than the actual change in total illumination.

The 1977 Kelly & van Norren paper was based on much more sophisticated test instrumentation, including definition of the color temperature used, that aids correlation with this work. However, they relied upon the "modern zone theory of color vision" prevalent at that time. Quoting them: "Our general conclusion is that flicker sensitivity is probably controlled by the pathways of the proximal retina, not by the temporal characteristics of cone cells." is based on the limited scope of that theory. The difficulty with the modern zone theory as they defined it is exemplified by their comment concerning the state of the literature at that time; "Unfortunately, no two of these techniques yielded the same results, so it is not certain that any of them succeeded in measuring the characteristics of independent cone classes." To circumvent those limitations, they adopted the earlier approach of Esteves & Spekreijse and introduced "silent-green flicker" and "silent-red flicker." These analytical crutches are not defendable by this work. By recognizing the parallel paths of the signal manipulation stage in this work (that can be described as an extended zone theory), the data can be interpreted in a more direct manner.

They also offered a premise that, although stated with less than the required precision, is easily interpreted using this extended zone theory. They stated: "For the red-green, opponent-color pathways, we make the following assumption: The frequency-dependent output of these pathways is determined by the *instantaneous value of the difference* between the (red and green) input signals they receive." When interpreted in terms of the New Chromaticity Diagram for Research and this work, the premise is obvious. However, it is important to recognize the *instantaneous value of the difference* is a difference in logarithms and determined by the spectral content of the two signals relative to the null at approximately 572 nm. in the performance characteristic of the signal manipulation channel (e. g., their red-green opponent-color pathway but also the difference between the L- and M-channels as represented in the Q channel of this work).

Using this work, the general conclusion of Kelly & van Norren can be expanded and stated more succinctly as, while the bandwidth of the visual channels recorded in flicker experiments is controlled by the P/D equation associated with the photoreceptor cells, it is the signal manipulation and signal projection stages of the visual process that control the sensitivity of the subject to flicker phenomena (excluding possible cognitive contributions that may be secondary and difficult to quantify at this time).

17.6.6.2 Sensitivity versus frequency

To illustrate the number of variables involved in flicker experiments, the theoretical foundation for figure 4 & 5 of Kelly will be developed. First it is necessary to postulate that no cognitive processes were involved and the impact of tremor can be ignored. In the absence of a prescribed characteristic of the source illumination, it is assumed that

the source temperature is 7053° Kelvin. If not, the effect of a different color temperature can be included with the effect of any filters used. In this case, since white light was specified, the assumption will be made that the source was of low color temperature as expected from a simple incandescent source. To simplify the analysis, it will be assumed to be completely devoid of light exciting the S-channel of vision. The ratio of M-channel to L-channel illumination is unknown but assumed to be fixed. (Although not critical to white light flicker studies, it is important to carefully control or measure the flicker frequency to correctly interpret any impact of the signal projection stage.) To avoid any impact due to the low frequency response of the adaptation amplifiers, the flicker frequency must be above 1-2 Hz. A flicker frequency in the 5 Hz area appears satisfactory. In the absence of a fixed specification on the illumination intensity, care must be taken to recognize the variable gain associated with the adaptation amplifiers associated with each chromatic photodetection channel.

With these parameters all eliminated, controlled or measured, it is possible to predict the sensitivity of the visual system as a function of frequency using the above equation. First, note that the terms x and y are variables given by $x=\sigma F_x\tau$ and $\psi=\sigma F_y\tau$. F_x equals to amount of the incident radiation absorbed by one of the chromatic channels and assumed to be the M-channel here. F_y equals the amount of incident radiation absorbed by the other channel, assumed to be the L-channel. A_x is the gain of associated with the x channel and A_y is the gain associated with the y channel. The unsubscripted A is the gain of the overall circuit represented by this equation. Here it is assumed to be the gain of the Q channel that is associated with the difference between the M- and L-channel signals. Second, note the form of the denominator. These two expressions define the high frequency poles of the overall signal (the signal and not the channel through which it is traveling). They are both a function of the illumination level. The gain, A, is reduced at frequencies above x and y. Third, note the form of the numerator. The expression associated with s is important. It describes the gain of primarily the adaptation amplifiers in each chromatic channel. If these gains are equal, this term disappears and the numerator is independent of frequency (an important special case). If the gains are not equal, their net value, along with the terms not including s control the slope of the gain characteristic at frequencies below the pole frequencies in the denominator. It is now possible to sketch the theoretical sensitivity of the visual system as a function of frequency, based on all of the caveats listed above. **Figure 17.6.6-1** illustrates the fundamental situation for three specific situations. In the first case, it is assumed that the term $A_x - A_y = 0$. The sensitivity, shown by the upper solid line, remains at a fixed value for a given illumination level until it begins to decrease due to the poles in the denominator. If the illumination level decreases, both the sensitivity and the half-amplitude point in the frequency response begin to move toward zero. This is illustrated by the lower solid line.

The condition, $A_x - A_y = 0$, is only a theoretical construct. It cannot exist in practice since it represents a null condition in the chrominance channel. All actual situations recorded in the laboratory are represented by the following cases.

If $A_x - A_y$ does not equal zero, two effects are noticed. First, the maximum sensitivity at low frequency is reduced. At a specific frequency, the sensitivity begins to increase. The slope in this region of the sensitivity versus frequency characteristic is determined by *all* of the terms in the numerator of the equation. This positive slope tends to be low and is soon overwhelmed by the negative slope introduced by the terms in the denominator. The result is a solution that shows a lower initial sensitivity that begins to rise to a peak and then fall steeply toward zero. The fall is actually steeper than shown here because two simple low pass filter terms were used in the denominator. In the P/D equation, there are actually two poles for each chromatic channel. One is defined by a time constant τ and the second by the expression $\sigma F\tau$. For the special case of $\sigma F=1$, each pole in the denominator becomes a double pole and the downward slope is doubled.

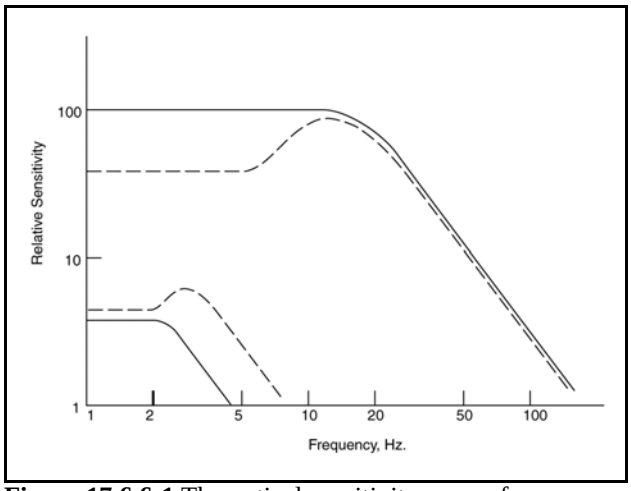

Figure 17.6.6-1 Theoretical sensitivity versus frequency for the visual system under a long list of specified conditions (see text). The solid lines are unrealizable theoretical constructs. The dashed lines are realizable and correspond to the measured data of Kelly (1961) subject to the discussion about the high frequency roll-off in the text.

As the illumination is reduce in this more complex case, a number of changes occur. First, σ, the absorption coefficient in the P/D equation remains fixed. Therefore, the product, σF, cannot remain equal to 1. Therefore, the two double poles in the denominator become four separate poles. This complicates the shape of the descending portion of the

characteristic. Second, the gain of the adaptation amplifiers associated with the terms, A_x and A_y generally increase independently toward their maximum value. However, the square-law process associated with translation in the L-channel drives the A_y term to zero. As a result, the overall characteristic begins to shrink toward zero in both sensitivity and frequency response, while maintaining an ever smaller hump due to the term associated with s in the numerator.

This analysis appears to correlate well with the data of Kelly for the conditions described. It is important to notice that the analysis is not based on interpreting the illumination as exciting a single channel responsive to "white light." It is based on the fact that the incident light is spectrally partitioned and sensed by two (or three) parallel chromatic channels that exhibit independent parameters. It is these independent (and independently varying) parameters that determine the performance of the visual system. The analysis is based on the operation of the chrominance channel, Q, and not the luminance channel, R. The response of the R channel appears to be negligible in this class of experiments. In general, the half-amplitude frequencies in the graph all decrease as a linear function of illumination as shown in his figure 4, although the relationship is obscured in his figure 5. The line connecting the m=1 values in the figure is a construct and does not represent a physical process. The subject of sensitivity is complex because it depends on th operation of the adaptation amplifiers., which are uncontrolled and invisible variables in his experiments. He did not discuss the state of adaptation of the subjects prior to the experiments explicitly, treating the background level during the experiment as equal to the adaptation level. His figure 4 shows the effect of these amplifiers in maintaining a relatively constant threshold amplitude down to about 0.65 trolands where the mesotopic illumination regime is entered. From 0.65 to 0.06 trolands, the change in sensitivity is approximately a square root relationship with illumination as expected. Somewhere below 0.06 trolands, the definition of threshold contrast will fail. The minimum signal level for detection will be fixed and depend primarily on image size.

This analysis suggests modifications to several of the conclusions drawn by Kelly. As an example, the hump in his figure 4 for 0.06 trolands appears to be real although he dismisses it in comment (a) related to the figure. For consistency, his term adaptation level should be replaced with background level. Further analysis requires considerably more discussion and evaluation of the unspecified parameters in that paper.

17.6.6.3 Flicker fusion experiments

One of the most widely studied fields of flicker has to do with the frequency at which the subject is no longer able to perceive a test signal that is changing repetitively with respect to one parameter or another. The number of options are endless and the complications caused within the visual system, particularly those related to the signal projection stage, are similarly endless.

There are many figures in the literature showing a significant kink in the graph of flicker fusion frequency as a function of illumination. The text invariably assigns this to the rod-cone transition without any significant discussion or justification. Only that it has been labeled so for many years. Most of the baseline work dates from Hecht & Shlaer[121] in the 1930's. Karp[122] has presented some more recent data, 1958, providing statistics on 100 subjects but little justification of the approach based on theoretical considerations. Armington reprinted their figure with a typographical error. Most of the subsequent articles referring to this early work suggests the portion of this curve occurring at lower illumination levels must be due to rods and the higher illumination part to cones.

Green has presented a series of experiments using Wratten filters but does not describe the physiological model of human vision[123]. He assumes a linear summation at the input of each photoreceptor but does not define the character of the output at any point in the system.

Using the top level schematic of this work along with the discussion of the P/D process as it applies differently to the L-channel than to the S- and M-channels, it is possible to interpret the exploratory data in greater depth. First, it is clear that the frequency response of the signals relating to the different photoreceptor channels are critically

---

[121]Hecht, S. & Shlaer, S. (1936) Intermittent stimulation by light. Part V. The relation between intensity and critical frequency for different parts of the spectrum. J. Gen Physiol., vol. 19, pp. 965-979. *Also* in Wyszecki & Stiles, figures 1 & 2 of [7.9.3]

[122]Karp, XXX (1958)

[123]Green, D. (1969) Sinusoidal flicker characteristics of the color-sensitive mechanisms of the eye *Vision Res* vol 9, pp 591-601

dependent on the illumination level applied to each chromatic channel. Second it is clear that the adaptation state of each chromatic channel is independent of the others. These states must be well understood before predictions can be made concerning the nature of the P, Q, & R signals created within the signal manipulation stage. These signals are then impacted by the asymmetry of the signal projection stage and then perceived in the cortex. It appears they are first perceived individually relative to a threshold level and then analyzed conceptually to determine the ultimate understanding of the image presented. Following this process to conclusion, it is proposed here that the kink is related to similar mode changes to those found in the dark adaptation characteristic. Armington[124] briefly discusses the difficulty in specifying the location of the kink along the lines of perception and cognition outlined above. The data of Hecht & Shlaer is interesting in that it shows the critical flicker frequency at low retinal illuminance is a monotonic function of spectral wavelength. Such a monotonic function extending from 450 nm to 670 nm is not compatible with the sensitivity profile of a monochromatic photoreceptor.

17.6.6.4 Examples of flicker phenomena

The examples of flicker phenomena in the literature are seemingly endless. Brindley has provided a good discussion and list of references through 1970[125]. One of the most well defined flicker phenomena is that of Bidwell in 1897. He suggested using the disk shown in **Figure 17.6.6-2** to cause scenes to appear in their complementary colors. Note the direction of rotation of the disk is quite critical to the appearance of the scene and the scientific interpretation of the results. The rotational rate, of six revolutions per second, is less critical but must be within a small band. Based on this theory, the process causing the perceived result is easily described.
[[need to show timelines here]]

A more complex disk for studying color contrast is presented in Graham[126].

Starting from point A, taking the notch as encompassing 45 degrees, and proceeding counterclockwise, the eye initially observes the black portion of the disk for approximately 74 milliseconds. During this interval, the subject perceives a black field. At the transition to viewing the scene, the subject perceives a change in the luminance channel of each group of photoreceptors viewing the scene in sequence. The observation time for each photoreceptor is approximately 21 milliseconds. This is sufficient time for the luminance channel to react to reasonably bright scenes by generating as many as 7.5 pulses (based on a maximum nominal rate of 60 pulses per second). However, the reaction time of the chrominance channels is asymmetrical. Since the pulses in the chrominance channel are asynchronous with the luminance channel pulses, the actual number of pulses transmitted to the brain during this 21 milliseconds can only be described statistically. It requires at least 30 milliseconds to merely report "white" following the initial pulse in each chrominance channel. During this 21 millisecond interval, the chrominance channels generally only generate one pulse.

Following the 21 millisecond interval, the photoreceptors are now presented with a bright white scene for approximately 74 milliseconds. This is more than enough time for the luminance channel to stabilize and report a significant change from the scene during the 21 millisecond interval. This change in brightness is nominally opposite to the change reported in going from black to the actual scene.

The chrominance channels also sense a change in the chrominance of the image that has now returned to "white." **[Da da da]**

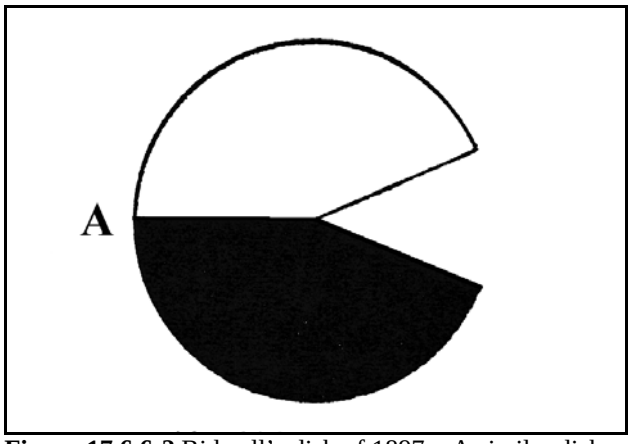

Figure 17.6.6-2 Bidwell's disk of 1897 . A similar disk can be constructed. To obtain the illusion of a complementary colored scene, the disk must be rotated clockwise at about 6 revolutions per second.

---

[124]Armington, J. (1974) The electroretinogram. NY: Academic Press pp. 320-326
[125]Brindley, G. (1970) Physiology of the retina and visual pathway Baltimore, MD: The Williams & Wilkins Co. 149-198
[126]Graham, C. et. al. (1965) Vision and Visual Perception. NY: John Wiley & Sons. pg 461

17.6.6.5 The bandwidth of the luminance & chrominance channels

[xxx This section will eventually include an evaluation of the bandwidth of the luminance and chrominance channels in support of the chapter on the tertiary circuits, Chapter 14. It will include the work of de Lange Dzn and Stockman, MacLeod & Lebrun.]

In the first of two papers in 1958[127], xxx. In the second paper[128], xxx. These two papers use only simple RC circuits as analogs. As a result, a few of his results are received with awe. A more realistic neural model would lead to a clearer interpretation of his results.

In the 1961 de Lange Dzn paper[129], he shows the signaling channel exhibits high frequency peaking approximating one-half log unit (about 3x) at 10 Hertz. He approximates this with a 4-stage RC filter with unlikely parameters in the absence of a better model of the neural system. The paper deserves more study.

Overall, these three papers have been referenced at the de Lange Dzn graphs of the temporal performance of the eye.

Sokol & Riggs addressed the separation of the signaling elements of color vision in 1971[130]. They demonstrate the wider bandwidth of the photoreceptors compared to the rest of the neural channels of the visual modality.

Stockman, MacLeod & Lebrun have provided flicker data focused on the blue photoreceptors that separated the high bandwidth luminance channel signals from the lower bandwidth chrominance channel signals[131].

17.6.7 After-image phenomena

The study of after-images has suffered severely from the lack of an adequate model of the visual system. The literature is based almost entirely on anecdotal data and generalized statements.

Palinopsia is a condition distinct from what most people think of as after-images. In this condition, images collected by the eyes are retained for an abnormal duration by the higher signal manipulation centers. The result is perception of a sticky series of images like occasionally seen in TV commercials as a special effect.

Brindley has also provided an interesting discussion of this phenomena along with an extensive biography through 1970[132].

Smerdon & Willshaw provided a paper in 1988 that describes after-image effects that lasted for days. However, the test protocol they provided was less than specific and the character of the illumination used can only be inferred from the technology of the day (they indicated a “green” phosphor monochrome kinescope display without defining the phosphor used).

Only a few technical papers have appeared in the 1989-2007 time period. The general assumption is that afterimages originate in a specific retina based on the predominant results of simple tests. Shimojo et al. have

---

[127]de Lange Dzn, H. (1958) Research into the Dynamic Nature of the Human Fovea -Cortex Systems with Intermittent and Modulated Light. I. Attenuation Characteristics with White and Colored Light *J Opt Soc Am* vol 48(11), pp 777-784

[128]de Lange Dzn, H. (1958) Research into the Dynamic Nature of the Human Fovea --Cortex Systems with Intermittent and Modulated Light. II. Phase Shift in Brightness and Delay in Color Perception Light *J Opt Soc Am* vol 48(11), pp 784-789

[129]de Lange Dzn, H. (1961) Eye's Response at Flicker Fusion to Square-Wave Modulation of a Test Field Surrounded by a Large Steady Field of Equal Mean Luminance *J Opt Soc Am* vol 51(4), pp 415-421

[130]Sokol, S. & Riggs, L. (1971) Electrical and psychophysical responses of the human visual system to periodic variation of luminance *IOVS* vol 10(3), pp 171-180

[131]Stockman, A. MacLeod, D. & Lebrun, S. (1993) Faster than the eye can see: blue cones respond to rapid flicker *J Opt Soc Am A* vol 10(6), pp 1396-1402

[132]Brindley, G. (1970) Op. Cit. pp. 149-155

recently provided a paper which proposes cortical involvement for some after-images[133].

The following tabulation is provided as an overview of the phenomenon and the mechanisms behind the phenomenon based on this work. As time permits, this overview will be expanded into a formal description and a proposed test program.

1. After-images and adaptation are closely related. Dark adaptation is more properly described as post-stimulus adaptation in the absence of any further stimulation. The post-stimulus adaptation characteristics are marginally different for the different spectral channels and their location in the retina.

2. The perceived color of after-images varies with time, frequently changing after 10-20 seconds. The interval before changing depends on the level of bleaching during the stimulus interval.

3. After-images are usually spoken of as positive or negative depending on the background during the post-stimulus interval. The nomenclature dates from the days of black and white photography, positives and negatives.

4. The after-images are usually not complementary to any degree of precision. The perceived image is the result of the transients from the spectral channels, S, L & M being processed by both the luminance (R) channel as well as the P & Q chrominance channels.

5. After-images generated using a large uniform screen result in a blotch of a different color in the center, representing the shape of the individual's foveola, compared to the surround. The blotch defines the nonuniformity associated with the foveola and known as Maxwell's Spot. See Davson, 1962.

6. In any laboratory experiment, it is absolutely mandatory that the difference between pink, maroon and magenta be precisely defined. Once these terms are defined, the subjects must be carefully advised as to what these definitions are before they are asked to describe their perceptions.

17.6.8 Temporal performance of combined visual-motor system

It is interesting to consider the time delay between acquisition of photons at the retina calling for an alarm response and the time of that response. Rodieck[134] has recently summarized some of the time delays related to the HVS in a classic "shoot out at the OK Corral." TABLE XXX modifies his presentation to associate the various time delays with the stages of this theory and to stress the variability of the first term and to differentiate between the **analytical path** and the **awareness path**. An further expanded version of this table is available in **Section 15.2.4**.

TABLE 17.6.7-XXX
TIME DELAYS WITHIN THE VISUAL-MOTOR SYSTEM

Path element	Time delay	Stage of Theory
Retina to optic nerve	20 ms. (a variable)	Stage 1 & 2
Optic nerve to striate cortex	10 ms.	Stage 3
Striate cortex to area 7	3 ms	Stage 3
	13 ms	
Optic nerve to pretectum	3 ms	Stage 3
Pretectum to area 7	3 ms	Stage 3
	6 ms	
Processing time in brain (Pretectum, LGN, striate and area 7)	110-130 ms.	Stage 4

[133]Shimojo, S. Kamitani, Y. & Nishida, S. (2001) Afterimage of Perceptually Filled-in Surface *Science* vol 293(5535), pp 1677 - 1680
[134]Rodieck, R. (1998) The first steps in seeing. Sunderland MA: Sinauer Associates pg. 294

Brain-spinal cord to finger muscles	20 ms.
Activation of finger muscles	20 ms.
Total	180-200 ms.

These numbers suggest that the dominant time delay is related to the cognitive centers. However, this finding is highly dependent on the task associated with the test. **Alarm path** responses, which do not involve the cortex, are much faster than indicated by the processing time in the brain suggests. Since both the efferent and afferent nerves are operating under pulse conditions, they do not reflect a change in time delay with the nature of the information they are transmitting. The photodetection process in the photoreceptor cells however, does exhibit a time delay that is a function of both temperature (slight in warm blooded animals) and of the average illumination level. Thus several milliseconds of the first 20 milliseconds is a variable associated with the time delay within the P/D equation. The rest is related to the compliment to Meyer's Loops found in the ganglion axons of the retina and is a variable with location within the retina. There is a clear advantage for you to be standing in a deep shadow if you are involved in a duel. Finally, the time for signals to reach area 7 from the foveola via the pretectum is considerably less than that for ex-foveola signals routed via the LGN and the striate cortex.

17.6.8 Temporal performance during saccadic eye movements

Brief discussions frequently arise in the literature concerning the operation of the eye during saccadic motions. The frequency has probably increased with the usage of stroboscopic marker lights on aircraft at night. The subject leads to a better understanding of whether the visual system employs a blanking system that prevents extraneous signals from being delivered to and processed by the stages beyond stage 1.

Brooks & Fuchs have provided good information on the visual sensitivity of subjects during saccades[135]. Merging their data with the model of this work, the need for a physical blanking mechanism appears small. It appears that any loss in sensitivity of the visual system during saccades is directly related to the integration time of the system and any smearing of the stimulus energy across portions of the retina. It can be inferred from the Brooks & Fuchs data that the cognitive centers and the saliency map do not reflect significant data acquired during saccadic motions because of the effect of these temporal and spatial bandwidth limiting mechanisms on the abstract data delivered to the saliency map.

17.7 The edge and area contrast performance of the human eye

The contrast performance of the human eye involves a wide variety of parameters and is very sensitive to the configuration of the task. It depends on the operational aspects of the task, the functional characteristics of the target stimulus, the architecture of the neural system, the performance of the physiological optics, and the topography of the retina.

In the broadest context, contrast performance is controlled by the nature of the operational task. If the subject must initially find the target in order to determine whether it was above contrast threshold, one result will be obtained. If the location of the target is known, a different threshold can be expected. If the subject must find the target, the question of whether the search routine used is cognitively directed or random is important. In a search experiment, the state of the physiological optics also plays an important role. In the absence of target cues, the optics will adopt quiescent focus and convergence condition that may make the target hard, if not impossible, to perceive without additional cues.

The form, as well as the size, of the target is quite important in contrast performance experiments. The neurological performance of the visual system varies significantly between the foveola (central 1.18° diameter), the fovea (from 1.18° to 8.68° diameter), the parafovea (out to 14.4° diameter) and the periphery or perifovea (extending to beyond 45° to 90° depending on the plane of interest. The foveola is specifically designed to perceive fine and complex details within an image. It easily differentiates between a circle, square and star as examples. However, its performance may not be optimum for less complex shapes because of its optimization. The fovea cannot achieve the detailed performance of the foveola. However, it can perform excellently on targets containing long relatively straight edges of up to several degrees in extent. It can also perform well on simple circular shapes because of the computational anatomy used in the visual cerebellum of the brain. The performance of the parafovea is much more

[135]Brooks, B. & Fuchs, A. (1975) Influence of stimulus parameters on visual sensitivity during saccadic eye movement Vision Res vol 15, pp 1389-1398

limited with respect to shape. However, by aggregating the signals from large numbers of photoreceptors in the retina, the parafovea can exhibit an enhanced contrast performance when viewing unstructured large (several degree diameter) targets. The performance of the perifovea has not been well characterized. It shares some of the capability of the parafovea in support of its Alarm mode responsibilities.

The size of the photoreceptors does not vary over the retina. All photoreceptors are nominally two microns in diameter. Since the color specific photoreceptors of the retina are organized in an interdigitated hexagonal matrix, the spatial resolution of the eye with respect to a narrow spectral range target is less than it may be for an achromatic target. When combined with the differences in neurological circuitry between the foveola and the fovea, the color contrast performance of the eye varies significantly with location in the field of view. The variations are so great, that considerable care must be taken in measuring the chromatic contrast sensitivity versus target size. This is vividly illustrated by "Maxwell's spot" (**Section 17.3.1.8**), a region corresponding to the foveola that gives very divergent contrast performance internally and when compared to the region surrounding it.

The physiological opical system is optimized to support the tasks associated with the above architectural and topographic design features. The system is highly anamorphic in order to achieve high resolution in the foveola while achieving a field of view of nearly 180° in each eye (obstructed by various facial features) at very low resolution levels.

The interpretation capability of the visual system is limited by its nominal frame interval of typically 1/30 to 1/50 second. This effective frame interval is defined more specifically as a function of illumination level by the flicker fusion characteristic (Section xxx). Because of the integrating characteristics of the eye over this interval, the stability of the target relative to the line of sight is critical. If the target moves within this interval, the detection probability will be greatly reduced. Similarly, if the intervening optical media is turbulent within this time scale, the image quality presented to the eye and the detection probability will be reduced. For complex targets, the role of eye tremor is also important. Motions of the target with respect to the line of sight, or intervening turbulence with frequency components in the range of 30 to 150 Hz will cause a loss in target detection probability (particularly at low contrasts).

Because of the above features of the system, the achievable contrast performance of the eye is frequently divided into two large classes of tasks; searching of a finite but not specifically defined area for a low contrast target, and evaluation of an edge presented by means of a bipartite field.

17.7.1 Area contrast performance under search conditions

Blackwell presented a massive, and very thorough, study of the achromatic low contrast performance of the eye under both cued and cognitively guided search conditions[136]. It was prepared as a result of military necessity during World War II and involved several million individual tests leading to excellent statistical precision.. Generally, a cue light was provided to insure correct focus and convergence at the start of the search and the subjects were told they could use either cognitively directed (a simple step wise search), random or higher cognitive search strategies to locate a target only known to be at one of eight compass positions along a three degree diameter circle.

The Blackwell study defined many critical parameters and differences in results as a function of the search profiles used. Circular targets were used. They were placed at the eight major compass points of a circle of three degrees centered on the cue light. Targets varied in size from 0.595 to 360 minutes of arc at distances of 10 to 60 feet and were illuminated for six seconds. Of particular interest was the natural transition from foveal search at high light levels to parafoveal search at lower levels. The transition occurred routinely at 7×10^{-4} foot-candles illumination. Note, Blackwell used the term brightness to represent what is now called luminance. Also of interest is the "critical visual angle" as a function of fully adapted light intensity. This characteristic defines the transition from perceiving "area" targets to point targets (such as lanterns at a distance). **Figure 17.7.1-1** shows his figure.

[136]Blackwell, H. (1946) Contrast thresholds of the human eye *J Opt Soc Am* vol 36(11), pp 624-643

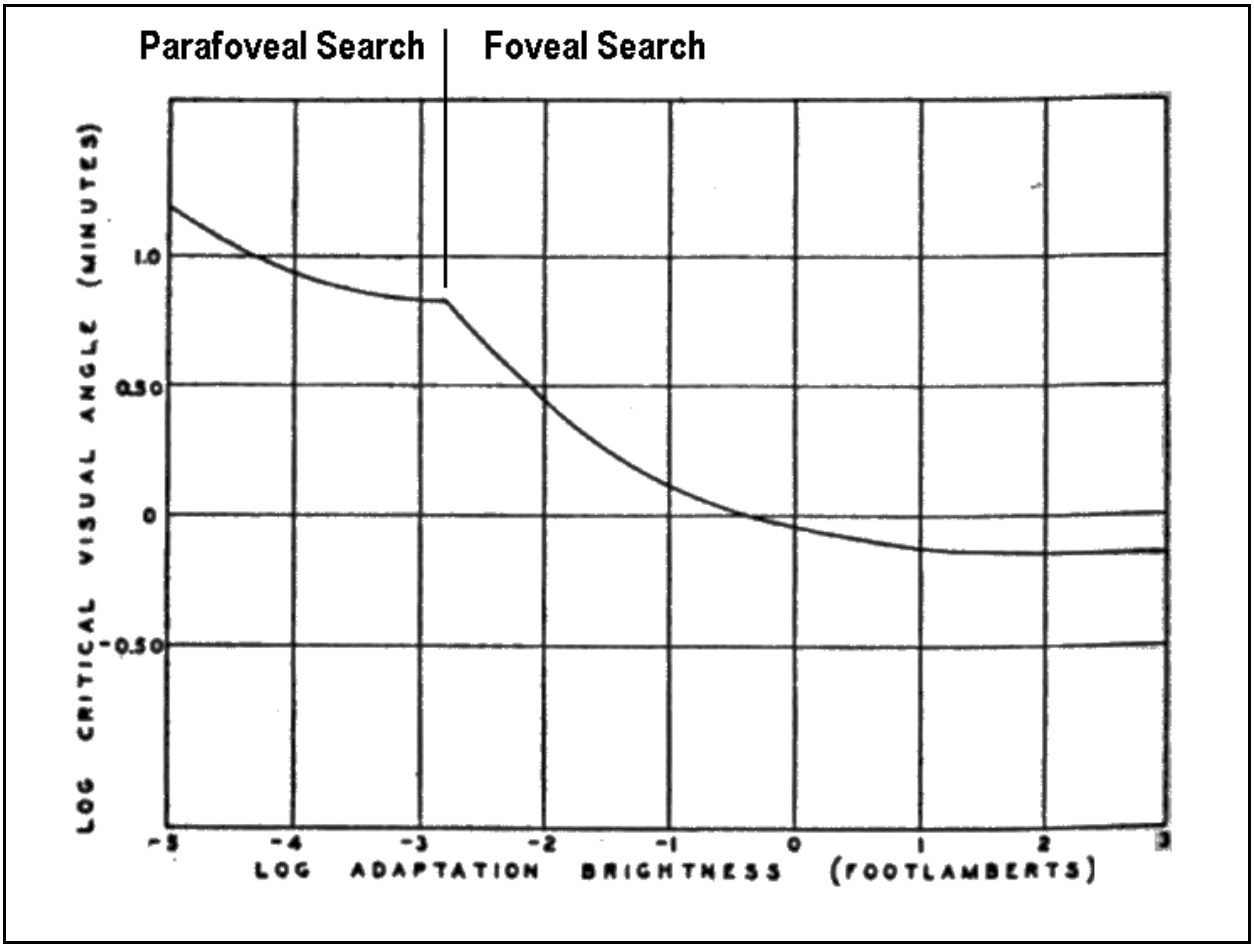

Figure 17.7.1-1 The Critical Visual Angle as a function of illuminance for the fully adapted eye. The area under the curve represents "point sources." Above the curve, the product of area times luminance is a constant. From Blackwell, 1946.

One of the young researchers in the Blackwell paper, S. Q. Duntley, went on to provide additional data on visibility under a variety of restricted conditions while operating the Visibility Laboratory of the Naval Electronics Command (San Diego) during the 1960's. Duntley provided a large number of papers identifiable via Google Scholar. The Blackwell paper also supported and motivated additional work by Farnsworth and others on the detectibility of lanterns over long distances.

In 1991, Wilson reviewed the same subject area but primarily from a users perspective[137]. He indicated "the sensitivity of the human eye as being able to detect targets differing in luminance from the background by less than 0.5%, and it can discriminate objects that differ in the locations of their features by only 5 arc seconds." These numbers were apparently chosen to impress rather than enlighten as he did not describe the hidden parameters associated with these values (example, the features have to be very long in order to for their displacement to be detected at the 5 arc second level–about one-third the diameter of a single photoreceptor and about one-sixth the amplitude of the tremor.

The text by Peli is now quite dated. It reflected the state of the art of a specific user community in that time period. While it speaks of quantitative models, the models are quite crude.

---

[137]Wilson, H. (1995) Quantitative models for pattern detection and discrimination *In* Peli, E. *ed*. Vision Models for Target Detection and Recognition. Singapore: World Scientific page 3

17.7.2 Contrast performance under bipartite observing conditions

Wyszecki & Stiles devote Chapter 5 and Sections 7.9 & 7.10 of their extensive work to various visual matching procedures and results, including area search and more complex multi-element targets, but primarily involving bipartite fields. Many of the bipartite tests involve a controlled background outside of a nominal bipartite circle. While their material lacks a coherent physical model, and does not employ the actual spectral responses of the visual chromophores, the empirical data is very extensive. Unfortunately, the analyses are based on both a linear and a trilateral interpretation of Maxwell's concept of color perception, rather than the logarithmic and rectilinear (quadrilateral) concept presented here (which is similar to a refined Hering color space). The Chapter will not be reviewed here at this time.

As noted above, Maxwell's spot introduces considerable complexity into the determination of color contrast under bipartite conditions. The relevant experiments must be very carefully designed, even to the orientation of the line separating the two test fields. The second complication is the change in neural signal processing between the foveola and the fovea. As a result, great care must be taken in extrapolating results crossing the 1.18° diameter boundary.

Because of experimental simplicity, much of the work concerning edge contrast performance is carried out in the spatial frequency domain where multiple line patterns lead to higher signal to noise ratio and therefore cleaner data reduction and cleaner results.

A major finding from bipartite experiments is that the threshold contrast depends strongly on the length, and the degree of straightness, of the line dividing the two test fields.

17.7.3 Edge effects EMPTY

17.7.3.1 Mach Bands EMPTY

17.7.3.2 Enhanced edge effects in the presence of flicker

Remole has performed a series of experiments that suggest enhancement of various edge effects in the presence of flicker[138]. His experiments included edges at eccentricities up to 1.5 degrees from the fixation point and employed three subjects.

17.8 The spatial performance of the human visual system

The spatial performance of the eyes can be considered from two initial perspectives, their ability to analyze imagery projected on the foveola and their ability to move over large angles in order to bring objects of interest to the line of visual fixation. A third perspective relates to the ability of the visual system to sum the signals from photoreceptors interrogating a finite area of the visual field in order to achieve an alternate objective such as threat detection.

The ability to move over large angles appears to be quite symmetrical except for a slight decrease in the ability to scan from bottom to top. This feature is illustrated by the practice of reading from left to right, right to left and top to bottom depending on the culture. **Chapter 19** will discuss reading in detail.

The pretectum of the POS provides a general two dimensional correlation capability that is not known to show any directional preference. This is illustrated by the nature of the characters found in writing. Some languages stress block characters with a vertical and horizontal dominance (the romance languages), others rely upon essentially circular characters (Sri Lankan) while the arabic languages are more script oriented with a dominance of wavy lines and corners.

The overall spatial performance of the animal eye will not be explored extensively in this work. The field has traditionally been divided into a clinical portion, examining the acuity of the system in everyday tasks, and a more research oriented activity to determine the spatial resolution of the system as a function of spatial frequency. The clinical activity has almost always concentrated on targets centered on the foveola. The spatial frequency work has occasionally deviated from the foveola position.

---

[138]Remole, A. (1975) Border enhancement during flicker stimulation: effect of retinal location *Vision Res* vol 15, pp 1385-1388

The performance of the POS has not previously been analyzed in detail. However, this mechanism is key to the ability of the human to recognize, interpret and perceive written communications and other fine details in works of art.

As seen in Chapter 11, the cortical portion of the visual system contains two distinctly separate signaling paths, the awareness path and the analysis path. The spatial performance of these two paths is distinctly different. The analytical path includes a two-dimensional image correlator involving some 23,000 photoreceptors. No similar processor is known to be present in the awareness path.

It is important that a more sophisticated framework be adopted to guide future effort in this area. This framework will differentiate between perception, interpretation and recognition. These terms were discussed in detail in **Chapter 15.**

This framework is significantly different from that used previously in the visual sciences. There is a large amount of empirical data available. The complexity of the neural interconnections within the signal processing area of the visual system of the eye is still far to great to allow detailed analysis. Much of the literature is inconsistent if not contradictory at the detailed level because of the many variables involved and the difficulty of understanding and controlling these variables without an available and adequate overall model. The framework provided here will support a re-evaluation of much of this material and contribute to the understanding of the spatial performance of both the human and animal eye. Such a framework must recognize that a majority of all animal species have at least trichromatic vision at the photodetection level. A very large percentage of all animals have tetrachromatic vison during at least part of their life cycle. Since much of the signal processing in the retina, involving the lateral cells, depends on inputs from multiple types of chromophoric photodetection channels, it is critical that test environments control the spectral variables carefully.

The impact of the vascular system on performance have already been discussed in **Section 17.5.2.** This effect can be represented in spatial frequency space but is not pertinent to the interpretation and recognition of signals above the CSF threshold level. This is the primary region of interest in this section. The effect due to the vascular system and perceived as Mach bands can be represented by its spatial frequency equivalent, a high frequency pre-emphasis filter. Based on the perceived width of the Mach bands, it appears the filter is of little importance in human vision. It is important to note that the spatial resolution of the eye is closely linked to both the spatial encoding of the signal projection stage as well as the spatial and temporal encoding of the signal manipulation stage. Any comprehensive technical description of the human eye must address all of its technical features and then predict and otherwise agree with the data resulting from psychophysical experiments. The following discussion will follow the top level block diagram presented in **Chapter 1** and used throughout the work.

To better understand the optical performance of the eye, it is useful to follow normal optical design and photographic practices. This entails determining the spatial resolution of the optical elements in the image projected on the Petzval surface of the system separately from the spatial resolution of the device sensing that image. Using this approach, it is possible to assign a contrast to the image (related to the scene as well as the scattering properties of the optics) as a function of spatial resolution. It is also possible to assign a function combining the spatial resolution and the threshold characteristic of the sensing device and not treat it as a mere checkerboard. When these two functions of spatial resolution and contrast are combined graphically or mathematically, it is possible to evaluate the quality of the overall optical system design. The intersection of these two functions is usually known as the “aim point” (the aerial image modulation point). In doing this, the overriding importance of the pupil as a controller of optical image quality becomes obvious. Its role as a controller of light level is seen to be trivial in comparison.

It is also clear from this model that most, if not all, animal vision involves change detection at the photoreceptor cell level. The animal eye does not perceive or preserve information at the photoreceptor level related to static scenes. It extracts change information. This information allows the brain to recreate boundaries of objects and note the change in (primarily brightness) contrast associated with that boundary. After creating a vector representation of that boundary, it assigns a single relative contrast level to the entire area within the boundary in a manner similar to a computer “paint program.” This overall methodology reduces the volume of data to be processed, and to be stored, immensely.

Change detection implies either a chromatic or luminance contrast change with time, usually brought about due to angular motion between elements of the scene and elements of the retina. To understand and properly interpret the possibilities within a given visual system, it is important to review the applicability of the Top Level Schematic of the Visual System as presented in **Figure 1.5.2-2**. Important characteristics such as whether the animals head can move relative to the remainder of the body are important. So is the question of whether the eye of the animal employs tremor, or some other method of introducing an internal source of angular motion along the line of sight.

It appears to be necessary to differentiate between two primary spatial regimes of animal vision. In the first regime, there is no significant motion within the scene relative to the optical system of the eye. The second regime is where there is intrinsic motion within the scene relative to the retina of the animal. These regimes can be explored relatively independently. They also allow the successful interpretation of eyes, such as those of the higher chordates at least, that are able to operate in a hybrid mode in order to extract useful information from both of these regimes.

As indicated in **Section 17.6.3**, much of the spatial performance of the visual system is based on the variable time delay associated with the location of the projection of the scene elements on the retina (exfovea) and on the conversion of spatial information into temporal signals via tremor (fovea). It is the processing of the time diversity information that gives rise to an apparent spatial filtering as a function of frequency. No lumped constant filter circuits with finite bandwidths have ever been defined in the visual system. It is important to note that in accordance with the underlying temporal frequency response, all plots of the spatial frequency response of the eye go to zero at zero frequency. Investigators frequently erroneously show the low frequency response as finite at zero frequency.

17.8.1 Background literature

The spatial performance of the visual system is usually reported differently in the clinic than in the research laboratory. The clinical data is usually in terms of acuity reported by the overall psychophysical system. The laboratory data is usually in terms of a modulation transfer function. Both measures are highly dependent on the illumination level which is seldom defined explicitly.

17.8.1.1 The general literature

Most of the early data relevant to the spatial frequency response of the eye has been collected using flicker techniques because of its experimental simplicity. However, these techniques necessarily involve the conversion of spatial information to temporal information and subsequent perception by the subject. Thus, the technique requires control of a great many variables if accurate and unambiguous results are to be obtained. Using these techniques, the spatial frequency resolution of the eye is often presented in terms of temporal frequency resolution units, i. e., Hz, while changing the spatial characteristics of the test targets. Flicker experiments, such as those addressed in **Section 17.6.6**, frequently introduce artifacts related to the asymmetries of the signal projection algorithms employed in stage 3.

Uttal has provide a discussion of the clinical capability of the human visual system[139].

17.8.1.2 Recent literature

Hay & Chesters have reproduced a figure from Mandelbaum & Sloan from 1947[140]. It presented visual acuity as a function of illumination. Their figure is reproduced in **Figure 17.8.1-1**. It shows a distinct shoulder near minus one log milli-lamberts. Below that level, the curve has a slope of two using the inverted scales shown. This slope is indicative of the photon noise limited region of vision and the necessity of integrating over a larger area to reach the same threshold level.

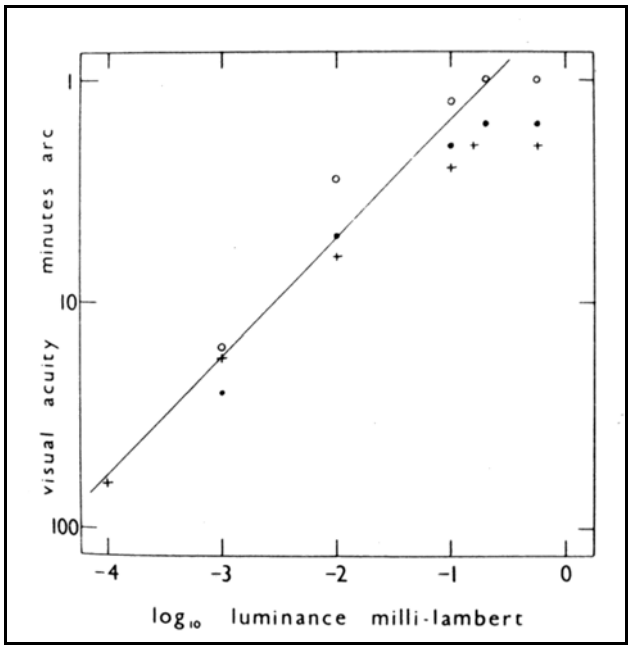

Figure 17.8.1-1 Visual acuity for unit contrast as a function of background luminance. The acuity is expressed as the threshold diameter in minutes of arc of black circular details on a light background. open circles, 0 degrees, filled circles 1 degree and plus marks 2 degrees horizontal temporal eccentricity. From Hay & Chesters, 1972.

---

[139]Uttal, W. (1981) A taxonomy of visual processes. Hillsdale, NJ: Lawrence Erlbaum Associates, pp 596-597

[140]Hay, G. & Chesters, M. (1972) Op. Cit. fg 7

Woods, Bradley & Atchison[141] have recently presented material on the contrast sensitivity function of the human eye with many references to earlier work. Although focused primarily on pathological conditions related to monocular diplopia, astigmatism among others, the approach is interesting. It does not rely upon the structure of the retina or the signal manipulation stages of the retina to evaluate the spatial performance of the lens system. It does appear to require the integration of the signal, projected as a line or series of lines on the retina, by the brain to perceive the result discussed. They were working with a cathode ray monitor with a central spectral moment of the luminance source at 605 nm. The original line on the monitor was described as 2.6 arcmin. by 93 arcmin. and was viewed through an artificial pupil of 6 mm. (diameter). The subject used a 632 nm. laser spot to designate the apparent location of each line in the perceived field of view. This technique does allow the calculation of a contrast sensitivity function, CSF, for the optical system and the authors did incorporate one of the Stiles-Crawford effects in their calculation, introducing apodization. It also provides sufficient accuracy to allow calculation of the location of nulls (or partial nulls, i. e., notches with a depth of a part of a log unit) in the contrast sensitivity function of the optics. However, the technique is limited in accuracy and the apparent approach was to assume the visual axis, passing through the center of the foveola, coincided with the optical axis of the eye. The actual optical axis is typically XXX degrees from the above visual axis. They also used a geometrical optics (Gaussian) model and employed numerical methods to perform a one dimensional Fourier (more likely Laplace, a symmetrical form of Fourier) transform on the simplified model. Such a model, and the assumption of on-axis operation, does not treat the phase error associated with the MTF of the optics appropriately. The two dimensional nature of the Airy disc calls for a two dimensional Fourier transform in the general case. The above assumptions are conventional in optometry.

Since the actual human optical system appears to be very near-diffraction limited along the optical axis of the eye (with pupil diameter less than 2 mm), a more sophisticated model would make better predictions related to diplopia, but the accuracy of the data generated by the technique may not warrant such effort. The assumption that diffraction effects were small for a 6 mm. pupil might be acceptable in a clinical environment but is not generally reasonable in a research environment (see **Section 2.4.5**). The assumption that only apodization is introduced by such a large pupil is not reasonable. The effect of the optical index gradient of the materials is a very significant factor in both the actual on-axis and off-optical-axis performance of the human optical system. The CSF data was presented on a logarithmic scale in units of cycles per degree.

[141]Woods, R. Bradley, A. & Atchison, D. (1996) Consequences of monocular diplopia for the contrast sensitivity function. Vision Res. vol. 36, no. 22, pp. 3587-3596

Mandelbaum & Sloan presented some of the best data available on acuity versus angle from the foveola, **Figure 17.8.1-2**. The figure shows how critical the light level is to achieving maximum acuity along the line of fixation.

Atchison et al. have provided very good clinical data on the acuity of the visual system as a function of illumination while carrying out other studies of apodization related to the Stiles-Crawford Effect[142]. Rynders et al. have provided clinical data on the Stiles-Crawford Effect in a well studied amblyope[143].

Curcio, et. al. have provided a summary of the off-axis acuity of the human eye when excited only by "blue" light[144].

Putnam, et. al. have provided very good data on the locus of fixation relative to the spatial features of the retina[145]. By co-collimating a large amount of equipment, including the active mirror ophthalmoscope at the University of Rochester, they were able to photograph the in-vivo retina and locate the locus of fixation to within about 1/5th of the diameter of a photoreceptor (taken as 2.5 microns). They note a systematic error in the locus of fixation relative to their determination of the center of the foveola. Their method of foveola location was a statistical one based on photoreceptor density (they speak only of cones). As seen from their imagery, the density is a very slowly changing function in this area. The calculated density peak is therefore more statistical than systemic. They also consider alternate definitions of the location of the highest performance point in the foveola, including the center of the foveal pit.

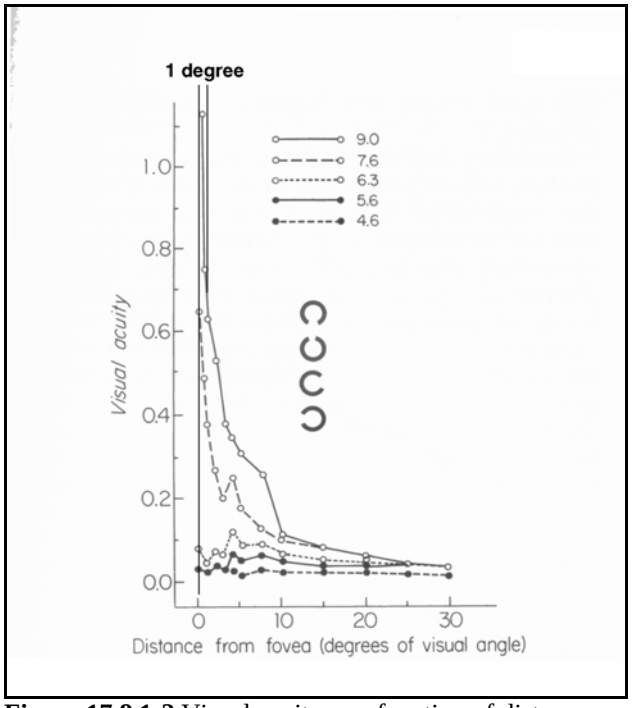

Figure 17.8.1-2 Visual acuity as a function of distance from the foveola at five stimulus intensities ranging from 4.6 to 9.0 micromicrolamberts. Visual acuity is expressed in arbitrary units on a relative scale. Modified from Mandelbaum & Sloan, 1947.

17.8.1.3 Recent collaborations– Modelfest

Beginning in the late 1990's and currently underway is a collaborative effort between a number of academic and industrial groups to quantify the spatial resolution of the HVS for what appear to be primarily engineering design purposes. The main activities of this group can be found at http://vision.arc.nasa.gov/modelfest . As of July, 2001, no theoretical or abstract models have appeared on that site in support of the efforts of the group. The website at http://4colorvision.com/files/contrastperf.htm reviews the current situation with regard to several potential models. Some early results have been presented. However, as a review of the "standardized" test procedure will show, the design of the baseline experiment is still inadequate with respect to the control of specified parameters and the recording of observed variables. This is particularly true with regard to the illumination level and the control of the spectral parameters of the illumination.

17.8.2 Technical Background

17.8.2.1 Terminology

---

[142]Atchison, D. Scott, D. Strang, N. & Artal, P. (2002) Influence of Stiles-Crawford apodization on visual acuity *J Opt Soc Am A* vol 19(6), pp 1073-1083

[143]Rynders, M. Grosvenor, T. & Enoch, J. (1995) Stability of the Stiles-Crawford function in a unilateral amblyopic subject *Opt Vis Sci* vol 72(3), pp 177-185

[144]Curcio, C. Allen, K. Sloan, K. Lerea, C. Hurley, J. Klock, I. & Milam, A. (1991) Distribution and morphology of human cone photoreceptors stained with anti-blue opsin. J. Comp. Neurol. Vol. 312, pp. 610-624, figure 12

[145]Putnam, N. Hofer, H. Doble, N. et. al. (2005) The locus of fixation and the foveal cone mosaic *J Vision (on-line)* vol 5, pp 632-639

This work requires a greater degree of precision in the terminology of spatial performance than normally found in the literature. **Figure 17.8.2-1** provides a simple summary of this material. In this figure, the diagonal lines represent the available acuity of the visual system based on geometrical optics alone. In the absence of diffraction, the acuity of just the optics would follow these two lines. The lower two curved lines represent the acuity limit due to the introduction of diffraction in the optics. This is followed by the limit established by the fact the foveola and the line of fixation are displaced from the optical axis. The predicted limiting spatial resolution at the foveal point is still several times better than that achieved under normal conditions. The nominal limit in human vision is a neurological limit due to the Precision Optical System. It is usually described as 20/20 (6/6 in metric notation) but is actually lower in a majority of the population. The peak in a distribution reflecting a large population is usually near 20/16. Note that there is no limit on the acuity of the system due to the size of the photoreceptors or their spatial density on the retina. The eye is a motion detection system, and is not pixel oriented. The major acuity limit is the capability of the correlator within the POS. At low illumination levels another limit due to signal to noise considerations. Hodos, et. al. have presented a simplified version of this figure showing their measured data based on pattern shift retinography in pigeon[146].

One diopter variation is equivalent to 330 microns (0.33 mm) in the above figure. A change from 20/20 to 20/70 involves an error of only about 0.12 diopters (40 microns). Curtin has provided several calculations relative to these scales[147]. They are in general agreement but are themselves inconsistent because of his use of a “reduced eye” and the formulas of Gaussian optics.

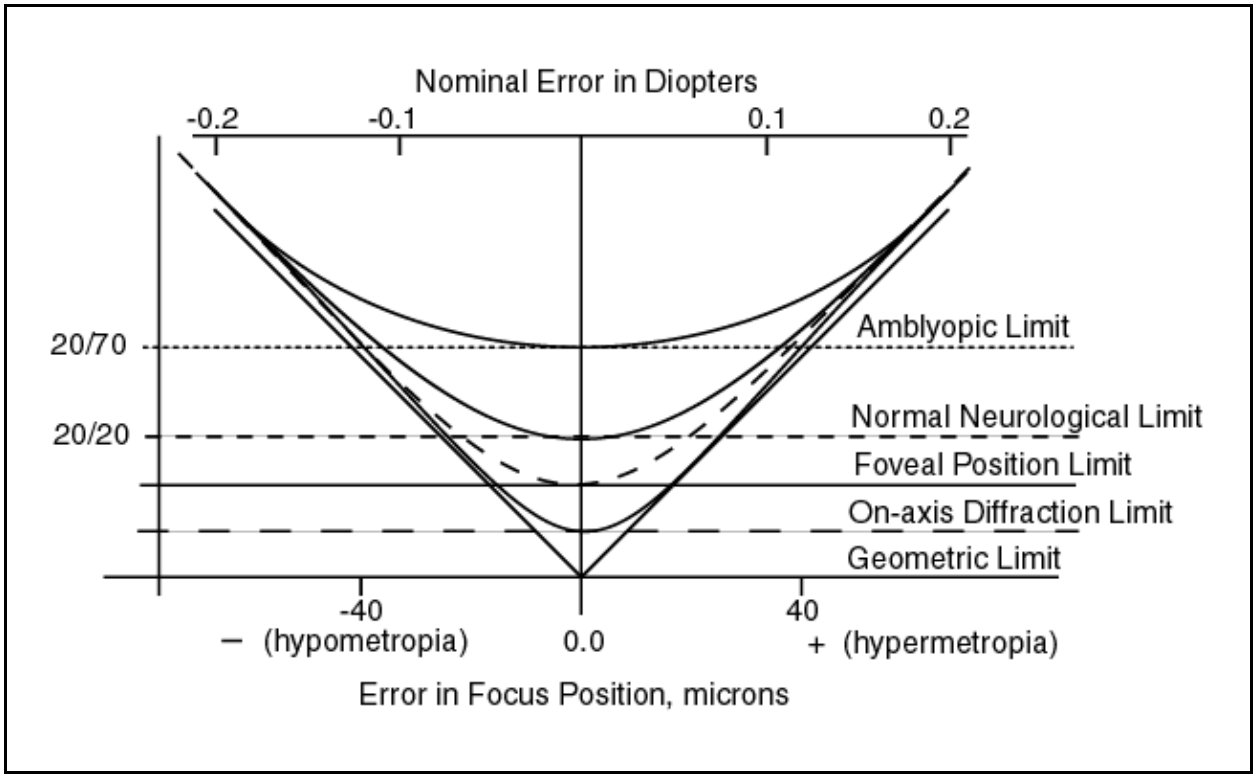

Figure 17.8.2-1 Simple acuity versus focus error diagram of vision. The straight diagonals indicate the theoretical spatial resolution of the optical system of the eye. The curved lines result from other limitations as indicated by the labels. See text.

In many ophthalmological diseases, the performance of the POS is limited in a variety of ways. These limitations

[146]Hodos, W. et. al. (1991) Normal and induced myopia in birds: Models for human vision. In Grosvenor & Flom, Op. Cit. Chapter 13, pp 235-245

[147]Curtin, B. (1985) The Myopias. NY: Harper & Row, pp 155-156

result is a series of diseases that include amblyopia, nystagmus and the broader syndrome known as achromatopsia. 20/70 is the nominal neurological acuity limit associated with these diseases.

It should be noted that these neurological limits are not related to the refraction of the eyes optics. They are described as uncorrectable in optometry since the error cannot be corrected with external appliances. The overall performance of the visual system is given by the RMS sum of the refractive and neurological limits of the system. It should be noted that the POS is most highly developed in humans. Its operation is probably shared with other higher primates (*Homonoidea*), note the way the great apes study things in detail, but it may not be shared with the lower primates (old world monkeys, etc.).

Graham has presented the data of Jones & Higgins that describes the acuity of the human eye as a function of distance from the center of the foveola[148]. It is seen that the acuity of the eye falls to 40% of nominal at the edge of the foveola, 350 μm from its center. This drop illustrates can be associated with a correlation due to the target reaching the edge, and extending out, of the field of the correlator.

As noted in **Chapter 18**, the term myopia is usually used to describe poor performance when examining fine details. This is normally accomplished at close range. Therefore, myopia has traditionally been assumed to be due to hypometropia alone. However, this condition can be equally well caused by neurological conditions not related to hypometropia.

The hypometropic eye can also perform below expectations due to neurological reasons. This work has not pursued the details but several conditions are apparent.

1. An eye that can be corrected for hypometropia with external lenses is operating outside of the dynamic range of the automatic focus circuit of the eye (in the absence of such auxiliary lens). This is the typical condition in textbooks where the image reaches focus before reaching the retina. In this case, the error in position is greater than can be accommodated by the automatic focus circuit.

2. An eye that cannot be corrected for hypometropia with external lenses can be suffering from at least two problems.

2a. The automatic focus circuit may be operating within the normal dynamic range of the automatic focus circuit. However, the circuit itself is operating improperly.

2b. The automatic focus circuit may be operating within its normal dynamic range but it may have suffered a loss in amplifier gain.

2c. There is a small possibility that the tremor signal may be operating at a higher frequency than the signal pathways between the photoreceptors and the pretectum can accommodate.

2d. There is a small possibility that the tremor signal may be operating at a lower amplitude level than required by the automatic focus circuit.

It appears that the eye adjusts for best focus by attempting to maximize the slope of the signal associated with a contrast edge in object space near the line of fixation. This circuit is associated with the POS found in the midbrain. If the circuit performing this function has an inappropriate offset bias associated with the output signal, this circuit will cause the eye to continually focus the image either in front of or behind the ideal location (regardless of auxiliary lenses). On the other hand, if the circuit has suffered a gain loss, It may not be able to drive the lens to the point of optimum perceived focus. The neurological limit shown in the above figure will move closer to the nominal amblyopic performance curve.

17.8.2.1.1 Performance criteria

Investigators have employed a variety of test stimuli to determine the performance levels (generally described as the acuity) of the visual system in the spatial domain. These configurations can be categorized and summarized in **Figure 17.8.2-2**. Each of the stimuli shown result in a different performance level, regardless of the test design. A most critical parameter in virtually every case is the aspect ratio. Extending the length of a line(s) invariably raises its acuity.

---

[148]Graham, C. et. al. (1965) Vision and Visual Perception. NY: John Wiley & Sons pg 329

Other than the recognition symbols, each stimulus can be described precisely using simple mathematics.

1. In the detection class, the left-most stimulus is the integral of the line stimulus in the middle.

2. In the recognition class, it is important to note the difference between the block B and the B with serifs. The difference in these type faces results in different performance levels.

3. As noted above, the aspect ratio between patterns of the same spatial frequency result in different performance levels. In the case of the right-most stimulus, the figure is frequently "windowed" by a Gaussian waveform, in either one or two dimensions, in an attempt to simplify the mathematical description of the stimulus. The resulting stimuli are called "Gabor Patches." The effect is merely to change the mathematical description of the stimulus.

4. Vernier tests, particularly when long lines are involved, frequently result in the highest performance level for a given test design.

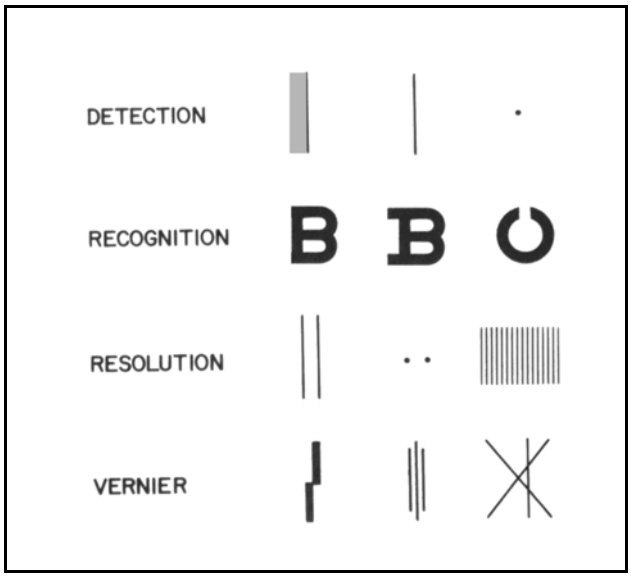

Figure 17.8.2-2 Test stimuli used in spatial performance evaluation experiments.

It is important to consider both the aspect ratio and the absolute size of the stimulus in human vision experiments because of the organization of the visual system into sectors. Results will vary with eccentricity. They will also vary when the stimulus is applied across a boundary between the foveola and the fovea or the fovea and the peripheral retina. To a lesser degree, the results will vary with orientation relative to the major axes of the visual system.

17.8.2.2 Performance of the physiological optics

The general capabilities of the physiological optics of man were discussed in **Section 2.4**. The dynamic performance of the optics is summarized in **Figure 17.8.2-3**. The typical human has a minimum point of adequate focus extending down to about 7 cm at an early age. This range gradually increases until it is typically 200 cm at 60 years of age . When expressed in diopters, this accommodation range extends from 68 to 54 diopters in young eyes to about 58 to 54 in young adult eyes. At 60, the range is typically less than one diopter. If the available range does not include the diopter value required to achieve focus on the retina, auxiliary optics will be needed for at least some distance intervals in object space. In the case of the author, this occurred at about age 48. At 68, he now required about +2 diopters of correction at both short (30 cm) and long distances. [As a result of the formation of a cataract in one eye at age 70, the lens of the right eye was replaced. He now has uncorrected vision of 20/20 in the right eye at distance but requires correction at short distances.]

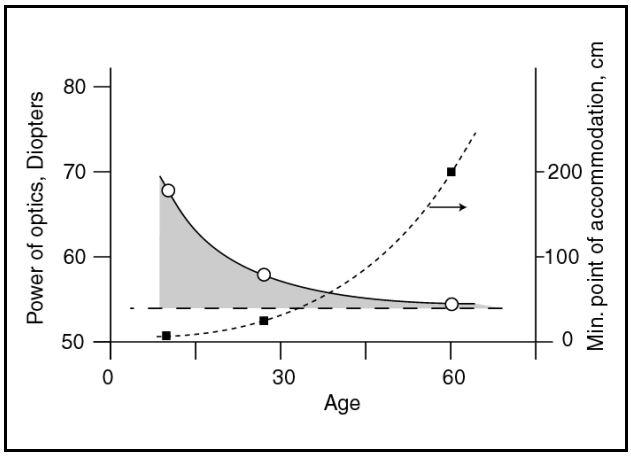

Figure 17.8.2-3 Near point of human optical system versus age and available variation in optical power. The dashed line is the power of the un-accommodated standard eye. The shading shows the range of accommodation versus age. The dotted line shows the typical near point of accommodation versus age.

17.8.2.2.1 Clinical explanations for myopia and hyperopia

The above information provides some background for discussing the clinical conditions of myopia and hyperopia (colloquially near-sightedness and far-sightedness).

The generally accepted cause of this loss in refractory performance with age involves the loss of elasticity in the "lens." Subsequently, the ciliary muscle (the sphincter muscle surrounding the lens) is no longer able to cause the necessary change in the shape of the lens.

The root cause of a failure to achieve focus automatically without auxiliary optics is interesting. The colloquial explanation is that the eyeball is mis-formed and results in an inability of the lens to focus the image properly. In the case of a young child, this appears unlikely to be the entire story. To be completely outside of the range of accommodation of such a child, the eyeball would need to be at least 4.2 mm larger in diameter along the optical axis than nominal. This is a nearly 20% enlargement. Other factors must be examined to account for this problem. Such an error could result in significant impact on the rotation of the ocular in its socket.

The goal of the physiological optical system is to maintain focus at the retina while significantly varying the optical power of the optical system. To accomplish this, it is necessary that the focal length of the system precisely equal the distance between the exit aperture of the system and the retina. There are a large number of factors that impact this equality. These factors are not easily separated because the system not only includes two separated lenses but these lenses are thick lenses. The rules applicable to a single thin lens are inadequate.

The literature reports that the lens moves laterally along the optical axis as it changes optical power. Both the absolute location and the relative location (with changes in power) of this lens play significant roles in the focus of the eye. They affect the location of the exit aperture and the focal length of the overall system (even in the absence of any change in power). These locations are difficult to measure externally. They can be determined by measuring the locations of the Purkinje reflections. A change in position of 300 microns relative to the cornea would cause a change in power of 0.1 diopters. However, a change in position of only 300 microns relative to the retina would also introduce a change in –0.1 diopters if the exit aperture location varied with it. The effects tend to cancel.

The cornea is the major physiological optical element. Whether it is a true meniscus lens or a plano-convex lens is not clear from the vision literature. The curvature of the first surface is about 7.6 mm. A 20% error in this dimension would be virtually unnoticeable and would not impact the rotation of the ocular globe in its socket. A change in the thickness of this lens would also be difficult to note except through careful measurement. In the case of an older person, only a marginal error in cornea radius of curvature could cause significant near- or far-sightedness. Such an error would not be correctable by the accommodation range of the "lens." It is the correction of this error that is the goal of surgery known as radial keratotomy.

17.8.2.3 Visual systems without angular motion in the scene

This regime includes two sub-regimes. In the first case, there is no motion within the overall scene but the scene *in toto* has an angular motion with respect to the eye of the animal (**Section 17.8.2.2**). In the second case (Section **17.8.2.1.1 & 2**), there is motion of elements of the scene relative to the line of sight but minimal or no motion of the overall scene. Animals have evolved who can exploit both of these sub-regimes. The first sub-regime appears to be most extensively exploited by flying insects for purposes of navigation, but it is used by all mobile animals including man.

The second regime accommodates motion of individual elements within the overall scene. This motion represents an angular motion relative to the visual system. This sub-regime is exploited effectively by many passive feeders, such as frogs. These animals remain passive for an extended period until something in their static field of vision moves. The sub-regime is also used as a fundamental alarm mechanism in nearly all animals.

Surveying the references listed below, it appears that the lowering of the illumination level causes many spatially oriented animal mechanisms to become less useful for the same reason that similar chromatically oriented animal mechanisms become less useful. At low illumination levels, the temporal response of the photodetection process is reduced and the chromatic signal levels in the P and Q channels approach zero.

17.8.2.3.1 No spatial change within the overall scene

Srinivasan, et. al. have provided a minireview of the data base related to insect orientation and navigation.[149] It provides extensive references and summarizes the significant empirical information available. However, it only

[149]Srinivasan, M. Poteser, M. & Kral, K. (1999) Motion detection in insect orientation and navigation Vision Res. pp. 2749-2766

includes conceptual, and floating, models of the mechanism involved. The presentation is couched in the language of gratings but clearly indicates it is the detection of a contrast transition, the edge, that is of primary importance. It does allude to the more probable use of summation algorithms than multiplicative algorithms. One of the most significant conclusions is that the temporal passband of the spatially oriented signal processing is similar to or identical to that found in the chordate, and particularly the human, eye. The paper explores a number of different operating regimes of the insect. These included:

+ the relatively slow yaw response, known as the optomotor response, resulting from a change in rate of scene angular motion during flight (presented to both eyes)

+ the centering response, a similar response during flight wherein the two eyes are presented with rates of scene angular motion that are in the opposite direction

+ the movement avoidance response, a tendency of bees to avoid flying toward rapidly moving objects.

Although neither the temperature of the animal or the light level was specified, a number of significant psychophysical test results were presented. The temporal range of the optomotor response was given as peaking in the 25-50 Hertz range and dropping to zero at 100 Hertz. The performance of the centering response however was still substantial at 100 Hertz. The movement avoidance response involved frequencies in the 50-200 Hertz range.

Some electrophysical test results were also given relative to “the so-called large monopolar cells of the insect lamina--the second stage of visual processing in the insect visual pathway.” The amplitude response of these cells to a moving contrast edge was reported to increase monotonically with edge speed over a range of 0-1000 degrees/second. A frequency range of 1-30 Hertz was reported in response to sinusoidal stimulation. It was noted that these responses were not entirely independent of the contrast of the edge used. The role of the adaptation amplifiers, if present, could not be determined from a reading of this paper.

It is interesting to note that many of the dynamic concepts alluded to in the above paper have been studied intensely in military bombing systems. In fact, they formed the basis of and were widely implemented in much of the hardware used for angle-rate bombing and image motion compensation (as used in aerial reconnaissance) prior to the 1970's.

17.8.2.3.2 Spatial change only within regions of the overall scene

One of the most powerful features of the visual system is its ability to detect small changes in the field of view of the animal. It is a major feature of the change detection mode of operation of the photoreceptors. Whereas a photoreceptor might require a 10-20 percent change in its total integrated photon flux within its pixel diameter and a finite integration interval to report a change based on its operation as an integrator, it is able to report a much smaller change as a change detector. In an integrator, the output signal would only occur at the end of the integration interval. In a change detector, this change is related directly to the **edge** of its photon-flux collection area and it can be reported at any time. Note that the reported change is fundamentally a change as a function of time and not spatial position.

As a result of the photoreceptors acting as change detectors in time and indirectly as edge detectors in space, the spatial performance of the eye is not directly related to the size of the pixels formed by the photoreceptor cells. The spatial performance of the eye is more directly related to the length of straight edges in object space and the threshold level of the signal processing system. It is this length of a straight edge that plays a dominant role in the criteria factor discussed in **Section 17.6.3.3**. Since the perception function involves a temporal correlation between a large number of signals from the foveola, the criteria is actually based on a more complex relationship than just the length of a single straight edge. The use of a tri-bar pattern in a standard Air Force 1951 resolution target recognizes this fact.

The change in luminance intensity resulting from local motion within a scene is a major driver for the **alarm mode** of operation of the visual system. Following the correlation in the LGN of the signals passed from the ex-foveola of the retina, the information extracted from the signals is routed directly to the response system in simpler animals or to the pretectum for further analysis before a response in the higher animals.

The classic example of the operation of the alarm mode of signal processing in animal vision is that associated with the frog. Normally, this animal can sit fixed in space for long period and observe its field of view without the benefit of tremor. It relies entirely on the relative motion of objects within local areas of its field of view. Based on the temporal changes in brightness caused by this motion, the frog initially computes the trajectory of the moving

object and then identifies the object. Based on this data, it determines whether to make a predatory response. This is the same methodology as used by all intercontinental missile detection systems. A military system was demonstrated during the 1970's that incorporated the same methodology as that of the frog visual system.

17.8.2.4 Visual systems with angular motion involving large fractions of the scene

The **awareness mode** of the visual system is able to accommodate the continuous motion of the entire field of view up to an angular velocity that results in loss of sensitivity due to the limited high frequency capability of the electrical signaling channels. However, the **analytical mode** associated with the foveola is much more limited because of the time required to scan the image projected onto the foveola. This time is usually described in terms of the fixation interval but more appropriately labeled the gaze interval since fixation does not occur at the minor saccades level.

As a result of these differences, the system is able to track a moving field in object space in what is described as a pursuit mode that can be relatively continuous. However, if the animal is to perceive and recognize objects within the field, the eyes must track the field using a look-ahead and pause series of major saccadic movements.

17.8.2.5 Hybrid systems

In this work, an attempt has been made to separate both the signal processing activity generally found in the retina from the perceptual processing occurring within the brain and the signal processing associated with the foveola and the ex-foveola portions of the retina. This differentiation has led to a clearer understanding of the two distinct signal paths leading to the cortex of the brain. The LGN path is obviously associated with the majority of the retina (the ex-foveola) and the wide visual field of the eye. The pretectum path is more closely related to the foveola area of the retina and is primarily concerned with detailed two dimensional analyses and perception of fine detail.

There is a large amount of literature reporting on psychophysical experiments concerning the spatial performance of the human eye. Unfortunately, most of this work has involved so many variables, controlled and uncontrolled, as to make analysis of the data nearly impossible. Most “surround” experiments have employed simultaneous changes in the luminance and chrominance channels as well as in the appearance channel(s). Even when attempting to work with only black and white images, these experiments have usually used illumination sources that have selectively excited more than one chrominance channel. Since these channels incorporate differencing circuits, the results have usually been corrupted by the introduction of uncontrolled chromatic information.

These exploratory psychophysical experiments have almost always ignored the presence of tremor.

Chapter 13-Secondary Signal Processing has explored two possible levels of spatial signal processing that are easily accomplished within the signal processing region of the retina. These modes include:

1. Simple differencing between the signals from adjacent photoreceptor cells but with the addition of a time delay in one channel. This is a very powerful method of detecting changes in a scene. If the location of these changes are collected in a “file,” it is very easy to calculate a trajectory of the feature moving in object space.

The presence of tremor in the above differencing must be accounted for. It may provide an additional, desirable or undesirable, dimension. If tremor is present, the differencing process will generate signals that are correlated in time with the tremor signals. If tremor is not present, the processing is less complex.

It appears that only the higher chordates and a few molluscs employ tremor. It also appears that in the highest level chordates, tremor is controlled by the autonomic nervous system and is not subject to the will of the individual. In some cases, this may be an unfortunate result of evolution. It complicates the stalking and capture of prey. It appears that the cat family can control the tremor function. It is almost a certainty that the frog family can control the tremor function. The ability of the frog to dispense with tremor makes it a very efficient tracker of prey. However, it makes the animal vulnerable to small boys with “frog sticks.”

2. Correlation of the signals from certain patterns projected onto the retina, particularly parallel lines of a given range of spacing and a given orientation. Such patterns appear to be sensed in the signal processing within the retina of the cat family. What is known about this sensitivity has been visualized in a videotape[150]. The implication is given that much of the additional appearance capability is used to sense irrelevant information, such as the presence

[150]"A Cat’s World” One hour videotape available from the History Channel Tel: 1-800-708-1776

of tall grass in the savanna, and discard it. This feature of the cat family visual system may provide an explanation for the stripped pattern of zebra.

17.8.3 Physiology and electrophysiology of the human eye

The only elements of the visual system that operate purely in the spatial domain are those of the physiological optics that create an image on the retina. While the majority of the photoreceptor cells of the retina exhibit an obvious spatial distribution related to the scene, their primary role in stage 1 is to convert the spatially oriented image into electrical signals that are temporal in nature. As a result, although the pedicles of the photoreceptor cells maintain a quasi-spatial relationship to the image (except for those of the foveola which are displaced to the edge of the foveola) **all signal processing subsequent to the pedicles is entirely in the temporal domain.** The relatively slow transmission speed of electrical signals within the retina contribute to and accentuate the temporal differences associated with the initial signal processing within stage 2.

> It is important to note that, contrary to frequent discussions in the psychophysical literature, there are no spatial frequency filters within the visual system. Whatever filtering is accomplished is performed within the temporal domain. Even the spatially related signal processing within the 2nd lateral processing matrix of the retina of some chordates is performed based on time delay differences rather than true spatial position.

Chapter 15 has presented detailed discussion of the electrophysiological and morphological structures of the visual system. **Section 17.6.3** of this chapter has explored the spatial performance of the system based on the underlying temporal signal processing mechanisms.

The mechanism of conversion of spatial signals to temporal signals takes two forms as discussed above. In the majority of animals (especially those without a functional foveola) the primary mechanism of conversion of spatial information to temporal information involves local motion within the field of view of the animal relative to the fixed orientation of the eyes. This is particularly true of the arthropods and most molluscs where the eyes are rigidly mounted relative to the body. In some of the higher molluscs and many chordates, the flexibility of the head contributes to the spatial to temporal signal conversion. A feature of the chordate family is the ability of the eyes to move independent of even the head (at least to the marginal extent required to introduce tremor). The addition of a continuous tremor between the animals line of sight and object space is what converts the visual system from a change detection system to an imaging system.

The tremor is believed to be a two-dimensional involuntary motion of the eyes. It is controlled by the pretectum as part of the Precision Optical System, POS, found in the midbrain. The phase relationship between the two orthogonal components of tremor are currently unknown.

The numerically large array of photoreceptors of the foveola, and their individual neurons connecting them to the pretectum, are the primary elements associated with the POS in the operation of the **analytical mode** of vision that is so critical to the visual acuity of the human species. It is the temporal relationship between the signals received at the pretectum from the array of photoreceptors in the foveola that are perceived by the pretectum and then interpreted and recognized within the cortex. Subsequent to the receipt of the signals at the pretectum, the information is converted into vectorial form that exhibits no physical or graphical relationship to object space. It is this information in vectorial form that is incorporated into the saliency map maintained in the mind of the subject (human or otherwise).

While selected signals from the ex-foveola maintain a spatial relationship to object space as they pass to the LGN and then to area 17 of the cortex, this relationship is preserved to support functions such as stereopsis and not perception and cognition. The major role of signals passed along this **awareness path** is to maintain awareness of the full field of view after identification of the individual elements of the scene by the mechanisms of the **analytical path**.

The distinction between these two paths is well documented and clinically recognized in cases of blindsight and macular (foveola) sparing. See **Chapter 18**.

17.8.4 Spatial performance of the higher processing centers of the human visual system

The spatial performance related to the higher processing centers of the visual system is much more interesting than the temporal performance. This is primarily because it is so much more complex. To place this performance in

context, it is important to make three clear distinctions.

+ The first is to differentiate between the different signal paths of the visual system, such as the **awareness path** and the **analytical path**, as done in Section 15.2.4.

+ The second is to recognize that the nominal spatial performance is actually performed in the temporal domain and primarily within the **analytical path** of the visual system.

+ The third is to differentiate between the perception, interpretation and recognition of patterns imaged on the foveola. These functions occur at different locations within the **analytical path**.

For purposes of first order discussion, perception occurs within the prectectum of the midbrain, interpretation also occurs within the pretectum with frequent help from the cerebellum, and recognition is primarily a function of area 7 and associated engines of the parietal lobe of the cortex. More advanced analyses, defined here as involving cognition, occur primarily in the frontal lobe of the cortex.

Using the above baseline, it can be said that interpretation and cognition do not occur at signal levels near the threshold associated with the contrast spatial frequency(CSF) function. The signal level must exceed this level for perception to occur within the pretectum. Once perception has occurred, the pretectum attempts to perform a temporal correlation on all of the signals received from the photoreceptor cells of the foveola. This is a process of interpretation at the individual scene element level. These correlations are generally performed in a time sequence covering up to 300-500 milliseconds for each area of significant interest in the field of view. The priority for interpreting these individual areas is subject to override by the alarm signal path. The pretectum may call on the cerebellum to analyze more unusual or unfamiliar signal vector derived from individual scene elements before completing its interpretation.

The degree of temporal correlation between the 23,000 signals derived from the foveola is poorly understood. Initial results relative to abstract and simple structure natural forms are discussed in **Chapter 7**.

It is the series of interpretations developed by the pretectum (at supra-threshold signal levels) that are forwarded to area 7 of the cortex via the Pulvinar Pathway for further correlation defined here as recognition. This higher level process may involve a large number of feature extraction engines as discussed in **Section 15.2.3**.

> The fact that these processes do not involve the striate cortex is significant. It has been demonstrated that these **analysis path** signals arrive at area 7 prior to the arrival of **awareness path** signals via the striate cortex[151].

While it may be of practical interest to quantify the performance of the HVS with respect to the spatial performance of the foveola, in order to meet certain application oriented needs, it is clear from the work in **Chapter 15** and **Section 17.6.3** that the spatial performance is actually a function of the temporal performance of the signal processing system and the intensity of the illumination. The initial perceptual performance in stage 2 is a function of the signal contrast in the P– , Q– and R–channels of vision, the threshold level of the circuits within the stage and the threshold criteria. Other than a minor role because of its asymmetry, stage 3 plays no role in th spatial performance of vision. Within stage 4, the performance is not directly related to the absolute spatial aspects of the imagery (and therefore the spatial resolution). In this stage, it is the correlated properties of the image impressed on the foveola (and filtered by stage 2) that are of greatest importance.

The spatial performance of the **analytical path** associated with the foveola far surpasses the spatial performance of the **awareness path** and **alarm path** associated with the ex-foveola. Because of the great mobility of the human eye, the study of its spatial resolution has been limited primarily to the on-axis or near on-axis condition associated with the foveola. This is the condition of concern to lay people and their optometrists.

17.8.4.1 Background

The visual systems in animals employ significantly different techniques and processes in accomplishing their multiple roles of threat alarm, predation and precision evaluation. In evolved (and hopefully civilized) man, the predation role is no longer important. It has been replaced to a great degree by technological skill beginning with the club, bow and arrow, etc. However, the alarm and evaluation roles remain very critical to the viability of the animal.

---

[151] Results of VEP experiments of XXX. in section xxx

The spatial resolution of the visual system is highly tailored to satisfy these two requirements, both in the optics and in the sensory mechanism. Both of these subsystems exhibit specific adaptations associated with each of these roles. To achieve the wide field of view required while accepting the highly curved Petzval surface necessary to achieve large angular agility of the overall visual system, the optical system has incorporated techniques man has only recently demonstrated in very sophisticated system (by his standards). The techniques employed in the eye include a design based on elliptical surfaces (not spherical) and materials exhibiting a gradient in their index of refraction. There are actually two gradients; a gradient as a function of radius from the centerline and a gradient with respect to position along the optical axis. Using these techniques, the optical system is able to maintain an adequate image on an extremely curved Petzval surface. The optical system of the eye can be related to the common integrating sphere of radiometry. In this case, the ocular globe is essentially spherical and the lens system is located at a small aperture in the globe. The lens system forms an image on more than one half of the total surface of the globe. To do this, it must exhibit a focal length that changes drastically with field angle. Furthermore, it must form an image at locations within the sphere forward of the back nodal point defined by Gaussian optics. A key feature in accomplishing this feat is the fact the optical system is of the immersed type. The outer surface is in a medium (air)of drastically different optical index than that of the inner surface (the vitreous humor) of the optics.

Most articles in the biological literature describe the great variation in the size of the photoreceptors of the retina as accounting for the significant differences in spatial resolution of the eye as a function of field angle. As seen in **Section 3.2.1**, this is simply not the case. The photoreceptors in a given species seldom vary by even a factor of two in either diameter or lattice spacing within the mosaic. The controlling feature in the spatial resolution of the human eye is the necessity of achieving the highly curved Petzval surface while maintaining the best possible resolution near the point of fixation. This compromise is achieved using the sophisticated techniques mentioned above. The spatial resolution of the resulting optical system falls off very rapidly with field angle. This fall off is much more rapid than the equivalent variation in the photoreceptor mosaic, no matter what assumptions are made about the structure of that array required to achieve the desired chromatic performance.

A primary thesis of this work is that there are no achromatic photoreceptors in animal vision. Therefore, the chromatic performance of the photoreceptors within the foveola must be addressed from the perspective of spatial resolution. How these photoreceptors are combined in the signal manipulation and signal projection stages, noting that it may be done differently relative to within and outside the foveola, also becomes an important question. These questions will be addressed below.

Based on personal experience and analysis of the literature, it appears that the perceived spatial frequency performance of the visual system relies upon the luminance channel. Although this channel accepts information from the S- and M-channels, it is dominated by the spectral performance of the M-channel. The perception resulting from the luminance channel alone is achromatic.

The arrival of the personal computer age has made many more aware of the problem of perceiving written words presented as blue characters on a red background, or worse, red characters on a blue background. Red characters on a blue background are all but invisible to a human, particularly if the luminance component of the two fields are made equal, e. g., the precision spatial information associated with the foveola is carried primarily by the luminance channel.

Because of the logarithmic nature of the signaling path in vision, the contrast performance (including the spatial resolution performance) is highly nonlinear in the large signal case. It can only be approximated using linear calculations in the small signal case.

There are a variety of techniques for evaluating the spatial frequency performance of the visual system. Some are more suited to evaluating specific components of the system than others.

17.8.4.2 Contrast performance (spatial resolution) of the optical system

Conventional wisdom has nearly always discussed the optics of the eye based on the Gaussian approximation. This is a very poor assumption. It has led to the inevitable conception by most people that the eye employs a fixed focal length lens system. Because of this conception, it is assumed that the optics can be discussed using nodal ray tracing. The optics of the eye are much more sophisticated than generally documented. The many facets of the Stiles-Crawford Effects are examples of this (see **Section 17.3.7**). In a research oriented analysis, the Gaussian approximation, also known as the thin lens approximation, *cannot be used*. It only applies to field angles of less than one degree, an angle smaller than that represented by the fovea. Not only are the individual lenses of the eye thick lenses, the system consists of two separated thick lenses with an adjustable pupil between them. As noted earlier, the complete optical system of the eye consists of the above two separated lenses (the cornea and the “lens”), the

pupil between them, the field lens consisting primarily of the neural tissue, including its blood supply, which are interposed between the lenses and the Outer Segments of the retina and the fluids found within the eye. The field lens, at least at the histological level, is not significant in humans. To the extent that the ellipsoids within the Inner Segments of the photoreceptors act as a large lenticular array in front of the Outer Segments, the field lens appears to play a major role in increasing the efficiency of light collection by the photoreceptors. This is extremely important in the human eye since the Outer Segments have a length that is far longer than is acceptable within the depth of focus of the optical system. Treating any light not captured by a photoreceptor as merely stray light not only reduces the sensitivity of the system, it reduces the effective contrast of the actual scene since much of the unabsorbed light would be absorbed by adjacent photoreceptors.

The performance of the physical optical system of the human eye, including its off-axis performance, has not been characterized to the level required to accommodate the current level of research. The best current estimates of the parameters of the eye are collected within the Standardized Human Eye of this work. Most studies have concluded that the limiting resolution of the entire visual system is near 30 cycles per degree in object space. Templates have been developed based on this deduction.

17.8.4.3 Spatial resolution of the sensing surface

The sensing surface of the human retina can be described as a fully populated array of nearly constant diameter cylindrical sensors in a closely packed array. The array appears to be described by the conventional notation of a hexagonal array, i. e., six sensors surrounding a central sensor. The lattice constants of the array are not precisely constant with position on the retina but the differences probably do not affect the spatial frequency response of the array. Since the eye was not designed as an imaging device, developing the criteria for determining its spatial resolution is difficult. The principle question is what elements of the array participate in determining the spatial resolution? Is it only the sensors of one spectral classification? Is it groups of sensors that sum their signals to form the luminance channel signal? Is it all of the sensors operating independently but participating in a sensory array? This work has not uncovered an answer to these questions. Therefore, it does not offer a theoretical description of the spatial resolution of the overall sensing surface.

17.8.4.3.1 Spatial resolution of the foveola

The sensors within the foveola enjoy a special status. They have individual signaling channels that connect directly to the Pretectum and are operated within the dynamics of the auxiliary optical system and musculature of the eye. It is reasonable to assume that all of these sensory elements are employed in determining the spatial resolution of the foveola. Based on this assumption, the spatial resolution can be calculated in two dimensions based on the lattice factors of a hexagonal array. The result can be displayed in a two dimensional drawing similar to those of XXX **[nice two dimensional plots, not in Woods, Bradley & Atchison.]**

17.8.4.4 Spatial resolution of the signal manipulation stage

Here again, the impact on the spatial resolution of the imagery falling outside of the foveola is not well defined. For the imagery falling on the foveola, the situation is different. The situation must be analyzed for each operating mode of the visual system. The most important mode is that of XXX **[perception of detail, what term did I introduce for this?]** During this mode, the image falling on the foveola is encoded by the minute physical motion of the retina relative to the line of fixation known as tremor. The information is encoded on a carrier frequency related to the fundamental frequency of the tremor. This places most of the signal information in the temporal frequency band from 30 Hz up to about 100 Hz, but possibly 150 Hz. In general, the circuits of the signal manipulation stage do not act as a constraint on the bandwidth of these data streams.

17.8.4.5 Impact of the signal projection stage on spatial resolution

The action potentials of the signal projection stage are designed to support temporal data streams up to at least 100 Hz and probably to 150 Hz maximum. Therefore, they are not a significant limitation in the Nyquist sense. However, the recovery of signals near the upper end of the signaling band may be degraded if inadequate decoding techniques are used. Little is known about the methods of decoding employed in the cortex at this time, particularly of the information transmitted from the foveola to the Pretectum on a subcarrier created by the tremor.

17.8.4.6 Perceived contrast in the periphery

Cannon has performed a series of experiments showing the contrast performance of the human visual system out to 40 degrees eccentricity[152]. Sine-wave gratings were presented on a monochromatic monitor and the data was presented with range bars. The results track the perceived threshold performance of the visual system as a function of stimulus intensity (which was developed largely on high contrast performance measurements). See **Section xxx**. They also support a slope (gamma) of 0.4 to 0.52 for the perceptual sensitivity function within the photopic regime. The results strongly support a concept of contrast constancy similar to that of color constancy. Such contrast constancy suggests the photoreceptors contributing to the dominant signal processing channel are adapting in unison. The photoreceptors were most likely the M–channel photoreceptors contributing to the R-channel signal.

17.8.5 Velocity performance of the eye EMPTY

[xxx See chapter 13 of Kulikowski, vision & visual dysfunction vol. 5

17.8.6 Spatial summation versus instantaneous visual field angle

It has long been recognized that the resolution of the visual system decreases drastically with field angle from the point of fixation. Along with this phenomenon is an apparent spatial integration of signal. Ricco studied this question in the 1870's as noted by Brindley[153]. Like most of the laws first formulated in the 19th Century, they have not proved sufficiently precise for modern purposes. Because of the initial appearance of simplicity, a great many studies have been performed attempting to rationalize the apparent areal summation processes found in vision. As a result, there has arisen a large volume of frequently conflicting empirical data. Looking at this data, it is clear that Ricco's "Law" must be restated to separate the mechanisms associated with the foveola, the fovea and the peripheral retina. In addition, the effect of the physiological optics and the adaptation mechanism must be considered. Many of these studies involved less than a statistically relevant number of subjects. It is also clear that the variation in the shape of the foveola and fovea varies significantly among individuals. The highly asymmetrical shape of one's own foveola is easily observed by the after-image formed at mesotopic light levels following a sudden bright flash of light involving a large part of the retina. As a result of these conditions, any study involving less than a statistically relevant number of subjects (probably near 50) is open to criticism.

To understand the role of channel summation in vision, it is important to appreciate the physiology of the system. In the human, multiple signaling channels are found that serve different purposes simultaneously. Some of these purposes can be associated with specific operating modes. The major signaling channels associated with a specific operating mode frequently use different computational anatomy to achieve different optimizations. The use of computational anatomy may occur serially as well as in parallel. [xxx develop further or reference **Section 15.xxx**].

17.8.6.1 Background

Hallett, Marriott & Rodger (1962, using one of two subjects) explored spatial summation in 1962 with very unusual results[154]. They used an array of point sources centered on 20° nasal eccentricity and a vertical range of +/– 3° but also made some experiments along the horizontal meridian.. The background was nominally zero and the source was an under excited automobile headlight. No color temperature of the source was provided. The data is presented in terms of the number of quanta required for detection at threshold. However, no discussion of how the number of quanta was determined was provided. The number of quanta required rose very steeply for a 10 arc minute source at low eccentricity angles (down to two degrees). The threshold rose by an order of magnitude for the eccentricity decreasing from 8° to 2°. They note the difficulty of employing simple laws to describe spatial summation in vision. Barlow's earlier assertion is repeated, "temporal and spatial summation in human vision are complex, interrelated phenomena which are not adequately described by the simple empirical laws (Bunsen-Roscoe, Ricco, and Piper) except within certain narrow ranges." They conclude, "The results of P.E.H. do not suggest tha Piper's Law has any general or fundamental validity." Following this work, Hallett provided a review of the literature concerning the peripheral retina at threshold up to 1963[155]. His only relevant finding regarding spatial signal summation was brief. "The only generally acceptable statement is that a few quanta need be absorbed for a threshold sensation and that there is probably more than one size of visual unit."

---

[152]Cannon, M. (1975) Perceived contrast in the fovea and periphery *J Opt Soc Am A* vol 2(10), pp 1760-1768

[153]Brindley, G. (1970) Physiology of the Retina and Visual Pathway, 2nd Ed. London: Edward Arnold

[154]Hallett, P. Marriott, F. & Rodger, F. (1962) The relationship of visual threshold to retinal position and area *J Physiol* vol. 160, pp 364-373

[155]Hallett, P. (1963) Spatial summation *Vision Res* vol 3, pp 9-24

Matin offered one of the few theoretical discussions of the applicability of Ricco's Law and the limits of that applicability[156]. His model was too simple to come to any general conclusion.

Davila & Geisler (1991, using four subjects) have provided very good data related to the on-axis situation, referred to here as involving the foveola[157]. Their data clearly shows that the output of the photoreceptors of the foveola are not summed as part of the Stage 2 signal processing but are connected directly to the thalamus by individual ganglion cells and the subsequent individual neural paths.

Volbrecht et al. (2000, using three subjects) have broadened the study area to include the point of fixation out to 20 degrees along the vertical meridian[158]. A series of threshold versus intensity experiments were carried out that were designed to separate the S- and L-channel photoreceptors. A stimulus interval of 10 ms to evaluate the L-channels is too short to be compatible with both the P/D mechanism at threshold levels and the fusion frequency at that level. The 50 ms interval for S-channel evaluation is also marginal. Their data uses a "bilinear" construct to place the simpler construct associated with Ricco's Law in perspective. That is the character of the signal summation mechanism changes drastically between the area near fixation and the areas more remote from that point. Their figure 5 shows significant variation between the so-called Ricco's area associated with the foveola (nominal diameter of 1.18°), the fovea (nominal diameter from 1.18° to 8.68°) and with the remainder of the retina. [xxx continue analysis]

Sakitt (1971, using three subjects) performed a series of experiments at 7° temporal that gave very conflicting results compared to their anticipation. He noted, "This experiment demonstrates the apparent paradox with respect to spatial summation." The variation in the results is worthy of review. The variation forced Sakitt to consider nonlinear as well as linear summation theories. The experiments were designed to be performed at threshold and no effort was made to differentiate between the performance of the S- and M-channel photoreceptors. His basic conclusion was "that spatial summation at absolute threshold is not related to a single variable like distance or separation but is (test) configuration dependent. No data was provided on the color temperature or spectral distribution of the stimulus. Many of the targets were quite small relative to the point spread function of the physiological optical system at 7° temporal. The 16 and 32 ms exposure intervals were very short relative to the rise and fall times of the P/D mechanism at threshold. They were also very short compared to the recognized fusion frequency at threshold levels. [xxx continue analysis] In general, Sakitt's results are compatible with a complex Stage 2 architecture involving the horizontal, bipolar and possibly amercine cells. This processing involves nonlinear processing by definition based on the theory of this work.

Scholtes & Bouman (1977, using three subjects) performed a set of psychophysical threshold tests covering the temporal retina from 4° to 40° eccentricity and a wide range of background intensity levels[159]. They noted the general conflicts in the literature and the lack of systematic studies. The stimulus duration was generally 10 ms using light of 510 nm generated using a narrowband interference filter. Targets ranged from seven to 280 arc minutes diameter. The data is unusual in that it provides range bars. However, the ranges only apply to the data for single individuals. They noted, "The breakdown of Ricco's law for 15° eccentricities and all further peripheral locations is a direct affrontation of the generally accepted concept of complete spatial summation of stimulus energy if applied in a sufficiently small area of the retina." They also concluded, "It would appear that all of the spatial possibilities of the retina are concentrated in the region subtending 20° with the fovea. It is thus not clear what function of the remainder of the retina is in this respect apart from the possibility of being a movement detector."

Wilson (1970, using two subjects in separate tests) studied an even wider angular range, 5 to 55° from fixation, using a tungsten source and long stimulus intervals of 130 ms. His data (figure 2) shows good agreement with the expected slope of -1 between log $\Delta I/I$ and the stimulus diameter for diameters below 8.5 to 40 arc minutes depending on eccentricity. For larger stimuli diameter, a response with a slope of less than 0.4, and approaching zero, was reported. Wilson uses a term to describe the area of complete summation that appears to agree with the widely used term, Ricco's area to describe the largest area that continues to follow the slope = -1.0 criteria. While this parameter varies significantly with eccentricity, the Weber fraction, log $\Delta I/I$, does not. His figure 5 is a composite showing the

---

[156]Matin, L. (1975) Ricco's Law: response as a power function of stimulus luminance and distance from target center *Vision Res* vol 15, pp 1381-1384

[157]Davila, K. & Geisler, W. (1991) The relative contributions of pre-neural and neural factors to areal summation in the fovea *Vision Res* vol 31(7/8), pp 1369-1380

[158]Volbrecht, V. Shrago, E. Schefrin, B. & werner, J. (2000) Spatial summation in human cone mechanisms from 0° to 20° in the superior retina *J Opt Soc Am A* vol 17, pp 641-650

[159]Scholtes, A. & Bouman, M. (1977) Psychophysical experiments on spatial summation at threshold level of the human peripheral retina *Vision Res* vol 17, pp 867-873

log threshold (ΔI/I) versus log stimulus area, with shifting of individual data sets to obtain a more presentable graph. The result shows a clear transition from a slope of -1 to a slope of zero over a range of three plus log stimulus area units. The range associated with a slope of 0.5 is less than one log unit of area. He concludes, "The data presented in figure 5 confirm Barlow's (1958) conclusion that Piper's law does not hold for any significant range of stimulus areas." He also notes the lack of sufficient electrophysiological data to make sweeping assertions concerning spatial integration with retinal angle. Based on this lack, he suggests there may be several invariant parameters defining the spatial summation mechanism and the possibility of multiple parallel processing paths cannot be dismissed.

[xxx address Vassilev, Reflect on Barlow's comments re: motion detection versus summation and contrast enhancement.]

Fischer and Glezer have approached the subject of convergence from a different perspective based on the concept of receptive fields of particular neurons within the CNS.

Glezer has provided a wide ranging summary of his 1962 doctoral dissertation that discusses receptive field size under a variety of conditions[160]. He used only a few subjects. Very good psychophysical data is provided for the on-axis condition in humans (one subject) and limited data is provided out to 40° eccentricity (one subject). However, a reinterpretation of Glezer's results are appropriate based on the fact that the effects of the physiological optics and the adaptation mechanism were not included in the original analysis. His introduction contains a mathematical formulation for discussing Ricco's Law.

Fischer has addressed a more significant physiological question than the majority of the psychophysical investigators. His studies capitalized on the greater flexibility associated with using cats as subjects compared to using humans. Fischer developed an early concept of computational anatomy to describe the variation of summation field diameter versus position in the instantaneous visual field[161]. Data on eccentricities up to 80° are provided.

The majority of the experimental data is the result of experiments using an unspecified tungsten filament light source. While, it is generally assumed such a source provides a spectrally uniform source of energy (or photons), this in not the norm. Such a source is invariably inadequate in the short wavelength portion of the spectrum.

Only a few of the above papers speculated on the morphological uniformity of the retina or on the presence of vascular conduits potentially shadowing the stimulus for small stimulus sizes. None of the papers reviewed showed any concern for the role of tremor in smoothing their data. The drastic spreading of the point spread function of the physiological optics was not addressed either. These effects all play a role that must be addressed in any systematic study of spatial signal integration in vision.

In spite of the goal expressed by Scholtes & Bouman, no comprehensive systematic study of sensory channel summation, leading to a clear understanding of the concept expressed so long ago by Ricco, has appeared in the literature. Such a study should explore the summation properties of the entire visual field of one eye for both broadband and at least the three primary spectral channels of human vision. It should also employ sufficient subjects to insure the conclusions represent the general population statistically. Lacking such a study, only a brief summary of the current state of knowledge regarding this subject can be presented.

Hansen et al. have reviewed the literature and provided new data on human color perception in the intermediate periphery using 5 and 8 degree diameter disks projected onto a curves screen[162]. They provide graphical data supporting their conclusion, "Color stimuli can be reliably detected and identified by chromatically opponent mechanisms even at 50 deg eccentricity."

17.8.6.2 Representative data

Figure 17.8.2-4 shows an annotated presentation from the work of Glezer. Modern luminance intensity scales have been provided. An exposure time of 115 msec was used. This interval is longer than that used by most investigators. The longer interval can be significant at low light levels where the time constant of the P/D

---

[160]Glezer, V. (1965) The receptive fields of the retina *Vision Res* vol 5, pp 497-525

[161]Fischer, B. (1973) Overlap of receptive field centers and representation of the visual field in the cat's optic tract *Vision Res* vol 13, pp 2113-2120

[162]Hansen, T. Pracejus, L. & Gegenfurtner, K. (2009) Color perception in the intermediate periphery of the visual field J Vision vol 9(4), article 26 http://journalofvision.org/9/4/26/

mechanism may be important.

The upper frames of the figure describe the derivation of the format of the lower frames. On the assumption that the integrated signal required to achieve a given threshold criteria is equal to the product of the luminous intensity at threshold, I_{th}, times the stimulus area S raised to a power n, the relationship between the luminous intensity versus stimulus area is given by graph (1). This is the graph used by the reports of many investigators found in the literature. In this graph, Ricco's Law is represented by a curve with a slope of –1.0, here labeled +1.0 to indicate the exponent of S when on the same side of the equality as the luminance intensity, I (as shown in the equations at upper left). Scholtes & Bouman and the Hallett team use graphs of this form.

An alternate graph can be produced by multiplying the ordinate by the stimulus area, S, to the first power. This is shown in graph (2). The ordinate of this final graphical form represents the total energy applied by the stimulus, not the intensity of that stimulus. The various lines drawn on these graphs define various conditions depending on the value of the exponent n. n = 0 corresponds to the condition defined by Ricco, the product of the luminous intensity times the area of the source equals a constant independent of the area S. An alternative condition, where n = 0.5, is known as Pilar's Law.

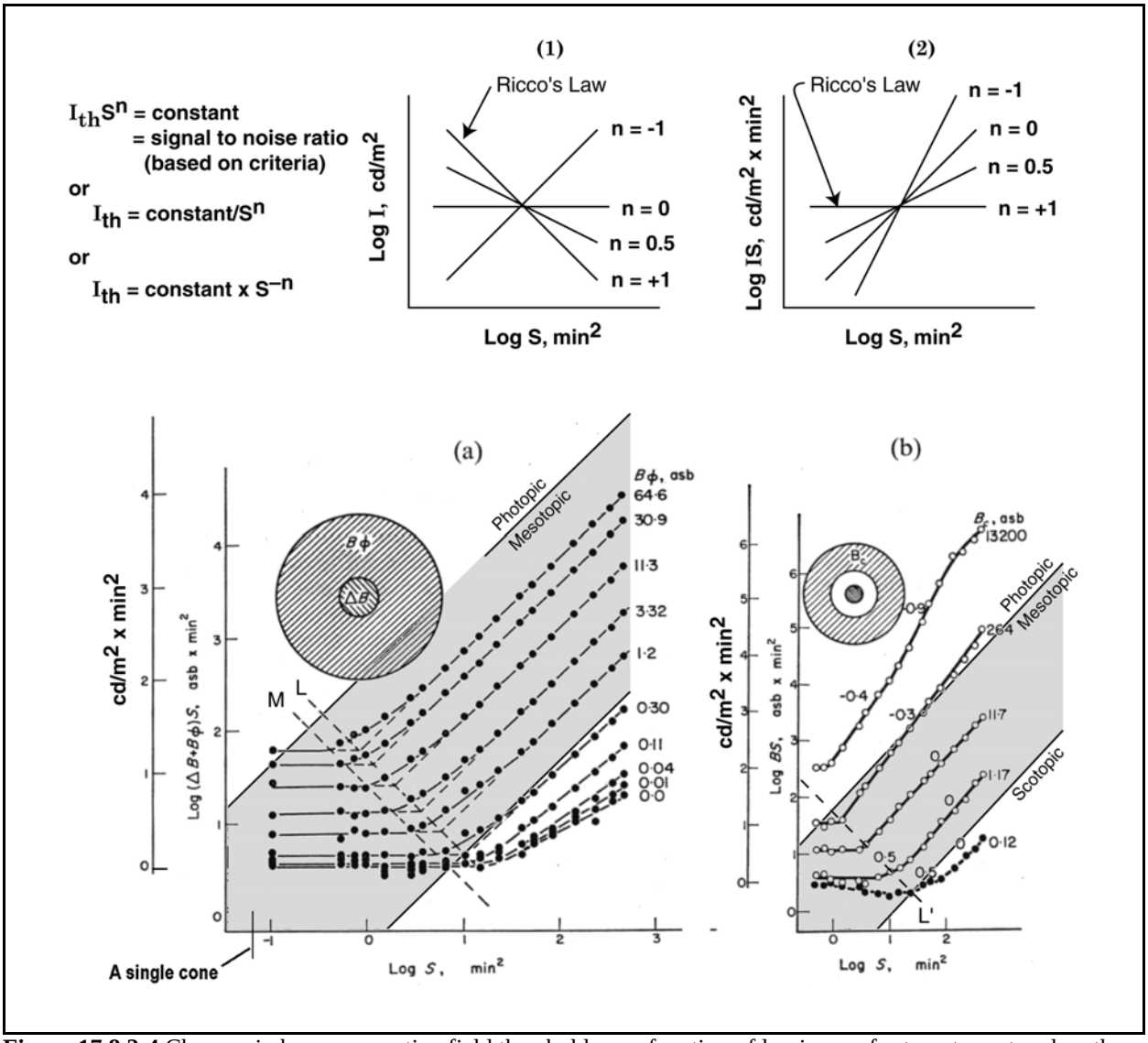

Figure 17.8.2-4 Changes in human receptive field thresholds as a function of luminance for targets centered on the point of fixation. Stimuli were presented for 115 msec. Upper frames; evolution of the format used in the lower frames. See text. (a) Threshold luminous flux as a function of the stimulus area background intensity. Subject V.G. (b) Changes in the zone of full summation and coefficient n beyond this zone as a fraction of luminance of the matching field. Subject Z.Z. Data from Glezer, 1965.

It must be noted that these criteria are based on the assumption that the visual system does not exhibit any nonlinearity or spatial limitations other than the threshold criteria itself. In reality, the simple equation is not realistic. The threshold is determined by the signal to noise ratio of the cognition mechanisms of stage 4 and 5 following all of the internal channel limitations. These limitations are introduced by the physiological optics, the P/D mechanism, the adaptation mechanism, the logaritmic signal conversion at the pedicles of the sensory neurons, and any correlation mechanism associated with interpretation, perception and cognition. The quantum nature of light must also be introduced at light levels in the mesotopic illumination range. At scotopic illumination levels, the quantum noise associated with the interpretation circuits must also be considered.

As a result, the simple equation should be expanded to compute the product of all of these effects on the input stimulus, and set the result equal to the constant defined by the test criteria.

Glezer has provided considerable data for the stimulus intensity versus stimulus area relationship for a stimulus centered on the point of fixation. Glezer did not discuss the significance of the lines labeled L and M in this revised figure, nor did he indicate the size of a single photoreceptor when he spoke of it in his text. The diameter of a nominal photoreceptor is shown in the lower left frame. The figure has been shaded to highlight the approximate limits of the luminance operating regimes involved (based on the levels in **Section 2.1.1.1**). By adding this shading, interpretation of the data is considerably simplified. Note that frame (a) only contains data derived from the mesotopic and scotopic luminance regimes. Note also that the threshold is determined by a change from the presence of both the background and the test luminance to the background illuminance alone. Within the mesotopic regime, the adaptation mechanism is not active and the internal noise limit is augmented by the photon noise associated with the stimulus. Within the shaded region, the slope of the curves for large stimulus areas have the slope of 1.0. This is consistent with an inactive adaptation mechanism. Based on this figure, the effect of the photon noise is not significant until the range below 0.3 abs (0.01 cd/m^2) is reached. Below this level, the slopes of the curves reduce to ½ which is consistent with the photon limited noise condition. It is noteworthy that only the area to the lower left corresponds to Ricco's Law. In the region of horizontal lines, the value of the exponent n is equal to +1.0. The system is operating as an area integrator in establishing the threshold criteria. For stimuli levels above this value, the threshold is based on the performance of individual sensory channels (pixels). In both cases, the presence of the surround at an illuminance of Bφ has no effect as is demonstrated in frame (b). The locus L appears to define the transition from the horizontal region representing Ricco's Law to the n = 0 slope region where the threshold is independent of the stimulus area. These curves do not exhibit any explicit region where n = 0.5, in agreement with Pilar's Law.

Frame (b) involves the same basic experiment except the background has been eliminated from the inner area to be occupied incrementally by the test stimulus. Thus, the threshold criteria is now determined by a change from the presence of the stimulus versus no stimulus. Note the compression of the ordinate scale in this frame. The mesotopic operating regime has again been shaded. This time, data was collected from the lower extent of the photopic operating regime but little or no data was collected from the scotopic regime. The curves are very similar to those in frame (a), confirming the fact that the surround is not playing a significant role in these experiments except possibly with respect to subject comfort and fatigue).

The curves labeled "0" have a slope of zero and the system is operating without the application of Ricco's Law. The threshold is based on a pixel by pixel determination of the stimulus. Only at the very lowest stimulus levels are the curves horizontal, suggesting the value of n = +1.0. This is the only area of the frame that corresponds to Ricco's Law.

As the stimulus intensity moves into the photopic regime, it is obvious that the adaptation mechanism is beginning to play a role. The slopes of -0.3 to -0.4 are similar to the slope of the perceived threshold as a function of intensity maintained by the adaptation process throughout the photopic regime (**Section xxx**). This characteristic slope defines the photopic regime. The dependence of the adaptation mechanism on the area of the stimulus is explained theoretically in **Section 12.5.3**. The relationship is the same as that demonstrated by the data of Glezer.

It is proposed that the region of the top curve labeled as slope = –0.9 is due to a statistical artifact. As noted from frame (2), the exponent of n changes very rapidly in this area of the curve. Replacing this line by its linear regression equivalent would eliminate this apparent change in slope. While it would be expected that this family of curves would bend over and become horizontal in the hypertopic regime due to saturation in the sensory neuron channels, this regime is at least four orders of magnitude above the luminance intensity of this curve.

Glezer's data strongly supports the model proposed in this theory. His data is entirely consistent with the predicted performance of the human eye based on the theory proposed here. He also shows that Ricco's Law is only relevant for extended test stimuli centered on the line of fixation with an area in the size range from 0.1 to 10 square arc minutes. For larger size targets, the threshold performance is determined on a pixel by pixel basis. Thus, incremental changes in the illuminance of small areas of the test stimulus can also be identified individually. In the light of this analysis, the suggestion by Glezer that inhibition (a binary concept) plays a role in his data should be replaced by the effect of adaptation (an analog mechanism).

The papers of the Scholtes & Bouman and the Hallett team confirm the key features of the above analysis over a range of eccentricities using figures based on frame (1) above. Their data does not support the existence of a substantial interval where Pilar's Law applies. The data does show that individual subjects show significant differences (0.3 log units) on a day-to-day basis.

Figure 17.8.2-5 from Scholtes & Bouman shows the variation in Ricco's diameter (the break point defined by the locus L in the previous figure, for a constant stimulus intensity using a 510 nm narrowband interference filter and a regulated tungsten source. The nominal stimulus interval was 10 ms as determined by a mechanical shutter. The

diameter is shrinking precipitously in the region of five to 15 degrees temporal eccentricity. The diameter is only one to three arc minutes diameter at the point of fixation based on Glezer (above).

Figure 17.8.2-6, also from Scholtes & Bouman, shows the variation among three subjects that accompanies the threshold versus eccentricity data. Their formulation is based on frame (2) above. The ordinate gives the total energy of the stimulus within an area of a given diameter. They note an anomaly in their data compared to the predicted performance based on Ricco's law. For eccentricities greater than seven degrees, they note a rise in the threshold for decreasing stimulus diameter. For very large angles, the increase is only a factor of 3-4, assuming the function does level off as shown.

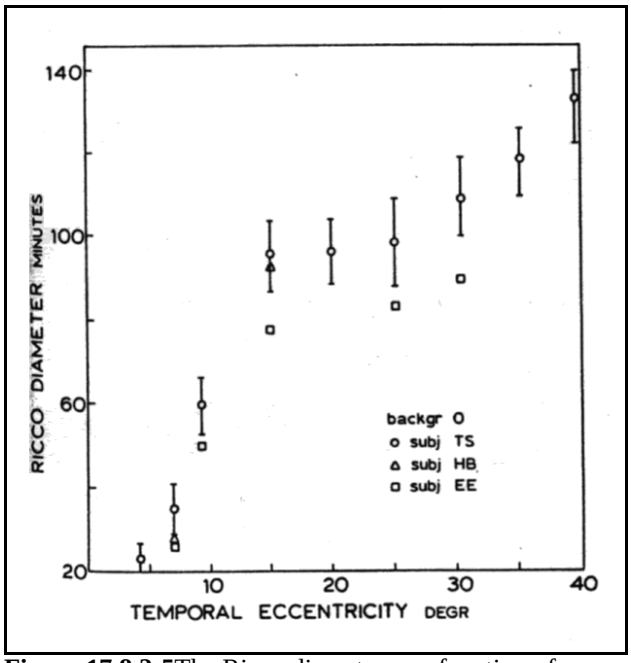

Figure 17.8.2-5 The Ricco diameter as a function of temporal eccentricity for three subjects for one stimulus intensity. The accuracy for the other subjects was similar to that for subject TS. From Scholtes & Bouman, 1977.

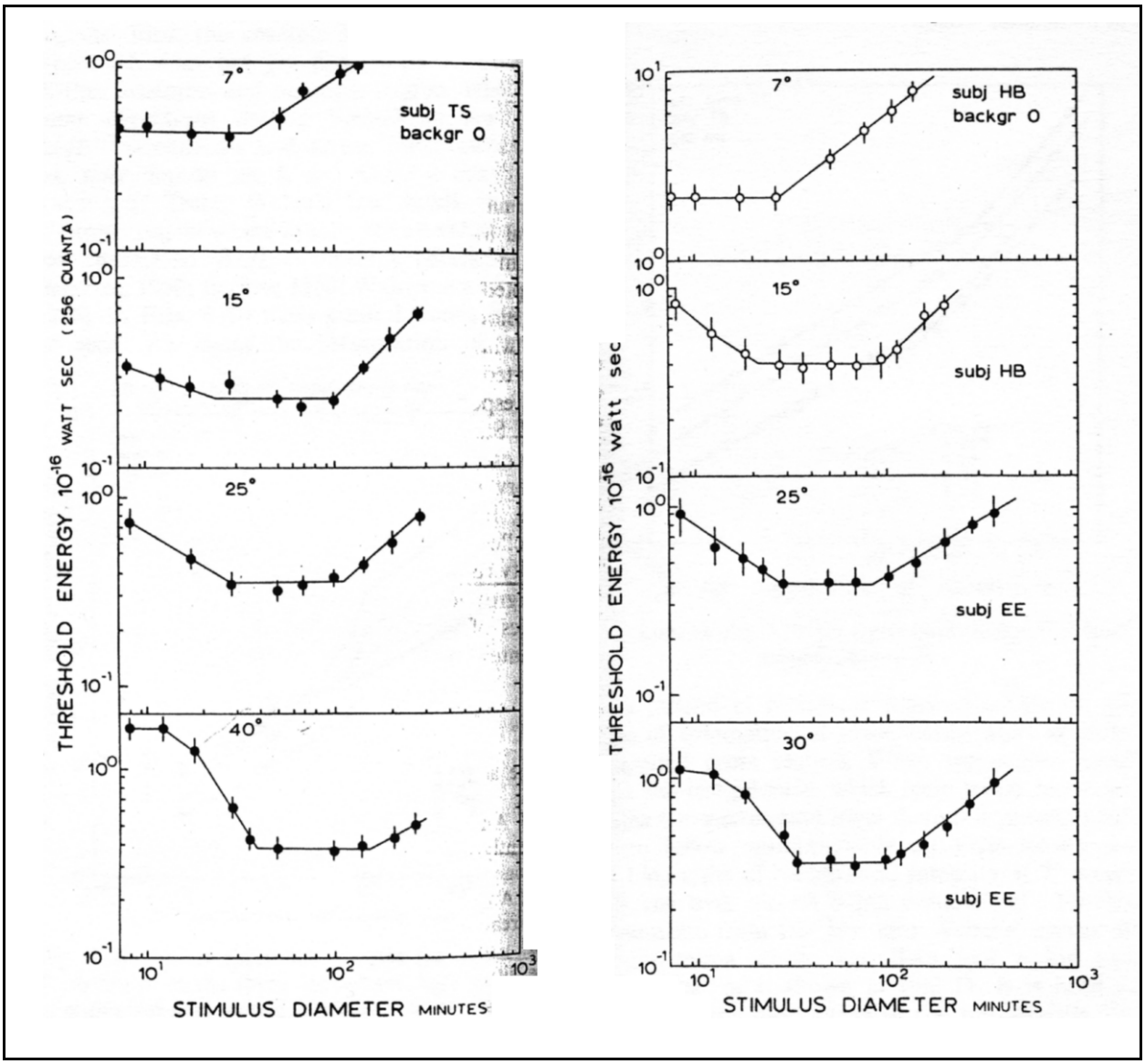

Figure 17.8.2-6 Threshold energy as a function of stimulus diameter at several temporal eccentricities following complete dark adaptation. The stimulus used a 510 nm narrowband source. Note different scale for ordinate at upper right for subject HB. From Scholtes & Bouman, 1977.

For larger spatial sources, a second effect becomes obvious. This effect causes the threshold to rise in proportion to the area of the stimulus for all eccentricities measured. Scholtes & Bouman speculate on the purpose of the retina beyond 20° based on this characteristic. "It is thus not clear what function the remainder of the retina is in this respect apart from the possibility of being a movement (sic, change) detector."

Volbrecht et al. presented their data using the framework of frame (1) above for angles from zero to 20°. Their goal was two-fold. First, to explore the threshold response versus stimulus area in the isolated S- and L-channels. Second, to relate that data with the density of ganglion cells within the retina. Their stimulus intervals were 50 ms and 10 ms respectively. The use of 10 ms may have led to difficulties in the L-channel. They did not evaluate the effect of their short stimulus intervals. Their method of channel separation was clearly inadequate based on their figure 2. The sensitivity of the M-channel remained ten times higher than the S-channel. However, their use of a narrowband source does allow the calculation of the nominal number of quanta required for threshold detection.

Their measurements did not show any anomaly at low source areas like the functions of Scholtes & Bouman. While

their data gave consistent values for Ricco's area over their test range, the values are at least an order of magnitude larger, when using either a 440 nm or 620 nm source, than those of Glezer . Without more complete channel separation, the discussion in the paper could not be conclusive.

17.8.6.1.2 A summary of the applicable psychophysical laws

Although many of the above papers discuss specific laws invoked to describe the convergence of photoreceptor signals as a function of position in the retina, they seldom provide adequate definition of these laws pertinent to their experimental protocol. The laws of interest are generally attributed to Ricco, Pilar, Bloch or Bunsen-Roscoe and frequently Weber or deVries-Rose. Weber's Law and the de Vries-Rose Law are generally associated with fixed stimulus areas while the first three are generally associated with variable stimulus areas.. It is difficult to find both a precise and global definition of these psychophysical laws. It is seldom possible to find a description of the range over which they apply.

In most of the situations explored here, the major parameters reflect different performance over three distinct intensity ranges. Above a certain level, the parameter exhibits a first power relationship to the independent test variable. Below a certain level, the parameter tends to be independent of the test variable. And in the intervening range, the parameter tends to reflect a square root dependence on the independent variable. In general, a complete law must address these relationships. Otherwise, the law is limited in its applicability (whether stated by the investigator or not).

Ricco's Law

Ricco's Law is the most quoted relationship involving spatial summation. Unfortunately the text-based quotations vary widely and are frequently contradictory. However, its formulation has not been very precise. Hallett, Marriott & Rodger say, "For very small areas threshold energy is independent of field size (Ricco's Law)." However, all of their data was given in quanta, not energy units. They generally found their statement to be true for diameters of less than 30 arc minutes regardless of eccentricities larger than five degrees (on the nasal side). Scholtes & Bouman found major discrepancies with that position for diameters below 30 arc minutes. As referenced above by several investigators, Barlow suggested both Ricco's Law and Pilar's Law verge on the inconsequential. This appears to be the case for most operational tasks.

Based primarily on the data of Scholtes & Bouman, Ricco's law can be stated as: For areas outside the fovea, under broadband illumination from an extended source smaller than Ricco's diameter, and in the absence of background illumination, the energy-based detection threshold is proportional to the area of the source.

Corollary: Ricco's diameter is the maximum diameter for which area summation, as implied by the above law, applies. Ricco's diameter is a monotonic function of eccentricity.

Corollary: To obtain statistically significant values for Ricco's diameter in humans, at least five times the number of subjects must be used as was used in any of the above investigations.

Corollary: For narrowband illumination, the variability in Ricco's diameter varies so drastically among individuals that no meaningful relationship can be given between Ricco's diameter and Ricco's law with respect to eccentricity.

Pilar's Law

Pilar's Law generally claims an association between the threshold stimulus intensity and the area of the stimulus. The association is a square root relationship. Such a relationship is only found as a transition condition between the region of Ricco's Law (n = 1.0) and the region of total independence of threshold as a function of stimulus diameter (n = 0).

17.9 Temporal performance of the human visual system

17.9.1 Visual tracking within complex backgrounds

Souto & Kerzel have analyzed the ability of the human eye to track objects within a distracting field of dots moving independent of the target object[163].

17.9.xxx Data obtained from transcranial magnetic stimulation (TMS)

There have been many attempts to use phosphenes (artificially generated visual perceptions not utilizing the optics of the eye) but these have generally suffered from the lack of an adequate schematic or block diagram of the visual system.

Marzi et al. have provided an extensive report[164] on their behavioral experiments without benefit of a realistic schematic of the overall system they were seeking to evaluate. They used a combination of visual and TMS stimulations involving both visual fields and both hemispheres of the cerebral cortex (at both occipital and parietal locations). Evaluation of their data under their protocol was heavily statistical in character but used well understood and developed statistical techniques.

The Marzi paper appears to exhibit some stylistic and semantic problems that leave it difficult to interpret with precision.

1.It appears to have been conceived in Italian and then translated into English by a good but not native speaker of English.

2. There is little calibration of their test set such as indicating whether the start time was when an electrical switch was commanded to take an action and when the actual stimulation was applied to the retina or the TMS coil was activated.

3. Their protocol does not make any attempt to determine the delay associated with the P/D mechanism when illuminating the retina at different intensities. The variation can be several milliseconds (Section xxx).

4. Using a very small subject set of only six individuals, and performing only 20 test runs per individual per experiment, they present their data with 5 digit precision when its accuracy appears to be 3 digits or less (based on the calibration problem described in item 2.

5. They appear to assume an unstated hypothesis that a stimulus to a temporal or nasal portion of the retina of one eye, to the ipsilateral operculum of the occipital lobe or the ipsilateral area of the parietal lobe must be transferred to the contralateral operculum of the occipital lobe or the contralateral region of the parietal lobe before any commands can be sent to the finger muscles to report perception of either a visual or TMS stimulus.

6. They offered no schematic or block diagram to support the hypothesis in item 4.

A clear result of the above items is that the data in their Table 1 (reproduced here as Figure 17.9.1-3) can be considered correct on a relative basis within a row, but the rows may not be comparable because of calibration difficulties.

They focus on response times (RT) along a single neural/motor signal path, interhemispheric transfer times (IT), and crossed-uncrossed differences (CUD). The CUD is described semantically on page 432 as, “With this method IT time is measured by subtracting RT of averaged uncrossed hand-hemifield conditions from that of averaged crossed hand-hemifield combinations. The latter require an IT and usually yield a longer RT than the former. The obtained value, the so-called crossed-uncrossed difference (CUD), is consistent across studies and is considered as a reliable

---

[163]Souto, D. & Kerzel, D. (2013) Ocular tracking responses to background motion gated by feature-based attention. J Neurophysiol DOI: 10.1152/jn.00810.2013

[164]Marzi, C. Mancini, F. & Savazzi, S. (2009) Interhemispheric transfer of phosphenes generated by occipital versus parietal transcranial magnetic stimulation Exp *Brain Res* (2009) vol 192, pp 431–441

measure of commissural IT time. On average it amounts to about 4 ms in health participants but is considerably slower in patients with either an agenesis or a surgical section of the coorpus callosum". *Unfortunately the average CUD of their putative healthy subjects in their Table 1 showed values an order of magnitude higher than 4 ms under a variety of stimulus conditions.*

Two figures are useful in interpreting the results of Marzi et al. **Figure 17.9.2-1** describes their experimental protocols using a profile view of the visual system. They performed two sets of experiments that avoided the foveola and focused entirely on the periphery of the visual field, generally three degrees each side of the vertical meridian and two degrees above or below the horizontal meridian. While using a skull cap to locate their points of TMS stimulation (their figure 1), they did in fact stimulate different areas of the cerebral cortex in the case of different subjects (their figure 3). Their TMS stimulation (using a 7 cm diameter magnetic coil) was generally perceived as several degrees in diameter as also indicated in their figure 3. Their subject set was small (six out of seven initial subjects were used) and the variation in perceived stimulation was large (about a factor of two among their six subjects. They asked each subject to draw their perceived field of TMS stimulation and subsequently used a back illuminated image of that drawing as a source of visual stimulation (using an unspecified, probably cathode ray tube, PC monitor). They also used a light projection system to present one degree white disks at six degrees to the left and right of the fixation point against a dark background.

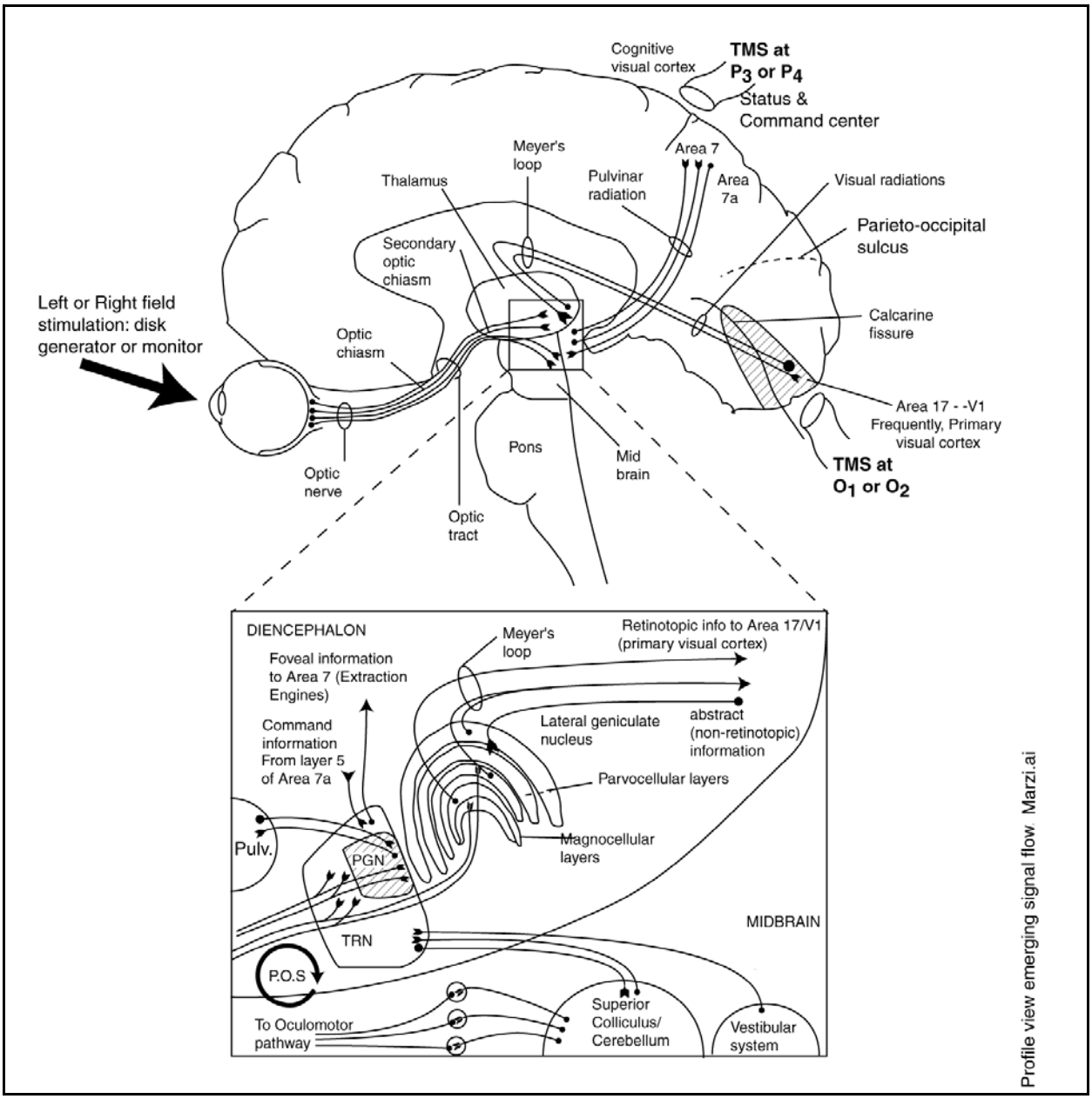

Figure 17.9.2-1 Profile view of visual and TMS signal flow. The visual stimuli are shown at upper left. The TMS stimuli to the Parietal lobe is shown at upper right. The TMS stimuli to the Occipital lobe is shown at center right. The skull cap establishes where the TMS coil is placed relative to the skull. However, the variability in location of specific areas of the CNS may cause differences in the area stimulated at the detailed level. Note the nominal horizontal meridian of vision is conventionally associated with the calcarine sulcus. See text.

By avoiding the foveola, all of their stimuli appear to have involved the pathways involving signals from the peripheral retina to the LGN to the occipital lobes, back to the TRN and then to the parietal lobe before being passed to the prefrontal cortex for evaluation. As shown in the next figure, subsequent signals were passed from the prefrontal cortex back through the motor portion of stage 6 (and the cerebellum) to the hands in order to actuate the space bar on a computer keyboard. While some familiarization was provided to the subjects, it will be assumed that they did not develop reflex paths through the cerebellum during these experiments (See figure in **Sections 4.6.3** or **12.5.1** for potential signal paths based on learning). Such reflex paths would change the interpretation of their

temporal reaction time results considerably.

Figure 17.9.2-2 shows a block diagram of the visual modality and a simple representation of the motor modality associated with it. Annotation has been added to indicate the protocol of Marzi et al. By avoiding the foveola, their afferent path stimuli avoided the PGN/pulvinar route shown. Both visual and TMS stimuli were focused on the LGN/occipital lobe couple leading to the parietal lobe and eventually to the fingers via the stage 6 neural circuits. The TMS stimulated signals were routed from their point of stimulation through the TRN at different points along their signaling path. The visual stimulation appears to have taken a short cut built into the system via the LGN to the superior colliculus (part of the Alarm mode discussed in **Section 15.2.4**). This short cut is used primarily to cause the eyes to turn to the source of the stimulus as quickly as possible in order to support the "fine feature extraction and perception" signal path through the PGN pulvinar to the parietal lobe. As part of their protocol, Marzi et al. trained their subjects to avoid redirecting their gaze from the artificial central target in their visual field.

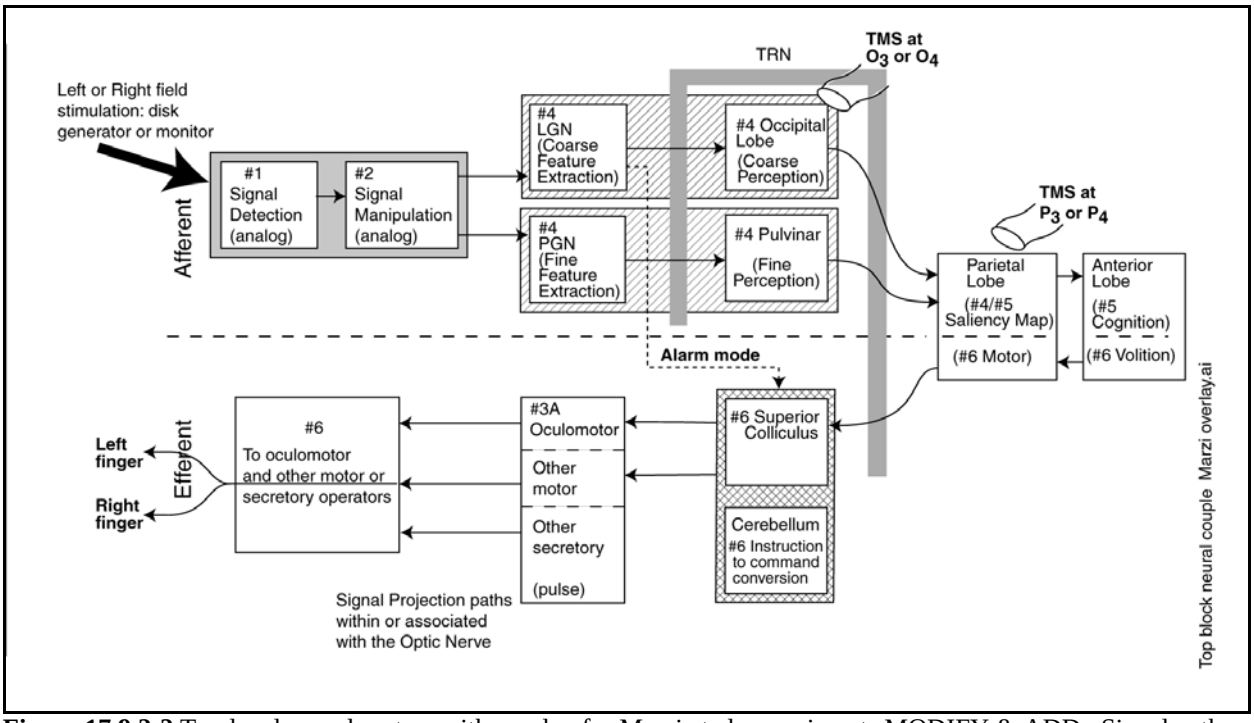

Figure 17.9.2-2 Top level neural system with overlay for Marzi et al. experiments MODIFY & ADD. Signal paths may originate with visual stimulation of stage 1photoreceptors, with TMS stimulation at the occipital lobe or with TMS stimulation at the parietal lobe as shown. The afferent paths are duplicated for the left and right visual fields. The efferent paths are duplicated for the left and right portions of the chordate body. The Alarm Mode associated with visual stimulation is also shown between each stage 4 LGN and the stage 6 superior colliculus. See text.

Figure 17.9.2-3 shows the perceived stimuli reported by the six subjects based on TMS stimulation of the occipitial lobe in **A** and the parietal lobe in **B**. In all cases, the subjects were asked to fixate continually on a point at (0,0) coordinates. In spite of using a skull cap and aligning the TMS coils with that aid, some of the subjects reported stimulation on either side of the horizontal meridian (traditionally associated with the calcarine sulcus of the cerebral cortex). The coils used were paired 70 mm diameter air core coils used routinely in clinical medicine. The magnetic fields generated were a rectified cosine pulse of nominally 1 Hz frequency reaching a strength of 1.2 Tesla at the manufacturer designated face of the coils. Marzi et al. chose to use the figure 8 coil assembly reversed without additional calibration. No comments appeared in the paper or the manufacturers instruction manual as to why magnetic pole pieces were not used to concentrate or shape the magnetic field. Based on the magnification factors detailed by Tootel et al. in 1988 between the object space interrogated by the human peripheral retina and the occipital lobe (~10 mm/degree), the effective magnetic stimulus diameter at the occipital lobe was on the order of 30 mm diameter.

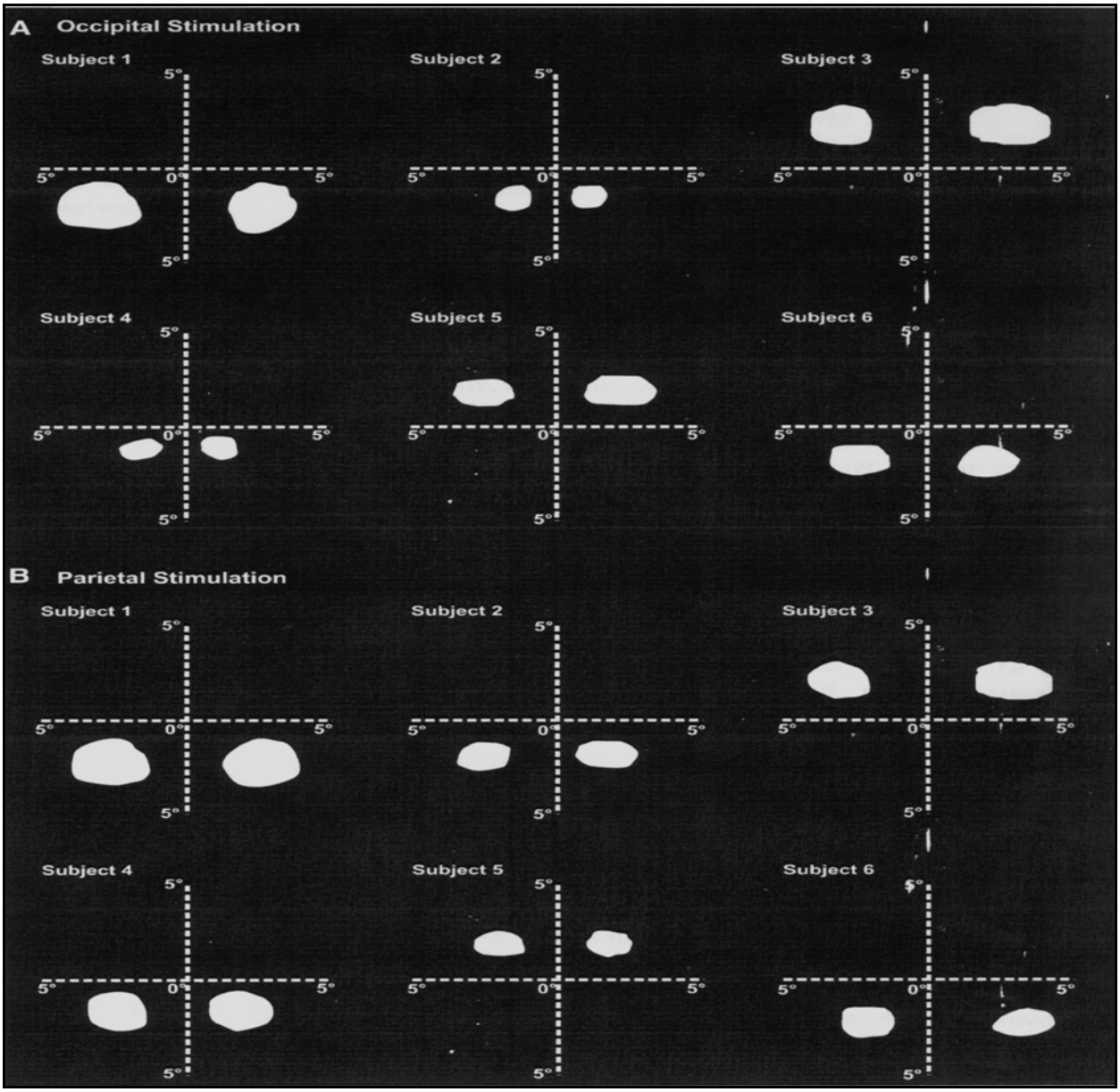

Figure 17.9.2-3 Position and shape of phosphenes for each participant in Exp. 1 & 2. Note the change in perceived phosphene location relative to the horizontal meridian when apparently using the same skullcap and 7 cm diameter TMS stimulation coil at the same cranial locations. The left-right symmetry is good for each subject. The perceived phosphene size varies by a factor of two. No foveal data was reported. See text. From Marzi et al., 2009.

Figure 17.9.2-4 is an annotated copy of their table 1 summarizing their results. The columns have been rearranged to group the crossed and uncrossed pairs. As noted in the leadin to this analysis, using a very small subject set of only six individuals, and performing only 20 test runs per individual per experiment, they present their data with 5 digit precision when its accuracy appears to be 3 digits or less (based on the calibration problem described in item 2). In addition, their taking the difference between two similar large mean values with significant standard deviations can lead to differences in the mean with standard deviations larger than the difference in the mean. It appears their CUD values are at best suggestive unless accompanied by standard deviation values.

			Uncrossed		Crossed			
Stimuli	Retinal stimulation	Stimul./partic./ per column	LH-LVF	RH-RVF	LH-RVF	RH-LVF	CUD	Mean
Experiment 1		40						
TMS-phosphene			390.28	376.49	409.16	438.31	40.35	403.56
Circle stimuli	✓		275.08	268.19	274.12	275.63	3.24	273.26
Phosphene-like	✓		264.18	273.13	275.31	269.67	3.83	270.57
Imagined anatomic			1006.82	998.70	1037.22	1045.32	38.51	1022.01
Imagined crossed			992.97	961.45	1046.99	980.00	36.28	995.35
Experiment 2		40						
TMS-phosphenes			385.06	391.85	389.53	397.30	4.95	390.93
Phosphene-like	✓		269.53	256.92	269.90	267.62	5.53	265.99

LH Left hand, *RH* right hand, *LVF* left visual field, *RVF* right visual field, *CUD* crossed–un- crossed difference

Marzi09pg436 annot.wpg

Figure 17.9.2-4 Mean response times (RT) to the various crossing conditions and sessions. Experiment 1; calculating CUD from the RT values elicited by TMS over the occipital lobe. RT's for the two imagined cases are measured from the onset of the audio tone, not from stimulus presentation. Experiment 2; similar to Exp. 1 but applying TMS to the parietal lobe. See text. Modified from Marzi et al., 2009

Looking at the rearranged columns;

1. The uncrossed pairs of RT's are not statistically different for the various conditions if their precision is reduced to three digits.

2. The crossed pairs of RT's are not statistically different for the various conditions if the small size of their sample group is taken into consideration and their precision is reduced to three digits.

3. The crossed and uncrossed pairs of RT's resulting from visual stimulation give significantly smaller values than do the TMS and the imagined values indicating different underlying signal paths.

4. The crossed and uncrossed pairs of RT's resulting from "imagined phosophenes," exhibit RT's much longer than for the visually induced and TMS induces perceptions.

Re-examining the values in the above table, the visual stimulations result in finger movements much earlier than for any of the TMS stimulations. This strongly suggests the initiation of visual stimulation is being detected at the Lateral geniculate nucleus (LGN) and is being passed directly to the superior colliculus (SC) via the Alarm Mode of the visual modality (**Section 15.2.4**) prior to and in parallel with any subsequent stage 4 or stage 5 processing (a common event within the visual modality). The result is the space bar is pressed prior to any perception of the stimulus by the higher cognitive centers of stage 5.

Their conclusion that the nominal commissural transit time (between equivalent areas located 2.5 degrees horizontally from the point of fixation) is 4 ms appears too long considering the minimum distance is on the order of

30 mm. Based on a nominal average stage 3 projection neuron signaling velocity of 44 mm/msec (**Section 9.4.2** of this work or **Section 7.3.7** in Processes in Biological Hearing), the expected value would be on the order of three-quarters of a millisecond. 4 ms would support a signaling path back through the thalamus and out to the other operculum if required. However, such a path does not appear to serve any purpose.

17.9.xxx.1 The unappreciated role of training in the Marzi et al. experiments

Training is only addressed superficially in Marzi et al. and from the perspective of whether the subject could perform easily and repeatedly. Their principle comment was that the subjects could maintain their point of fixation without difficulty, particularly if they avoided blinking during an individual test interval. They did not discuss the effect of telling the subject what hand to use for a given test sequence.

From the point of view of the neural system, their training to maintain the subjects point of fixation during a test sequence clearly established the goal of maintaining fixation from the perspective of the cerebellums task of relieving the stage 5 cognitive engines of this responsibility. This training also had a role in suppressing the normal Alarm mode operation within vision where the appearance of the stimulus causes the LGN to instruct the SC to diverted the eyes to a new point of fixation centered on the stimulus and to make any focus adjustment required. This point is important from the perspective of the TMS experiments where stimulation bypasses the role of the LGN in its alarm mode responsibilities.

Instructing the subject to use the index finger of a specific hand to press the space bar (both to start the test cycle and to respond to the stimulus) is an act of training within the neural system. There is no requirement for the neural system to evaluate whether the stimulus is in the left or right visual field before selecting which finger to use when taking action.

As a result of these training steps, there appears to be little if any need for the stage 5 cognitive engines to participate in the experiments involving visual stimulation. The same is true for the TMS stimulations. However, for the imagined stimuli test sequences, the role of the stage 5 cognitive engines play a major role in accessing declaratory memory before responding. Accessing declaratory memory is a time consuming process.

17.9.xxx.2 Experiments imagining a phosphene

In the final phase of the first experiment of Marzi et al., the protocol and neural procedures are entirely different from the visual and TMS stimulating protocols of the earlier phases. In this case, following an alerting audio tone, the subject was asked to recall their previous perception of a phosphene and then press the keyboard space bar when such a perception is first perceived.

The afferent blocks of the top level neural system apply equally well to both the auditory and visual modalities with minor changes in nomenclature, but the task beyond the afferent path is entirely different. The cognitive engines of the CNS are asked to interrogate the memory system to recall an image of a previously observed phosphene and then instruct the efferent system (as used in the earlier experiments) to press the space bar of the PC when this image has been retrieved. The RT's for this operational sequence is about four times longer than that for the RT to a phosphene projected onto the PC monitor (labeled "phosphene-like" in the above table). This protocol requires the participation of a host of additional stage 5 neural engines such as highlighted in the Top Level Signaling Plan illustrated in **Section 1.2.1** involvng the afferent neural engines of stage 6 and the musculatura.

17.9.xxx.3 Recapitulation of the Marzi et al. and a proposed revision of the General Conclusions

It is difficult to determine any global null hypothesis for the work of Marzi et al. in their first 2009 paper (beginning on page 431) They did not describe their understanding of the neural signal paths involved, either semantically or graphically. The fact that they did not relate their measured results to any comprehensive schematic of the neural system forces them to discuss the operation of the relevant elements of the neural system in only the most general terms (even though a handful of other papers are cited). Many of their comments could be further perfected using an adequate schematic and/or block diagram.

- - - -

They did present a set of corollary stand alone hypotheses to the unstated main null hypothesis;

1.“An off-center stimulus processed by V1 and adjacent visual areas should take longer to cross to the other hemisphere in comparison to a stimulus processed by parietal areas with widespread callosal connections (page 432).”

2. Exp. 1: “Stimuli that use callosal connections at the level of V1, such as TMS-generated or imagined phosphenes should yield a substantially slower IT than visually presented stimuli that, as shown by various studies are likely to undergo IT at the level of parietal or prefrontal cortical areas (page 432).”

3. Exp. 2: “The slow IT of phosphenes is related to a callosal transfer through the sparse callosal connection of the visual cortex (page 438).”

- - - -

Their abstract concluded by comparing the interhemispheric transfer times for the TMS stimulation of both the occipital and parietal lobes and the imagined stimulations. However, it did not address the fact their measured data for visually induced responses exhibited significantly smaller IT values than any of these other approaches. This situation would suggest one of two possibilities; the occipital and parietal lobes of the CNS did not play a role in the visual signal path between the eyes and the neuro-muscular portions of the response system **OR** their concept of signal flow within the visual modality was unsupportable.

- - - -

Marzi et al. address the border area between V1 and V2 at several locations in the paper. However, they appear to rely upon only a cartoon and discussion of this interface on page 1538 of Tootel et al[165]. Tootel et al. actually cite several papers that argue against their position. addxxx

- - - -

Marzi et al. did make two important observations relative to the spatial organization of the information represented at the occipital and parietal lobes. The first was that the spatial organization of the occipital lobe was retinotopic, i.e., the perceived phosphenes followed the eyes, as expected. On the other hand, their wording was less precise about the spatial organization of the information represented in parietal lobe and suggested it was worthy of further study. This work asserts the information related to the visual stimuli in the parietal lobe and the saliency map it populates do not move with the eyes but are organized inertially. The map represented the external environment with respect to the subject’s head and not with respect to the eyes.

- - - -

Based on the schematics and block diagrams presented above, it can be said that their protocols are exploring distinctly different operating modes of the visual modality combined with selected elements of the higher cognitive engines and a selected path of response involving the dextrous (specifically the finger portion) of the motor system. Their visual stimuli used cause activity within the Alarm mode of the visual modality in the normal manner. Their TMS stimuli involve parametric (non-normal) signal insertion into the visual modality that does not involve the orthodromic operation of stages 1 through 4. As a result, the neural system must manipulate signals in an unnatural signal format and operating mode.

Their protocol calling for the subject to retrieve their memory of a previously perceived blob from declarative memory involved a totally different chain of events from those involving visual or TMS stimuli. The processes resulted in significantly longer overall RT’s.

Because of the application of the visual stimuli to the peripheral fields of vision, the Alarm mode of operation was implemented under the direction and control of the TRN (without the participation of the other stage 4, 5 and 6 information extraction, cognition and instruction engines. Because of the prior training involving the cerebellum, the eyes did not divert their point of fixation to the centroid of the stimuli. These steps did not occur for the parametric stimuli involving TMS. The TMS stimuli applied to the occipital lobe in experiment 1created unnatural signals that

---

[165]Tootell, R. Switkes, E. Silverman, M. & Hamilton, S. (1988) Functional anatomy of Macaque striate cortex. *J. Neurosci*. vol. 8, pp 1500-1624

were passed back through the TRN to the thalamus and then to the parietal lobe for insertion into the saliency map and presentation to the stage 5 cognitive engines as an undefined "blob" in the visual field. In experiment 2, the TMS stimuli were applied to the parietal lobe (at a later part in the signal processing chain) with the result, they were inserted into the saliency map after a shorter time delay as an undefined "blob." These blobs were presented to stage 5 as undefined generally disk shaped bright white or gray signatures. The stage 5 engines instructed the motor system to report the cognition of the blobs using the index finger based on the previous training.

As a result of these different methods of passing the signals resulting from the stimuli, the RT's of the visual stimuli were the shortest, followed by those for TMS applied to the parietal lobe, followed by those for TMS applied to the parietal lobe, followed by those involving recalling perceived blobs from the declarative memory by the stage 5 engines.

No rationale can be defined requiring, or suggesting, the passing of the signals generated from the TMS stimuli between operculuma of the occipital lobe via stage 3 signal projection circuits (or between left and right portions of the parietal lobe) in order to satisfy their experimental protocols. The calculation of the "so-called crossed-uncrossed difference (CUD) in RT's appears to be superfluous to their experiments. The CUD may be the result of taking the difference between large mean values associated with significant standard deviations. No numerical standard deviations were presented for the CUD related calculations (page 435) but their figure 4 showed the standard deviations of the CUD's were essentially equal to their mean values (resulting in a 1 in 6 chance that the CUD value was zero in a given trial).

Rearranging and annotating their Table 1 as presented above, suggests that all of their CUD's resulting from real stimuli

17.10 Characterizing psychophysical experiments based on the model

There has been little effort on assembling a framework characterizing the profusion of psychophysical experiments reported in the literature. Lacking such a framework, investigators have not been able to relate their work to that of others in a formal and precise way. Lacking such a framework, investigators have frequently overlooked and failed to control variables that are crucial to the precision and the interpretation of their work. To achieve such a framework, a comprehensive model of the visual system is required. Such a model is required to delineate the functional borders that need to be addressed in the design of any research experiment. In some cases, the analyst can determine whether a given experiment was performed without violating these borders. In other cases, it is clear that the experiments have straddled significant borders.

> A typical example of an experimental set straddling a border is that of Wolfson & Graham[166]. The describe their approach as using a probed-sinewave paradigm without completely characterizing that paradigm. In a set of experiments varying the intensity of a center stimulus of ten degrees diameter, they adopted two frequencies for the variation based on the refresh characteristics of a particular computer display monitor. The frequencies of 1.2 Hz (75 Hz/64) and 9.4 Hz (75 Hz/8) actually straddle a time constant in the adaptation amplifiers of the human photoreceptor cells. However, this fact was not recognized in their analyses. It does appear to be clearly represented in their figure 3. Their experiments also straddled the foveola- fovea border at a nominal diameter of 1.2 degrees and the fovea-periphery border at 6.2 degrees. What is the impact of changing the size of the fields in their experiments to avoid straddling these borders?
>
> In a second example from the same paper, the authors interpret their results as suggesting that "processing associated with detecting the probe is primarily in the retina (or any place with monocular input)." They then proceed to caveat this statement (at two different levels) on page 1004 and by adding the word likely to the title of the paper. They faced two major problems. First, they did not describe what they meant by "processing" or provide a scientific definition of the term detection. Second, their non-invasive procedures provided no information concerning where such processing actually occurred. The model of this work suggests that considerable signal processing (analog signal manipulation) occurs in the retina but no signal processing associated with detection, perception or cognition occurs there. The mechanisms of detection and perception (monoptic, dichoptic and binocular) are better described as occurring in the midbrain. This work

---

[166]Wolfson, S. & Graham, N. (2001) Processing in the probe-sinewave paradigm is likely retinal. *Visual Neurosci*. vol. 18, pp 1003-1010

would suggest that detection is a primary responsibility of the LGN (especially for stimuli falling outside of the foveola). A finer degree of detection leading to perception is associated primarily with the pretectum. The LGN is particularly well positioned for handling all three of the types of signal presentation defined above.

Repeating the above experiments at 2.4 Hz and 4.8 Hz would highlight the role of the adaptation time constant in their figure 3. As shown below, further defining their experiments to include a displaced fixation point would have highlighted the role of the pretectum and LGN in performing the detection task. Similarly, by stabilizing the optical image during one phase of the experiments, the un-quantified effects of the Precision Optical System (primarily related to the oculomotor system) could be removed rom the data.

17.10.1 Preliminary characterization of psychophysical experiments

The number of variables involved in the visual process is very large. It is useful to have a framework, eventually leading to a definitive code describing each type or class of experiment. Such a code cannot be defined at this time. However, a preliminary framework can be described that encompasses, and suggests methods of isolating, most of the variables. **Figure 17.10.1-1** is a preliminary framework for such a codification. It is based on the following theses:

1. The visual system is based fundamentally on change detection as opposed to imaging.

2. The detection of a characteristic of a stimulus is distinctly different from the perception and/or cognition of such a stimulus.

3. The tremor mechanism (associated with the Precision Optical System) plays a critical role in the perception and ultimate cognition of stimuli presented to the foveola.

4. The Precision Optical System defines three separate time periods crucial to the interpretation, perception and cognition of stimuli applied to the foveola.

Several brief remarks are appropriate concerning the framework.

I. The detection methodology of human vision is quite different from the perception and cognition methodologies. The acquisition of an simple interpretable image usually requires about 50 msec. Cognition usually requires the acquisition of multiple interps obtained during individual 50 msec intervals. Detection, on the other hand can occur following presentations of stimuli for only microseconds if the source is sufficiently bright.

IA. The mode of testing may affect the results of the experiment substantially. The selected mode must recognize the time constants inherent in the first three Stages of the visual system as well as the level of cognition required of the brain in order to satisfy the test criteria. The delays associated with that level of cognition can be significant. In timed experiments, it may also be important to factor in the time delay associated with the peripheral nervous system (finger responses occur sooner than foot responses).

II. The visual mechanisms employed between the retina and the midbrain as well as within the midbrain differ considerably depending on the location of the stimuli applied to the retina. It is vitally important to differentiate between stimuli presented totally within a given region of the retina and those presented so as to bridge a border between regions of the retina.

III. The difference between a background upon which a center stimulus is added, is significantly different than a surround with a hole in it where the center is placed. In this second case, the center stimulus is not summed with the background.

IV.

V. While a bite bar may restrict the casual motions associated with breathing and room vibration, it does not control the normal oculomotor motions of the eye. It specifically has no influence on the fine motion, tremor, of the eyes. However, there are stabilization techniques that do control or eliminate the effects of tremor. The performance of the visual system when stabilized is quite different from its performance under normal conditions.

VIA. The dichoptic mode, where different stimuli are introduced into the portions of each field of view of each eye

which they share, can provide useful information concerning the detection and interpretation capabilities of the visual system.

VIB. The state of adaptation is sometimes treated inadequately in experiment planning. There are numerous examples in the literature where the state of adaptation changed during an experiment without the knowledge of the investigator. The investigator must be aware of the asymmetry in the dark adaptation versus the light adaptation process, and how easily the adaptation state can be changed by even the briefest exposure to an unplanned light level. An incidental glance at a glowing cigarette or a pilot light can significantly upset the state of dark adaptation.

VII. The character of the light stimulus used in psychophysical experiments has seldom been matched to the performance boundaries associated with the spectral absorbers of the eye. This has frequently led to imprecise results. At other times, the results have been less than optimium. The overlap in the spectral absorption of the individual spectral channels complicates this selection.

VIIA(3) & **VIIB(3).** The color temperature of the sources used in psychophysics experiments is critical to the quality of the results. This factor is the defining factor in why the psychophysical school teaches that blue light is not a significant factor in the luminous efficiency function in direct conflict with vision physicists like Judd. In most psychophysical experiments, inadequate light sources have made the light passing through a blue filter inconsequential. As a result, there results do not reflect the performance of the visual system.

VIII. Symbols play a unique role in human (and possibly other higher primates) vision. This role is different between stimuli presented to the foveola and the remainder of the retina. There is a fine line between the perception and cognition of symbols and other fine patterns within the foveola. Most symbols are understood apriori due to previous training. The interps related to such symbols are already stored in the brain (probably in the cerebellum). Fine patterns can be learned in the course of the overall experiment, and may thereby become symbols. While the orientation of patterns may be significant in some experiments, the orientation of symbols placed within the foveola is much less important (after initial training). It should also be noted that there are no known spatial frequency filters within the electophysiology of the visual system. While spatial correlation is performed within the pretectum, this correlation is highly time dependent. While pseudo spatial filtering occurs within the retina, this filtering is actually performed in the time domain using time delay techniques not temporal frequency filtering.

IX. The temporal content of any portion of a test environment must be considered with respect to the variety of time constants and the signaling asymmetries found in the visual system. These features play a major role in determining how the visual system responds to a given stimulus. Proper interpretation of the stimulus in terms of these features leads to clearer understanding of many flicker effects and other effects of a novelty nature.

It is proposed that the term protocol is better than tradition, as used by Wolfson & Graham, to describe the procedures associated with a given experiment.

Based on this framework, the experiment of Wolfson & Graham could be described as an achromatic detection experiment using a center and background format. Detection was characterized by a yes or no in response to a staircase intensity variation of the center probe viewed for 1/75th second in the presence of a background available for at least two seconds. The protocol used a spatially uniform but apodized probe slightly larger than the foveola. The probe intensity was variable but always additive to the background. A spatially uniform but apodized background with a diameter of 10 degrees varied periodically in the temporal domain. The subject was coached to fixate his monocular or binocular but unstabilized line of sight (except for a bite bar) at the expected location of the probe.

It is interesting to note that the probe presentation interval is considerably shorter than the 50 msec usually associated with the dwell time of the eye in reading. This would suggest that the detection process is associated with the alarm mode of the human visual system more than it is associated with the analytical mode. The probe presentation interval is also short in terms of the duration of the continually occurring minisaccades of normal eye motion. This would suggest that some presentations of the probe will be missed due to the normal oculomotor motions of the eye.

A similar parsing of other experiments can be performed based on this framework. This leads to a more definitive description of what parameters were controlled, varied and left uncontrolled in a given experimental sequence.

I.	Time Domains involving the foveola	<50 msec	200 msec	>500 msec
IA.	Detection methodology	Free	Forced	Timed
II.	Spatial Domain of stimuli	within foveola	within fovea	within periphery
III.	Spatial Character of experiment	Center	Center & Background	Center & Surround
IV.	Fixation point	Stimulus point On line of sight	Stimulus point displaced from LOS	
V.	Line of Sight	Free at micro radian level	Stabilized to microradian level	
VI	Mode of application	Monoptic	Dichoptic	Binocular
VIX	State of adaptation	Dark	Ambient	Chromatic
VII.	Stimuli with zero spatial frequency content			
VIIA.	Character of center stimulus	Constant center chrom.		Constant center lumin.
VIIA(1)				Constant Red-Aqua ratio
VIIA(2)				Constant Yellow-Violet ratio
VIIA(3)	Color Temperature of source	7053 K	6500 K	<3600 K
VIIB	Character of surround/background (repeat analysis as in VIIA)			
VIII	Stimuli with pattern or symbol spatial content			
VIIIA	Patterns larger than foveola	Fixed orientation		Variable orientation
VIIIB	Patterns smaller than foveola	Abstract patterns		Recognizable symbols
VIIIC	Symbols	Known to the subject		Requiring learning
IX	Temporal content assoc. with VI & VII			
IXA	Variable in--	Center	Background	Surround
IXB	Variation is --	Transient	Periodic	Aperiodic

Figure 17.10.1-1 Preliminary framework for categorizing psychophysical experiments. The factors to the right of each characterization on the left are only suggestive. Future variants of this figure will develop more relevant terms.

17.10.2 Averted vision as used in astronomy

Popular writing in the field of astronomy frequently discuss the practice of averting one's vision to place an image at a point other than the point of fixation in order to achieve higher threshold sensitivity when viewing dim objects such as distant galaxies and nebulas. However, the reader is frequently left without any description of what angular measure of aversion should be used. It is quite clear from perimetry measurements that the peak sensitivity of the human eye falls rapidly outside of the foveola at photopic light levels (**Section 17.2.4.2**). Similarly, the visual acuity of the eye also falls dramatically outside of the foveola at photopic light levels (**Section 2.4.7**).

Data on the performance of the visual system at very low light levels is very limited, and generally incomplete. Aulhorn & harms has provided data on the absolute sensitivity of the eye as a function of background level (**Section 17.2.4.2**). The size of the source used in these experiments was not given. This data shows an apparent maximum sensitivity, at very low background levels (well below 0.01 asb or 0.00318 cd/m^2), at eccentricities of about 10 degrees as high as ten times the sensitivity at fixation. However, the data collected by Randall suggest a loss in visual acuity of between 5 and 20 to one at this same eccentricity. When these values of visual acuity and the absolute sensitivity at 10 degrees eccentricity are combined, the performance may or may not be better than that at the point of fixation.

When seeking maximum combined sensitivity and acuity, the mosaic structure of the retina (including the foveola) may become significant. When trying to resolve the arms of a spiral galaxy, the precise alignment of the arms and the pattern of photoreceptors may become significant. The photoreceptors are approximately two microns in diameter in the foveola resulting in a visual field of 20 seconds of arc in diameter. This is also the nominal pitch of the closely packed photoreceptors. These numbers, combined with the fact the eye is a scanner and not an imager, indicate that features of less than 20 arc seconds in dimension may be perceived differently depending on the precise position on the foveola mosaic. For "long" features, the Nyquist frequency limit of slightly less than two cycles/minute of arc can also be used as a guide. That criteria suggests perception of long features approaching 20 arc seconds in width may fade in and out at threshold.

The above discussion assumes virtually ideal seeing conditions. Very low background illumination must be achieved to obtain the potential sensitivities described by Aulhorn & Harms. Simultaneously, very stable conditions in the atmosphere must be present. Otherwise, the turbulence of the air will introduce both spatial and temporal variations in the brightness of small image details that will exceed the levels involved in the above discussion.

The above discussion also assumes the observers foveola has not been damaged at the point of fixation. If the foveola has been damaged, only a detailed ophthalmological evaluation of the foveola can account for its performance.

As noted by some writers, performance gains by aversion of the line of sight is a skill claimed to be developed by experienced observers. An astronomer observing with the naked eye should not expect a performance gain by averting the image by more than 0.5 degrees from the normal point of fixation. This is approximately the diameter of the full moon when high in the sky.

17.11 Summary

The analyses in this chapter have built on the structure developed in earlier chapters. Points of critical importance were the detailed definition of the adaptation amplifier within the photoreceptor cell and the unique square-law characteristic of the L-channel in human vision.

The very high degree of negative internal feedback within the adaptation amplifiers, and the low pass time constant related to that feedback play crucial roles in the overall performance of the HVS. The level of feedback is controlled almost completely by the diffusion characteristics of the bioenergetic materials powering the photoreceptors. This factor insures the very high degree of amplifier gain uniformity achieved throughout the retina.

The very high degree of negative internal feedback, approximately 85% with a low pass time constant on the order of one second, insures that the signal processing section of the retina operates in an essentially constant amplitude regime. The wide swings in illumination presented to the eye are almost completely removed from the signal from all of the photodetection channels before further processing.

The primary signal of the photodetection section of the visual process is a current. This current creates a voltage at the pedicle of each photoreceptor cell that is the logarithm of this current. The luminance signal processing channel uses the voltage at the pedicles to compute the psychophysical perception of brightness via a weighted matrix. The

chrominance signal processing channels use the same voltages at the pedicles, via a different matrix with different weightings, to compute the psychophysical perception of chromaticity.

The above matrixing highlights an important fact. The chrominance information is not derived from the luminance channel of vision. They are both derived from the more fundamental spectral channels.

> The signal gain in each of the spectrally specific photodetection channels proximal to the adaptation amplifiers is not the same in the luminance channel or in the chrominance (or in other differencing) channels. Each matrix defining these channels contains different coefficients.

17.11.1 Operation of the luminance channel

Using a constant photon flux per unit wavelength input illumination, it is possible to develop a single equation that describes the perception of brightness in the HVS at all levels of illumination intensity. This equation automatically changes character as the illumination intensity varies from the scotopic, through the mesotopic, to the photopic region. Based on this equation, it is possible to define the nominal signal amplifier gains used in the photodetection channels proximal to the adaptation amplifiers and presented to the luminance signal channel for signal processing.

In passing through the scotopic, mesotopic, photopic and hypertopic regions, the above equation correctly describes the special effects known as the Purkinje phenomena and the Bezold-Brucke phenomena. It also defines the enhanced nature of these phenomena that can be perceived under unusual spectral adaptation conditions.

17.11.2 Operation of the chrominance channels

Using a constant photon flux input spectrum, it is possible to demonstrate three important aspects of signal processing in the chromatic channels.

+ The characteristics of the signals at the output of the differencing circuits, the axons of the lateral cells, are the same as the characteristics of the output of the cortex. No significant chromatic signal processing occurs within the cortex, other than the fill function used to interpolate the “color” of large constant luminance, and other “null,” areas. These null areas include the “blind spot” and other scotomas of the retina.

+ There are two orthogonal chromatic signal processing channels in human vision. These channels correspond to a S- minus M-channel and a L^2- minus M-channel. There is a balance point in each of these channels wherein no signal information is passed to the cortex. When both of these channels are at the balance point, no chromatic information is transmitted to the brain; the subject reports the illuminated scene is achromatic. This “white point” is independent of the actual spectral characteristics of the scene.

Although the Trichromatic Color Mixing Theory is correct that it requires three chromatic samples to exactly match an arbitrary sample, only two properly selected chromatic samples are required to produce the sensation of “white.” These two pure spectral colors are XXX and XXX under conditions of adaptation to a constant photon flux per unit wavelength.

+ The signal gain in each of the photodetection channels proximal to the adaptation amplifiers is essentially equal as presented to the lateral cell dendrites of the chrominance channels.

17.11.3 The perception of color under chromatic adaptation

Changing the color temperature of the scene results in a change in spectral luminosity as reported on a photoelectric photometer. However, the photometer cannot represent the apparent color seen by a human. After a short period of adaptation, the adaptation amplifiers of the human eye will compensate for this change in spectral luminosity. The subject will then perceive a portion of the scene as white, regardless of its actual spectral distribution, under a very wide range of conditions. This process can be understood and accounted for using the new Chromaticity Diagram and its extensions. In this way, it is possible to explain and quantify the apparent whiteness of the various standard illuminants, A thru E, compared to the inherent whiteness under constant photon flux conditions, illuminant F.

17.11.4 Efforts to create a “color solid”

There have been many attempts to create a three dimensional Luminance/Chrominance Diagram. They have been

useful for pedagogical purposes but have usually foundered in practice. Although it is possible to create a three dimensional "color tube," where the brightness of a light along the spectrum locus can be plotted as a third dimension perpendicular to the two dimensional new Chromaticity Diagram, the utility of this presentation is questionable. The actual perceived brightness for a given scene defined only by spectral colors is given by the integral of the brightness function included within these wavelengths. This is also true for the brightness corresponding to points within the spectrum locus on the new Chromaticity Diagram. However, the perceived brightness at a given chromaticity in response to a real scene in object space is not unique. The perceived brightness may result from both mixing different colors in object space, and differential adaptation by the photoreceptors with time. The result is different perceived brightnesses for the same scene under apparently the same conditions.

By using scene elements illuminated by multiple sources of different color temperature, it is possible to create many unusual effects. These techniques relate closely to and explain many of the effects demonstrated by Land[167] and presented in his Retinex Theory of color vision.

17.11.5 The temporal performance of the human eye

Investigators have had difficulty in describing and modeling the temporal characteristics of the visual system, and particularly the HVS, because of several factors. There are three major factors associated with perceived brightness and one associated with perceived color.

The two primary factors are related to the performance of the adaptation amplifiers. These amplifiers are highly non-linear and their time constants are asymmetrical. Third, the phototransduction process involves a time delay that is illumination level dependent. This time delay is often considered a simple time constant in the proposed models. The illumination level dependent feature of this time delay makes the typical experiment difficult to confirm by repetition. These factors affect all of the photoexcitation channels of the animal.

Because the amplitude transfer function of the adaptation amplifier involves an exponential term of the fifth or sixth power that is time dependent, many investigators have attempted to model the overall passband of the HVS using as many as 12 cascaded stages of simple RC filters, occasionally with one or more variable resistance values. More careful experiment design will illustrate that this multi-stage filter approach is inappropriate.

The chrominance channels exhibit another temporal effect that has not been discussed or properly modeled in the past. The midget ganglion cells are biased so that they generate a continuous pulse stream at a nominal 30 pulses per second. With higher levels of excitation, these cells can increase this nominal rate to at least 70 pulses per second. Upon reduced levels of excitation, the pulse rate is reduced significantly. However, as the rate approaches zero pulses per second, the information transfer rate becomes very low or non-existent. This situation would suggest that the rate of color perception, in the human at least, may be related to the polarity of the chrominance signals applied to the midget ganglion cells. The data is sparse in this area. However, it appears this feature accounts for the relatively slow perception of changes in the saturated blue and saturated red regions of the chromaticity diagram. Zworykin & Morton[168], working with tristimulus values to define the NTSC color television system, showed that the relative passband of the blue channel is only about 17% of that of the green channel. The red channel passband is only about 40% of that of the green channel. These numbers apply to highly saturated colors. These finding would tend to say that signals in the chrominance channels of the visual system affect the midget ganglion cells differently as suggested above. It appears that an increase in the S-channel signal amplitude causes the midget ganglion cell of the P-channel to lower its pulse frequency. Similarly, an increase in the L-channel signal appears to cause the midget ganglion cell of the Q-channel to lower its pulse frequency. In both cases, the pulse frequencies are increased in the presence of higher levels of M-channel illumination.

Some animals exhibit a very distinct lead-lag network at the input to the parasol ganglion cells of their eyes. This has not been reported in humans. It is hard to quantify.

17.12 Colloquy showing the usage of the Performance data presented here

Several correspondents have asked questions of how the performance data of Chapter 17 is used in field

---

[167]Land, E. (1974) The Retinex Theory of color vision. Proc. Roy. Inst. of Great Britain, vol. 47, pp. 23-58
[168]Zworykin, V. & Morton, G. (1954) Television, 2nd ed. NY: John Wiley & Sons. pp. 817-825

applications. As an aid to others, several of these colloquies will be included here.

17.12.1 Colloquy with DK (2016)

DK is a well founded engineer working in lighting in Australia.

8/28/2016 Response

I apologize for being a few days slow in responding. I had total knee replacement surgery on 22 August 2016 and was not really up to technical discussions until Saturday when I first reviewed your messages.

Your website presents an interesting Resume. I will not talk down to you but the first paragraph or two is needed to get us onto the same page. I will also take the license to copy your four emails of last week onto this single page in order to discuss them in a cohesive manner.

You have raised a number of questions in an area with an unfortunately long history involving groups that typically did not talk to each other very much, the technical (scientific) community and the combined printing and expressive art (arts) communities. The first has dealt almost exclusively in what is called additive color with a significant focus on narrow spectral bandwidth sources (when available). The latter has dealt almost exclusively with what is called subtractive color with a significant focus on only three to (occasionally) six palette colors.

-----Original Message-----
Sent: Wednesday, August 24, 2016 10:32 PM

I am an electronics designer. Thank you so much for all your fascinating web pages. I think your New Chromaticity Diagram will be helpful in bridging from a wavelength specification (such as the dominant wavelength given in the datasheet for a LED) to a perceptually-even system such as Munsell.
http://neuronresearch.net/vision/files/chromaticity.htm

But I'm stuck on one point. Why do you call 494 nm (Munsell 5BG) "azure"? Why not "cyan"?

*** This question is very pertinent to the New Chromaticity Diagram and the state of the commercial arts (subtractive color). As I developed my materials it became important to differentiate between these two terms at the technical level, even though I may need to go back and do some editing for consistency. Basically, my intent is to define the Chromaticity Diagram with a greater precision than ever before. I believe I have claimed a precision in my definitions of color names and wavelengths to an accuracy of +/-2 nm. This is an extraordinary precision (on the order of +/-0.4% at 500 nm) in Color Science.

*** In the commercial arts, the colors cyan, yellow and magenta are precisely standardized BROAD spectral colors. Both the gelatin color separation filters and the printer's inks used have been highly standardized by a number of manufacturers.

*** Only with the arrival of the personal computer and CGI techniques has an intersection of additive and subtractive color appeared. Who ever heard of a choice between RGB and CYM color spaces until the PC arrived?

*** In my work, Azure is described as a narrow SPECTRAL color, at 494 nm, that also describes the nominal center wavelength of the broad (non-spectral) color known as Cyan. I can provide you copies of the Kodak spectrums for the CYM separation filters. Even these consists of sets to satisfy different artistic and commercial communities.

*** In my work, I attempt to define the SPECTRAL colors based on the actual physiology and performance of the human eye. That eye is best described using on additive color spaces (crudely by Maxwell, Hering, Munsell, the CIE and many others). See Section 2.1.1 of
http://neuronresearch.net/vision/pdf/2Environment.pdf#page=1

When I look at this Munsell colour wheel
https://en.wikipedia.org/wiki/Munsell_color_system#/media/File:MunsellColorWheel.svg
and compare it to the named colours here
https://simple.wikipedia.org/wiki/List_of_colors
with saturation 100% and luminance >= 50%,

I find that the colour named "azure" in the above list looks to be more like 450 to 460 nm (Munsell 10B to 5B). Other searches on the meaning of "azure" always call it a kind of blue and sometimes call it purplish, but never greenish. And its etymology relates it to lapis lazuli which has no hint of green.

*** I do not intend to defend the un-named sources that appear in Wikipedia. The material is easily objected to by noting alternate sources in my **Section 2.1.1.**

Then I noticed that in
http://neuronresearch.net/vision/pdf/17Performance1b.pdf
you used the name "aqua" for 494 nm/5BG.

In the above comparison I find "aquamarine" to be more like 505 nm/10G.

*** I will go back and review the terminology of these pages, with the intent of sticking with "Azure" and "Cyan" and eliminating "Aqua."

*** I will note that Munsell, who did a fine job in the 1910 time period, ARBITRARILY divided his color wheel into ten zones of 30 degrees each and then further subdivided each zone. If he had divided the 360 degrees by nine, he would have defined a totally different color wheel.

The "cyan" in the above list appears to be a much better hue match to 5BG/494 nm. The 5BG square appears to have luminance between that of "cyan" and "teal".

*** I agree with the naming of BROADBAND Cyan. Teal is an arbitrary name that has been used variously by many, see **Section 2.1.1**.

Add to that the fact that "cyan" is already accepted as the name of a subtractive primary used for printer ink, and there seems to be a good case for you to use the term "cyan" rather than "azure" (bluer than cyan) or "aqua" (greener than cyan). Just wondering why you don't?

*** See the above discussion, some authors in Section 2.1.1 place azure as bluer than cyan and others place aqua as greener than cyan. In fact a printers cyan is broader than, and encloses both the noted labels of azure and aqua. In this work, azure is a NARROWBAND color at the nominal center of the "printers" BROADBAND ink cyan and nominally at the center of the separation preparers Broadband gelative filter labeled Cyan.

I love your "blocked tetrachromat" stuff too. At one time I was designing systems that used UV-C lamps for sterilisation. I couldn't help occasionally glimpsing them and was fascinated that they appeared to be an unsaturated cyan or unsaturated blue (hard to say which). I have normal lenses and normal colour vision. I once saw a CIE-style chromaticity diagram for aphakics that showed the violet tail continued into the ultraviolet by curling back upward into the unsaturated blue region, ending at the infinite-temperature black-body point, which made perfect sense to me.

*** I looked into the work you cite many years ago. It remains correct but uses the CIE Chromaticity Diagram of 1931-4. It and subsequent modifications to it are entirely empirical and provide no theoretical foundation.

How does your tetrachromatic chromaticity diagram explain the perception of UV as unsaturated cyan/blue?

*** The colors you describe as unsaturated are in fact nulls at specific wavelengths occurring within the neural signaling system (Section 16.2 in

http://neuronresearch.net/vision/pdf/16Equations.pdf#page=11

Azure occurs at P = 0.00 (at 494 nm), yellow occurs at Q = 0.00 (at 572 nm) and a color not discussed yet, Lilac occurs at O = 0.00 (at 400 nm) with tolerances of about =/- 2 nm.

*** Demonstrating these null values in the laboratory to the desired tolerance is difficult because of the protocol required to ensure equal adaptation among the various spectral channels and equal stimulation of the channels (recognizing their variable sensitivity as a function of stimulation wavelength) as the data is collected.

It would be interesting to see what the black-body curve looks like on your diagram. Is it smooth or does it have a kink?

*** The New Chromaticity Diagram is a Uniform Color Space (UCS) using the CIE nomenclature. It is in fact a 3-dimensional color space with O-, P- & Q axes. Such a color space cannot be represented entirely adequately on a 2-dimonsional paper or monitor (as is the case with the CIE diagrams). Section 17.3.3.3 of

http://neuronresearch.net/vision/pdf/17Performance1a.pdf#page=228

describes the choices leading to the New Chromaticity Diagram.

***Section 17.3.3.6.3 shows the optimal representation in

http://neuronresearch.net/vision/pdf/17Performance1a.pdf#page=245

Note the triangular space at upper left. Note also the rectangles representing the achievable additive color space using current monitor (phosphor generated) color space and the subtractive (process) color space achievable.

*** I have not performed the calculations needed to display the Black Body locus on the New Chromaticity Diagram. If you can find a CIE UCS Lab or Luv representation with the Black Body locus shown, I would appreciate your forwarding me a copy. As noted above, the New Chromaticity Diagram incorporates a discontinuity at 437 nm to achieve a 2-dimensional representation. The Black Body locus will pass through the white point at 494,572 at a nominal 6500 Kelvin and then rise until it reaches the discontinuity at 437 nm at a temperature exceeding a roughly estimated 20,000 Kelvin. Below 6500 Kelvin, the Black Body locus will curve off to the lower right becoming parallel to the horizontal axis at 532 nm.

My apologies. I should have read more of http://neuronresearch.net/vision/pdf/17Performance1b.pdf

I see that your reason for not using "cyan" for the hue of 494 nm/5BG is that it is associated with a broadband colour in the printing industry.

But I don't understand why, in naming a hue, it matters whether the colour it derives from is narrowband or broadband.

*** Go into the laboratory and see how much energy at 494 nm is needed to achieve a given intensity of azure or yellow using an LED versus a wideband source.

"Yellow" is also associated with a broadband colour in the printing industry, and yet you use it as the name of a hue.

*** It is difficult to rationalize the use of Yellow as a name in both the additive and subtractive regimens other than to note history. Yellow in fact does not appear in the intermediate neurological signal processing of the brain. It is a perception within the stage 5 (cognition) circuits of the brain arising for a high value of R-channel signal (brightness) simultaneous with a null in the Q-channel.

There are LEDs (narrowband sources) that are sold as "cyan".
http://www.digikey.com.au/product-search/en/optoelectronics/led-indication-discrete/524729

Admittedly they aren't really cyan, since they have a dominant wavelength of 505 nm, but that's due to the historical "redshift" in _all_ LED hues relative to their marketing names, by about 5 to 10 Munsell units. Historically LEDs were developed from red to violet, so we can guess that the first to produce a reddish-orange LED heralded it as the first "orange" LED, then the first to produce an orange heralded it as the first "amber", etc.

*** You provided the answer to your own question. In the commercial world, a manufacturer can assign any name to something that he wants in the absence of some industry or governmental requirement.
I previously took yellow (10Y) to be in the range 575 to 581 nm and cyan (5BG) in the range 487 to 493 nm, based on
https://www.ecse.rpi.edu/~schubert/Light-Emitting-Diodes-dot-org/chap17/F17-03%20Chromaticity%20diagram%20(Gage).jpg
It puts the central yellow at 578 nm as opposed to your 572 nm, and the central blue-green (cyan) at 490 nm as opposed to your 494 nm. Pretty close.

*** As an aside, I graduated from RPI long before they opened their "lighting Center."

*** Ask Professor Schubert for a tolerance in nm on his spectral labels. I think my values will stand the test of time better.

***For several years, researchers attempted to develop a simple LED that produced white light. This is impossible. Simple LED's generate a SPECTRAL wavelength source. White is a non-spectral color at 494, 572 nm. Mixing the light from two LEDs, with wavelengths at 494 and at 572 nm and appropriate intensities, will produce a very excellent white light. Many textbooks insist that three LEDs are required to achieve a good quality light. This is based on an archaic Chromaticity Diagram concept. (Section 17.3.4)

- - -

Found your discussion of "canary" versus "yellow" on page 193 of
http://neuronresearch.net/vision/pdf/17Performance1a.pdf
Still don't understand why it matters.

*** Canary is the trade term for the "BROADBAND yellow" separation negative prepared in the printing industry before printing with a "BROADBAND yellow" ink. If you prepare a canary separation negative after exposing the film through a NARROWBAND yellow filter, your resulting final print will look like it was produced by a partially color blind reproduction system.

*** It is another subject, but if you use a NARROWBAND Sodium Vapor lamp as a street light, the color rendition index (CRI) will be just terrible. A bright red material will be reproduced as a fecal brown (as will a bright blue or green material. I had a bright red coat at RPI (school colors).

- - -

I see that UV-C lamps simple produce some visible spectral lines, that presumably give rise to the unsaturated blue.
http://www.negativeiongenerators.com/UV-C_spectrum.html

*** Your citation shows their "high quality source on the right and an inferior commercial source on the left. It produces a variety of low intensity lines that may be labeled anything in the purple to red area depending on the specific source and the state of adaptation of the observers eyes. The labels UV-A, UV-B & UV-C are largely undefined and developed empirically during the 1930-60's time period.

8/30/2016 Response

Thank you for the information about the Kojima et al. paper. I will study it a little more carefully before commenting. The value of 380 nm is clearly supportive of my work but without a tolerance value, I can not put it into my work. The actual value for the peak sensitivity of the absorber, after all possible adjustments are made (such as lens absorbance), should be closer to 342 nm or possibly 350 +/- 10 nm.

It will take me a week or so to rationalize the New Chromaticity Diagram with the Black Body Locus because it depends on multiple parameters. In general, the New Chromaticity Diagram is a Perceptual Chromaticity Diagram and only relates to the illumination in the external physical environment under conditions of "Color Constancy," that generally coincide with the photopic range of illumination. If the environment is not provided by a light source of 6500 Kelvin, a condition known as D(sub 65), additional parameters must be controlled and reported

I hope you realize the CIE 1976 Luv and Lab color spaces are entirely calculated (with numerous mathematical adjustments made to accommodate a connection to the CIE 1934 space that was also entirely empirical and based on data of quite limited precision at that time). The New Chromaticity Diagram is easily traced to the actual neurological signals within the eyes and brain when certain parameters are properly controlled in the laboratory protocol. The CIE 1934 Color Space has virtually no redeeming scientific value, except that it has been widely reproduced and accepted as factual over a very long period of time.

8/31/2016 Response

Your comments below are pretty much on target. But there are some subtleties that I would like to share with you.

First, when thinking of "cyan" as labeled in additive (conventional) color space, it can be described as a center wavelength of 494 nm and a bandwidth of +/- 100 nm., i.e., it covers almost the entire visual spectrum. On the other

hand, the label, "azure" has a center wavelength of 494 nm but a bandwidth that can be defined as 0.00 nm, but with an accuracy of +/-2 nm.

Until more experiments are carried out the values of 494 nm for "azure" and 572 nm for "yellow," the precision of these values are estimated from reviewing a large amount of the applicable literature.

-----Original Message-----
]
Sent: Tuesday, August 30, 2016 7:16 PM
To: James T. Fulton
Subject: RE: UV-sensitive photoreceptor protein OPN5 in humans and mice.

Hi Jim,

Yes, I always assumed the black body locus was telling me what I'd see if the general illumination was with the standard illuminant, while I was looking at a small-area black body at the given temperature, such as yesterday when I drove up to a T-intersection in the middle of the day and there was a lighting store with glass walls in front of me. Many of the luminaires looked quite yellow (as expected) and yet I have the same at home and they seem white enough indoors at night (as expected).

*** You are encountering spectral channel adaptation while the overall eye is operating in the photopic region. This dynamic spectral adaptation on an individual channel basis insures what is called "color constancy" in your perceived response. It is achieved by the chromophores of the different spectral sensory neurons changing their individual sensitivity with a time constant measured in milliseconds.

*** Contrary to Kojima et al., (2011) and the general belief in the pedagogy of the visual community, the chromophores are not proteins. What is generally called "rhodopsin" is actually a structural substrate protein that is coated with a distinctly different chemical, one of the rhodonines. The rhodonine family is a set of four retinoids, that are modifications of vitamin A. When in their active state, they are conjugated all-trans-retinoids. They do not change to a cis-form on activation. Instead they are electronically excited into an excited state that can release an electron into the plasma of the sensory neuron dendrite.

Yes, I'm very impressed by the neurological plausibility of your chromaticity diagram, but I'm still having trouble understanding how to use it to determine the expected chromaticity of a combination of 1, 2 or 3 spectral (or narrow band e.g. LED) sources.

*** Fair question, I tried to introduce this subject in the last email. The next step is to appreciate that the New Chromaticity Diagram is a perceptual Diagram. It does not apply directly to object space. Thus, to determine exactly what a subject will perceive, you must consider both the chromaticity space and the intensity space associated with each illuminant just as Munsell did (and the current day empirical version of his theory still does). This is where the experimental protocol becomes so important. If the subject is exposed to a gray field surrounding the test illuminant, the gray field is at a photopic intensity level, and the subject has not been exposed to a high contrast field other than the gray field for at least 20 minutes, the results will be quite repeatable, estimated s.d. = +/-2 nm, even between individuals. However, if any of the above conditions are not maintained, the results will differ to the extent of +/-10% or more. So, it is important to determine what the goal of the investigator is.

It seems that the only thing I can read directly off your chromaticity diagram is what I get with _two_ narrowband sources. Otherwise I'd have to assume you're telling me that the combination of equal amounts of 532.1 nm and 655 nm has much the same chromaticity as 655 nm alone and that this is an orange of about Munsel 2.5YR. Even a 630 nm LED looks far less orange and far more red than that, to me. So how do I read the chromaticity of a single narrowband source?

*** You must adjust, or control, the perceived brightness of each of your individual light sources at the sensory layer of the retina. To achieve the optimum desired results, you must determine the product of the stimulus intensity and the spectral sensitivity of the retina at a specific wavelength (done easily with LED sources). For more broadband sources, integration over specific spectral ranges must be employed. The best available spectral sensitivity of the human eye is that of Babucke, 2007 shown in Figure 17.2.5-13 at

http://neuronresearch.net/vision/pdf/17Performance1a.pdf#page=63

Chapter 17Performance Part 1a is still subject to considerable editing but the figures are all correct. The figure on page 63 is introductory with the more detailed figure 17.2.5-13 on page 98. As you can see, there is a variation with wavelength of about a factor of four across the spectrum when working within the central 2 degree field of vision centered on the center of the foveola of the retina, the "point of regard" in object space.

I would recommend you ignore any data related to the CIE visibility function dating from 1924. It is archaic and obtained under poorly understood and controlled conditions. I would also recommend you ignore any data with the name Stockman attached to it. Stockman et al. were, and are, a group of psychophysicists (actually psychologists working way beyond their educational background). While Stockman is reasonably charismatic to the uninitiated, he has difficulty defending his positions. His, and his groups, understanding of mathematical precision is almost non-existent.

As shown in 17Performance1a.pdf, the visual system does not employ linear (conventional) algebra. All summations are done in logarithmic space. This makes a big difference. The broadband brightness function, the R-channel of this work is a logarithmic summation of the signals at the output of the sensory neurons. Figure 17.2.6-1 shows a pedagogical difference in the visual sensitivity functions obtained based on several different models. Only the logarithmic model even approaches the actual function.

- - - -

But even when looking up the combination of two narrowband sources, your diagram seems to be telling me that I can produce a white light by combining 494 nm and 572 nm in equal quantities. But the solid curve in your figure 17.3.4-4 (Wright 1972) appears to be telling me I'd need more like 480 nm and 586 nm. Can you explain this apparent contradiction? By the way, I don't understand what the dashed curves are in that figure.

*** Wright performed a majority of his excellent work on complementary colors (for the time period) in 1929 before both you and I were born (and before the CIE was formally established. He provided a comprehensive report on his work in 1946[169]. In later years (ca. 1969), he ridiculed the work of the CIE committee, including the ones he was chairman of (page 125 in 17Performance1a.pdf). I do not, and cannot, defend any of the work of the CIE and their reliance upon simple linear algebraic expressions to describe clearly logarithmic relationships. Even in their highly empirical and adjusted CIE 1976 Luv and Lab representations, the axes u, v, u', v', a* & b* lack any relevance to the actual visual modality of biology. I will address this subject further in a future message related to the Black Body locus.

The CIE Standard Observer of 1931 does not relate to human vision. It was a construct defined to be compatible with the other CIE data of the time period and is *archaic*. A real spectral response of a human eye under well characterized conditions is that of Babucke (2007) cited here.

I do not support the data in Wyszecki & Stiles, (1982), section 3.5. The data was derived by scaling from the archaic CIE 1931 Chromaticity Diagram which lacks any theoretical model and is totally *archaic.*

Based on Figure 17.2.5-13, it is necessary to operate the 494 nm narrow band source at 175% of the 572 nm source to achieve equal stimulation of the retina after accounting for the absorption of the lens of the eye, etc. when working at the point of regard.

It remains tough to achieve a precision better than +/-20% reproducibility among humans, even after reviewing Wright's remarks and the above elements of an adequate protocol. Most laboratory work previous to this theoretical work lacked an adequate foundation on which to develop an effective protocol. The investigators were happy to achieve reproducibility within a much larger field, typically by a factor of 3:1.

- - -
Response of 1 Sept 2016

Take my confusion over the recipe for white = narrowband xxxx/azure/xxxx + narrowband yellow.
Am I misreading your chromaticity diagram when I conclude that I should ideally use 494 nm and 572 nm?
Am I misreading Wright's graph when I conclude that I should ideally use the more widely spread 480 nm and 586 nm?
They can't both be correct, since they differ by 14 nm, and you claim +-2 nm for these unique wavelength on your diagram and you claim that Wright's work was excellent [[[for the time period]]].You also note that your unique

[169]Wright, W. (1946) Researches in Normal and Defective Colour Vision. London: Kimpton

xxxx/azure/xxxx and unique yellow correspond to _asymptotes_ to Wright's curve, and therefore do not correspond to the coordinates of its central white.

*** I have xxxx'd out two of your terms. The term aqua has been eliminated from my material in favor of azure and cyan is not a narrowband label.

*** You are misreading Wright's data in Figure 17.3.4-4. I chose my words carefully and you truncated them somewhat. Wright did excellent work in the late 1920's but recognized its shortcomings as noted in the previous email. He had difficulty in obtaining adequate source luminance using a spectrometer and a low color temperature incandescent light bulb (2400 Kelvin comes to mind). He also had difficulty in measuring the radiance of the source post spectrometer in the age before electronic amplifiers (well before the introduction of the transistor in 1946). I have not found any record of his protocol but it is likely he used spectral bandwidths significantly wider than +/- 2 nm to approach the required photopic levels. Also, as the experimenter approaches the cross-over at 494,572 nm, it requires a large cohort of subjects to obtain statistically accurate results. He did not have such a cohort available. Maxwell's Spot (the uniformity of human retinal sensitivity) varies significantly among humans. I was working with people trying to develop LED headlamps for cars during the first decade of 2000. It was demonstrated that two tunable LED sources at 494 and 572 nm provided a very good narrow band white. However, the narrowband white could not be used as a satisfactory IllUMINANT since the color rendition index (CRI) was extremely poor. The research rapidly moved to very bright LED's in the UV region that were used to excite broadband phosphors providing a wide spectral band source that resulted in much better CRI values. Even the definition of the CRI index was found to be faulty when used to evaluate non-incandescent light sources. The auto industry and the street lighting community has ignored the CRI index ever since. I could tell "war stories" about this evolution.

If I understand you correctly, 494 nm excites S and M equally, and 572 nm excites M and L equally. In that case Wright's recipe makes more sense to me because, putting it crudely, if you have 494 and 572 together then you're getting a double hit of M. But I understand that perceptually it's not a double hit because of the logarithmic response. In electronics we'd say the signal is only 3 dB higher. So I'd expect 494 nm plus 572 nm to give me a faintly greenish white. But that's not what appears on your chromaticity diagram at the intersection of the orthogonal 494 and 572 lines. As implied by Wright's graph, I'd expect to need to move them slightly apart in wavelength to compensate for the additional M and eliminate the green tinge.

*** My calculations are theoretical and await laboratory verification. The colors portrayed in the New Chromaticity Diagram are meant to be illustrative. To achieve precise color renditions would require calibration of my computer and your display, along with a transfer table connecting the two. This has been an area of significant investigation since about 1990 (without an acceptable calibration technique arising suitable for general use.

So why doesn't your chromaticity diagram show a greenish-white at the intersection of 494 and 572?

*** This question involves a more complex situation than you may realize. As noted above, 494,572 nm provides an excellent white for a large percentage of the human population. To achieve this degree of uniformity, it is important that the observer not encounter any stimulus in the UV region at wavelengths shorter than 400 nm. If it does, the criteria for a unique white requires O=P=Q=0.00 That is, a three dimensional color space must be utilized. This situation can generally be ignored unless very detailed data is needed under daylight intensity conditions.

Have a great day.

(Active) SUBJECT INDEX (using advanced indexing option)

(Inactive) DEFINITIONS INDEX (Use individual marks)